

1989

## Dielectric and Kinetic Analysis of Thermosetting Polyester Resin

Patricia Haverty Tully

*College of William & Mary - Arts & Sciences*

Follow this and additional works at: <https://scholarworks.wm.edu/etd>



Part of the [Polymer Chemistry Commons](#), and the [Polymer Science Commons](#)

---

### Recommended Citation

Tully, Patricia Haverty, "Dielectric and Kinetic Analysis of Thermosetting Polyester Resin" (1989).

*Dissertations, Theses, and Masters Projects*. Paper 1539625521.

<https://dx.doi.org/doi:10.21220/s2-0020-q714>

This Thesis is brought to you for free and open access by the Theses, Dissertations, & Master Projects at W&M ScholarWorks. It has been accepted for inclusion in Dissertations, Theses, and Masters Projects by an authorized administrator of W&M ScholarWorks. For more information, please contact [scholarworks@wm.edu](mailto:scholarworks@wm.edu).

DIELECTRIC AND KINETIC ANALYSIS OF  
THERMOSETTING POLYESTER RESIN

---

A Thesis

Presented to

The Faculty of the Department of Chemistry  
The College of William and Mary in Virginia

In Partial Fulfillment

Of the Requirements for the Degree of

Master of Arts

---

by

Patricia Haverty Tully

1989

APPROVAL SHEET

This thesis is submitted in partial fulfillment of  
the requirements for the degree of

MASTER OF ARTS

*Patricia H. Tully*  
-----  
Patricia Haverty Tully

Author

Approved, April, 1989

*David E. Kranbuehl*  
-----  
David E. Kranbuehl

*Robert A. Orwoll*  
-----  
Robert A. Orwoll

*Stephen K. Knudson*  
-----  
Stephen K. Knudson

## DEDICATION

To my husband, whose prayer support accomplished more than my own will.

## ACKNOWLEDGEMENTS

I thank the faculty for selflessly- instinctively- providing encouragement and help. A special appreciation to Ray Hoffman of Aristech whose complete knowledge and willingness to share his insights were of immeasurable assistance. My sincere thanks to Dr. Kranbuehl, Dr Knudson and Dr. Orwoll for their investments of time and wisdom. My acknowledgements would certainly be incomplete without recognizing Melanie Hoff who was always just a shout away.

## TABLE OF CONTENTS

	PAGE
ACKNOWLEDGEMENTS.....	iv
LIST OF TABLES.....	vii
LIST OF FIGURES.....	viii
ABSTRACT.....	ix
INTRODUCTION.....	2
CHAPTER I. CHEMISTRY OF UNSATURATED POLYESTER RESIN...4	
CHAPTER II. DIFFERENTIAL SCANNING CALORIMETRY.....13	
A. DSC THEORY.....13	
EXPERIMENTAL.....20	
B. KINETIC EVALUATIONS.....22	
1. PATRICK LAM ANALYSIS.....22	
2. LEAST SQUARE KINETIC FIT.....30	
3. RYAN-DUTTA ANALYSIS.....41	
4. BATCH-MACOSKO ANALYSIS.....47	
C. DISCUSSION OF RESULTS.....51	
D. RELATIONSHIPS BETWEEN REACTANTS AND THE EXPONENTIAL FACTORS, $m$ AND $n$ .....58	
CHAPTER III. DYNAMIC DIELECTRIC ANALYSIS.....65	
A. THEORY	
1. POLARIZATION.....66	
2. ELECTROSTATIC RELATIONS.....70	
a. CAPACITANCE.....70	

b.	PERMITIVITY .....	72
c.	ELECTRIC DISPLACEMENT.....	73
d.	RELAXATION.....	75
3.	DYNAMIC RELATIONS.....	76
a.	CIRCUITRY.....	76
b.	COMPLEX PERMITIVITY.....	79
c.	DIPOLAR AND IONIC CONTRIBUTIONS.	82
B.	EXPERIMENTAL.....	85
C.	DIELECTRIC RESULTS/DISCUSSION	
1.	PERMITIVITY AND LOSS	
a.	ONSET OF POLYMERIZATION.....	86
b.	ONSET OF SOL-GEL TRANSITION.....	88
c.	COLLAPSE OF PROCESSING WINDOW...	89
d.	APPROACH OF GLASS TRANSITION....	91
2.	IONIC MOBILITY.....	126
3.	TIME-TEMPERATURE DISCUSSION.....	134
CHAPTER IV.	CONCLUSIONS IN SUMMARY.....	135
APPENDIX A:	DSC DATA.....	138
APPENDIX B:	LEAST SQUARE FIT PROGRAM.....	152
APPENDIX C:	RYAN DUTTA DERIVATION.....	153
APPENDIX D:	DERIVATION OF COMPLEX PERMITIVITY.....	154
APPENDIX E:	VISCOSITY AND BARCOL HARDNESS.....	157

## LIST OF TABLES

TABLE	PAGE
2.1	Kinetic Parameters for Lam fit.....23
2.2	Kinetic Parameters ( $k_0, k_1, m$ and $n$ ) for Least Square Fit.....31
2.3	Kinetic Parameters ( $k_1, m$ and $n$ ) for Least Square Fit (narrow range).....31
2.4	Kinetic Parameters ( $k_1, m$ and $n$ ) for Least Square Fit (broad range).....31
2.5	Results form Ryan Dutta Analysis.....42
2.6	Evaluation of Components of Kamal's Equation.....60
2.7	Correlation of $d(\alpha)/dt_{\max}$ with gel.....61
3.1	Component of LCR Circuit.....77
3.2	Reaction onset , Cure Temperature and Temperature of Exotherm.....87
3.3	Correlation of Gel Times from dielectric and rheometric measurements.....89
3.4	Evaluation of dipolar relaxation region.....90
3.5	Approximation of times to Tg from $d\varepsilon'/dt$ .....92
3.6	Relationship of alpha to $\log(\sigma)_{\max}$ .....126
4.1	Summary of all Kinetic Data.....136-8

## LIST OF FIGURES AND ILLUSTRATIONS

FIGURE		PAGE
2.1	Isothermal cure 25°C.....	17
2.2	Alpha versus Time (all temperatures).....	18
2.3	Reaction Rate as a Function of Time.....	19
2.4	Reaction Rate as a Function of Alpha.....	19
2.5-10	Lam Analysis: $\ln(d\alpha/dt) / \alpha^2$ versus $\ln((1-\alpha)/\alpha)$ ..	24-26
2.11-16	Comparison of Lam Fits with Experimental Data...	27-29
2.17-22	Least Square Fits (4 parameters).....	32-34
2.23-28	Least Square Fits (3 parameters, narrow range)..	38-40
2.29-34	Least Square Fits (3 parameters, broad range)...	35-37
2.35-40	Ryan Dutta Fits.....	44-51
2.41-46	Batch Analysis.....	48-50
2.47-52	Evaluation of the Function of $k_0$ .....	54-56
2.53	Evaluation for Activation Energy ( $k_1$ vs $1/T$ ).....	57
3.1-11	vs time.....	93-103
3.12-22	LOG $\epsilon'' * \omega$ versus time.....	104-114
3.23-31	$d\epsilon'/dt$ versus time.....	115-123
3.32-33	Barcol Hardness versus time.....	124-125
3.34-39	Time/Temperature Transition .....	127-133
3.34	$T_{cure} = T_g$ versus Alpha.....	134
A.1-6	Isothermal Cures.....	139-144
E.1-4	Rheological Data.....	152-155

## ABSTRACT

An orthophthalic polyester resin was cured with benzoyl peroxide (initiator) and N,N-dimethylaniline (promoter). The exothermic reaction of the unsaturated maleic anhydride with the comonomer/diluent styrene was monitored isothermally both dielectrically and calorimetrically over the temperature range of 0°C to 60°C.

The data obtained from the differential scanning calorimeter was used to evaluate a simple, mechanistic kinetic equation proposed by Kamal:  $d(\alpha)/d(\text{time})=k_1(\alpha)^m(1-\alpha)^n$ . The rate expression is dependent only on the degree of cure and its rate of cure. Three methods were used to solve for  $k_1$ ,  $m$  and  $n$ . The first is a method Patrick Lam proposed under the assumption that  $m+n=2$ . The slope of  $\ln-\ln$  plot of  $d(\alpha)/dt$  vs  $(1-\alpha)/\alpha$  provided  $n$ ; from its intercept,  $k$  was determined. All temperatures were fit via non-linear least square fit. Thirdly, Ryan and Dutta engineered a technique which is dependent upon the maximum rate of reaction and  $\alpha$  at that point and an initial rate constant  $k_0$ . This method represented the data most precisely due to its inherent dependence on the maximum rate of reaction. All fits, however fail as the reaction approaches the glass transition point and becomes diffusion controlled. The DSC reaches its limit of sensitivity and valuable information concerning  $t_g$  is unattainable.

The frequency dependent electromagnetic sensing technique, however, is highly sensitive and distinctly marks the shut down of cure at extremely longer times than the DSC suggests- due to glassy structure. The technique shows clearly the history of the cure process: reaction onset, onset of sol-gel transition, build up in ionic mobility, dipolar relaxation before approach of the glass transition, and the completion of cure.

The reader will gain awareness of the necessity of dielectric sensing to the comprehensive evaluation of thermosetting polymer resins and understanding of the dynamics of autocatalysis.

DIELECTRIC AND KINETIC ANALYSIS OF  
THERMOSETTING POLYESTER RESIN

## INTRODUCTION

Polyester resins were prepared as early as 1883 but not until World War I did they become industrially significant. At this time, Glyptal was introduced for coating and impregnating. While this class of chemicals has served in that capacity to the present day, their functionality has greatly diversified.

By changing the formulation slightly, the final product may range from tough and resilient, soft and flexible, to brittle and hard. Furthermore, combining the resin with glass fibers economically enhances the strength and the resistance to heat, water, fire and chemicals. While 20% of the 500,000 tons of unsaturated polyester resin consumed in the United States in 1986 was used without the fibers for casting furniture parts, the remaining 80% was reinforced with fibers. The applications are numerous: automotive, housing and construction and electrical .

The resin discussed in this paper is chiefly used for the construction of boat hulls . Due to the size of these parts, production is generally by the spray-up process. This process is highly economical in the production of low quantities of large glass fiber reinforced plastics (GRP) and is restricted only by the need for controlled reaction

at ambient temperatures and pressure without the evolution of volatiles.

Valuable to successful molding is the knowledge of the chemistry of the system. By evaluating the kinetic, mechanical, electrical, and/or rheological properties of the polyester resin during its cure, questions concerning the ideal processing conditions can be answered.

## CHAPTER I: UNSATURATED POLYESTER CHEMISTRY

Unsaturated polyester resins are cured by free radical copolymerization of the resin with styrene, which serves as diluent and co-monomer. Typically, the resin is composed of the dibasic acid and an unsaturated dibasic acid (or its anhydride). These condense with dialcohols (glycols) to form a polyester. The linear polyester contains all three species, usually eleven to twelve units in length. The unsaturated acid anhydride retains its double bond; it is this degree of unsaturation which controls the properties of the cured resin.

There are two main steps in the manufacture of a thermosetting polyester. The first is the synthesis of linear (uncrosslinked) chains from the saturated and unsaturated dibasic acids (or their anhydrides) and the dihydric alcohol(s). These chains are then crosslinked with styrene via the aide of an initiator-accelerator system.

Fusion melt is the conventional choice of manufacturing polyester chains from liquid glycols and low melting dibasic acids (which includes phthalic anhydride). The reactants must be stoichiometrically balanced, and 5% excess of glycol added to compensate for its vaporization at elevated temperatures. Due to the difunctionality of the reactants

there are many possible routes to reaction. Both maleic anhydride and phthalic anhydride may react with either the propylene glycol or the ethylene diglycol. The maleic anhydride has a statistical preference to form esters with the primary alcohols of propylene glycol. This leaves the secondary alcohols available for reaction with phthalic anhydride which is a tediously slow process. For this reason, the resin is processed in two stages.

The first stage is the reaction of phthalic anhydride with the glycols ( $>200^{\circ}\text{C}$ ). This reaction is complete in approximately eight hours after which the melt is cooled and the maleic anhydride added. Condensation commences at about  $180^{\circ}\text{C}$ . (Fractionating columns remove any water formed during condensation.)

As shown in the reaction scheme on page 8, the maleic anhydride isomerizes to trans-fumarate. During the initial esterification, maleic anhydride isomerizes to cis-maleate diester. In this configuration the double bond is highly strained by steric hindrance. At temperatures less than  $160^{\circ}\text{C}$ , the maleate esters remain in this configuration; at temperatures in excess of  $180^{\circ}\text{C}$ , the thermal energy is sufficient to transform the molecule to the more planar trans-fumarate ester.

Incomplete conversion of maleic anhydride to trans-fumarate introduces the problem of incomplete cure. The cis-maleate isomer is distorted from planar configuration and reacts less readily with the styrene radical than does the

trans-fumarate ester. When linear glycols (DEG) react with maleic anhydride, the reaction occurs more rapidly at lower temperatures; the isomerization process may be only partially complete. However, bulky aromatic dibasic acids (ie., phthalic anhydride) promote isomerization by increasing the steric hindrance. (Hence, it is seen that a slight change in formulation may change the properties of the resulting polyester significantly.) The resulting chains are, on the average, twelve units in length and are dissolved in styrene. Since styrene may generate free radicals by the addition of oxygen across the double bond, inhibitors -such as quinone or other substituted phenols-are added to the solution to prevent premature gelation. (Example shown in reaction scheme III.)

The free radical initiator consumes the inhibitor and crosslinks the unsaturated polyester resin with the styrene to form the desired product- a tough thermosetting resin. Crosslinking proceeds rapidly and establishes a three-dimensional network. The free radical concentration increases and the termination rate constant decreases due to the immobility of polymer chains and monomer; this leads to an exponential increase in the styrene initiated copolymer growth.

The choice of initiator depends on time and temperature. Generally, initiators are activated thermally at temperatures much higher than typical spray-up temperatures. Therefore, promoters ( or accelerators) are

used to initiate the reaction at the temperature desired for the application.

The commonly used promoters are either transition metal ions or tertiary aromatic amines. Dimethyl aniline (DMA) was selected because the times to gelation and to completion of cure over the range of temperatures required in this study were better than corresponding times with diethyl aniline (DEA) or N,N-dimethyl-p-toluidine (DMPT). A comprehensive study on the effect of DMA, DMPT, DMMT(dimethyl-m-toluidine), and combinations thereof, was completed by Storey, Sudhakar, and Hogue(6). DMPT and DMMT reactions were considerably faster- much too rapid for the purposes of this study.

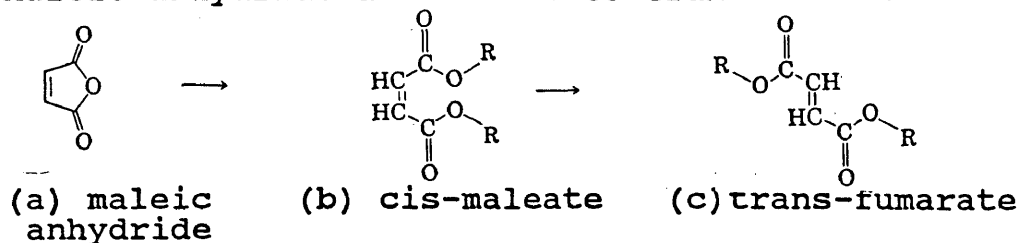
The schematics of the reaction of the promoter with benzoyl peroxide is shown on page 9. The tertiary aromatic amine attacks benzoyl peroxide to produce a radical cation (I), N-benzoyloxydimethylanilinium ion, which in turn decomposes to form a benzoyl radical (III) and a radical cation of the tertiary amine (II). The benzoyl radical initiates the reaction of the cure.

Electron releasing substituents on the aniline ring enhance nucleophilic attack of nitrogen on the peroxide oxygen and lead to faster gel and cure times ( seen with DMMT, DEA, DMPT). The effect is even greater when the substituent is in the para position relative to the amine group. Corresponding ortho isomers were not very effective promoters due to the steric hindrance of the amine group.

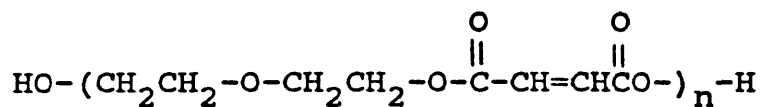
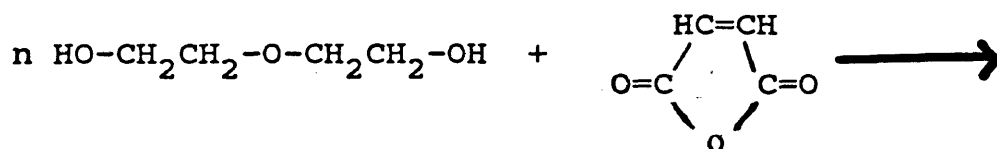
DMPT promoted more efficiently than DMA and DMMT, according to Storey et al., because it produced larger exotherms and higher glass transition temperatures—approximately  $10^{\circ}$  higher than corresponding runs with equal concentrations of the other promoters. The experiments were conducted at low temperatures, (10 and  $15^{\circ}\text{C}$ ) where, they explain, a high exotherm is desirable for cure completion. Our conditions demanded isothermal treatment at temperatures considerably higher.

## I. REACTION MECHANISM

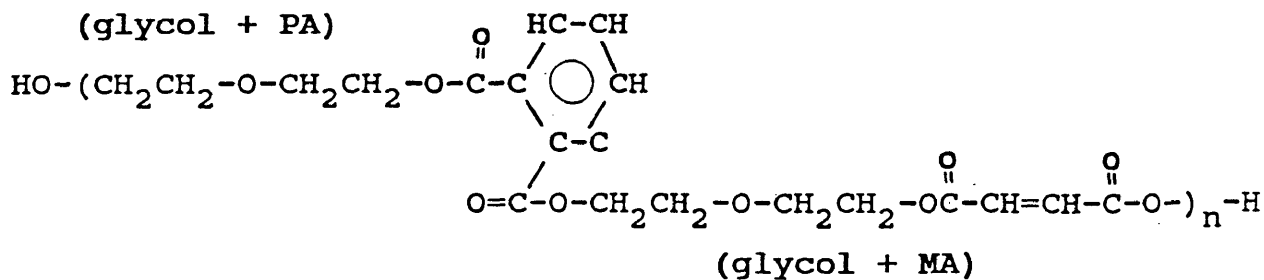
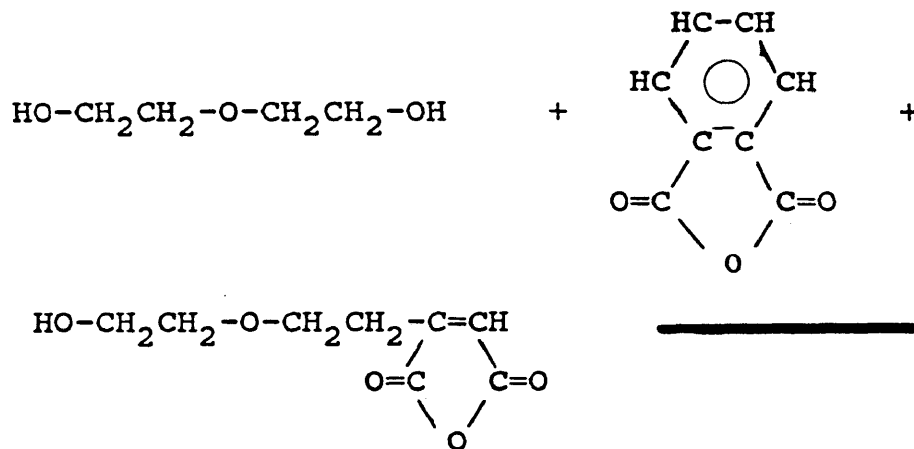
## A. Maleic anhydride isomerizes to trans-fumarate



## B. Glycol reacts with maleic anhydride

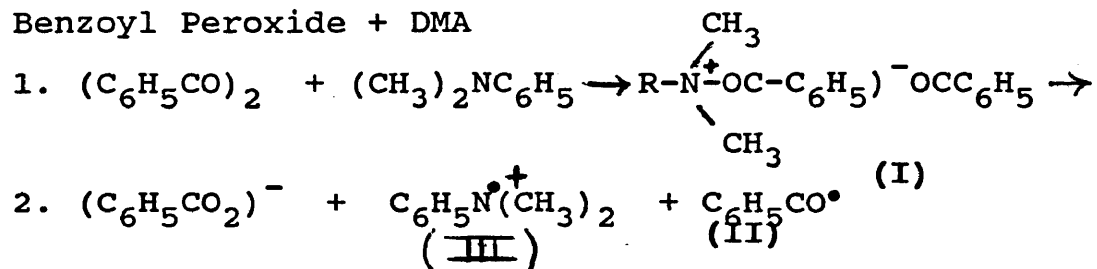


## C. Phthalic anhydride may also react with hydroxyl groups of glycol

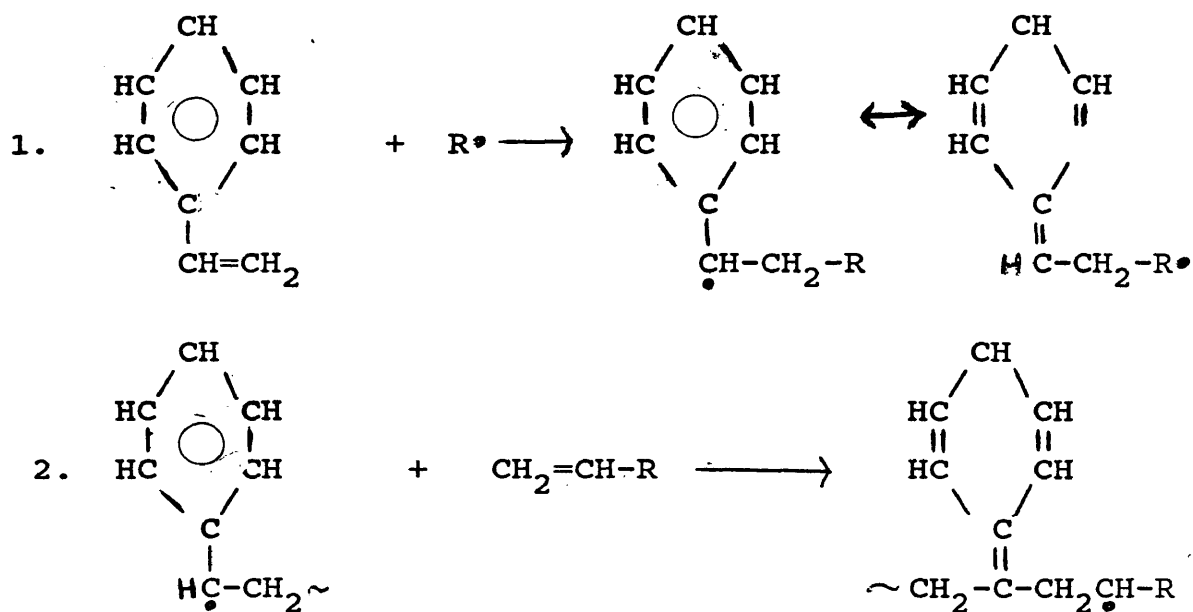


## II. FREE RADICAL FORMATION

### A. Benzoyl Peroxide + DMA

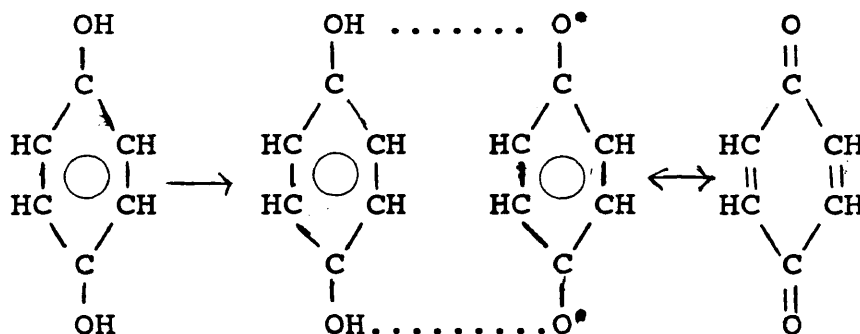


### B. Styrene



The styrene radical attacks at the double bond of the maleic anhydride in the unsaturated polymer chain or other styrene molecules.

### III. Free Radical Scavengers : example, benzoquinone

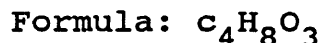


The resin used in this study is a general purpose orthophthalic polyester resin. The components of the system are listed below:

A. 98.75% by weight resin as received:

1. Dibasic Acid

a. Diethylene Glycol (DEG)



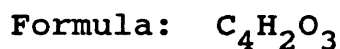
b. Polyglycol (PG)

Formula:

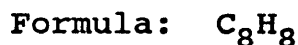
2. Phthalic Anhydride (PA)



3. Unsaturated acid anhydride: Maleic Anhydride (MA)

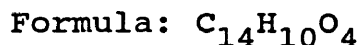


4. Diluent and Crosslinker: Styrene



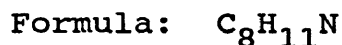
B. 1.00% by Weight Initiator

Initiator: Benzoyl Peroxide (BP)



C. 0.25% by Weight Promoter

Promoter: N,N-dimethyl Aniline (DMA)



The composition of the resin as received is 60/40 molar ratio of PA/MA; 84 mole % PG and 22 mole % DEG based on a ratio of 100 mole % dibasic acid. The mole% ratio of styrene to the total moles of styrene and maleic anhydride is 70% ( $ST/(MA+ST)=70\%$ ).

## REFERENCES FOR CHAPTER I

1. "Polyesters, Unsaturated," Encyclopedia of Chemical Technology, 1982 ed.
2. "Polyesters, Unsaturated," Encyclopedia of Polymer Science and Engineering, 1986 ed.
3. "Antioxidants," Encyclopedia of Polymer Science and Engineering, 1986 ed.
4. David H. Morton-Jones and John W. Willis, Polymer Products: Design, Materials and Processing (London: Chapman and Hall, 1986) 159-169.
5. Chanda Manes and Salel K. Roy, Plastics Technology Handbook (New York: Marcel Dekker Inc., 1987).
6. Robson F. Storey, Dantiki Sudhakar and Melissa Hogue, "Tertiary Aromatic Amines as Cure Reaction Promoters for Unsaturated Polyester Resins: II Low Temperature Studies," Journal of Applied Polymer Science, 32 (1986), 4919.

## CHAPTER II: DIFFERENTIAL SCANNING CALORIMETRY

### A. THEORY OF INSTRUMENTATION

Understanding the kinetics of polymerization is crucial to the precision of processing parts. Much research has been invested to develop manageable and realistic equations which describe the chemical reaction of thermosetting resins. While most research has focused on epoxy and phenolic systems, unsaturated polyester resins are being studied more closely as their industrial consumption increases.

The differential scanning calorimeter (DSC) is used nearly universally in evaluating the unsaturated polyester resin. Its operation will now be discussed.

The DSC compares the heat flow into and out of the sample against an inert reference; both sample and reference are maintained at the same temperature by independently operated sensors within both chambers. As the measurement is a power difference ( $J/s=Watts$ ), there is no need to know the thermal resistance to heat flow. This allows for the enthalpy of a change in state or progress of a chemical reaction to be easily calculated.

$$\text{Power}=J/\text{sec}$$

$$\text{Enthalpy}=J/g= \text{Power output}*\text{time}/\text{sample weight}$$

If the material absorbs heat from its surroundings, power is

supplied to the sample chamber. The corresponding endotherm is recorded. If the material gives off heat, the power will be reduced to equilibrate the temperatures of the two chambers.

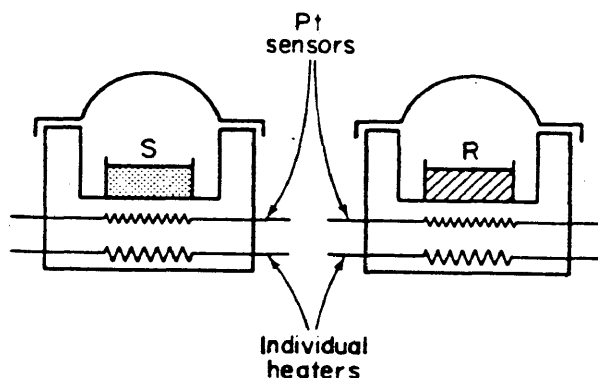


Illustration 1

Since styrene reacts with maleic anhydride, the unsaturation of the polyester molecule, to produce heat, the isothermal data is exothermic. (5,6). The power output is a direct measure of the heat generated or absorbed by the reacting system. The extent of the reaction,  $\alpha$ , is then easily calculated by determining the enthalpy at a given reaction time and dividing it by the total enthalpy.

$$\alpha = H_t / H_{tot}$$

The instantaneous change in the enthalpy is also proportional to the rate of reaction,  $dH/dt$ .

$$d\alpha/dt = \frac{dH/dt}{H_{tot}}$$

where  $H_{tot}$  is the enthalpy of the isothermal reaction plus

the residual enthalpy due to incomplete cure.

$$H_{\text{tot}} = H_{\text{iso}} + H_{\text{res}}$$

Isothermal cures are characterized by two transitions: gelation and vitrification. Gelation marks the transition from a liquid state to a rubbery, elastic state due to infinite crosslinking of polymer chains. The polymer does not flow (has high modulus) and, hence, is not processable beyond this point. Gelation is dependent on the reaction mechanism- functionality, reactivity, stoichiometry-and occurs at constant degree of cure as long as the reaction mechanism is temperature independent. Vitrification marks the transition from a liquid or rubbery state to a glassy state as a result of molecular weight buildup; the polymer chains are essentially "frozen" into their configuration thereby ceasing the reaction.

Enns and Gillham (14) constructed a time-temperature-transition (TTT) diagram that depicts the influence and interplay of these transitions for thermosetting systems.  $Tg_0$  represents the glass transition temperature of an unreacted resin. At this characteristically low temperature, the molecules are constrained by weak dipolar forces- too weak to maintain most low molecular weight substances in a solid state; but on the macroscopic scale of most polymers , the magnitude of these forces is sufficient at low thermal energy to maintain a solid state. By increasing the thermal energy, these short range forces are overcome with time.  $Tg_{00}$  is the glass transition temperature of the completely cured resin. If  $Tg_0 < T_{\text{cure}} < Tg_{00}$ , then the reaction will shut

down before completion of cure due to vitrification. If  $T_g = T_{cure}$ , the glass transition temperature has increased to the isothermal cure temperature. Theoretically the lower the cure temperature, the lower the degree of cure at the glass transition as the thermal energy of the lower temperatures is insufficient to overcome forces and spur on the reaction.

A typical DSC trace is illustrated in figure 2.1. General features are the reaction onset (designated by A) and the primary peak in the exotherm or maximum rate of reaction (B). The secondary peak (C) is observed in all isothermal cures but is not understood at this point. This "shoulder" appears in data collected by Salla and Martin(15) but is neither reported nor discussed. There is some uncertainty concerning the origin of the maximum in the reaction curve (B). Lam(7) and Pusatcioglu (10) credit the autocatalytic effect but it has been questioned whether the effect is autocatalytic, diffusion controlled, or a combination of the two (7).

DSC Data File: 0212d  
 Sample Weight: 20.580 mg  
 Fri Feb 12 02:23:45 1988  
 aristech polyester

PERKIN-ELMER  
 7 Series Thermal Analysis System

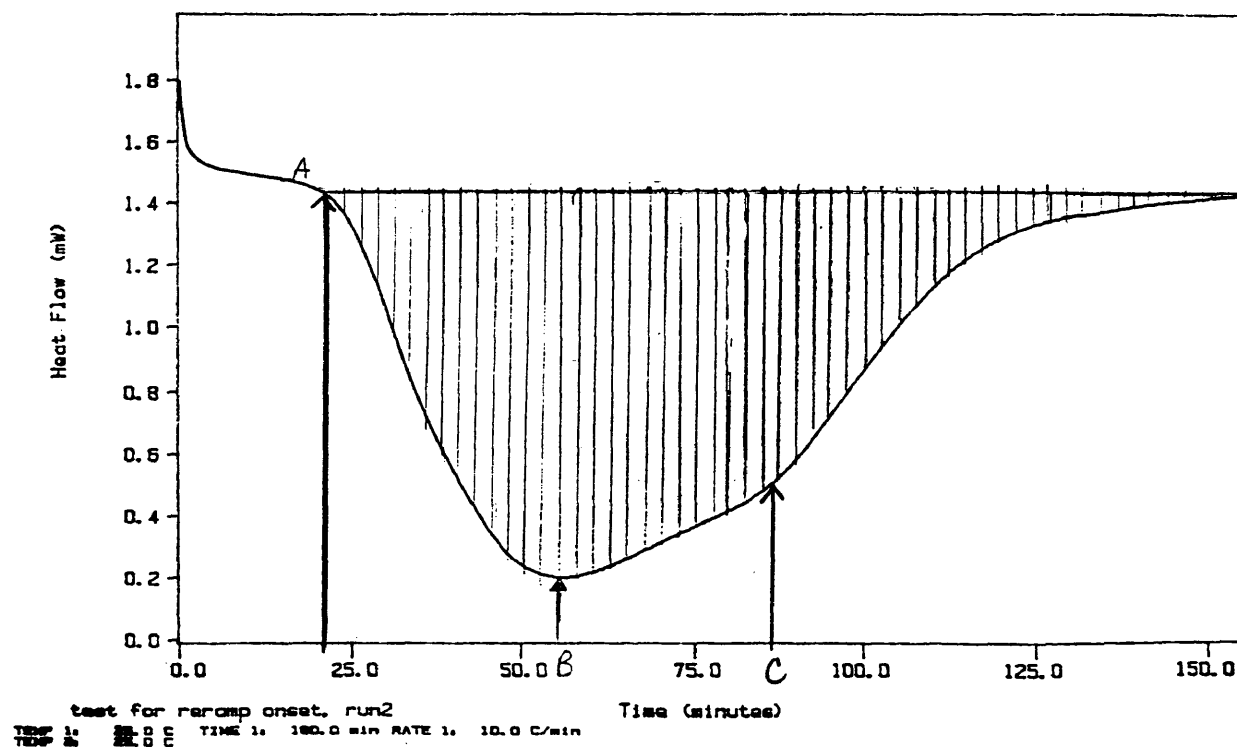
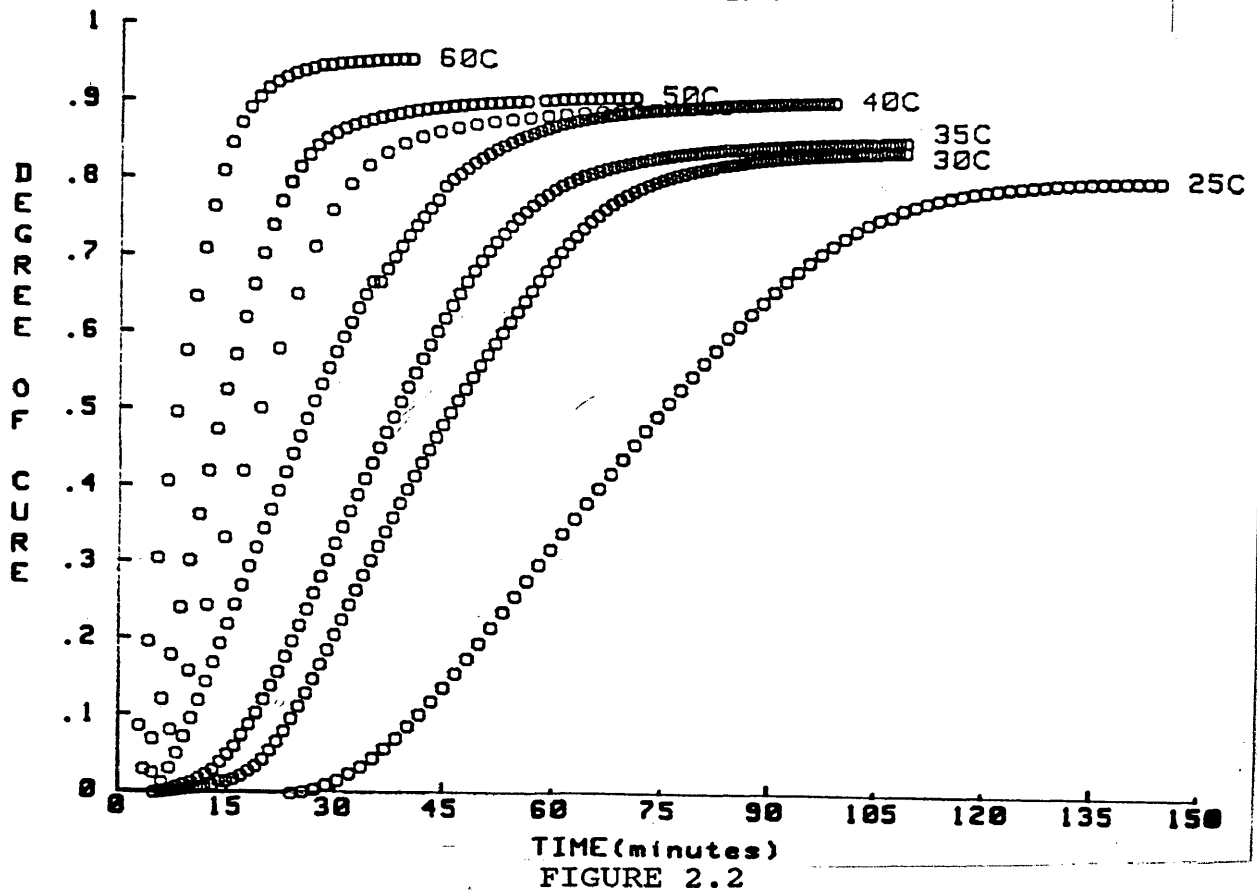


FIGURE 2.1



A complete picture of the cure as a function of time and temperature is provided in figure 2.2. The raw data for each of the isothermal runs is provided in Appendix A. It is seen that for higher temperatures the cure progresses more quickly and completely, as expected.

Figures 2.3 and 2.4 display reaction rates as a function of time (figure 2.3) and of  $\alpha$  (figure 2.4). It is evident, from figure 2.3 that a small difference in the temperature profoundly effects the reaction rate of the polyester resin. Figure 2.4 calls to attention the singular fact the maximum rate of the reaction for all temperatures occurs at approximately the same  $\alpha$ .

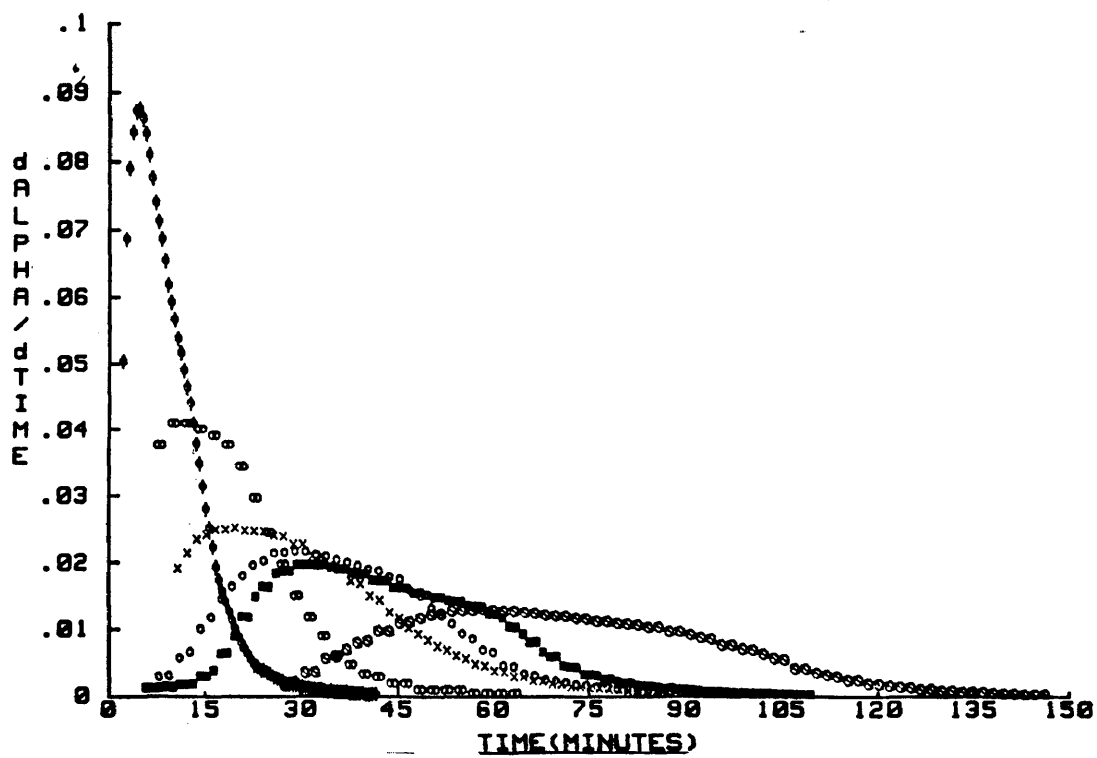
REACTION RATE AS A FUNCTION OF  $\alpha$ 

FIGURE 2.3

## REACTION RATE AS A FUNCTION OF ALPHA

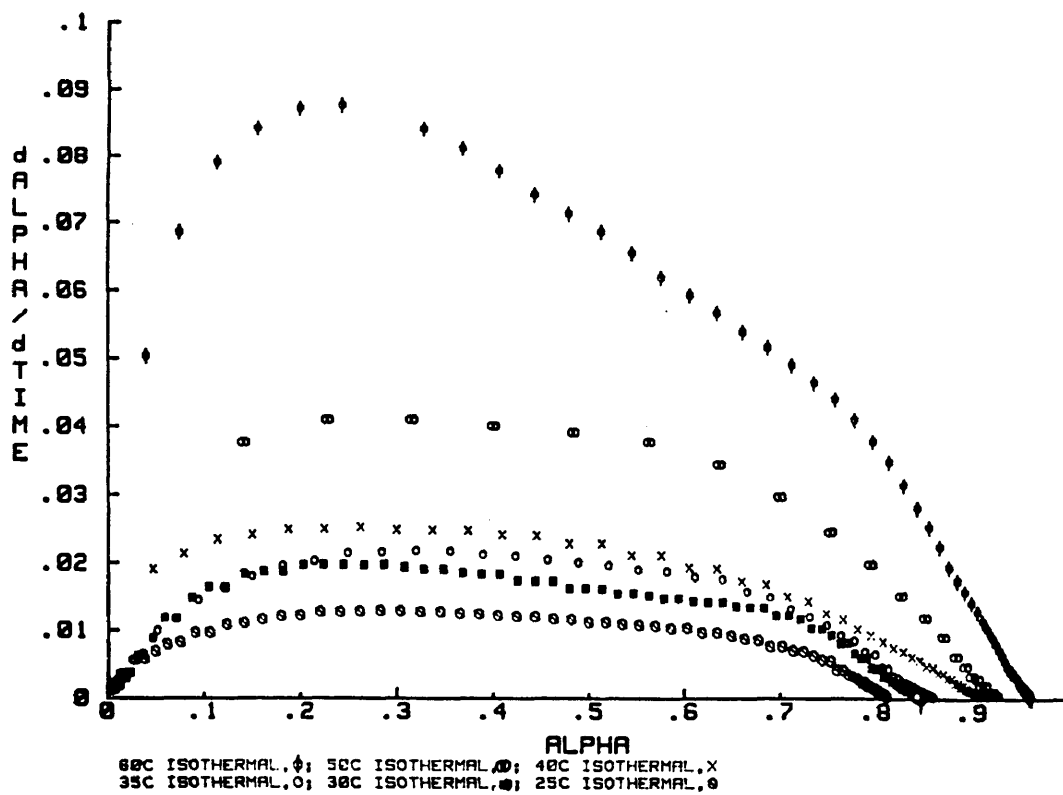


FIGURE 2.4

Several approaches, both mechanistic and phenomenological, have been tested to understand the cure kinetics. Emphasis, here, will be on the latter and efforts to fit Kamal's equation (3)

$$1 \quad d\alpha/dt = (k_0 + k_1 \alpha^m)(1-\alpha)^n$$

Lam, along with most of his contemporaries, simplifies the above equation by assuming that  $m$  and  $n$  sum to 2 and that  $k_0$  is negligible. (7)

$$2 \quad d\alpha/dt = (k_1 \alpha^m)(1-\alpha)^n$$

The data collected from the DSC scans will be analyzed using three different means to determine the kinetic parameters  $m$ ,  $n$ , and  $k$ . Comparison of the resulting fits follow after discussion of the three methods for treating the data.

## EXPERIMENTAL

All experiments were conducted on the unsaturated polyester resin provided by Aristech Chemical Corporation. A mixture consisting of 98.75% by weight of the resin, 1.00% benzoyl peroxide, and 0.25% DMA was stirred for three minutes in a nitrogen atmosphere.

For DSC scans, a portion of the resin was transferred to preweighed aluminum pans, sealed hermetically under a nitrogen environment, and placed in the DSC chamber which had been preheated to the desired temperature. The isothermal cure continued until the curve returned to the original baseline. At this point the resin was quenched to room temperature and ramped at  $10^\circ$  or  $40^\circ$  per minute to

200°C to determine the residual heat of the reaction. (The residual was the same in either case.) Sample size ranged between 15 and 20 mg. To reduce the risk of introducing oxygen into the system and hence oxygen inhibition, larger sample size was necessary.

## B. KINETIC EVALUATION

### 1. LAM ANALYSIS

Patrick Lam (7) offers a simplified technique for evaluating the kinetic expression suggested by Kamal and co-workers (equation 1).

$$1. \quad d(\alpha)/dt = k(\alpha)^m (1-\alpha)^n$$

The standard interpretation of the rate constant  $k$ , where  $A$  is the pre-exponential factor,  $E$  is the activation energy, and  $T$  is the absolute temperature:

$$2. \quad k = A \exp(-E/RT)$$

Limiting the sum of the exponents, based on the findings or restrictions of previous researchers(4-9), provides easy analysis of the maximum rate of cure and the degree of cure at this maximum cure rate by the scheme offered below.

$$3. \quad m + n = 2$$

Differentiating equation 1 with respect to  $\alpha$  and setting the value equal to zero provides the solution to finding the value of  $\alpha_{\max}$ .

$$4. \quad \alpha_{\max} = m/2$$

Substituting equation 3 into equation 1, dividing both sides by  $\alpha^2$  and rearranging yields equation 5.

$$5. \quad \ln[d(\alpha)/dt * 1/\alpha^2] = \ln k + (n * \ln [(1-\alpha)/\alpha])$$

Using the values of  $k$ ,  $m$  and  $n$  obtained from DSC thermograms, the values of  $k$ ,  $m$  and  $n$  can be determined from the above equation. A plot of the left hand side of equation 5 versus  $\ln[(1-\alpha)/\alpha]$  provides the slope  $n$  and intercept  $\ln(k)$ . (Review figures 5-10 where  $X$ = degree of cure) The parameter  $m$  is dependent on  $n$  through equation 3.

Other variables can be explored. The theoretical values of the maximum cure rate and the time required to reach this maximum are given below.

$$6. \quad d(\alpha/dt)_{\max} = k * (m/2)^m * (n/2)^n$$

$$7. \quad t_{\max} = k * (n-1)^{-1} * (m/n)^{(n-1)}$$

The calculated values of these parameters are listed in the table below. Discussion of these findings will be delayed until the next chapter when these results will be compared to those of other methods.

TABLE 2.1 (figures 11-16)

TEMP	$k_0$	$m$	$n$
60	.328	.86	1.14
50	.187	.79	1.21
40	.095	.66	1.34
35	.081	.76	1.24
30	.076	.76	1.24
25	.049	.59	1.41

## ARISTECH POLYESTER RESIN: 25 C

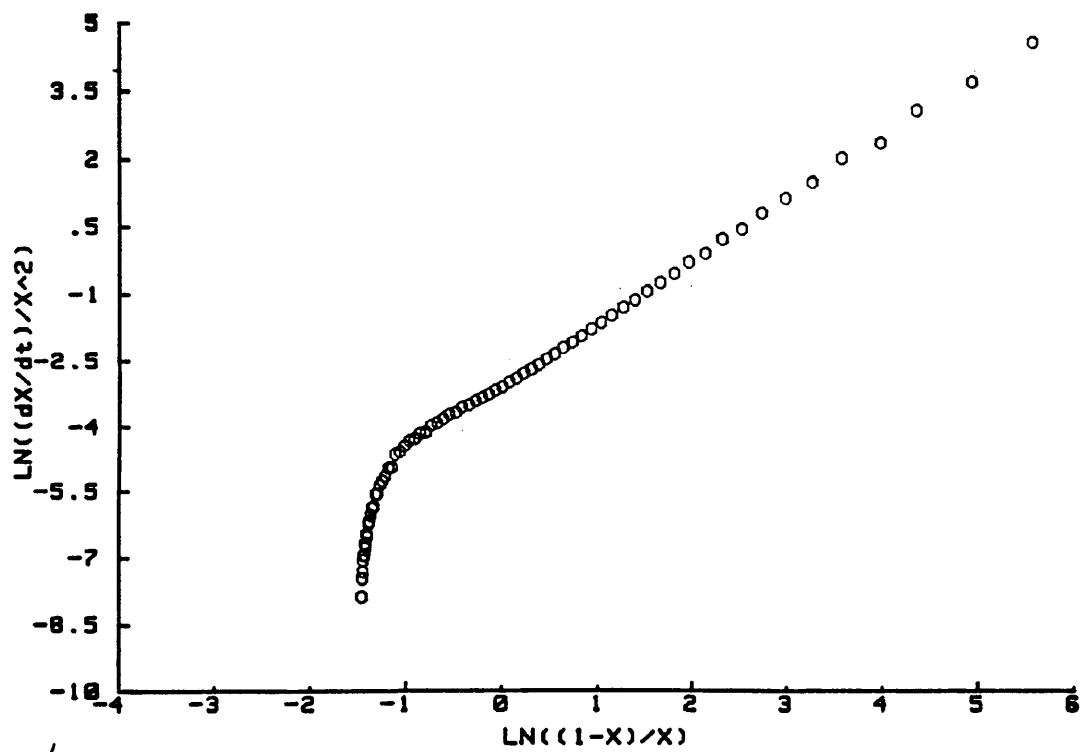


FIGURE 2.5

## ARISTECH POLYESTER RESIN: 30 C

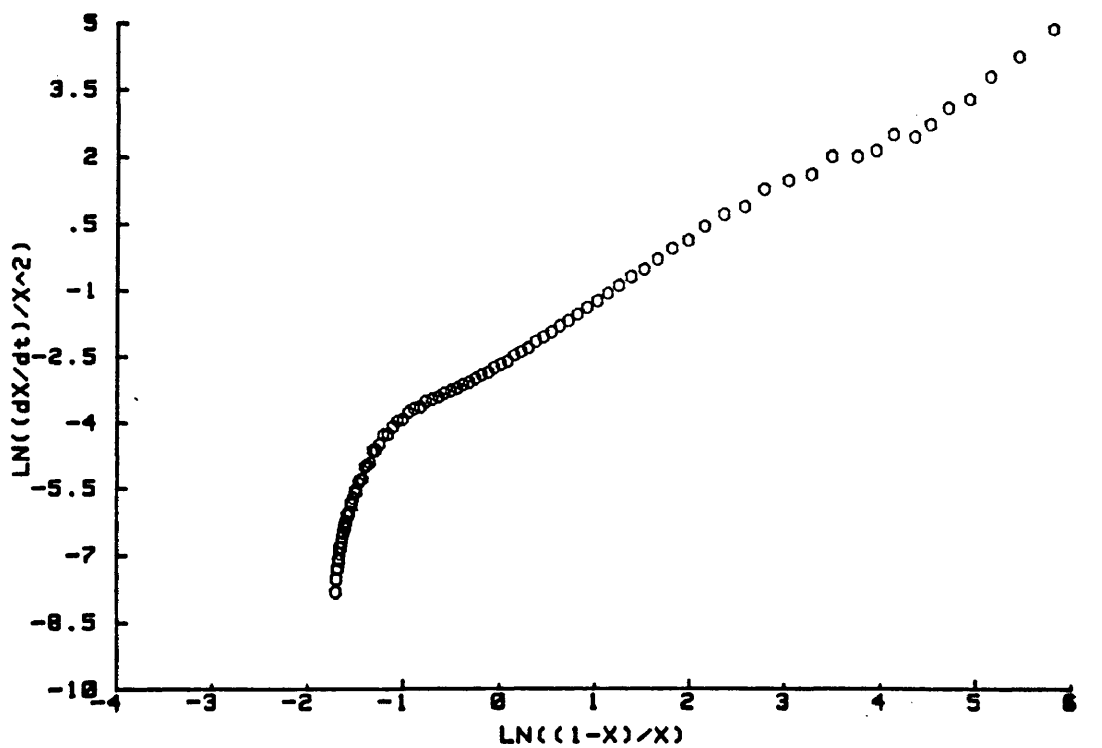


FIGURE 2.6

## ARISTECH POLYESTER RESIN: 35 C

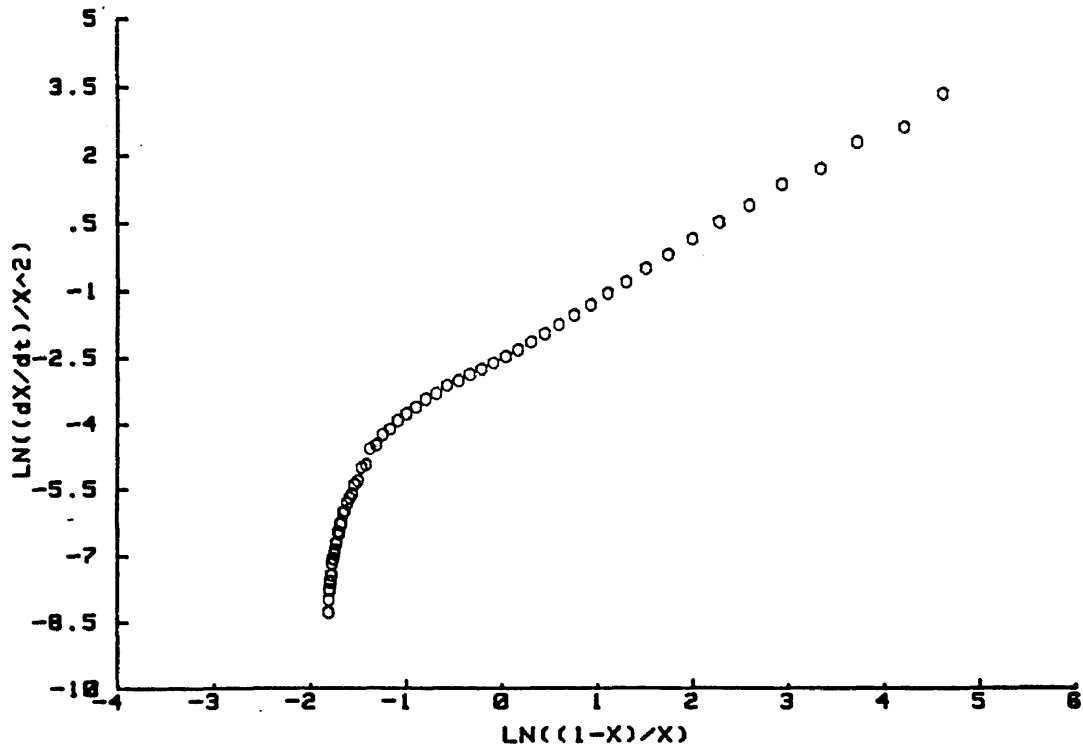


FIGURE 2.7

## ARISTECH POLYESTER RESIN: 40 C

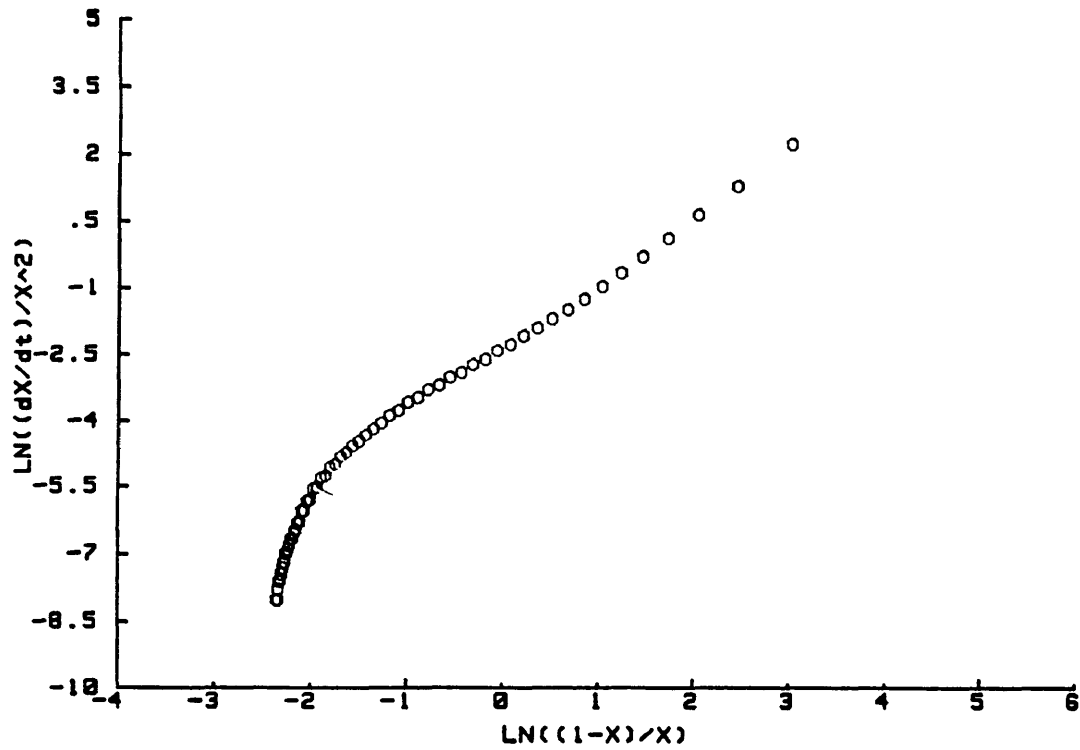
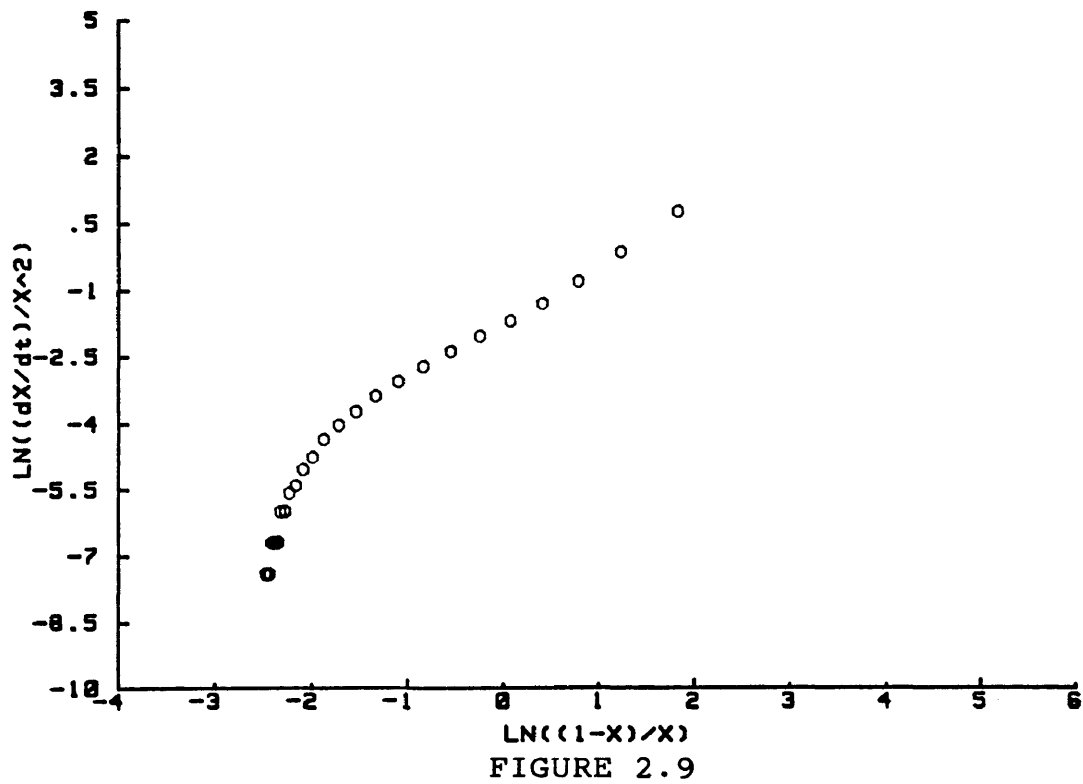
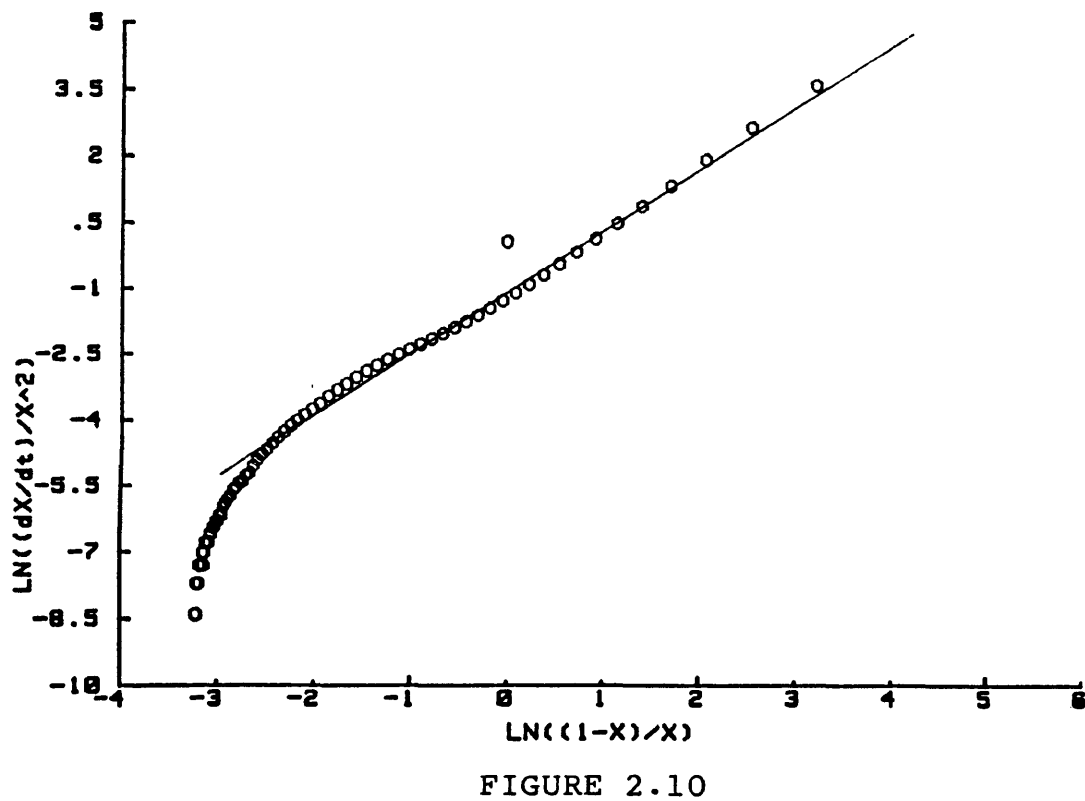


FIGURE 2.8

## ARISTECH POLYESTER RESIN: 50 C



## ARISTECH POLYESTER RESIN: 60 C



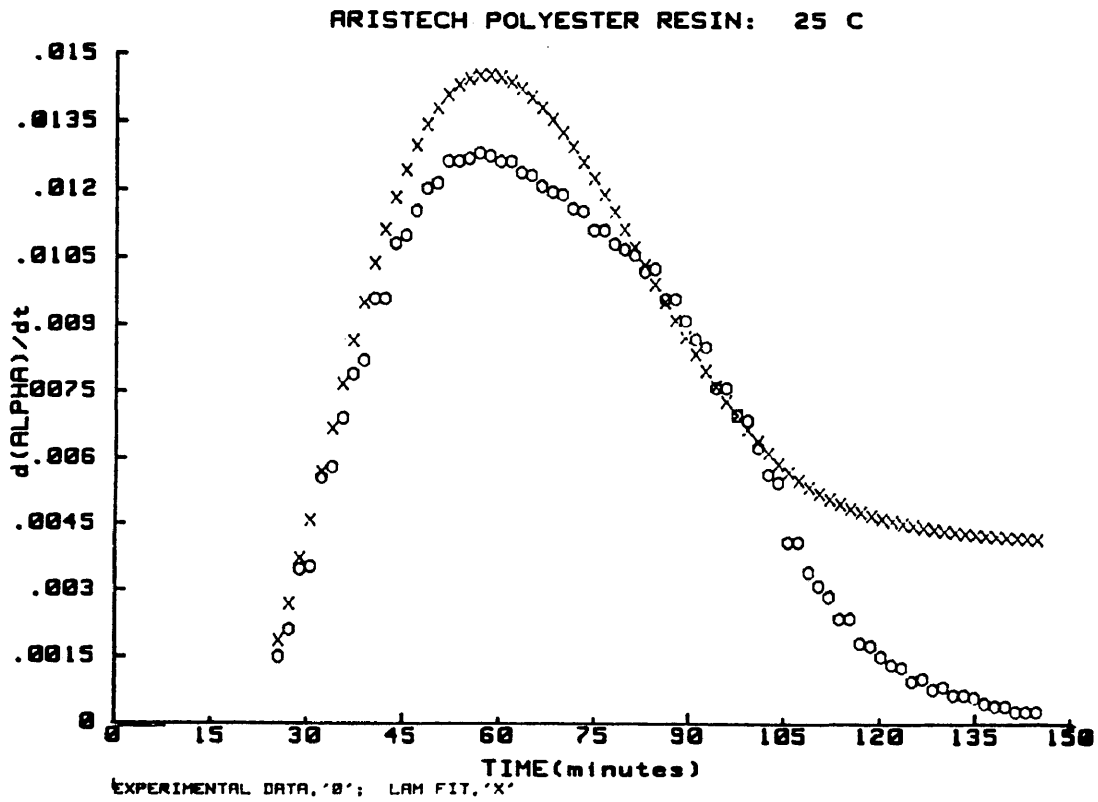


FIGURE 2.11

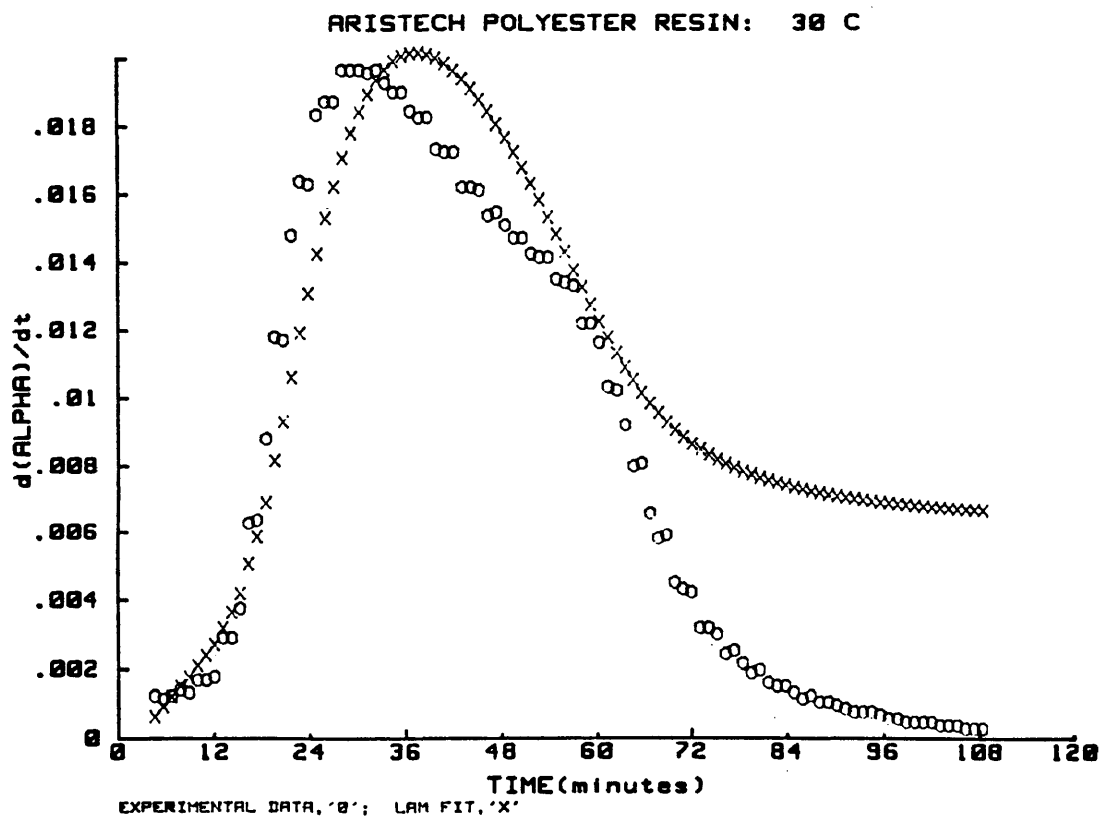


FIGURE 2.12

ARISTECH POLYESTER RESIN: 35 C

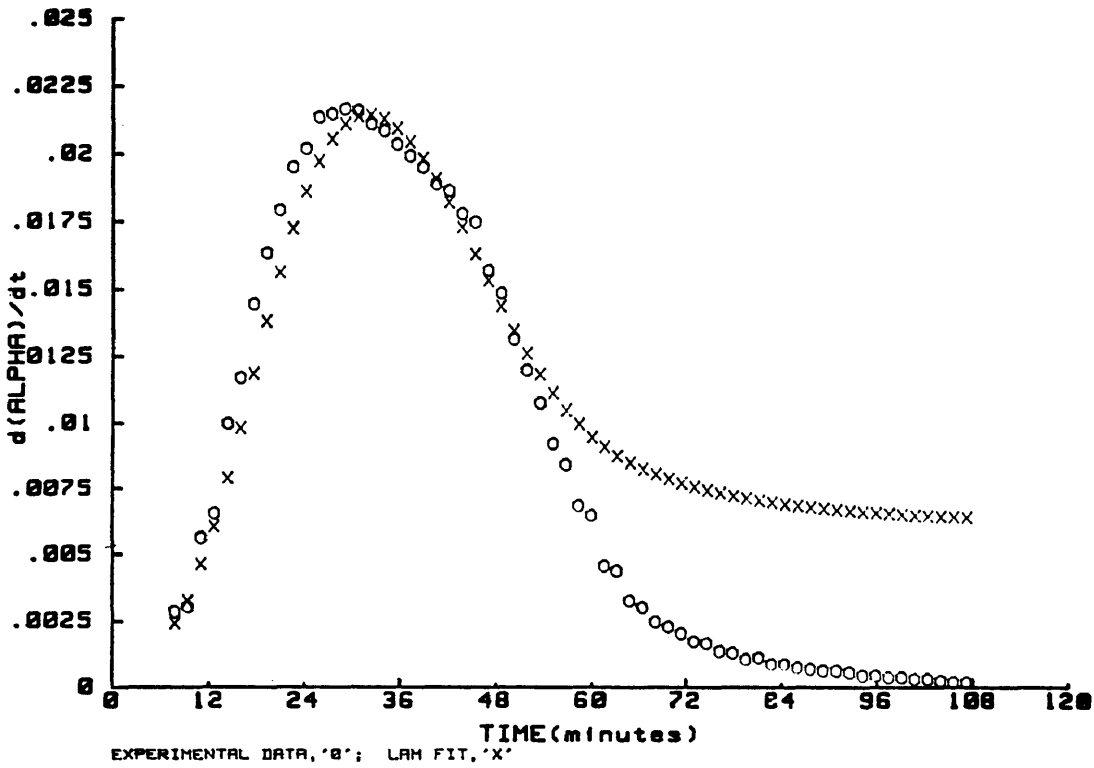


FIGURE 2.13

ARISTECH POLYESTER RESIN: 40 C

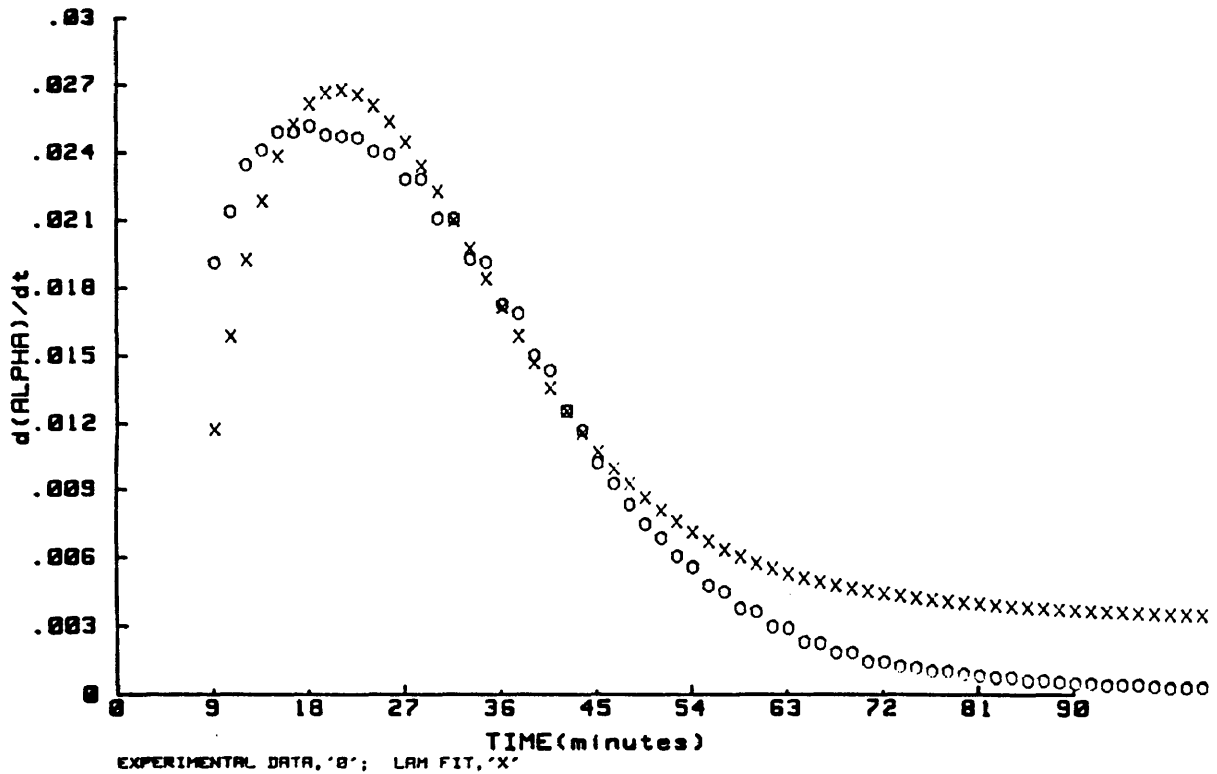


FIGURE 2.14

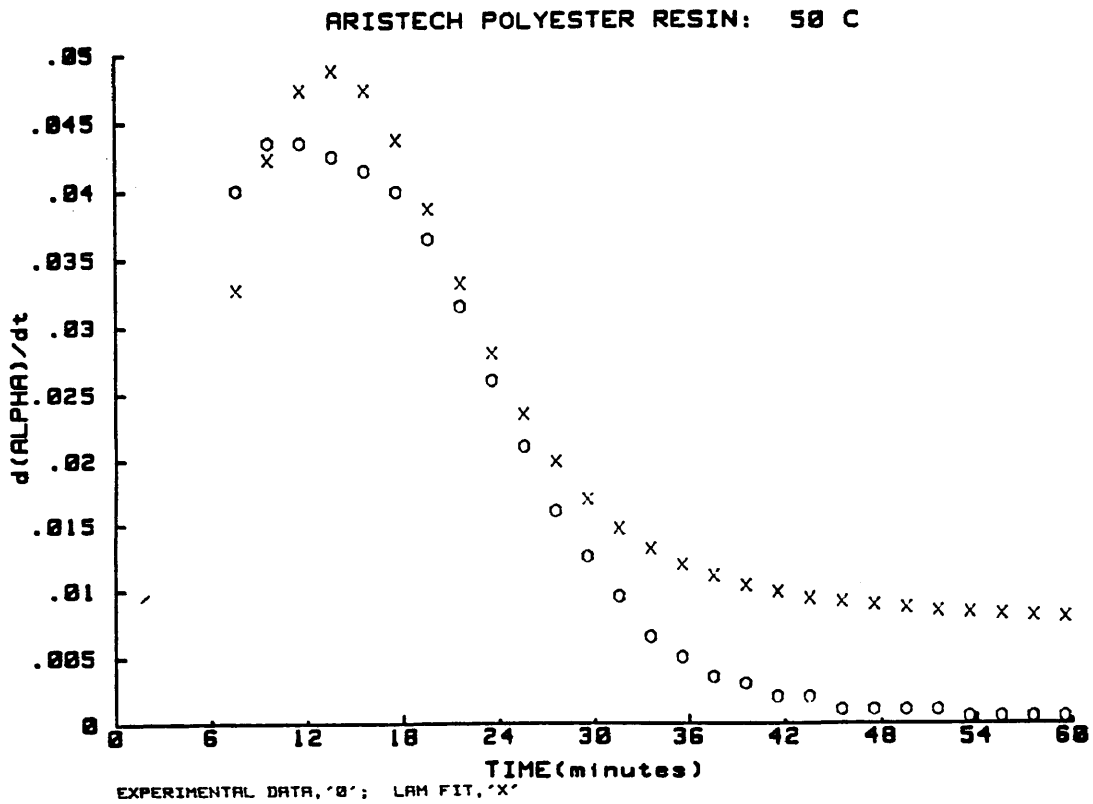


FIGURE 2.15

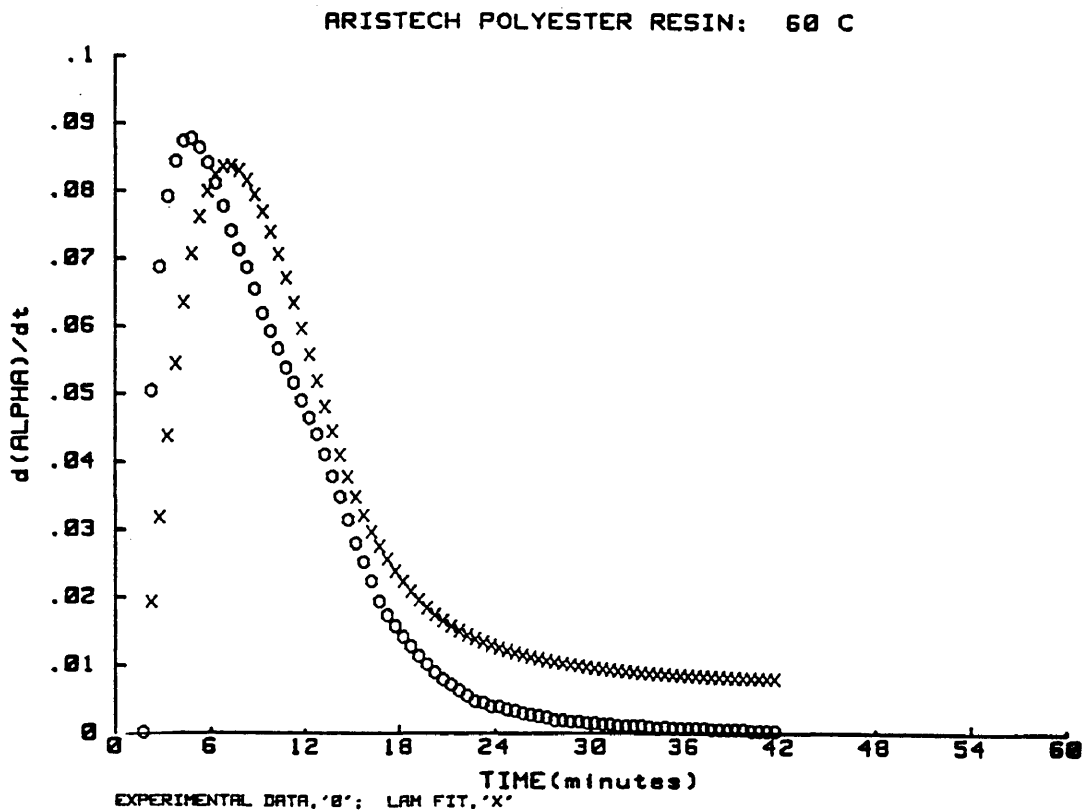


FIGURE 2.16

## 2. LEAST SQUARE FIT ANALYSIS

The data were fit to equation 1 using a least squares technique. A sample program is provided in Appendix D.

The degree of cure ( $\alpha$ ) and the rate of the change in      with respect to time were read into the program. The initial and final values of the parameters and the step function between the two were defined. Combinations of the four parameters were evaluated; the combination which yielded the smallest residual value was then iterated by small amounts until the residual converged (changed by less than  $10^{-8}$ ).

The values determined in the Lam analysis provided an initial estimate for the parameters. While  $k_0$  was previously ignored, it was retained in the original fit (table 2) to determine if it indeed was significant. The range of the values was expanded as there did not seem to be any theoretical reasoning for restricting the sum of m and n to 2. Next, the equation was evaluated with  $k_0=0$ . On the following page, two tables compare the fit with and without  $k_0$ . Table 3 reflects results from a fit with a restricted range and step size.

TABLE 2.2 (figures 17-22)

PARAMETERS:	$k_0$	$k_1$	$m$	$n$
RANGE:	0-.01	0-0.50	0-5.0	0-7.0
STEP SIZE:	.0015	.040	.30	.30

TEMP	$k_0$	$k_1$	$m$	$n$
60	.0142	.2225	.5059	1.1778
50	.0075	.2000	.9000	1.5000
40	.0144	.0994	1.0155	1.3978
35	.0015	.1200	.9000	1.8000
30	.000535	.1177	.9036	1.8106
25	.000452	.0371	.4995	1.5595

TABLE 2.3 (fig. 29-34)

PARAMS:	$k_1$	$m$	$n$
RANGE:	0-1.50	0-3.0	1-3.0
STEP :	0.025	0.100	0.100

TEMP	$k_1$	$m$	$n$
60	.320	.4020	1.4000
50	.1995	.8001	1.4982
40	.0900	.6000	1.4000
35	.1002	.7497	1.7239
30	.0600	.6000	1.2000
25	.0388	.3919	1.4717

TABLE 2.4 (fig. 23-28)

PARAMS:	$k_1$	$m$	$n$
RANGE:	0-1.5	0-5.0	0-7.0
STEP :	.05	.25	.25

TEMP	$k_1$	$m$	$n$
60	.2038	.4034	1.0951
50	.1995	.8001	1.4983
40	.0962	.6283	1.40
35	.1961	1.1052	2.19
25	.0993	.8029	2.3992

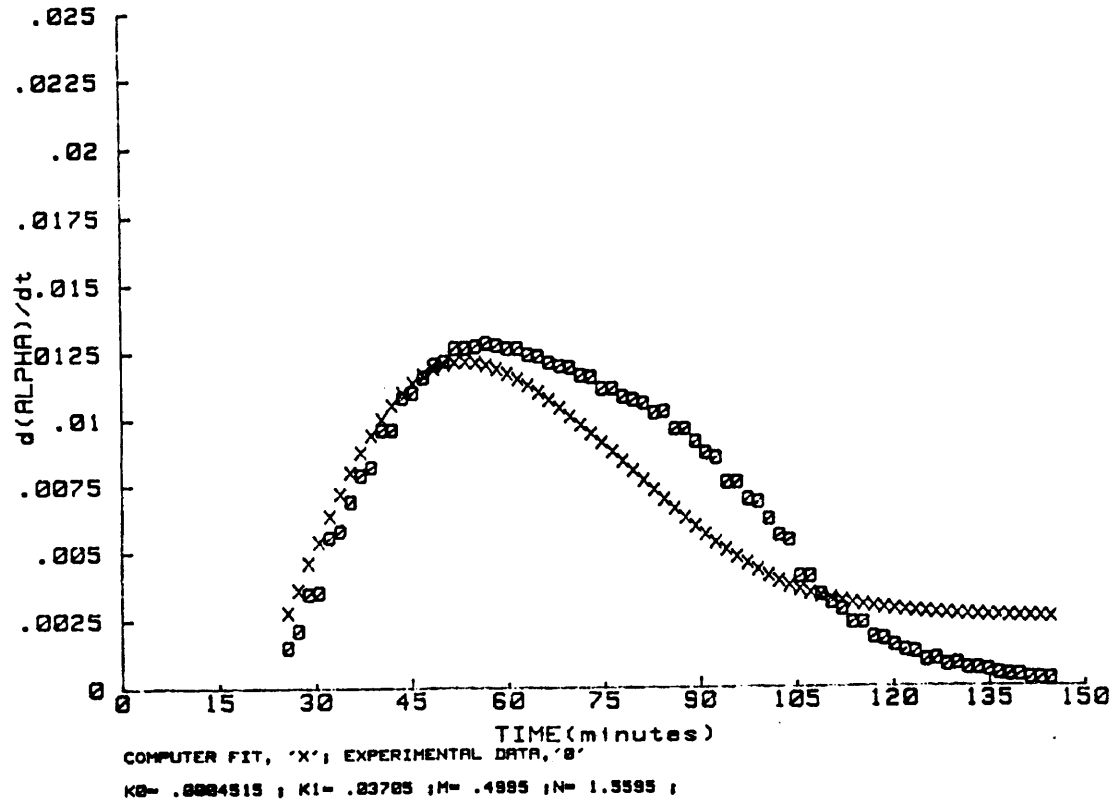


FIGURE 2.17

ARISTECH POLYESTER RESIN: 30 C

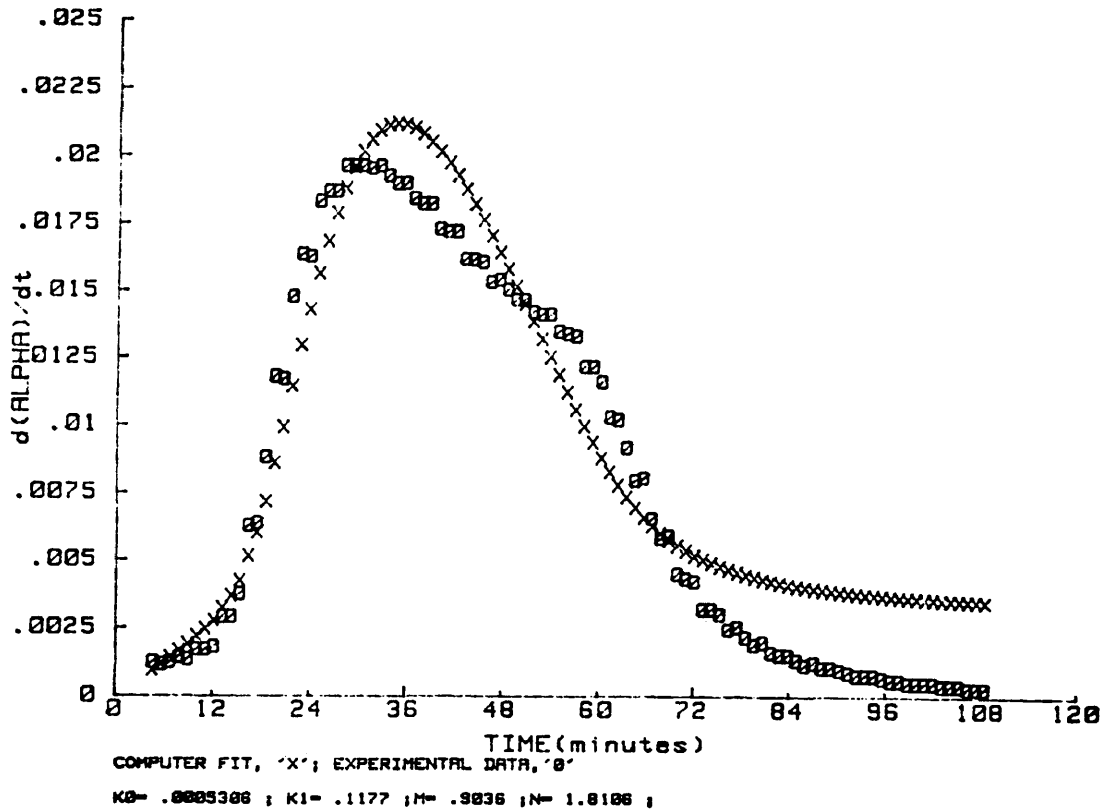


FIGURE 2.18

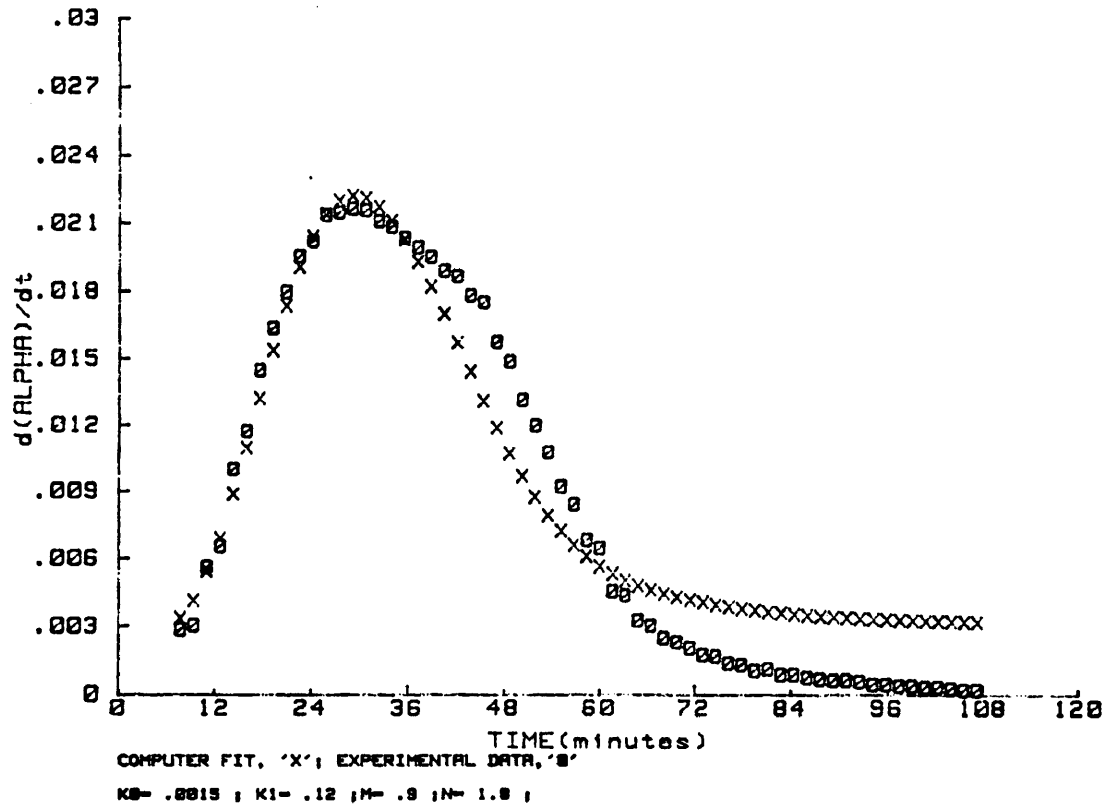


FIGURE 2.19

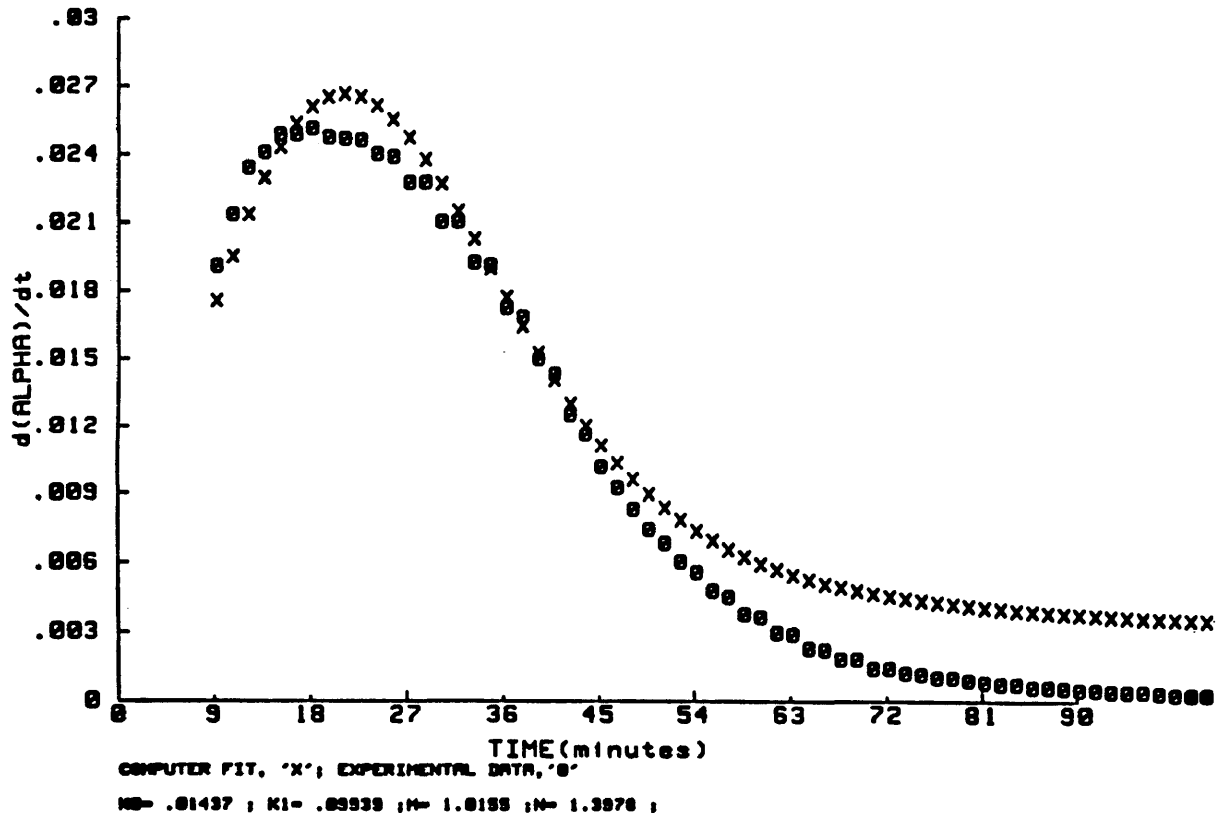


FIGURE 2.20

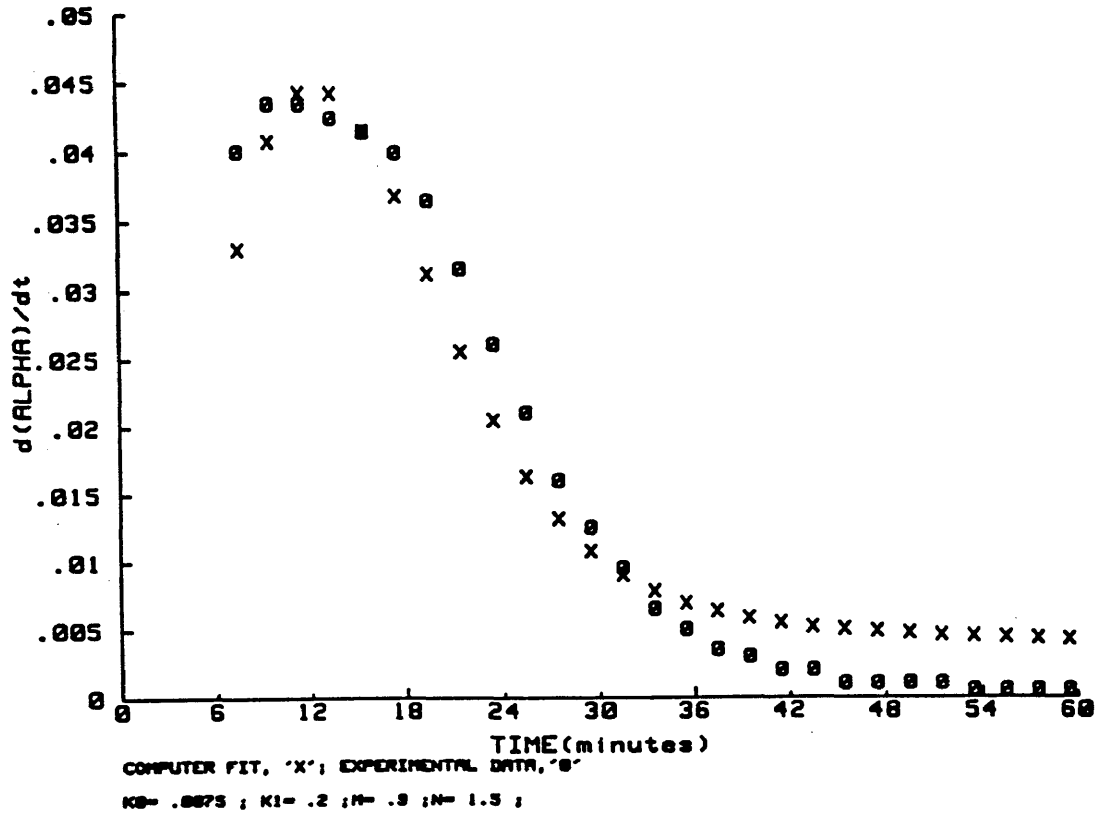


FIGURE 2.21

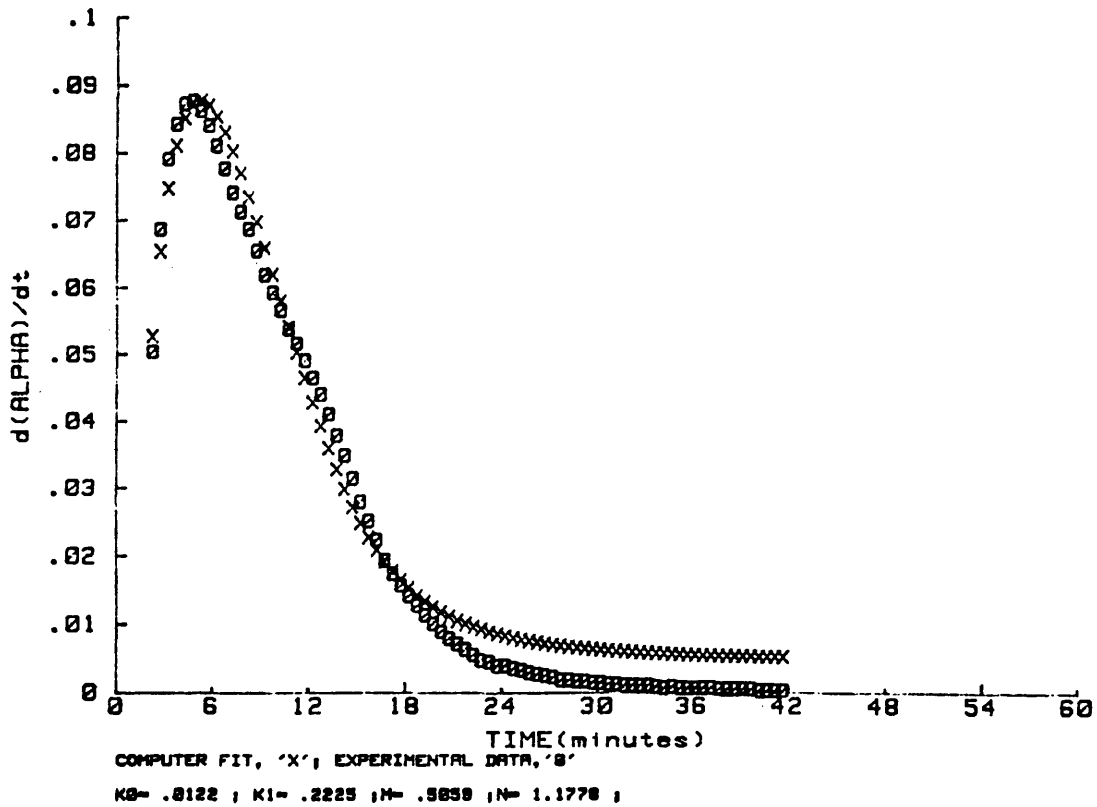


FIGURE 2.22

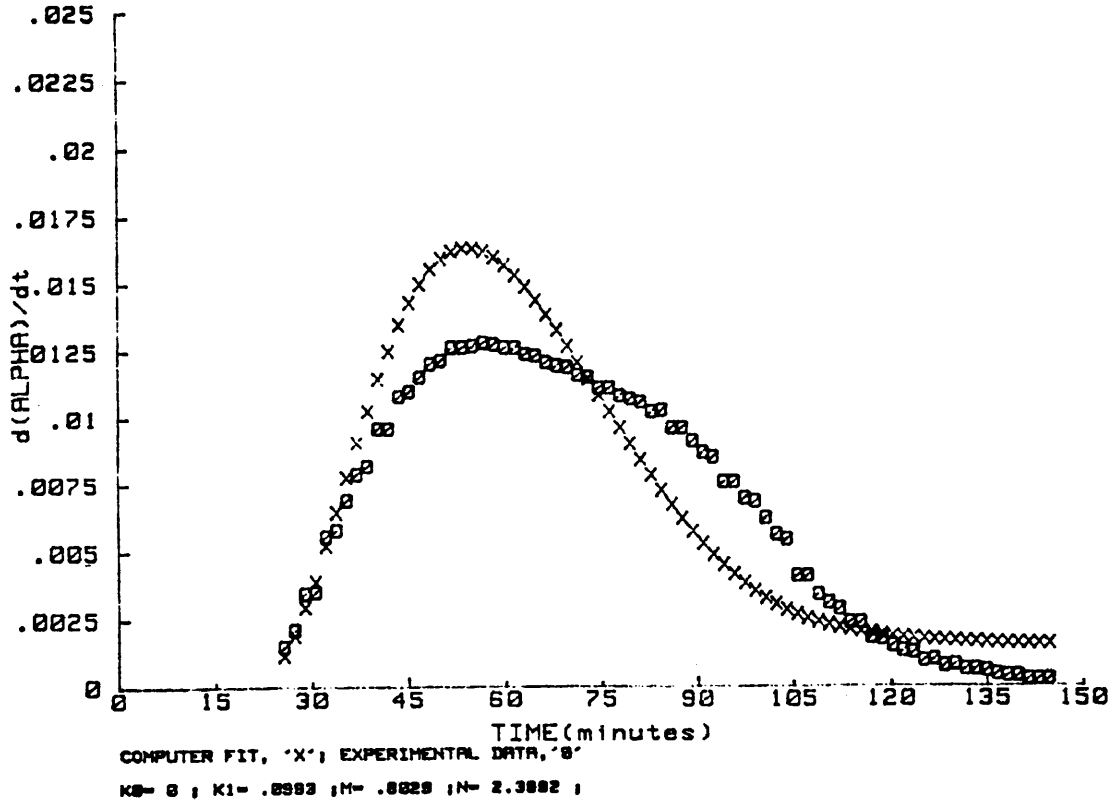


FIGURE 2.23

ARISTECH POLYESTER RESIN: 30 C

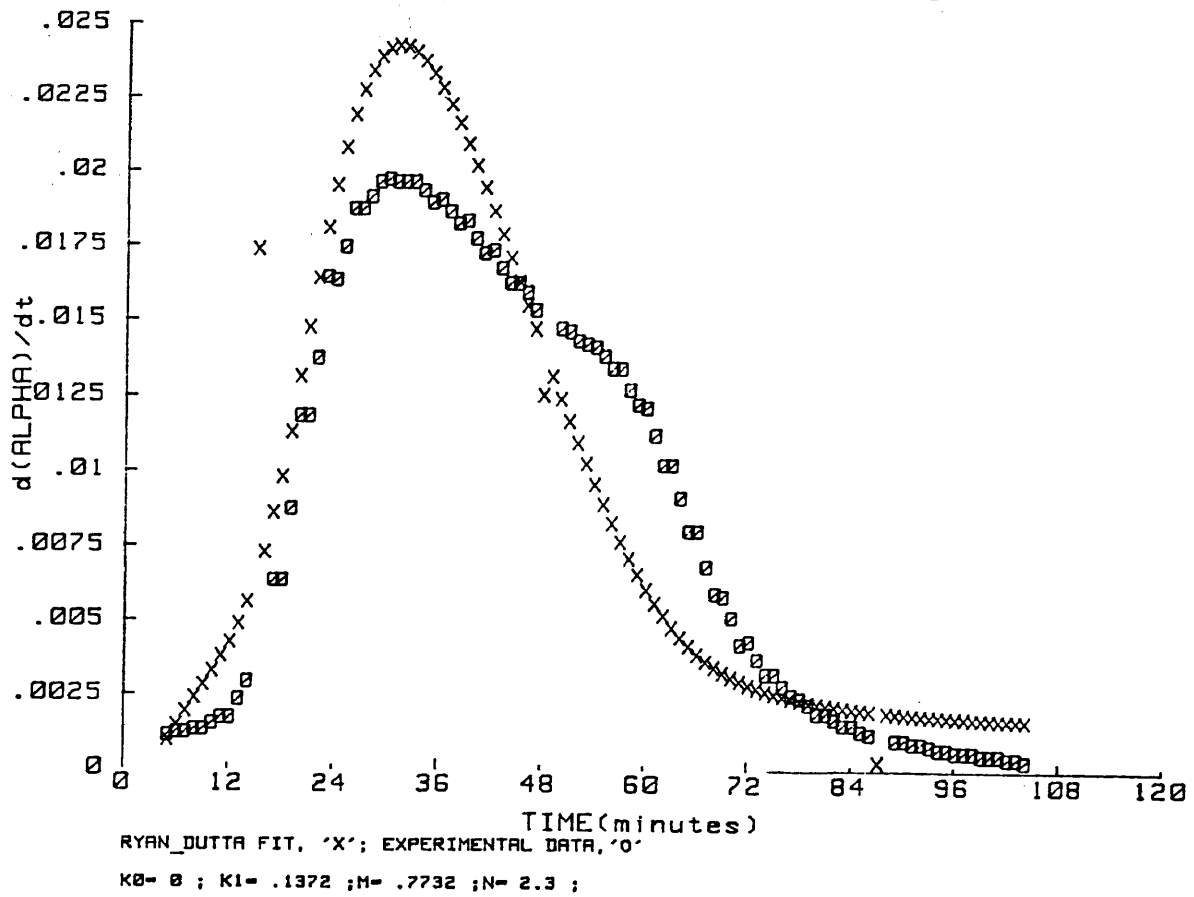
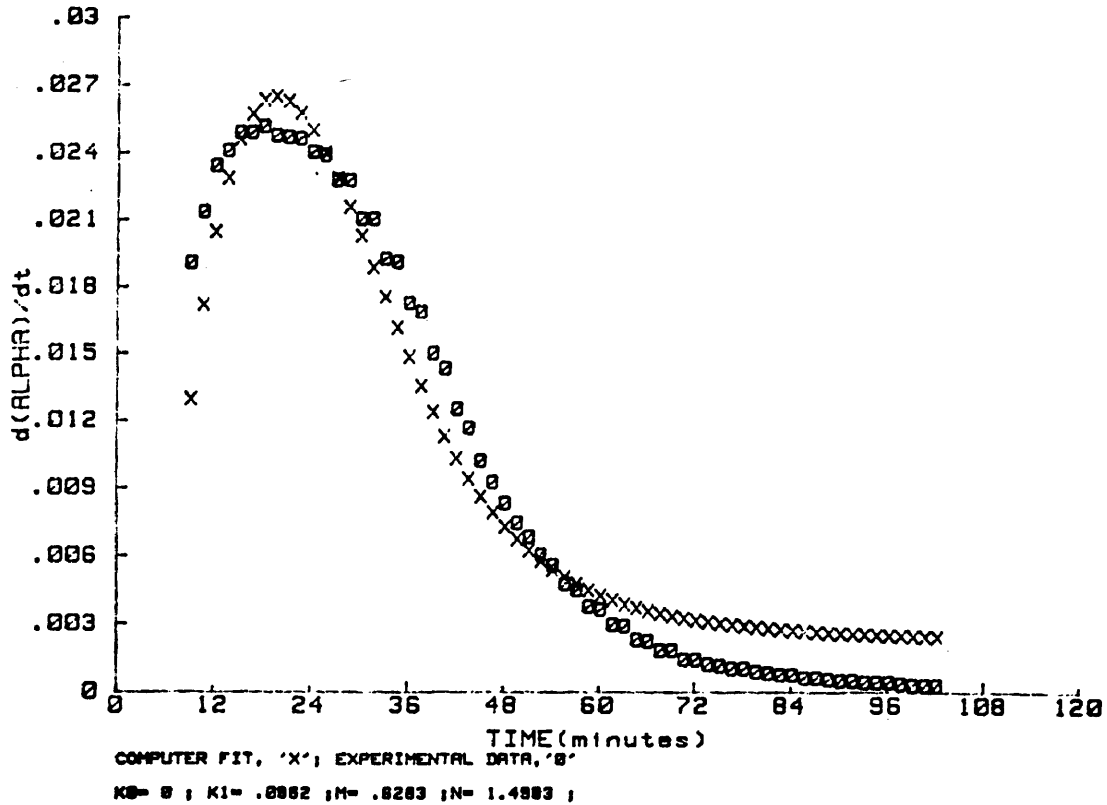
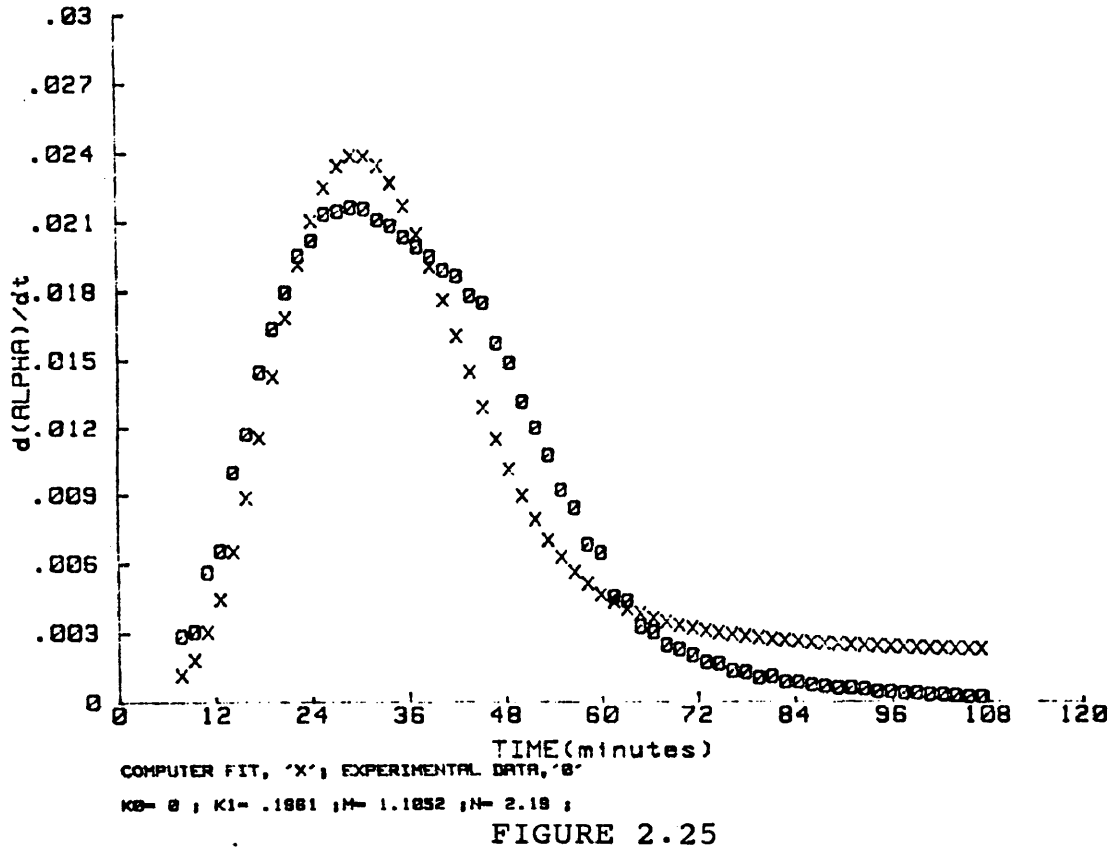


FIGURE 2.24



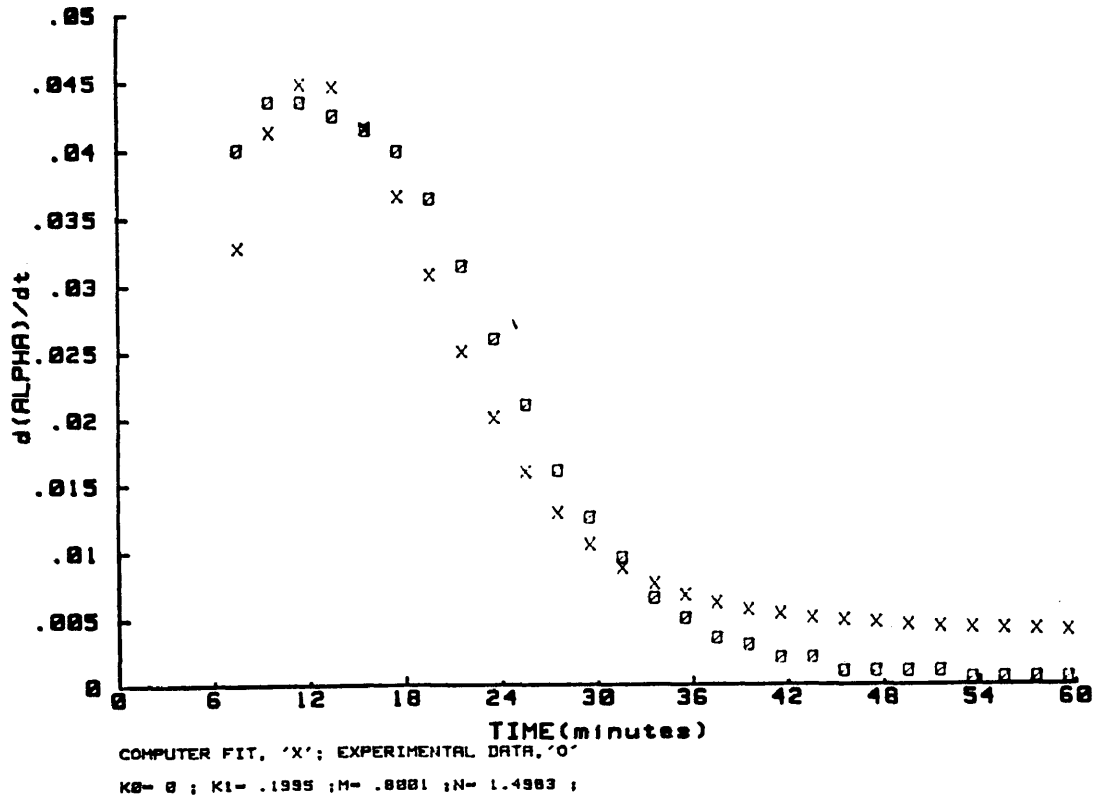


FIGURE 2.27

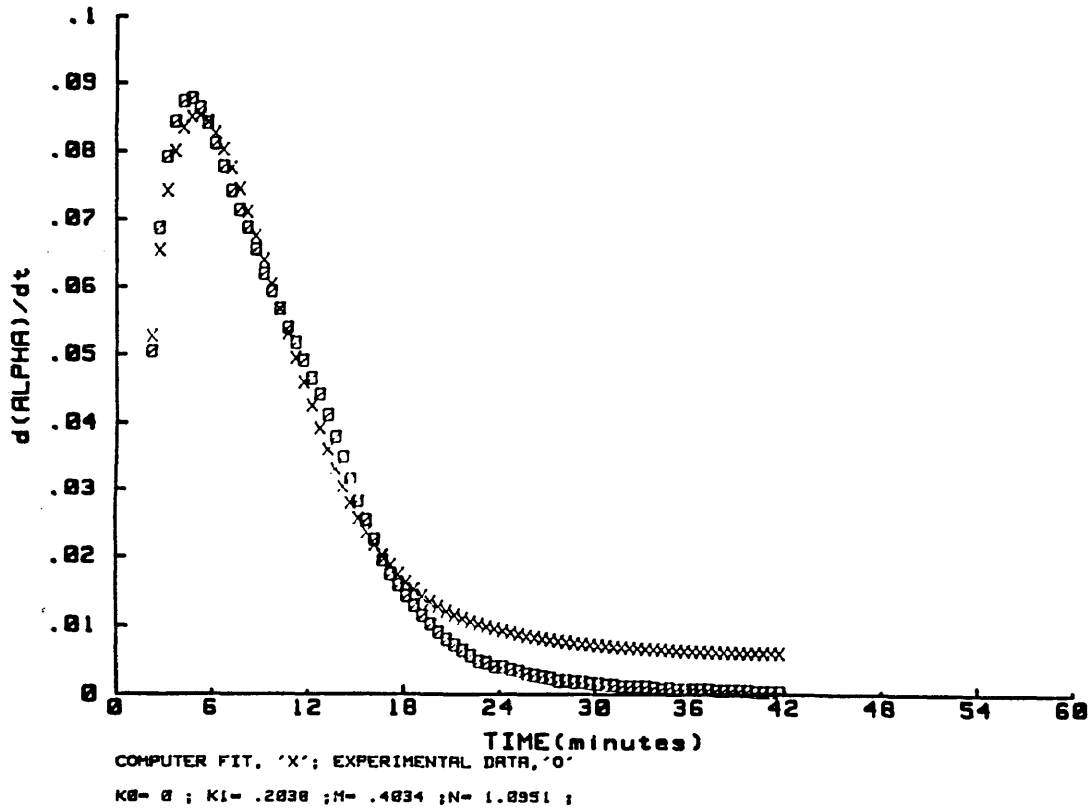


FIGURE 2.28

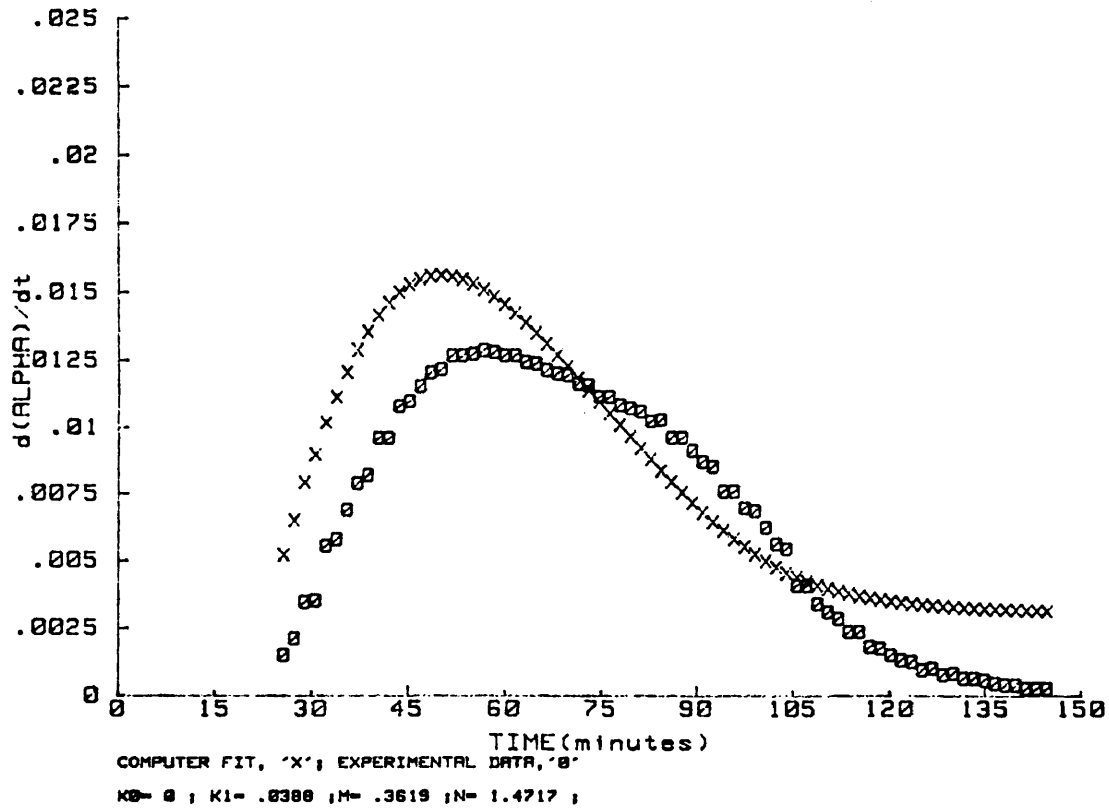


FIGURE 2.29

ARISTECH POLYESTER RESIN: 30 C

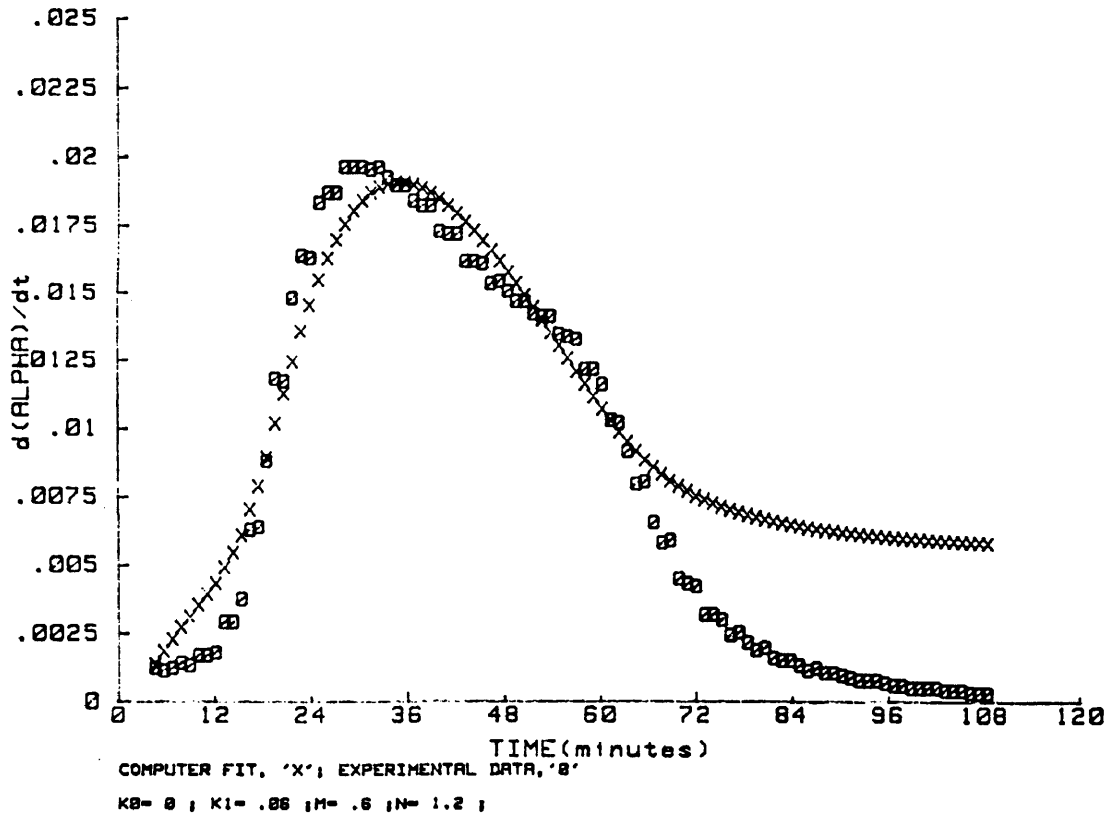


FIGURE 2.30

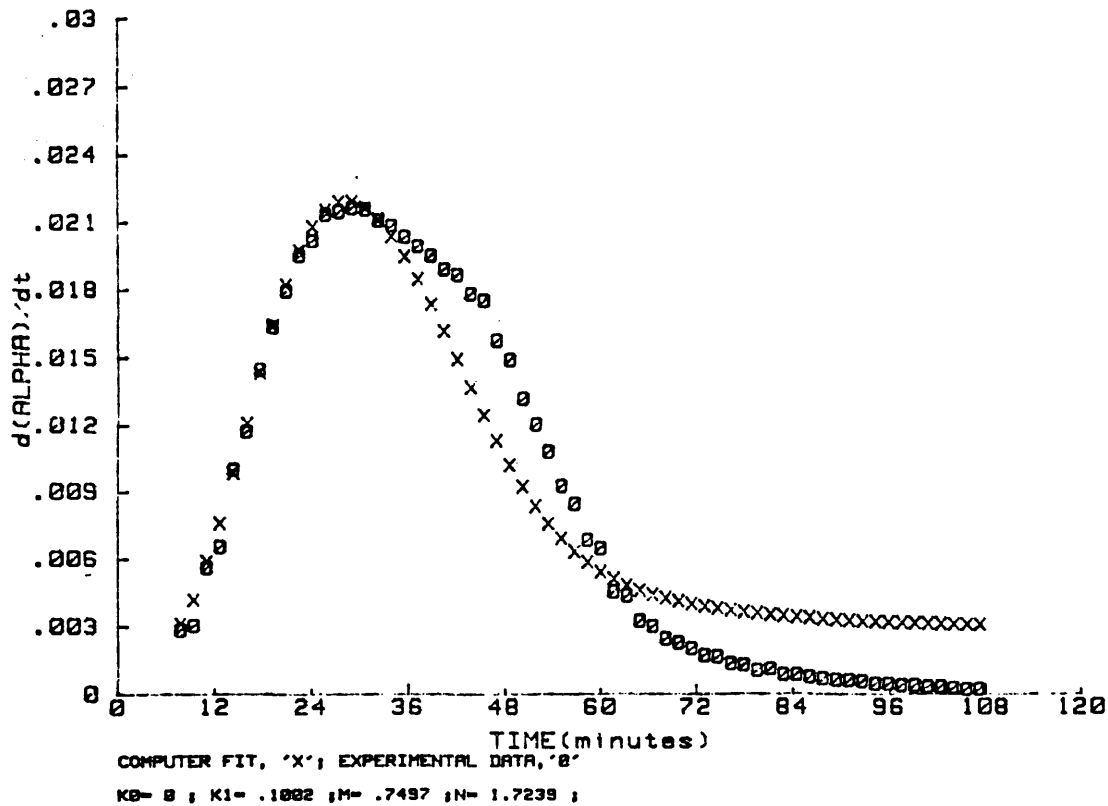


FIGURE 2.31

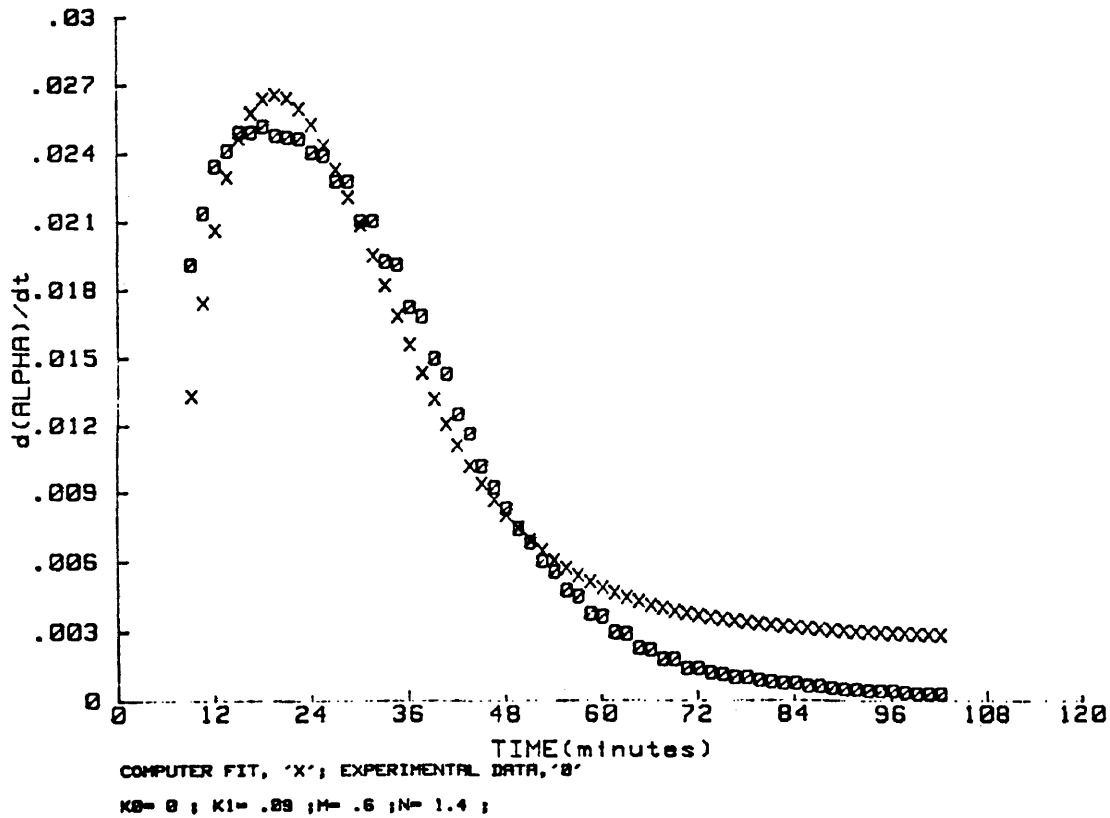


FIGURE 2.32

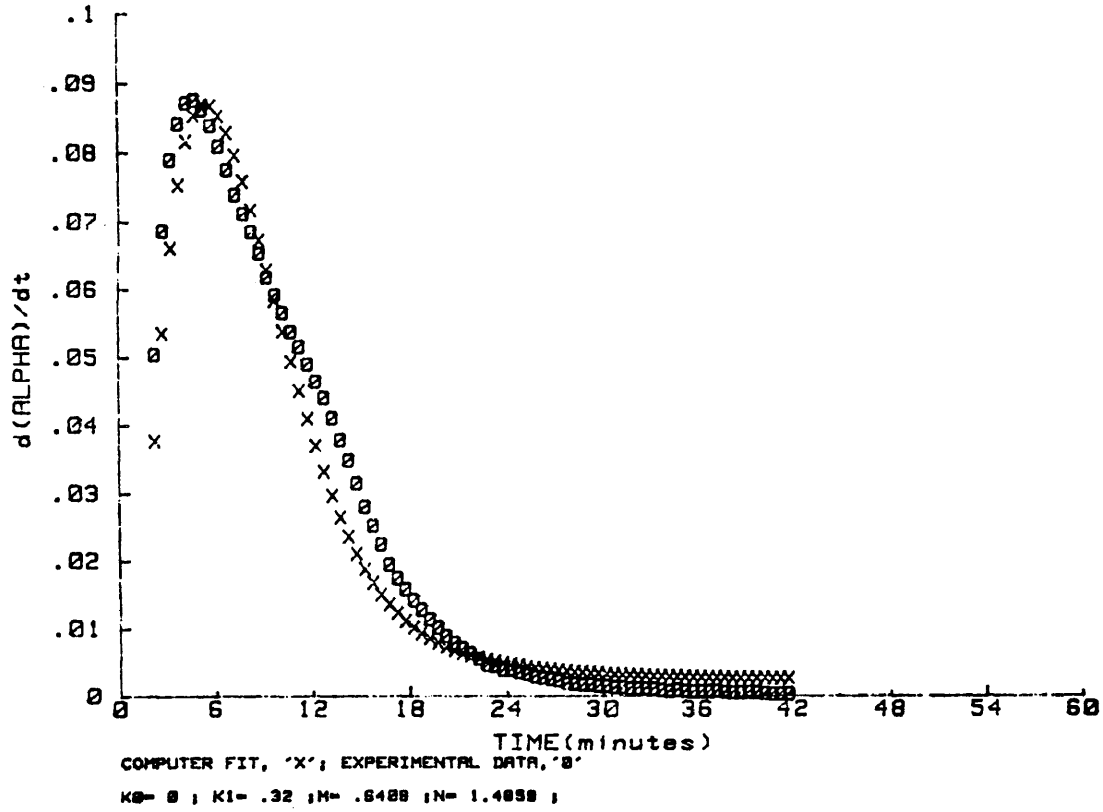


FIGURE 2.33

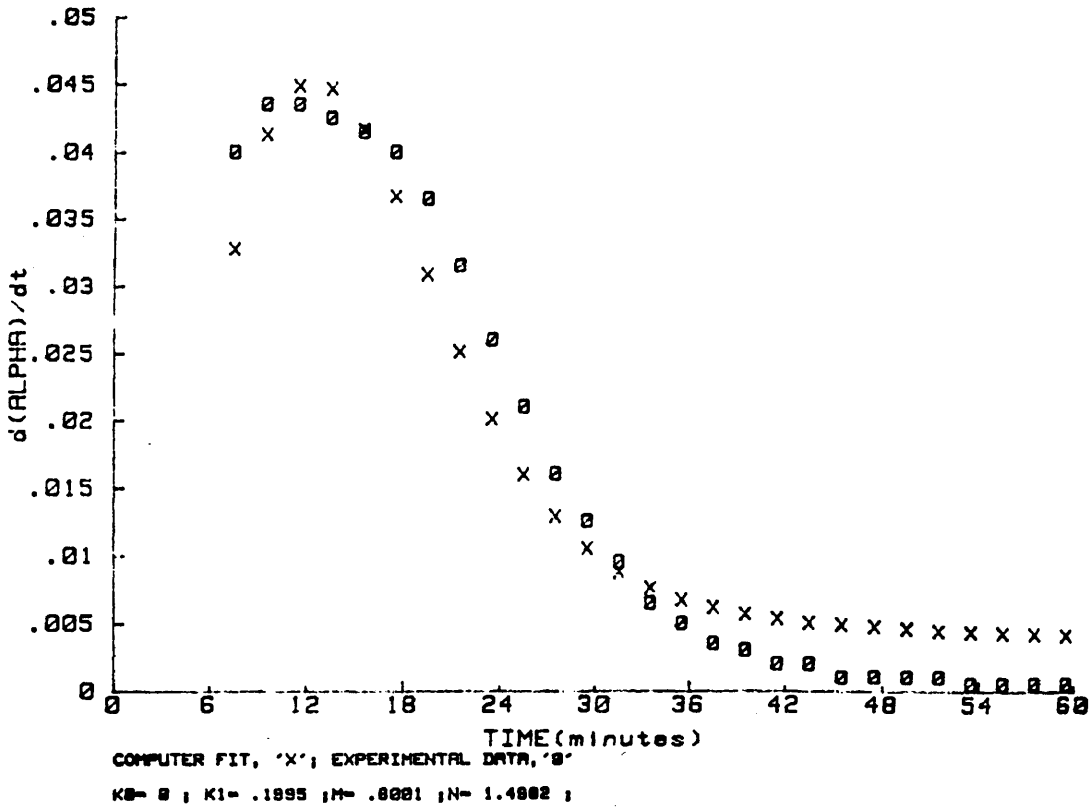


FIGURE 2.34

### 3. RYAN DUTTA ANALYSIS

#### a. THEORY

M. E. Ryan and A. Dutta of State University of New York developed a method to simply analyze the kinetic expression proposed by Kamal and Sourour. Maintaining that an accurate prediction of the characteristic peak in the reaction rate is the distinguishing and defining feature of the autocatalytic reaction, they focused on the maximum rate of reaction. In doing this they eliminated the lengthy process of determining the parameters through least square analysis.

The procedure evaluates an expression for the exponent  $m$ , which is dependent on  $n$ , the degree of cure at the exothermic peak, and the rate of cure at that point, and  $k_0$ . The derivation follows below.

$$8. \quad \dot{\alpha} = (k_0 + k_1 \alpha^m) * (1-\alpha)^n$$

$$9. \quad \dot{\alpha} / (1-\alpha)^n - k_1 = k_1 \alpha^m$$

The value of  $m$  can be found simply by rearranging the above equation and evaluating its natural log:

$$10. \quad m = \ln \left( \frac{(\dot{\alpha} / (1-\alpha)^n - k_0)}{k_1} \right) * (\ln \alpha)^{-1}$$

At the peak of the reaction curve  $\alpha_p$ , the derivative of the reaction rate is zero. Values of  $\alpha$  and  $d(\alpha)/dt$  at this point will be distinguished by subscript  $p$ .

$$11. \quad \frac{\delta^2 \alpha}{\delta t^2} = 0$$

Applying this to equation 8:

$$12. \quad 0 = nk_1 (\alpha_p)^{1-m} + (k_1(m+n)\alpha_p - nk_1)$$

The value of  $m+n=2$  is assumed. Therefore, the above equation can be rewritten to evaluate  $k_1$ . This is necessary as  $k_1$  can not be calculated from the raw data as can  $p, d p/dt$ , and  $k_0$ . the rate constant  $k_0$  is evaluated as the initial instantaneous change in with time

$$13. \quad k_1 = \frac{(2-m)k_0\alpha_p(1-m)}{(m-2)\alpha_p}$$

Substituting this value back into equation 12, an expression for  $m$  is obtained (equation 14) which can then be solved for  $m$  with computer analysis. The value of  $m$  is then used to determined  $k_1$  from equation 13.

$$14. \quad m = \frac{\ln \left[ \frac{\alpha_p / (1-\alpha_p)^n - k_0}{2 - mk_1\alpha_p(1-m)} \right] * (m-2\alpha_p)}{\ln \alpha_p}$$

#### b. RESULTS FROM RYAN-DUTTA ANALYSIS (figures 35-40)

TABLE 2.5

TEMP (°C)	$k_0$	$\alpha_p$	$\alpha_p$	$m$	$k_1$
60	.0551	.0875	.2416	.7269	.1953
50	.0060	.0496	.2722	.5767	.1524
45	.0058	.0361	.3353	.6869	.1157
40	.0034	.0373	.2789	.5934	.0602
35	.0026	.0214	.2637	.5514	.0663
30	.0009	.0248	.2891	.5273	.0606
25	.0005	.0116	.2809	.5767	.0375

**c. COMMENTS**

Ryan and Dutta found  $\alpha_p$  to increase with increasing temperature. In the present study  $\alpha_p$  was essentially constant. ( I qualify "essentially" because the data collected at 60°C and 45°C varied slightly from the average value of 0.28.) Where  $\alpha_p$  is constant,  $m$  is ,within error, constant. A small deviation in  $\alpha_p$  produces a more substantial difference in  $m$  due to the dependence of equation 14 on  $\alpha_p$ . This difference is exaggerated due to the logarithmic function. It should be noted that a precise determination of the parameter  $\alpha_p$  for the reactions which proceed rapidly at the higher temperatures, is much more difficult.

In addition,  $k_0$  must be extrapolated from the data instantaneously, and it must be evaluated consistently at the same minute reaction time for each temperature. The value, unlike in the other methods discussed, contributes to overall height of the curve.

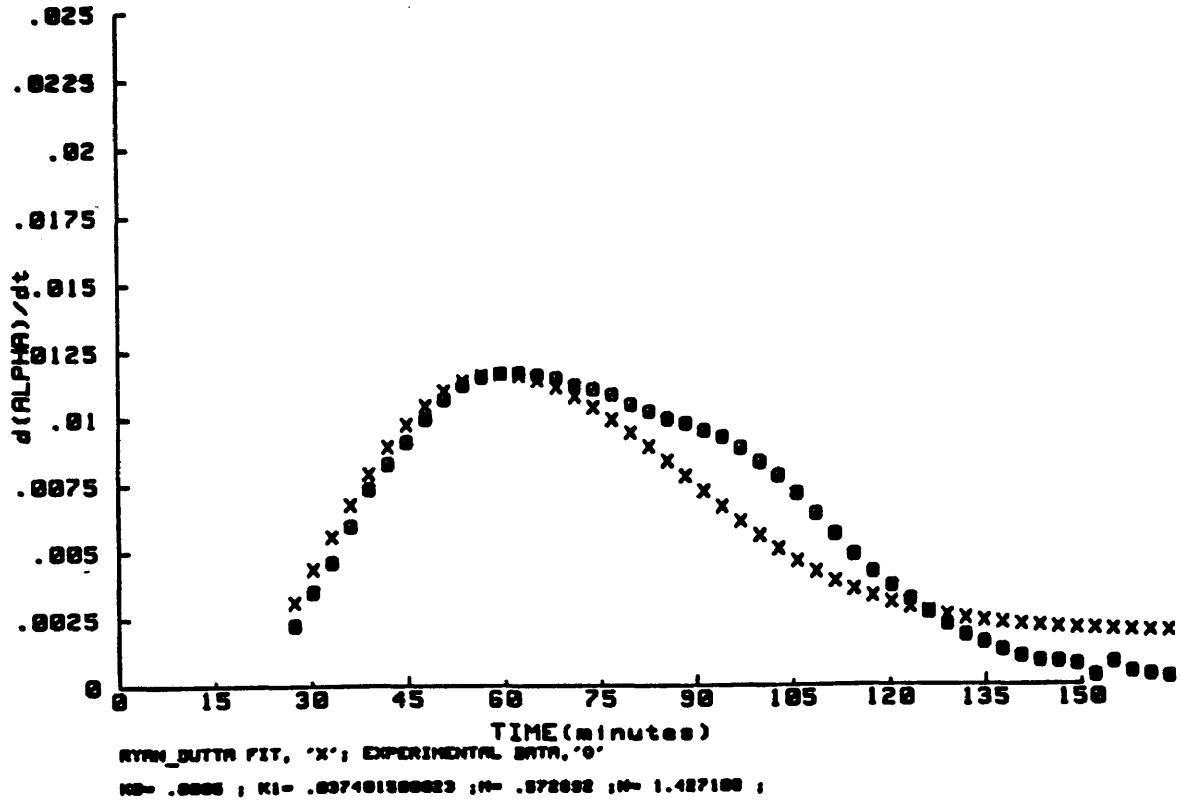


FIGURE 2.35

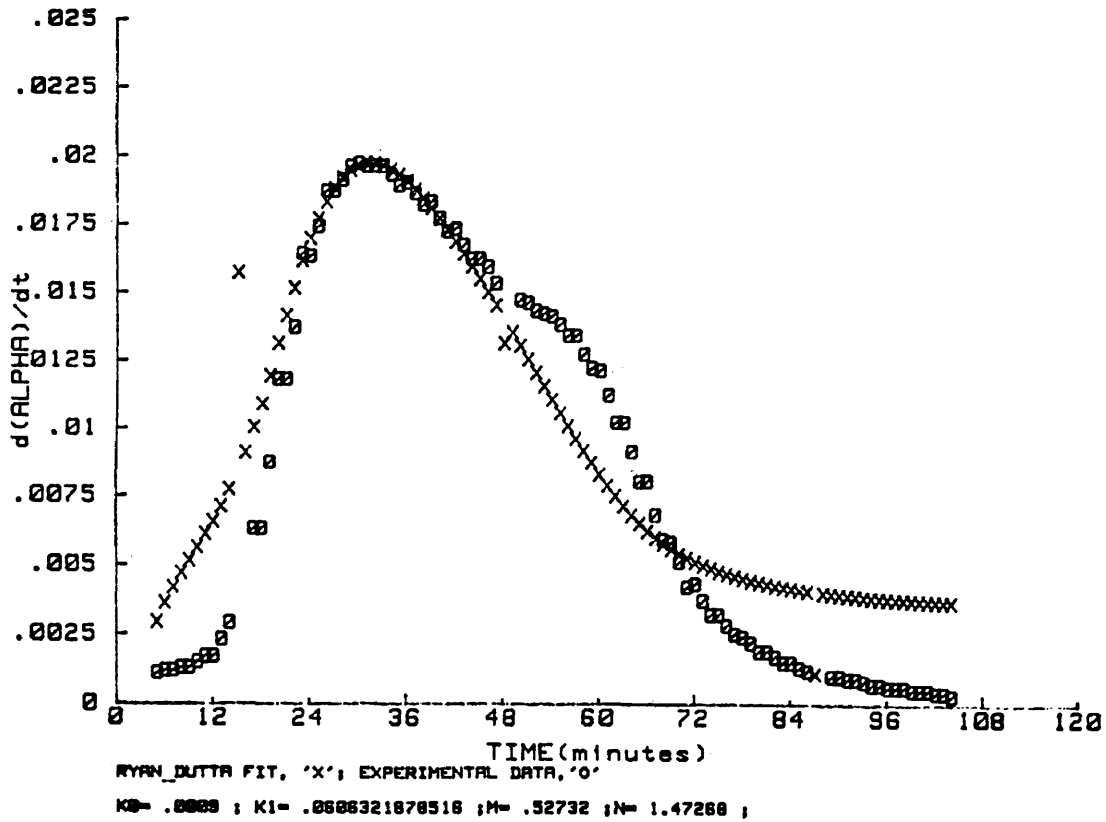


FIGURE 2.36

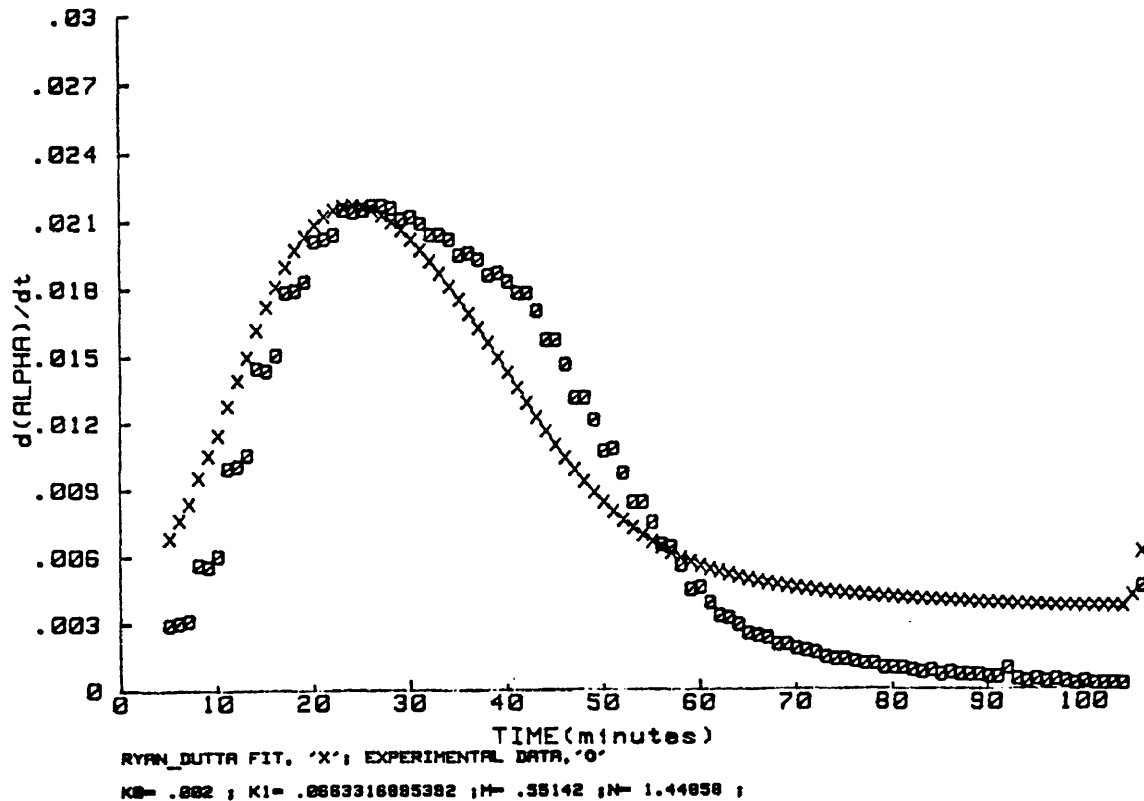


FIGURE 2.37

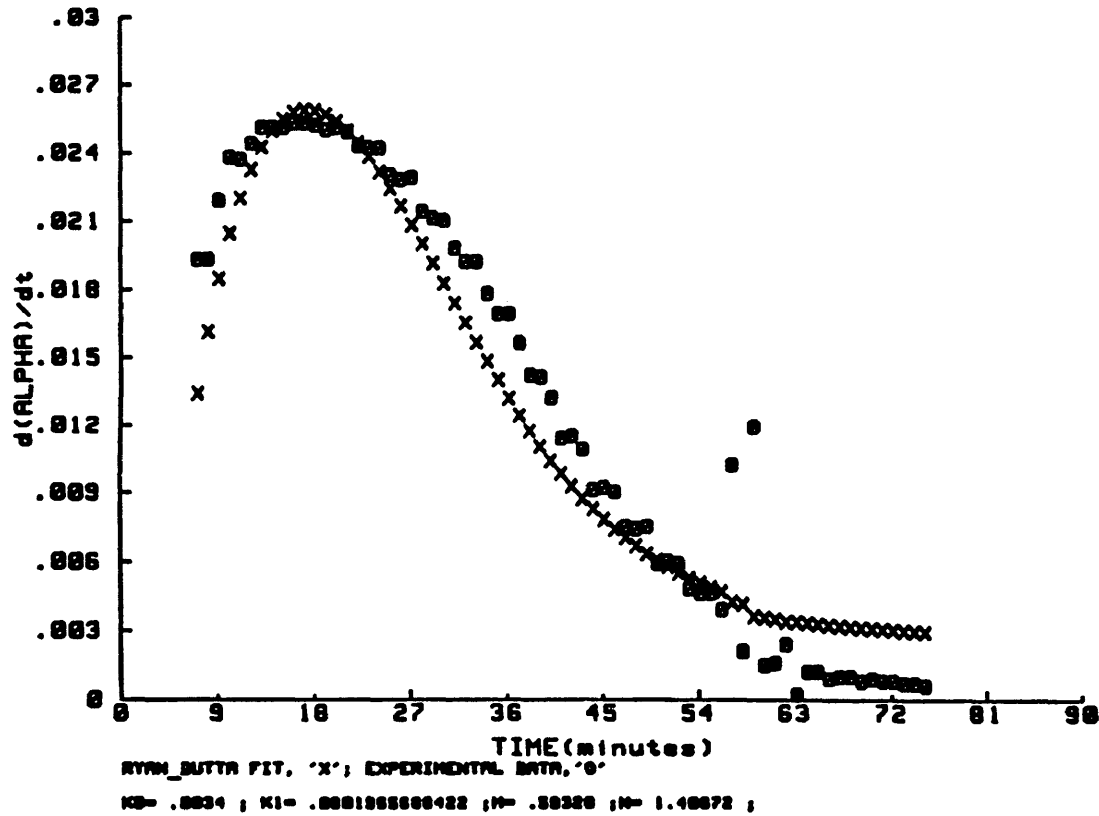
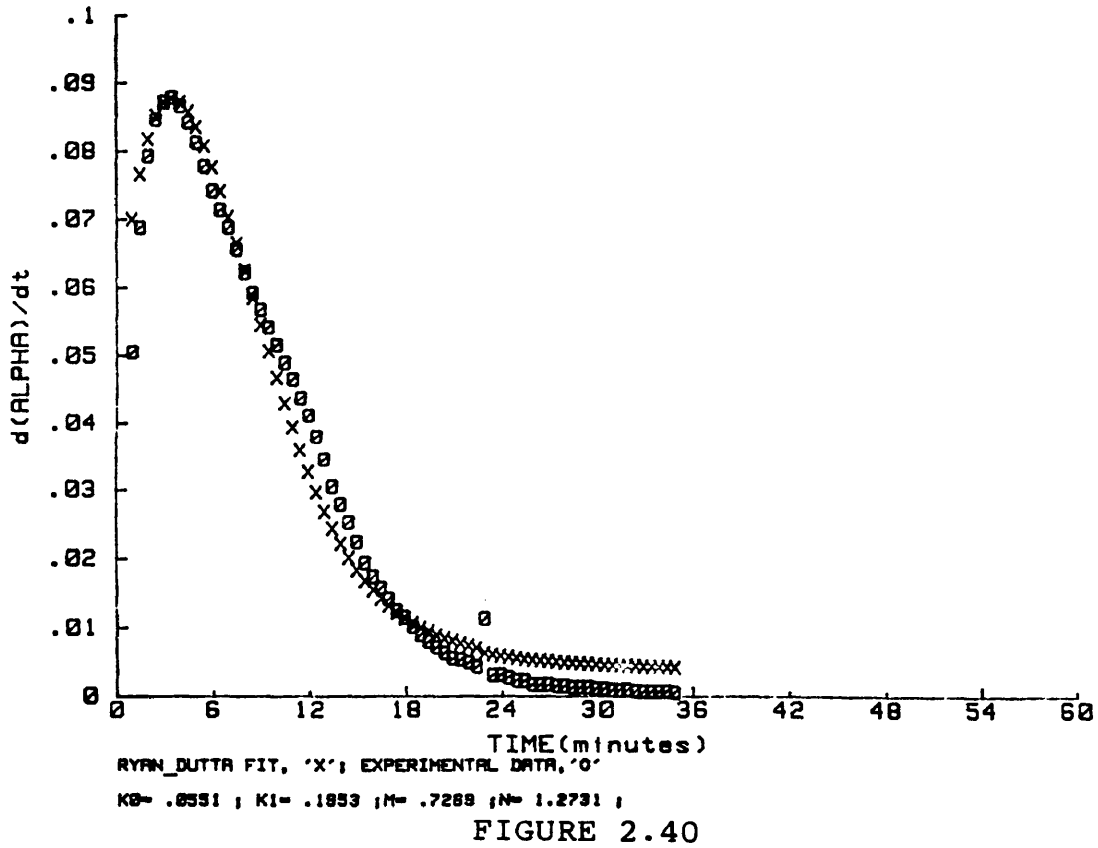
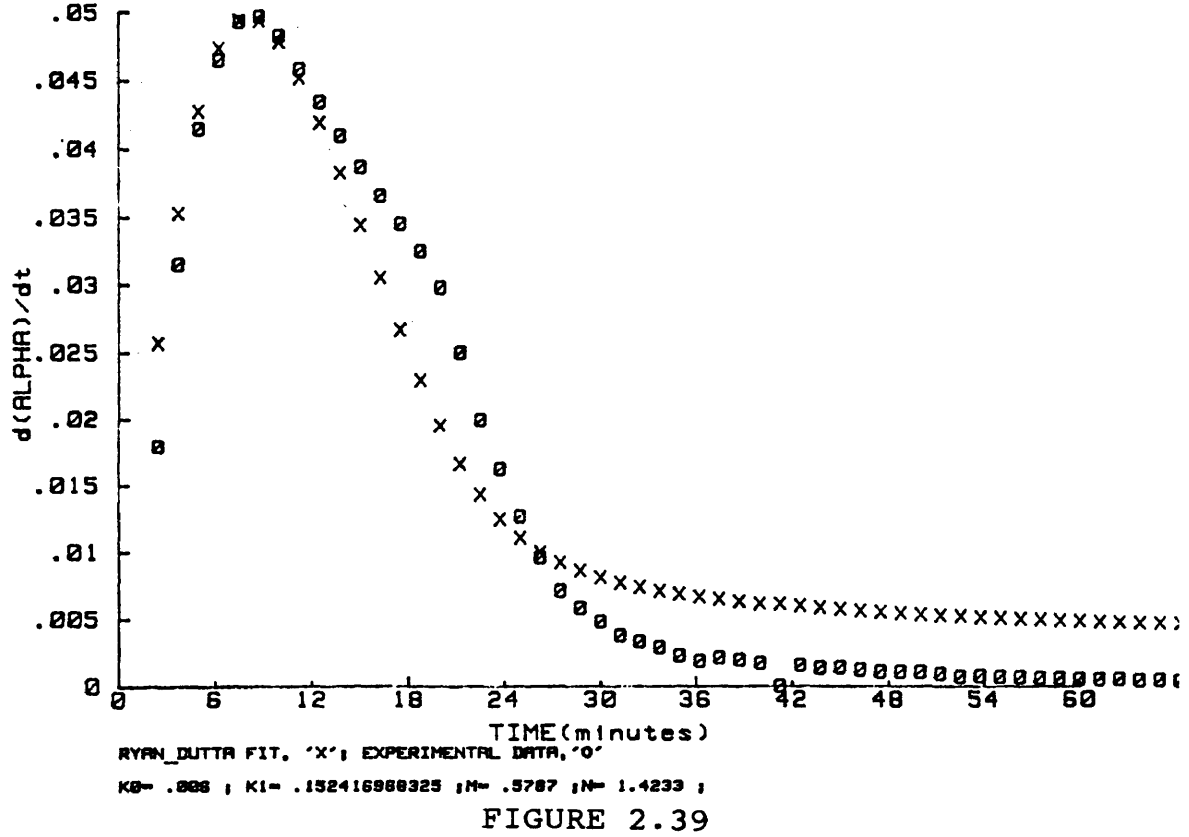


FIGURE 2.38



#### 4. BATCH AND MACOSKO ANALYSIS

In deriving a mechanistic model for the reaction kinetics of a progressing unsaturated polyester cure, Batch and Macosko(12) draw on models formulated by Stevenson(13), Huang and Lee(11), and Gonzalez-Romero (17). The goal of the study was to derive a set of equations dependent on the initiator and inhibitor concentrations. This allows for a much more direct analysis of the system than does a phenomenological model in which all the parameters must be reevaluated with each change in initiator concentration.

They divided the reaction into three time periods: 1) inhibition, 2) propagation, and 3) diffusion controlled propagation. The first period, inhibition, is the time to reaction onset, designated  $t_z$ . During this time, the free radicals react with the inhibitor which has a much larger rate constant than does the propagating monomer. Once all inhibitor is consumed, the radicals react readily with the unsaturated diacid species. This propagation continues until diffusion dominates; the peak in the reaction rate clearly marks this point.

ARISTECH POLYESTER RESIN: 25 C

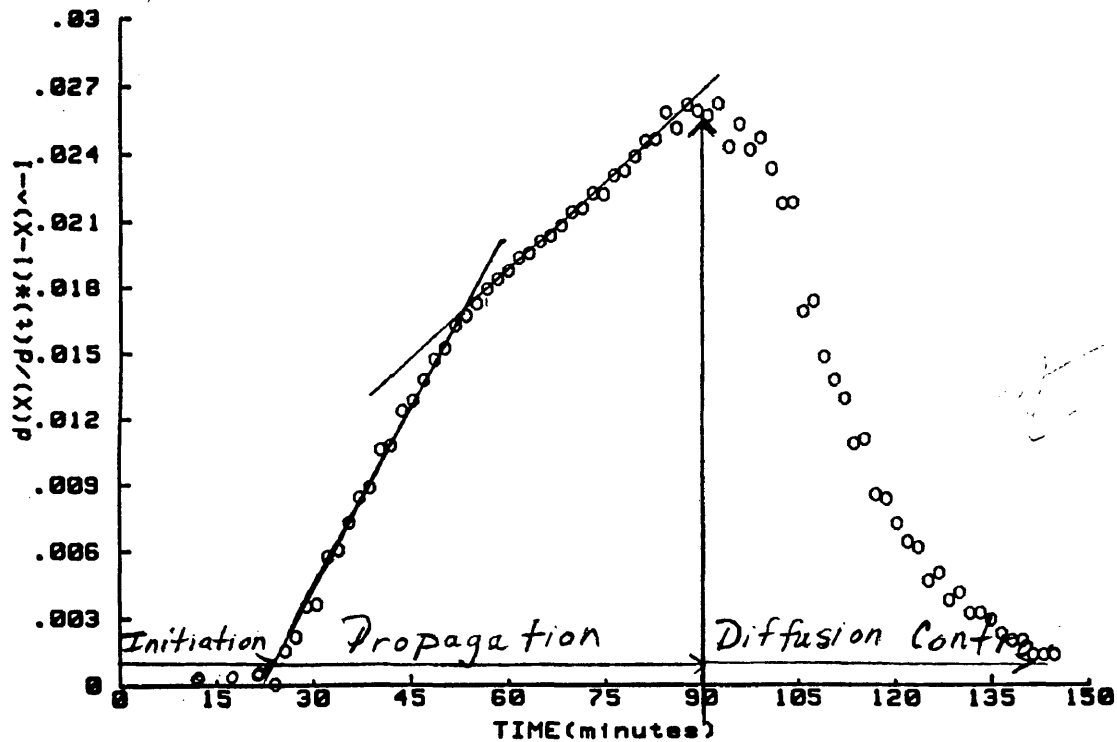


FIGURE 2.41

ARISTECH POLYESTER RESIN: 30 C

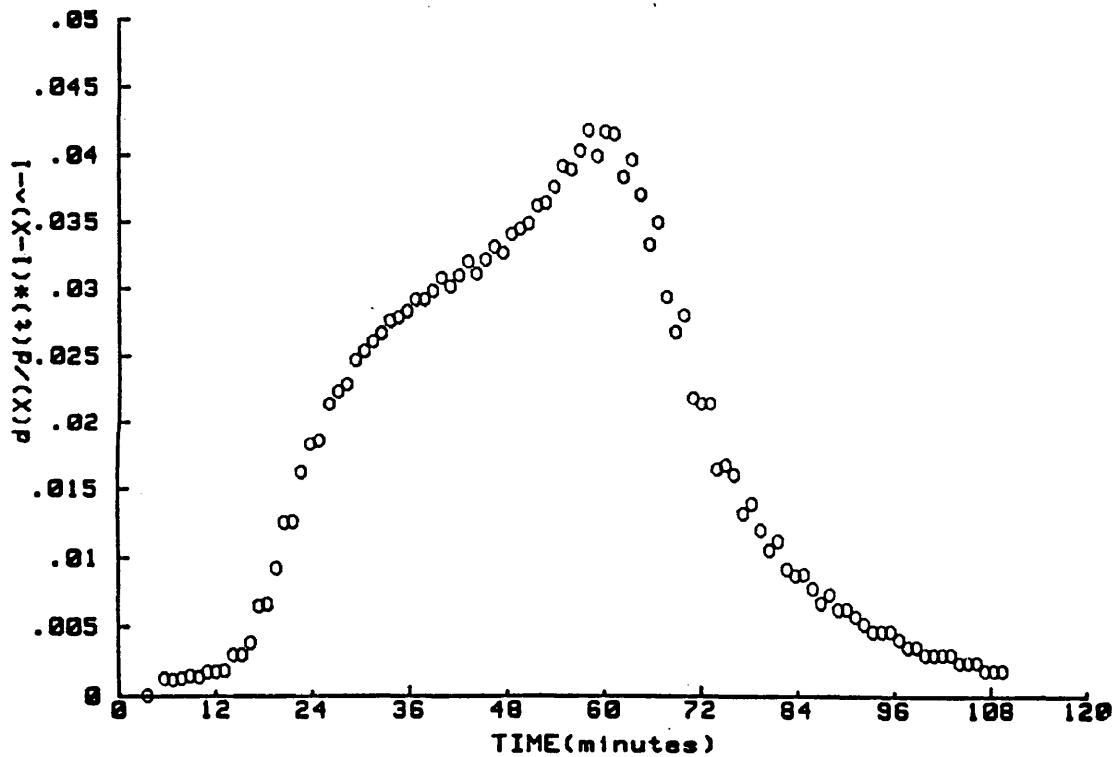


FIGURE 2.42

## ARISTECH POLYESTER RESIN: 35 C

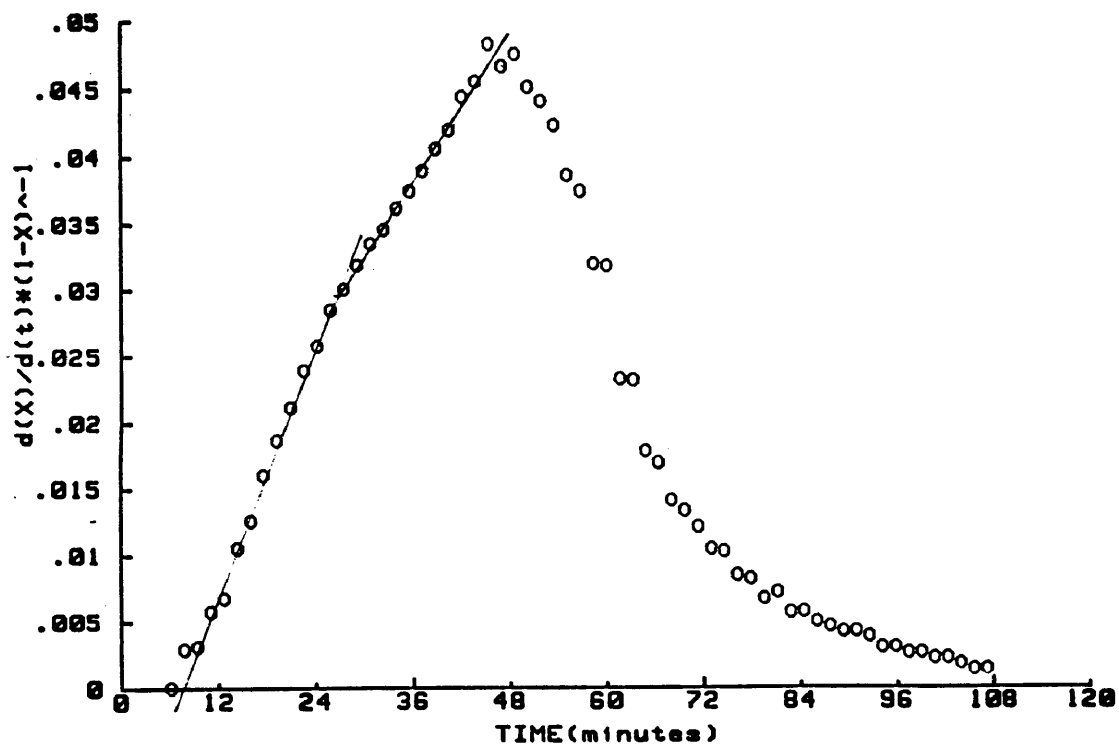


FIGURE 2.43

## ARISTECH POLYESTER RESIN: 40 C

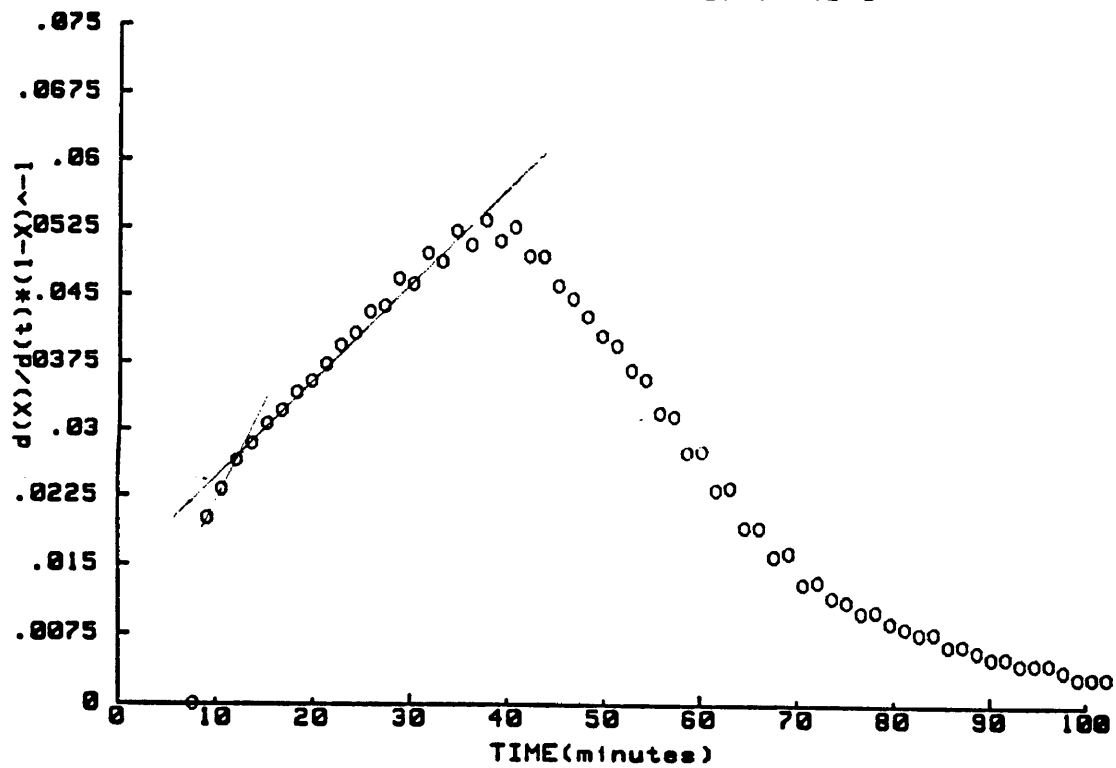


FIGURE 2.44

## ARISTECH POLYESTER RESIN: 50 C

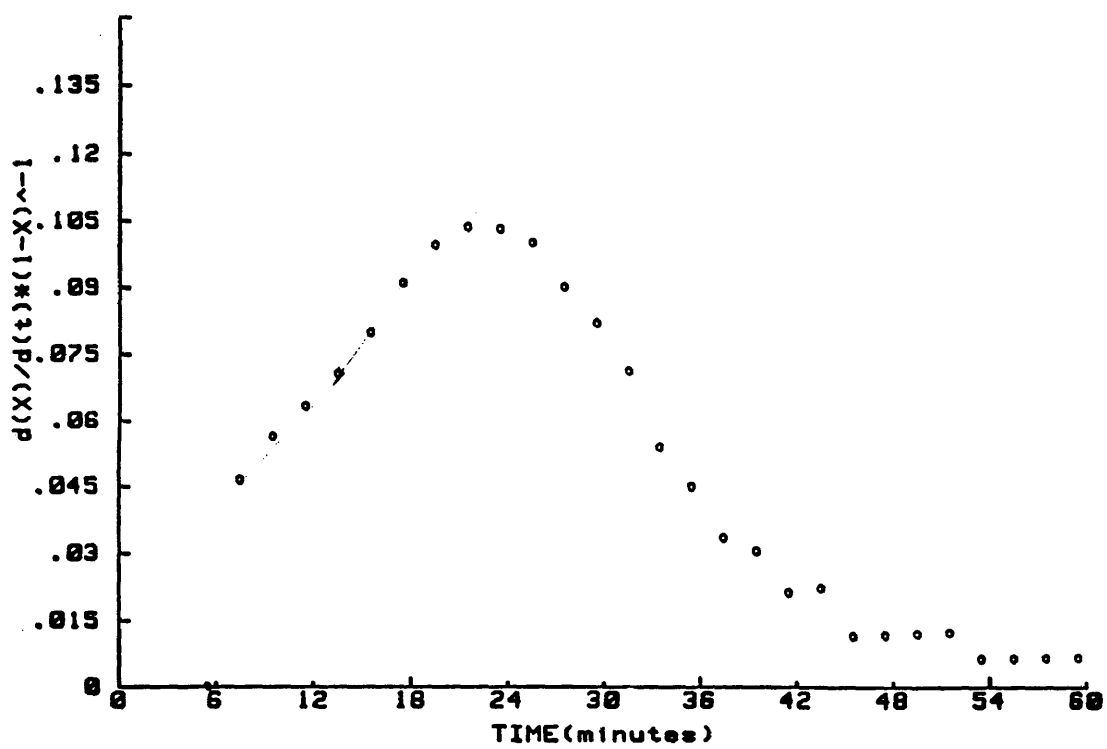


FIGURE 2.45

## ARISTECH POLYESTER RESIN: 60 C

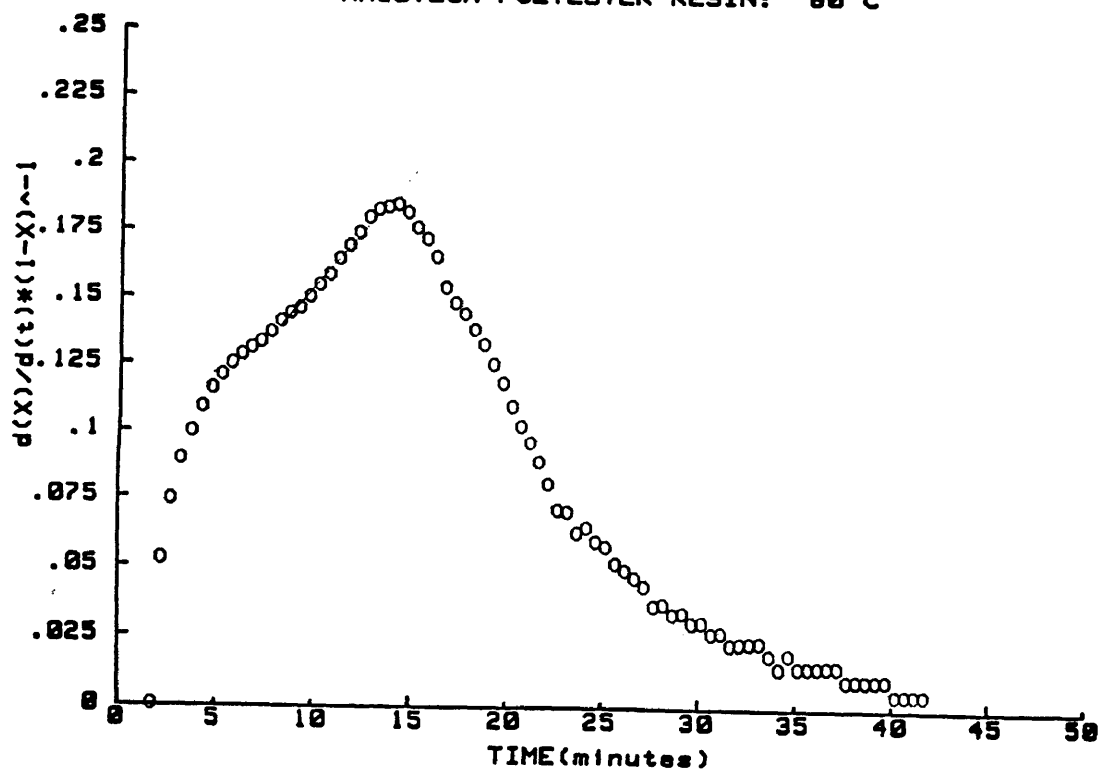


FIGURE 2.46

### C. COMPARISON OF KINETIC FITS

The Ryan Dutta method- without question- fits the curve most precisely; the Lam fit was the poorest of the three. The success of the RD method is attributed to its intrinsic dependence on the peak of the autoacceleration curve; it predicts the maximum rate of reaction and the time to this peak throughout the temperature range. The computer analysis (without  $k_0$ ) accurately estimates the time to  $d(\alpha)/dt_{\max}$ , but overestimates its value as compensation for the underestimation at higher degree of cure ( $>.7$ ) where diffusion begins to dominate the cure process. Both the LSF and the RD fits are consistent in their deviations at this point. The Lam fit, however, yields the greatest error in  $d(\alpha)/dt$  at later stages of the reaction. Kamal's equation itself can be partially blamed for the lack of precision beyond the maximum rate of cure because it can not compensate for the secondary peak (shoulder) in the reaction rate, which is briefly discussed in the opening paragraphs of this chapter.

The fact that better fits and a more linear relationship in  $k_1$  were obtained with the least squares method when the  $k_0$  term was neglected indicates that the term is not significant. The reaction rate as a function of time as defined by the data listed in table 2 (in previous section) is separated into two terms:  $k_0(1-\alpha)^n$  and  $k_1(\alpha)^m(1-\alpha)^n$ . It is seen (in figures 47-52) that in all cases, with the exception of the 40°C reaction where  $k_0$  is one or two magnitudes larger than for other temperatures,

the term plays no role at all. This indicates that  $k_0$  is of little importance to the overall reaction rate, this factor is usually added to allow for instrumental equilibration. (It should be noted that it may be a function of the step size, which was rather large.)

It is also important to note that the sum of  $m$  and  $n$  was not restricted to 2 in the computer analysis. However, for the two different fits shown previously, the value of  $m$  was almost always less than 1 and that of  $n$  between 1 and 2. The resulting fits of table in which the step size was considerably larger than in the corresponding evaluation of data in table 2.4, are not precise fits. In reviewing figures 23-28, the larger exponential values gives less than desirable results. While the assumption that the sum of the exponents is equivalent to two is qualified in the accuracy of the Ryan Dutta fit, the least square data provides no concrete evidence of this. It results in neither a consistent increase or decrease in the sum as a function of temperature nor a constant value of the sum of  $m$  and  $n$ . But, for the most part- and for the better fits- the value does oscillate around the value of 2. Further justification for this exponential sum is provided in the analysis proposed by Lam. Linearity of curves 2.5 through 2.10 depends on  $m$  and  $n$  summing to 2; deviations from linearity occur only as diffusion controlled propagation becomes dominant.

The activation energies are 43.57, 51.62, and 38.13 kJ/mol for the Lam, LSF and RD fits respectively. (see plot 54 on following page). These values agree with those in literature on similar systems (8-11kcal/mol).

ARISTECH POLYESTER RESIN: 25 C

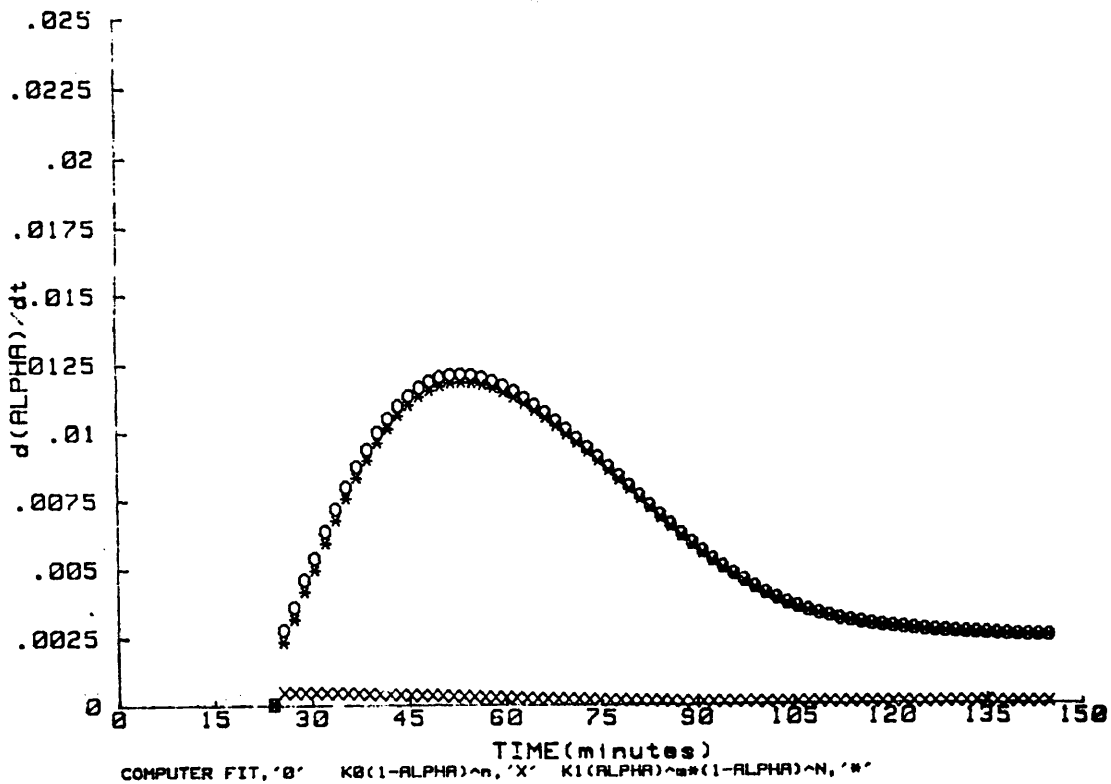


FIGURE 2.47

ARISTECH POLYESTER RESIN: 30 C

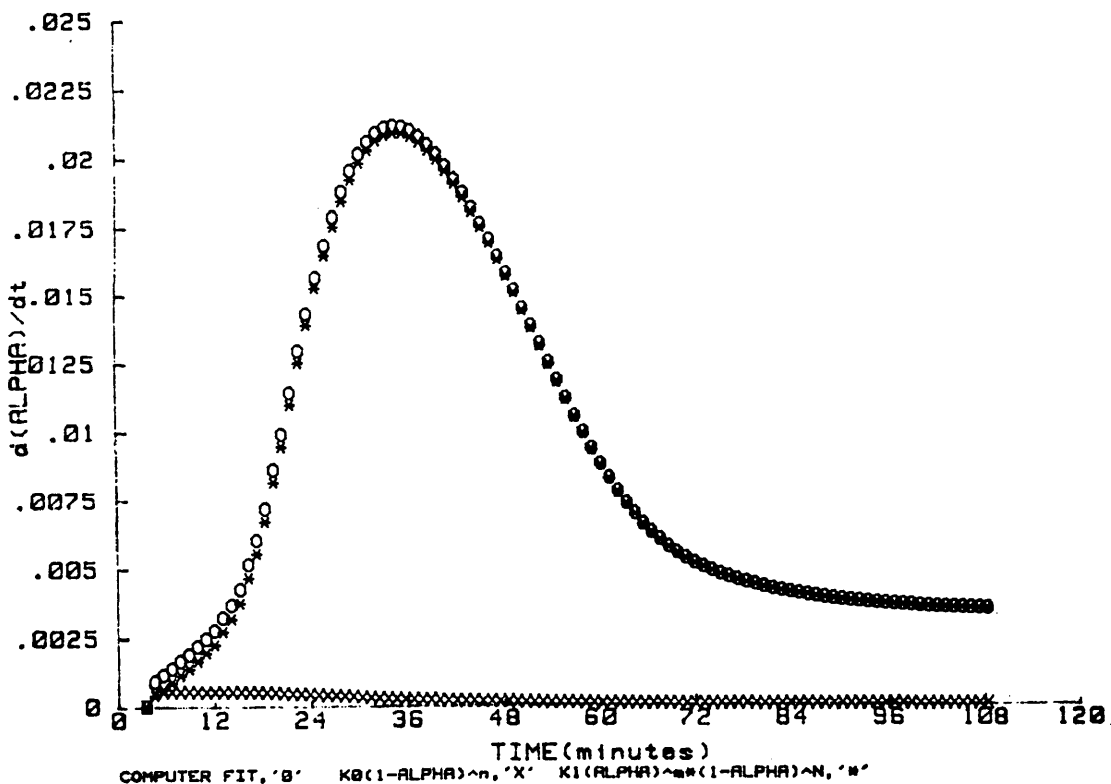


FIGURE 2.48

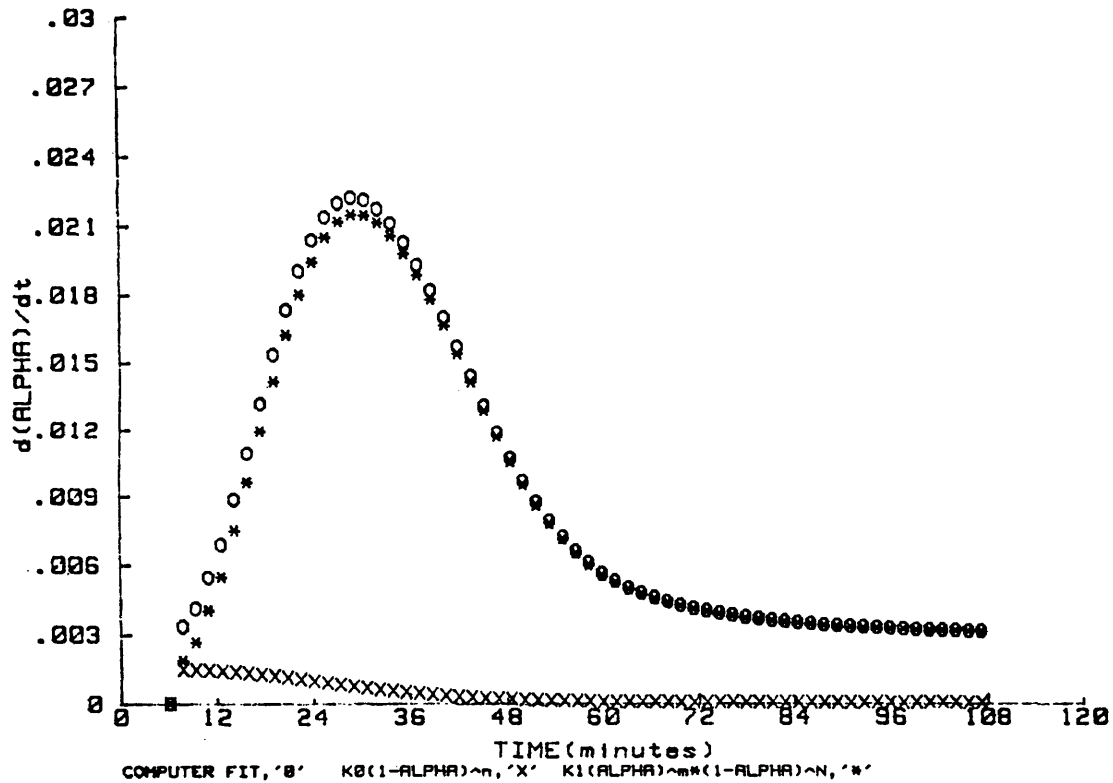


FIGURE 2.49

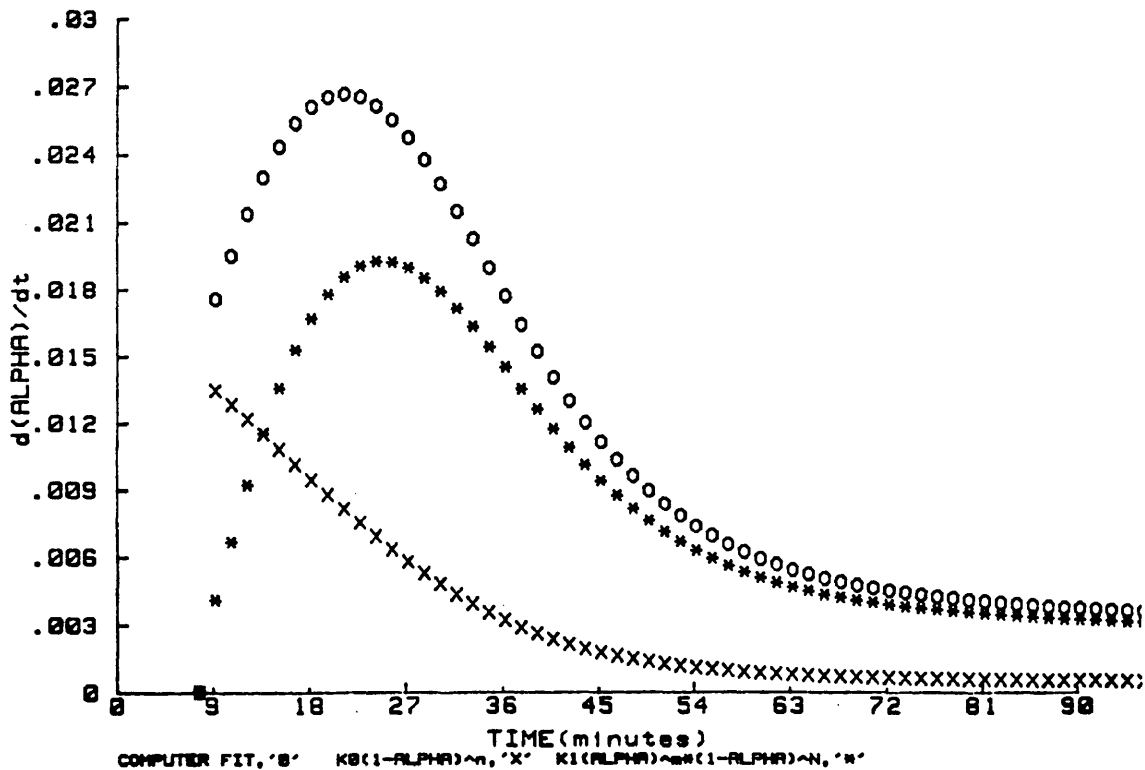


FIGURE 2.50

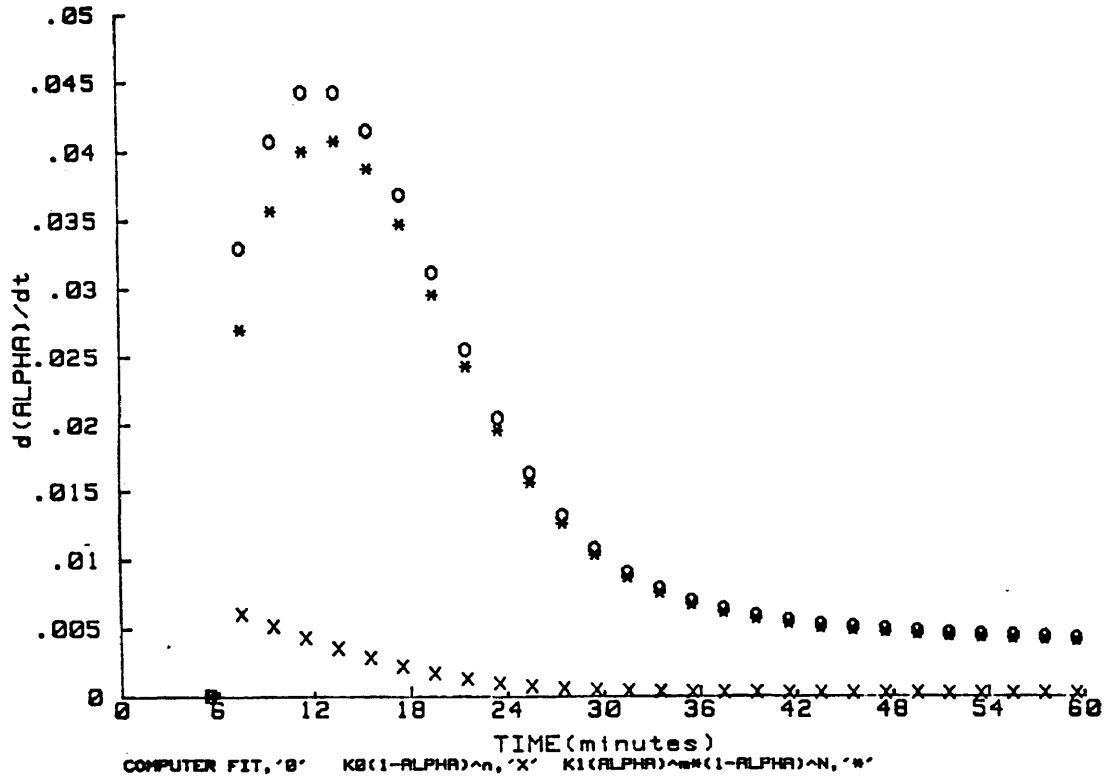


FIGURE 2.51

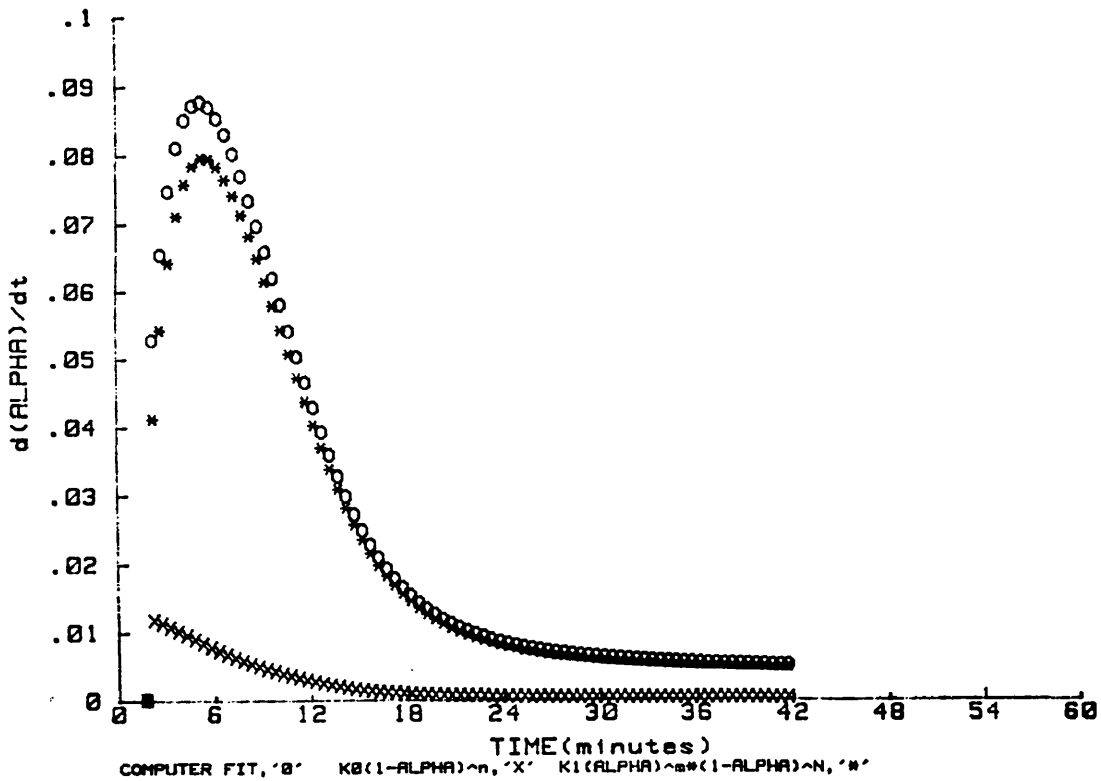


FIGURE 2.52

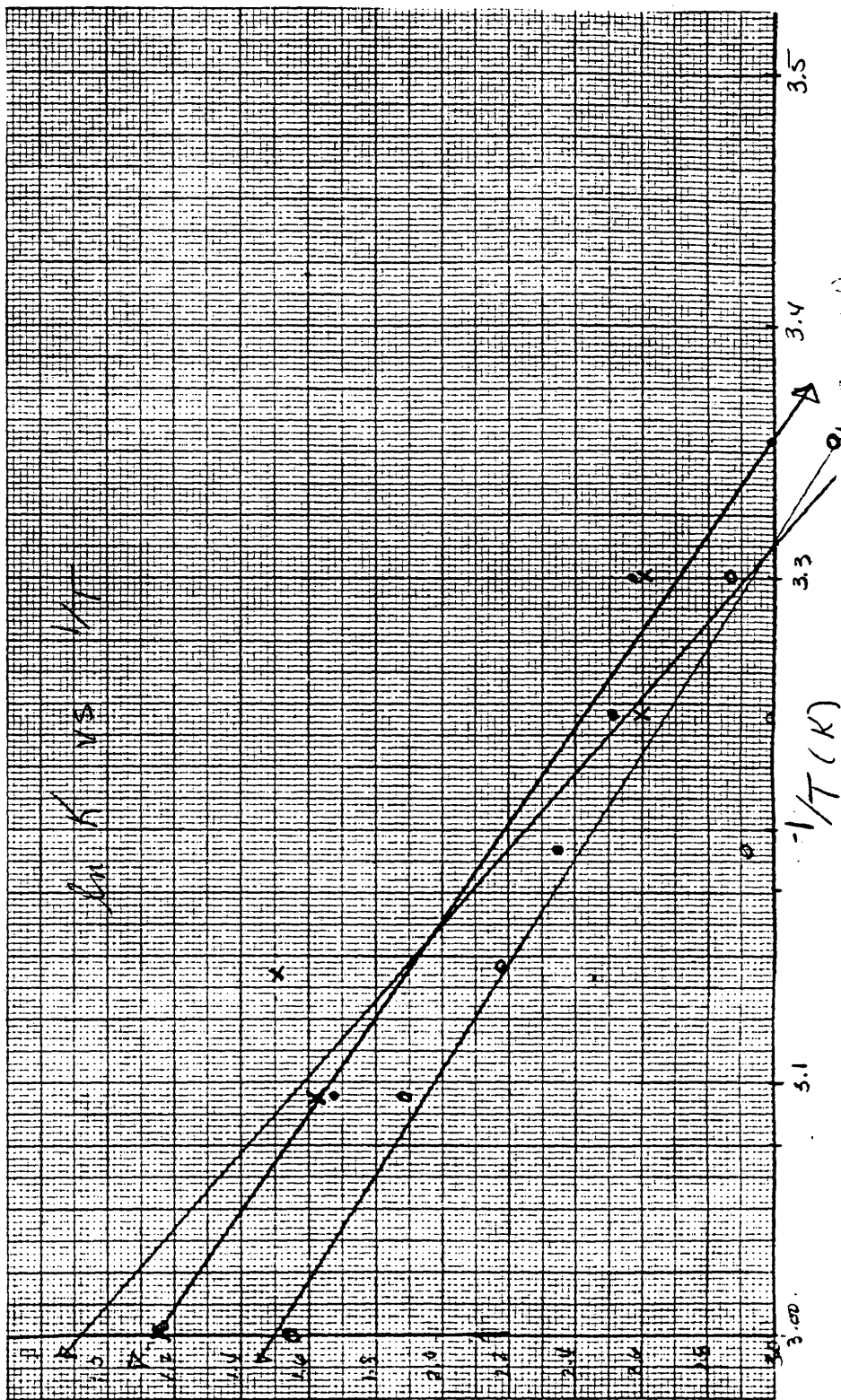


FIGURE 2.53

ln K

D. RELATIONSHIPS BETWEEN REACTANT CONCENTRATIONS,  $m$ , AND  $n$ 

In free radical polymerization, the rate of polymerization ( $r_p$ ) depends on the concentration of the monomer radical



From the propagating reaction scheme represented above, the rate of the reaction,  $r_p$  can be represented as :

$$15 \quad r_p = k_p [M]_t [R \cdot]$$

Both the rate of polymerization and  $\alpha$  can be defined in terms of decreasing monomer concentration, where  $[M]_0$  is the initial monomer concentration and  $[M]_t$  is instantaneous monomer concentration:

$$16 \quad r_p = -d[M]/dt = \frac{[M]_0 - [M]_t}{dt}$$

$$17 \quad \alpha = ([M]_0 - [M]) / [M]_0$$

The change of  $\alpha$  with respect to time also expresses a reaction rate albeit unitless. Differentiating equation 17 with respect to time yields an expression proportional to  $r_p$  (represented in equation 16) by a factor of  $[M]_0$ .

$$18 \quad d\alpha/dt = - (1/[M]_0) d[M]_t/dt$$

Therefore,

$$19 \quad r_p = [M]_0 (d\alpha/dt)$$

Solve equation 17 for  $[M]_t$ .

$$20 \quad [M]_t = (1-\alpha) [M]_0$$

Substitute the above value in equation 15.

$$21 \quad r_p = k_p (1-\alpha) [R.] [M]_0$$

Equating equations 19 and 21 gives an expression very similar to the equation used by Kamal and co-workers wherein the initial rate constant was negligible.

$$22 \quad \frac{d\alpha}{dt} = k_p [R.] (1-\alpha)$$

If, in the above derivation, a steady state concentration of free radicals is valid, the reaction rate should decrease linearly as a function of  $\alpha$ . However, if the reaction is autocatalytic- the reaction generates species which accelerate the rate of the reaction- the free radical concentration changes. As this changes the kinetics of the reaction, it is reflected in the nonlinear curve of  $\log d\alpha/dt$  versus  $\log (1-\alpha)$ .

Equation 22 is strikingly similar to equation 2. Both contain an increasing term, a decreasing term and a rate constant. A simple inquiry into the nature of the equation elucidates, that a peak is the natural result of the equation. This is demonstrated in the table on the next page( table 2.6) where  $m=.7$  and  $n=1.3$  (chosen arbitrarily). The value of  $m$  and  $n$  determine the point at which the curve will maximize. This indicates that for a constant maximum rate of reaction, a constant value for  $m$  and  $n$  should exist. Therefore, if the factor  $(1-\alpha)^n * \alpha^m$  is constant for a given

for all temperatures,  $k_1$  alone controls the rate at which  $d\alpha/dt$  maximizes for each temperature, acting in the true role of a rate constant.

The similarities between the true kinetic expression of the reaction rate and the one proposed by Kamal provides some mechanistic insight into the approach that has been criticized for being purely phenomenological. The decreasing term is proportional to the radical concentration and the increasing term, to the monomer concentration (as  $\alpha$  itself is).

TABLE 2.6

$\alpha$	$\alpha^m$	$(1-\alpha)^n$	$\alpha^m * (1-\alpha)^n$
0.1	.2	.87	.174
0.15	.27	.81	.219
0.20	.32	.75	.240
0.25	.39	.69	.262
0.30	.43	.63	.271
0.35	.48	.57	.274
0.40	.51	.52	.265

Experimentally, the peak in the exotherm of the cure occurs at a constant degree of cure and is, therefore, independent of the temperature but dependent on the mechanism of the reaction. It should also be noted that the peak occurs after the gel point, which is reached at 5-10% conversion. (This early gelation is consistent with thermosetting polyester resins(5).) At this point the polymerizing thermoset is sufficiently crosslinked and the viscosity of the reacting mass is large.

TABLE 2.7

TEMP	TIME TO $d\alpha/dt$ max	ALPHA AT $d\alpha/dt$ max	GEL TIME	ALPHA AT GEL
25	54.2	.28	39	.10
30	30.7	.28	20	.05
35	25.5	.26	15	.05
40	17.7	.28	7	.09
45	12.9	.35	--	--
50	9.9	.27	--	--

After the reaction rate maximizes, the decrease in the reaction rate progresses linearly, or nearly so, until 70-90% conversion (depending on the temperature) when the reaction slows considerably. Refer to figure 2.2, keeping in mind the discussion of three zones proposed by Batch and Macosko. At lower temperatures, there is inhibition. The propagation period is recorded as a steadily increasing degree of cure. A significant change in the slope of the degree of cure is evident in each of the reactions. The intersection of these two slopes corresponds to the time at which diffusional propagation begins as ascertained through the Batch-Macosko analysis. Correlating this change in the Lam analysis, these times also represent the deviations in linearity of  $\ln[(dX/dt)/X_2]$  vs  $\ln[(1-X)/X]$ , where  $X=\alpha$  (figures 2.5 through 2.10).

With much supporting evidence, it can be stated that diffusion controls the propagation of the free radicals as the degree of cure slows considerably. This point is also

closely associated with the glass transition.(6) The molecular structure of the reacting resin is rigid and glasslike; hence, the molecular motion is greatly restricted. Although, monomer and radicals remain, the only route to collision is diffusion of these species through the highly crosslinked matrix.

According to Batch and Macosko, the time at which diffusion propagation begins to dominate is the point at which  $d(\alpha)/dt[1/(1-\alpha)]$  maximizes. From equation 20, it can be seen that the parameter evaluated in these figures 2.41 through 2.46 is  $k_p[R.]$ . The presence of a maximum necessitates either a decreasing radical concentration or decreasing rate constant with time and extent of cure. The first of these assumptions is more likely, although a changing rate constant has been suggested but not confirmed(7). If the rate constant were changing it would indicate changing mechanism (as in the change from autoacceleration domination to diffusional propagation). A change in either of the two variables- a sudden decrease in radical concentration or a change in the rate constant or both- indicates a deviation in the reaction scheme. It can be concluded that the fit described by equations 1 and 2 fails beyond  $\alpha=0.7$  (for  $25^{\circ}\text{C}$ , and correspondingly higher with increasing temperature) because it can not encompass this change.

## REFERENCES FOR CHAPTER II

1. J. L. McNaughton and C. T. Mortimer, Differential Scanning Calorimetry (rpt. London: Buttersworth, 1975).
2. Harry R. Allcock and Frederick W. Lampe, Contemporary Polymer Chemistry (New Jersey: Prentice-Hall, INC., 1981), pp.436-442.
3. S. Sourour and M. R. Kamal, "Differential Scanning Calorimetry for Characterization of Thermoset Cure," SPE Technical Papers, 18 (1972), 93.
4. M. R. Kamal and S. Sourour, "Kinetics and Thermal Characterization of Thermoset Cure," Polymer Engineering and Science, 13, no. 1 (1973), 59.
5. S. Sourour and M.R. Kamal, "Differential Scanning Calorimetry of Epoxy Cure: Isothermal Cure Kinetics," Thermochemica Acta, 14 (1976), 41.
6. Musa R. Kamal, "Thermoset Characterization for Moldability Analysis," Polymer Engineering Science, 14, No. 3 (1974) 231.
7. Patrick W. Lam, "The Characterization of Thermoset Cure Behavior by Differential Scanning Calorimetry: Part 1 Isothermal and Dynamic Study," Polymer Composites, 18, No. 6 (1987), 427.
8. Ryan and A. Dutta "Kinetics of Epoxy Cure: A Rapid Technique for Kinetic Parameter Estimation," Polymer, 20 (1979), 203.

9. G. Batch and C. Macosko, Antec, (1988), 1039.
10. S. Y. Pusatcioglu, A. L. Fricke, J. C. Hassler, "Heats of Reaction and Kinetics of a Thermoset Polyester," Journal of Applied Polymer Science, 24 (1979), 937.
11. Chang Dae Han and Dai Soo Lee, "Curing Behavior of "Unsaturated Polyester Polyester Resin With Mixed Initiators," Journal of Applied Polymer Science, 34 (1987), 793.
12. Gibson L. Batch and Chrisotpher W. Macosko, "Kinetics of Crosslinking Free Radical Polymerization with Diffusion Limited Propagation," Antec, (1987), 974.
13. James F. Stevenson, "Free Radical Models for Simulating Reactive Processing", Polymer Engineering and Science, 26, No. 11 (1986), 746.
14. John B. Enns and John K Gillham, "Time-Temperature-Transformation (TTT) Cure Diagram: Modeling the Cure Behavior of Thermosets," Journal of Applied Polymer Science, 28, (1983) 2567-2591.
15. J. M. Salla and J. L. Martin, "Dynamic Isothermal and Residual Heats of Curing of an Unsaturated Polyester Resin," Thermochemica Acta, 126 (1988) 339-354.

## CHAPTER III: DIELECTRIC ANALYSIS

### A. THEORY

A dielectric is an insulator, a material which contains few or no free electrons. Therefore, charge does not readily flow through these materials when voltage is applied. This property allows for the construction of capacitors which store electrical charge and oppose changes in electrical voltage. Since most polymeric substances are dielectrics, they may be used as capacitors and their electrical properties studied as they serve this function.

## 1. POLARIZATION

A dipole moment arises when the centers of positive and negative charge within a molecule are separated a distance  $l$ . As illustrated below, it is a vector quantity of magnitude  $L \cdot q$  and is directed from the negative toward positive charge.

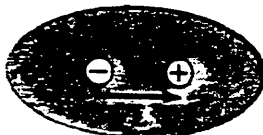


Illustration 3.1

In terms of separation of these charges, molecules are divided into two classes: polar and nonpolar. Molecules with noncoincident positive and negative charge centers, due to asymmetrical composition or association of unequally electronegative atoms are by definition polar molecules and possess a permanent dipole moment,  $\mu$ . However, since the motion (orientation) of the molecules is random, the average dipole moment,  $\langle \mu \rangle$ , however, is zero.

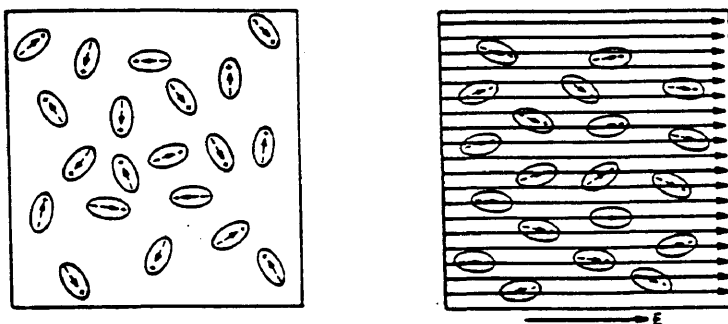


Illustration 3.2

All atoms and the majority of molecules are nonpolar,

meaning the centers of positive and negative charges are coincidental; these do not possess a dipole moment in their natural, unperturbed state. In an applied electric field, charges align themselves with the field. If the field is uniformly applied, a polar molecule experiences a net torque produced by two equal and opposite forces, causing the molecule to make an angle,  $\theta$ , with the field. The resulting torque has magnitude  $FL\sin\theta = qEL\sin\theta = pE\sin\theta$ .

1

$$\tau = \mathbf{p} \times \mathbf{E}$$

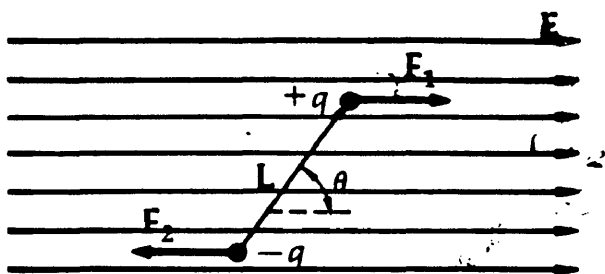


Illustration 3.3  
(uniform)

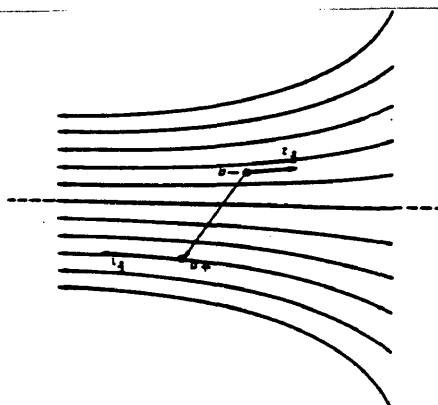


Illustration 3.4  
(nonuniform)

If the dipole is rotated through an angle  $d\theta$ , the potential energy is described as

$$2a \quad dU = pE\sin\theta \, d\theta$$

$$2b \quad U = -pE\cos\theta + U_0$$

$$2 \quad U = -\mathbf{p} \cdot \mathbf{E} + U_0$$

$U_0 = 0$  when the dipole is parallel to the field.

In a uniformly applied field, nonpolar molecules experience an induced dipole moment as the charges are

separated by the field. There is, however, neither a net force nor net torque produced because the induced dipole is parallel to the axis of the applied field.

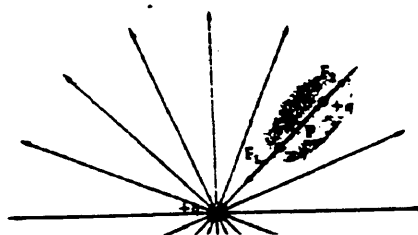


Illustration 3.5

The results become more interesting in a nonuniformly applied field such as one generated by an alternating current. Both polar and nonpolar molecules experience a net force which distorts the electronic and atomic clouds. Hence the term distortion polarization is used in reference to this phenomenon. The electronic distortion polarization is rather small due to weakness of the applied field ( $10^8 \text{ Vm}^{-1}$ ) with respect to the intra-atomic field ( $10^{11} \text{ Vm}^{-1}$ ). This polarization does, however, react to extremely high frequencies ( $>10^{15} \text{ Hz}$ ). Since the movement of the heavy nuclei is more laborious than for electrons, the atomic distortion polarization is observed at frequencies somewhat lower ( $10^{12} - 10^{15} \text{ Hz}$ , near IR).

In the nonuniform field the molecule experiences a net force as well as a net torque responsible for the orientation polarization. Orientation polarization is highly dependent on molecular interactions. The dipoles make a significant contribution to the average dipole moment (total

polarization), but it may be slow to develop, possibly covering a frequency range of  $10^0$  to  $10^{12}$  Hz. Much more discussion will be directed toward the subject of orientational polarization once fundamental circuitry and capacitance are elaborated in the reference frame of dielectric materials.

Distortion polarization occurs in both polar and nonpolar molecules and is independent of a permanent dipole moment. It has two components, atomic and electric. These are induced by the electric field. The electron cloud is distorted by the electric field ;the nuclei may also be displaced which alters the bond lengths and angles. These changes are quite rapid and are able to follow oscillating fields of high frequencies. With increasing temperature, this distortion varies minutely; the orientation polarization, conversely, shows a characteristic decrease as the thermal motion enhances the more random orientation. As a result, the permattivity of polar molecules decreases more rapidly than the nonpolar molecules with increasing temperature.

In summary the orientation and distortion polarization are understood as follows

$$3 \quad P_{\text{polar}} = P_0 + P_{\text{atomic}} + P_{\text{electronic}}$$

$$4 \quad P_{\text{nonpolar}} = P_{\text{atomic}} + P_{\text{electronic}}$$

## 2. ELECTROSTATIC RELATIONS

Understanding the circuitry of a parallel plate capacitor is essential to fully appreciate the behavior of a material in an electric field. In this section, electrostatic relations will be discussed prior to the more complex subject of dynamic relations.

### a. CAPACITANCE.

Capacitance is the ability of a passive circuit element to store electrical charges. A capacitor is constructed by placing a dielectric between two equally but oppositely charged conductors (plates) and applying a potential difference, or voltage, between the two conductors.

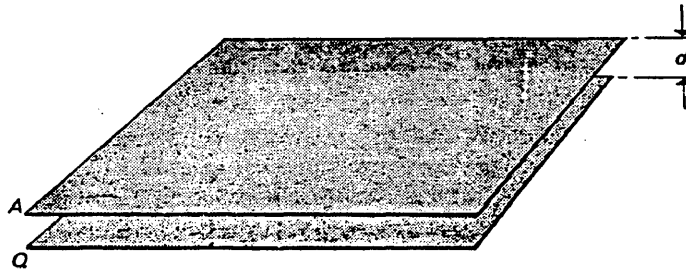


Illustration 3.6

Charge is transferred from one plate to the other until the potential between the two plates is equivalent to the voltage drop across the battery terminals. The capacitance,  $C$ , is the ratio of the charges on the conductor to the applied voltage. The value of  $C$  is specific for the dielectric material and conductor geometry.

Neglecting edge effects and treating the conductors as infinite planes of charge with charge density  $Q/A$ , the field within the plates is

$$6 \quad E = Q/A \cdot 1/\epsilon_0$$

where  $\epsilon_0$  is the permittivity of free space ( $8.85 \times 10^{-12} \text{ Fm}^{-1}$ ). Outside of the plates the fields cancel; inside, they add (field lines are directed from negative charge toward positive charge). Illustration 3.7 shows the field in vacuo.

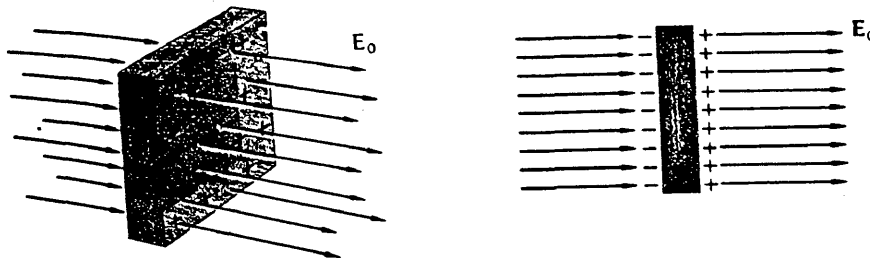


Illustration 3.7

By definition, the potential difference between the plates,  $V$ , is the cross product of the field and instantaneous displacement of the charge. Therefore,  $V$  can be defined by charge and geometry of the capacitor.

$$7a \quad V = E \int \delta d \quad \text{where } d \text{ is the distance between the plates}$$

$$7b \quad V_0 = E_0 d$$

$$7 \quad V_0 = Q_0 d / \epsilon_0 A$$

Using equation #6, capacitance is redefined:

$$8 \quad C = Q/Ed$$

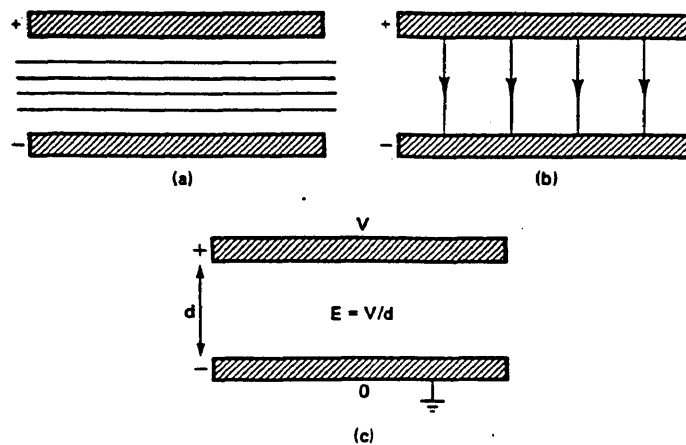


Illustration 3.8

### b. PERMITTIVITY DEFINED THROUGH CAPACITANCE

Once a dielectric is inserted between the plates, the orientation polarization changes the field and capacitance : this partially cancels the original field. The molecules orient themselves with the positive ends of the dipole toward the negative electrode and the negative toward the positive.

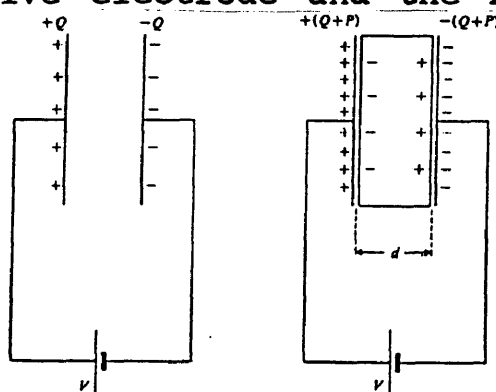


Illustration 3.9

While the interior of the material remains fairly neutral, the surfaces adjacent to the electrodes build up excess charges. These charges are bound strongly to the plates and are, therefore, restricted in movement. These bound charges reduce the effective strength of the applied field. The

battery maintains constant voltage by supplying more charge to the plates. While more charge is stored on the plates, the free charge,  $Q$ , on the plates remains constant. The end result is increased capacitance. This increased capacitance due to the dielectric is related to the capacitance of a vacuum through the dielectric constant of the material.

9

$$\epsilon = C/C_0$$

### c. ELECTRIC DISPLACEMENT

The value of  $\epsilon$  depends on the amount of polarization within the material. Defining polarization as bound charge per unit area,  $P$  can be redefined as

10

$$\epsilon = (Q + P)/Q$$

where the emf remains unchanged. Since the electric field changes, it is useful to describe the charge in terms of the field:

11a

$$\epsilon = (\epsilon_0 E + P)/\epsilon_0 E$$

11b

$$P = (\epsilon - 1) \epsilon_0 E$$

11c

$$P = \epsilon_0 \epsilon E - \epsilon_0 E$$

11

$$D = P + \epsilon_0 E = \epsilon_0 \epsilon E$$

The quantity  $D$  is the electric displacement (flux of free charges), a fundamental field equation applying at any point in an isotropic medium.  $\epsilon_0 \epsilon$  is absolute permittivity of the material. Thus, the dielectric constant is relative with respect to  $\epsilon_0$ .

An alternative approach to deriving D.

The field within the material is the applied field minus the field arising from polarization.

$$12a \quad E_{int} = E_o - E_{pol}$$

$$12b \quad E_{int} = E_o - 1/(\epsilon_o)P$$

But the applied field is also described as  $E \epsilon$

$$12c \quad E = E \epsilon - (1/\epsilon_o)P$$

$$12d \quad P = E \epsilon_o \epsilon - \epsilon E$$

12

$$D = \epsilon_o \epsilon E$$

This quantity will be used again to discuss a material's electrical properties in a sinusoidally oscillating field.

#### d. RELAXATION TIME

In a static field, polarization equilibrium is obtained. When the field is removed, the polarization decreases with a characteristic time,  $\tau$ , to zero. In an alternating electric field, the molecules attempting to reach equilibrium experience a lag. Orientation polarization causes this delayed response. Electronic and atomic polarizations are too fast to be considered here. The rate of dipolar relaxation is out of phase with the applied electric field; because of this, the dielectric material will absorb energy and dissipate excess energy in the form of heat.

### 3. DYNAMIC RELATIONS

#### a. RC CIRCUITRY AND IMPEDANCE

Simply, an alternating electric field is generated by a coil rotating in a uniform magnetic field as diagrammed below.

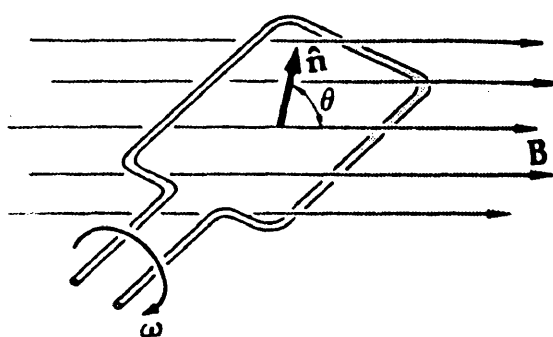


Illustration 3.10

$B$  is the magnetic field,  $\theta$  is the angle created by the vector normal to the plane of the coil,  $n$ , with the magnetic field, and  $\omega$  is the angular frequency of the rotations expressed in radians per unit time.

The magnetic flux through the coil is  $\phi = NBA \cos \theta$ , where  $N$  is the number of turns the coil makes,  $A$  is the area of the coil. If an external force rotates the coil an emf will be generated within the coil equivalent to  $d(\alpha)/dt = NBA \sin(\omega t)$ . Maintaining constant angular velocity within the magnetic field generates a sinusoidal potential which converts mechanical energy to electrical energy.

Table 3.1 defines potential and current by the three components inductance ( $L$ ), capacitance ( $C$ ), and resistance ( $R$ ). The derivation of which can be found in any fundamental

physics text. The terms are expressed as sine functions to draw attention to the phase difference between the components.

TABLE 3.1

COMPONENT	VOLTAGE	CURRENT
L	$LdI/dt, V\sin(\omega t)$	$(V_{\max}/\omega L)\sin(\omega t - 90^\circ)$
R	$IR$	$(V_{\max}/R)\sin \omega t$
C	$Q/C$	$(CV_{\max}\omega)\sin(\omega t + 90^\circ)$

It can be determined from the above relationships that the voltage and current are in phase. The capacitance and conductance originate from the same point but in opposite directions (phasor diagram, figure #3.11). The inductance and current are  $90^\circ$  out of phase with the voltage; the inductance trailing and the current leading.

As the dielectric material between the plates of a capacitor behaves like a resistor and capacitor in series (or parallel), the remaining discussion will be limited to RC circuits.

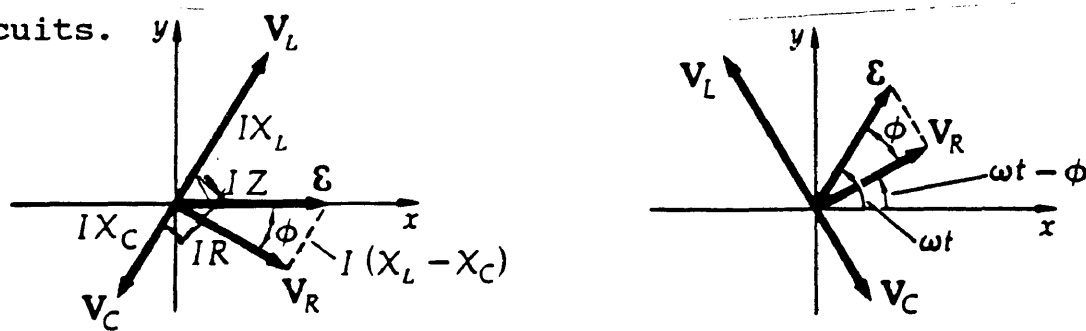


Illustration 3.11

As the phasor diagram illustrates, the applied voltage

is the summation of the y components of the emf in accordance with Kirchoff's Second Law (Conservation of energy). Therefore,  $V_{\text{appl}} = V_c + V_r$ . But by geometry,  $V_{\text{appl}} = [(V_r)^2 + (V_c)^2]^{.5}$ . And by comparing the two equivalent expressions it follows that  $b^2 = (V_c)^2$ .

$$13 \quad V = [(IR)^2 + (I/\omega t * (\cos \omega t))^2]^{.5}$$

Representing the voltage in such a manner shows the voltage in both of the passive elements to be proportional to the current. This proportionality constant is Z, the impedance, measured in ohms.

$$14 \quad V = \sum ZI$$

Therefore, for this circuit, the impedance is defined as

$$15 \quad Z = R + [C\omega(\cos \omega t)]^{-1}$$

Or following the same derivation but representing the field as a complex quantity,  $V = V_0 e^{i\omega t}$ , the impedance is described as

$$16 \quad Z = R + 1/(i\omega C)$$

$$17 \quad \tan \phi = 1/(i\omega CR) = -1/(\omega CR)$$

### b. COMPLEX PERMITTIVITY

An applied alternating emf alternates the field. Therefore we must expand the definition for the static permittivity to include an oscillating field. The alternating electric field will produce polarization of changing magnitude and direction within the dielectric material. If the angular frequency is high enough, the orientation of the dipoles will lag behind the field. This lag,  $\delta$ , is expressed by the dielectric displacement. Illustrated below is a typical sinusoidal displacement curve;  $\tau$  is the time at which the displacement reaches its maximum.

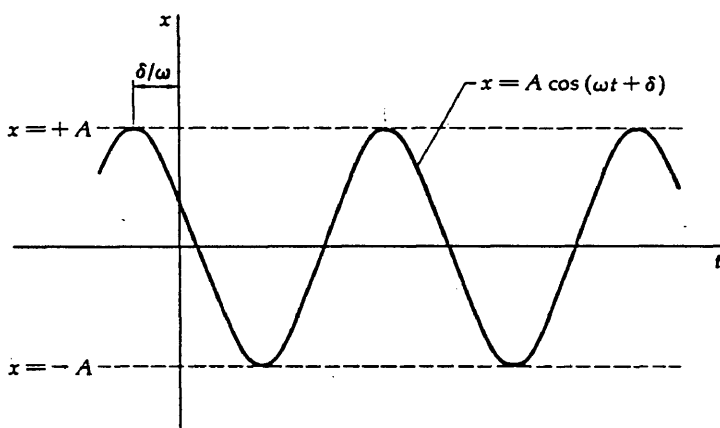


Illustration 3.12

$$18a \quad D = D_0 \cos(\omega t - \delta)$$

Using the trigonometric relationship for the difference:

$$18b \quad D = D_0 \cos(\omega t) \cos(\delta) + D_0 \sin(\omega t) \sin(\delta)$$

and separating into two terms

$$18 \quad D = D_1 \cos(\omega t) + D_2 \sin(\omega t)$$

where  $D_1$  and  $D_2$  define the in phase and out of phase displacements, respectively.

This separation of terms can also be extended to the dielectric constants. (Recall  $D = \epsilon_0 \epsilon E$ )

$$19 \quad \epsilon' = D_1 / \epsilon_0 E$$

$$20 \quad \epsilon'' = D_2 / \epsilon_0 E$$

$$21 \quad \frac{\epsilon''}{\epsilon'} = \tan \delta$$

Summing the two constants and employing complex notation, the dynamic permittivity is defined by equation 22.

$$22 \quad \epsilon^* = \epsilon' - j\epsilon''$$

The material has a dual functionality, one in phase and the other  $90^\circ$  out of phase. This is represented more clearly when seen in the circuit with alternating voltage.

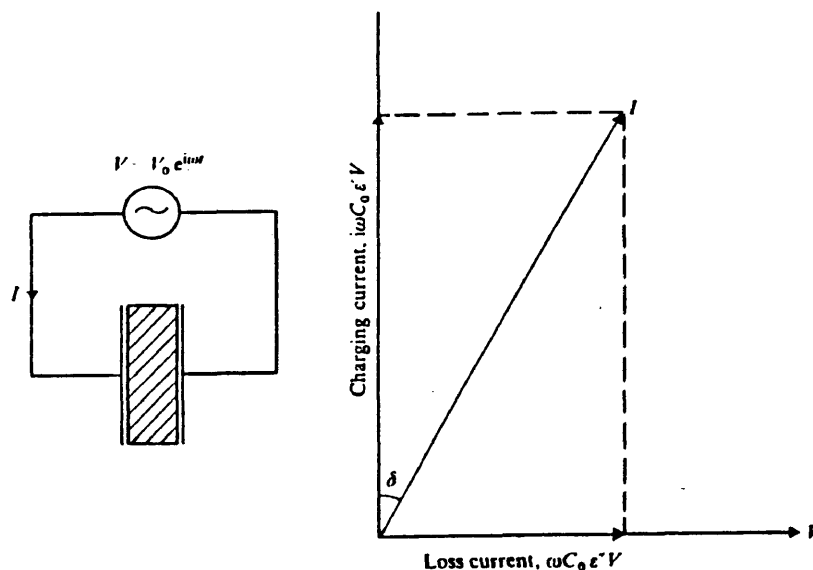


Illustration 3.13

Recalling equations ( $I=i\omega CV$  and  $C=\epsilon*C_0$ ), the following derivation defines the behavior of the dielectric material between the plates of a parallel capacitor as a resistor and capacitor in series.

$$\begin{aligned}
 I &= i\omega\epsilon*VC_0V \\
 I &= i\omega(\epsilon' - i\epsilon'')C_0V \\
 I &= \omega C_0(\epsilon'' + i\epsilon')V \\
 23 \quad I &= \omega C_0 \epsilon''V + i\omega\epsilon'VC_0
 \end{aligned}$$

The real portion is in phase and the imaginary portion out of phase with the voltage.

$$24 \quad I_R = \omega C_0 \epsilon''V \quad \text{and} \quad I_C = i\omega C_0 \epsilon'V$$

The current represented in this way is identical to the current for an RC circuit. Therefore, the dielectric material between the plates eliminates the need for a resistor within the circuit. And it allows for the determination of the dielectric constant of materials by measuring the impedance of an element with known capacitance and frequency of oscillation.

The impedance of the series circuit is

$$25 \quad Z = R_s + 1/i\omega C_s$$

Similarly the impedance of a parallel circuit is

$$26 \quad 1/Z = 1/R_p + i\omega C_p$$

Application of an AC voltage results in both an in phase and

out of phase current

$$V = Z \cdot I$$

$$26a \quad I_C = V(i\omega C_p) \quad (\text{as previously found})$$

$$26b \quad I_R = V/R_p$$

And as we found earlier, two dielectric components

$$26c \quad \epsilon' = C_p/C_o$$

$$26d \quad \epsilon'' = (1/R_p) * (1/C_o\omega)$$

$$26e \quad \tan \delta = 1/(R_p C_p \omega)$$

### c. DIPOLAR AND IONIC CONTRIBUTIONS TO PERMITTIVITY

Debye derived the frequency dependence of the resistive and capacitive components of the complex permittivity as follows (derivations provided in appendix A)

$$27 \quad \epsilon'(\omega) = \epsilon_\infty + (\epsilon_s - \epsilon_\infty) / (1 + \omega^2 \tau^2)$$

$$28 \quad \epsilon''(\omega) = \omega \tau (\epsilon_s - \epsilon_\infty) / (1 + \omega^2 \tau^2)$$

using the quantity  $\tau$  as the characteristic relaxation time. The terms  $\epsilon_\infty$  and  $\epsilon_s$  refer to instantaneous dielectric constant and static dielectric constant respectively. The first measures the dielectric constant at zero polarization, immediately after the field is applied.  $\epsilon_s$  is the highest observable dielectric constant, corresponding to maximum polarization.

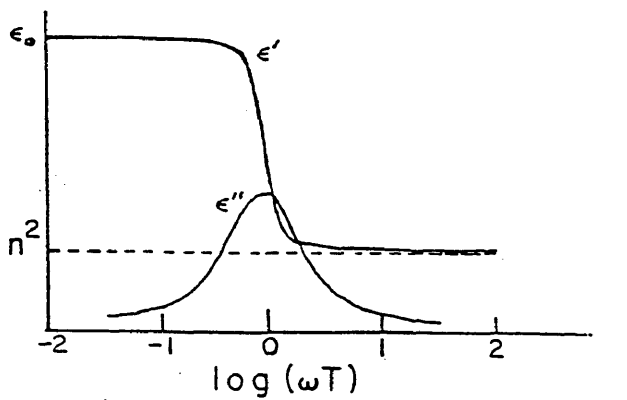


Illustration 3.14

The figure above shows the ideal behavior of a Debye relaxation. The relaxation of most polymers, however, is more broadly dispersed than the Debye derivation allows. This led Davidson and Cole (1950) to modify the above equation to

$$29 \quad \epsilon_d^* = \epsilon_\infty + (\epsilon_s - \epsilon_\infty) / (1 + i\omega\tau)^\beta$$

The parameter  $\beta$  has no theoretical function but it gives an improved fit.

The two components of the dielectric constant can each be separated into dipolar and ionic contributions.

$$30 \quad \epsilon' = \epsilon'_i + \epsilon'_d$$

$$31 \quad \epsilon'' = \epsilon''_i + \epsilon''_d$$

At low frequencies, low viscosities and higher temperatures, the ionic component of the complex permittivity often dominates. Johnson and Cole derived the following empirical equations for the ionic contributions of the molecule.

$$32 \quad \epsilon_i'(\omega) = C_o Z_o \sin(n\pi/2) \omega^{-(n-1)} (\sigma / 8.85 \cdot 10^{-14})^2$$

$$33 \quad \epsilon_i''(\omega) = (\sigma / 8.85 \times 10^{-14} \omega) - C_0 Z_0 \cos(n \pi / \omega) \omega^{-(n-1)} + (\sigma / 8.85 \times 10^{-14})$$

$Z_0$  is the impedance.

$C_0$  is the capacitance.

$\sigma$  is the conductivity, an intensive variable.

The first term in equation 33 is due to conductance of ions translating through the medium; the second term is due solely to polarization. At high frequencies where the electrode polarization is not generally significant, (less than 10Hz), sigma and tau can be evaluated through equation 33. When values of  $\epsilon'' \cdot \omega$  lie along the same line in the lower frequency region, sigma can be determined. In turn, sigma is subtracted from  $\epsilon''_{\text{meas}}$  to determine  $\epsilon''_{\text{dipolar}}$  from which tau is extrapolated. Tau is evaluated at the time when  $\epsilon'' \cdot \omega$  peaks.

## B. EXPERIMENTAL

The dielectric measurements were made using a Hewlett-Packard 4192A LF Impedance Analyzer controlled by a Model 9826 Hewlett-Packard computer. The resin was applied in a thin layer over a geometry-independent Dek Dyne/180 sensor positioned in a beaker. The beaker was then immersed in a water bath of the desired temperature, purged with nitrogen gas and sealed. Due to the exothermic nature of the reaction, the water bath was required to maintain constant

temperature within the environment of the curing system. Measurements of the complex permitivity over frequencies from 5 to  $5 \times 10^6$  Hz and temperature were recorded at regular intervals and stored on computer disk. The temperature was monitored with an iron-constantan thermocouple embedded in the resin; the temperature was displayed by a Keithley 179 TRMS Digital Multimeter. The recorded data was plotted using a Hewlett-Packard 7475-A six pen plotter.

Dynamic Mechanical Measurements were made using a Rheometrics model RDS 7700 rheometer.  $G'$  (dynamic storage modulus) and  $G''$  (dynamic loss modulus) were measured. The freshly mixed resin was poured onto the lower 50mm parallel plate and the upper was adjusted to 0.5-1.0mm gap. The material properties were measured to the material stiffness limit of the apparatus ( $10^6$ - $10^7$  dynes/cm<sup>2</sup>).

Barcol Hardness measurements were made with a hardness tester model GYZJ-935 provided by Paul N. Gardner Company. This model, one range lower than the one normally used for polyester resins, was more sensitive to early cure development. The hardness data was recorded in triplicate and the average of the values used in computations.

## B. RESULTS AND DISCUSSION

### 1. ANALYSIS OF $\epsilon'$ AND $\epsilon''$

Monitoring a curing polyester resin by DDA is useful in that it measures the onset of the reaction, the time to maximum in the exotherm, as well as the completion of reaction- knowledge of which is crucial to successful application. This technique also defines the regions of ionic and dipolar molecular motions which provides insight into the flow state and hence important transitions.

#### a. ONSET OF POLYMERIZATION

It has been shown that the onset of polymerization corresponds to a change in the real component of the permittivity,  $\epsilon'$ , (5). Traces of the temperature of the reacting system are superimposed on the plots of permittivity (figures 3.1-3.9). These figures show the onset of the reaction throughout the temperature range of 0 to 60° C and the sensitivity of the technique in monitoring the fluidity of the system. The formation of a charge layer causes a rise in permittivity. In fluids, ions migrate to the electrode surfaces and may form an electric "double layer". These ions diffuse through the layer and discharge at the electrode causing polarization. Decreasing viscosity enhances this phenomenon and is detected by increasing permittivity.

$\epsilon'$  rises almost imperceptibly in the lower

temperatures before dropping off sharply. The point at which  $\epsilon'$  drops marks the beginning of the reaction. The molecular weight begins to build up instantaneously. A large exotherm effects the permitivity as seen in figures 3.10 and 3.11. The permitivity drops initially as the molecular weight builds up but there is bump in the downward trend. This is attributed to a sudden increase in temperature which decreases the viscosity, hence, increasing the permitivity (marked B).

TABLE 3.2

TEMPERATURE	TIME TO ONSET OF REACTION	MAX TEMPERATURE OF EXOTHERM
25	27	25
25	27	85
30	18	32
34	6	35
35	6	42
40	3	40
45	2	45
50	0	52
60	0	66

The higher temperatures (>35) effect the flow of the resin; the viscosity decreases with these higher temperatures and the permitivity increases.

The 60 degree reaction shows the competition between the viscosity increasing as a result of the rapidly

increasing molecular weight of the propagating reaction and viscosity decreasing as a result of the increase in temperature. The molecular weight build up is instantaneous, reflected by the initial decrease in  $\epsilon'$ . At this elevated temperature, a "run away" reaction is created- the styrene/maleic bonding occurs so quickly that there is not sufficient time for the heat to be absorbed by the surroundings water bath; the added heat further accelerates the reaction. The large exotherm follows this rise in temperature. As the temperature increases sharply to its maximum, the permitivity peaks in the lower frequencies; these frequencies follow the motion of the ions in the flow state. But this motion is quickly overcome by the increasing molecular weight.

The fact that the permitivity is sensitive to minute changes in the viscosity is seen even in low temperature runs that are nearly isothermal, with temperature changes of only 2.3 degrees celsius. The downward trend in  $\epsilon'$  is interrupted by the exotherming reaction. Point B marks the effect in the 30<sup>o</sup> reaction.

These details are also observed in the loss component of permitivity,  $\epsilon''$  (figures 3.12-3.22).

#### b. ONSET OF SOL-GEL TRANSITION

The onset of the rubbery state, referred to as the sol-gel transitions, occurs very early in the polymerization of

unsaturated polyester resins, generally at 5-10% conversion. This transition may be identified by scaling  $\epsilon''$  by  $\omega$ . Overlapping of these values indicates that the loss is dominated by ionic effects. Figures 3.12-3.22 show ionic effects dominate until the point marked B. This point is associated with the point at which the viscosity changes rapidly. These resulting gel times are compared with rheometric measurements in table 3.3 below. They are in excellent agreement.

TABLE 3.3

TEMP	TIME TO GEL ( $\epsilon'' \times \omega$ )	TIME TO GEL (VISC)
25	41	40
30	20	20
35	12	12
40	4	5
45	3	-
50	2	-

### c. COLLAPSE OF THE PROCESSING WINDOW

Soon following gel, the build up in modulus and viscosity can be accurately monitored by the dipolar relaxation time,  $\tau$ . Plots of the imaginary component of the dielectric constant,  $\epsilon''$  (figures 3.12-3.22) provide insight into motions of bound charges in a molecular system. The peaks in the dipolar contribution to the loss, usually identical to the peaks in  $\epsilon''$ , can be used to determine the times to the characteristic relaxation time  $\tau$ ,  $1/2 \pi$  frequency.

Scaling  $\epsilon''$  by  $2\pi \cdot \text{frequency}$ , puts the molecular motions as a function of time and frequency in clear perspective. During the initiation period, ionic motion dominates the term; this is seen as an overlap of the low frequencies.(6) As the reacting radicals grow in chain length, their motions become hindered and successful combination is restricted to rotational diffusion. These bound charges attempting to align with the oscillating electric field, experience a lag. The times to are specific to the molecular makeup, the kinetics and the state of the system. Figures 3.34 and 3.35 display the relaxation times as a function of cure temperature.

TABLE 3.4

TEMPERATURE	TIME(min) AT PEAK 1000kHz/5kHz	WINDOW	ALPHA	dalpha/dt(max)
0	249/385	136	--	--
10	130.5/183	52.5	--	--
25	57.5/70	13.5	.30/.45	54.2
30	37/50	12.5	.30/.46	32.4
35	27/36.7	9.7	.29/.46	25.5
40	18.7/25.3	6.6	.30/.47	17.7
45	13/17.5	4.5	.27/.43	12.9
50	10.8/15	4.2	.25/.42	9.9

Relaxations for the entire temperature range occur at approximately the same alpha for a given frequency. That is,

the dipolar relaxation depends on the amount of reacted resin. Also the highest frequency relaxes just after the maximum rate of reaction in DSC scans. Furthermore, this is not related to the sol-gel transition. At this point, the motion of the bound charges are viewed in the window of dipolar relaxation. Most of the free radicals are carried on growing chains with restricted movement.

#### d. APPROACH OF GLASS TRANSITION STATE

The permittivity also monitors the change from a rubbery state to a glassy state. This transition has been difficult to determine with differential scanning because the reaction shuts down as this point is approached under isothermal conditions and the sensitivity of the machine is reached. The time at which  $d \epsilon' / dt(5\text{kHz})$  is reduced to .001 corresponds to the time necessary to reach a glassy state at a specific temperature (figures 3.23-3.31). Table 3.3 reiterates what the DSC suggests.

Measurements of Barcol hardness at  $25^{\circ}$  and  $35^{\circ}$  were made to locate the rubber/glass transition. The results shown in figures 3.32 and 3.33 are in good agreement with the results reported for the two temperatures in the table 3.2. The change in the barcol number reaches the limit of instrument precision in 240 minutes and about 140 minutes for  $25^{\circ}$  and  $35^{\circ}$  respectively. Low frequency viscosity data contributed by Hoffman of Aristech also corroborates these times.

TABLE 3.5

TEMPERATURE (°C)	TIME TO $d\varepsilon'/dt$ 5kHz <.001	TIME TO DSC END (min)	ALPHA AT DSC END
0	900	---	---
10	460	---	---
25	240	150	.76
30	120	145	.81
35	140	107	.86
40	95	100	.91
45	81	83	.90
50	63	65	.92
60		45	.96

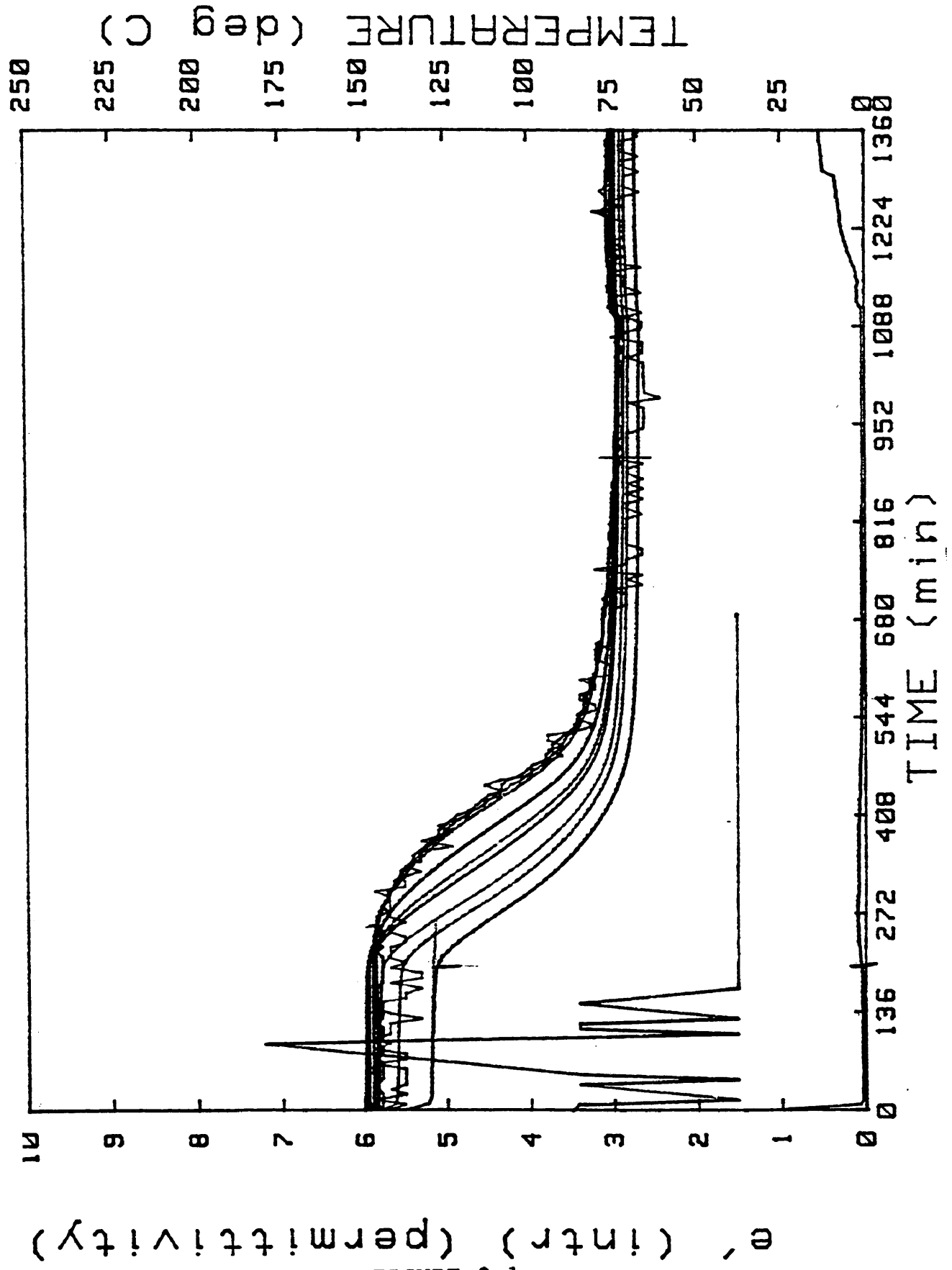


FIGURE 3.1

TEMPERATURE (deg C)  
250  
225  
200  
175  
150  
125  
100  
75  
50  
25

TIME (min)

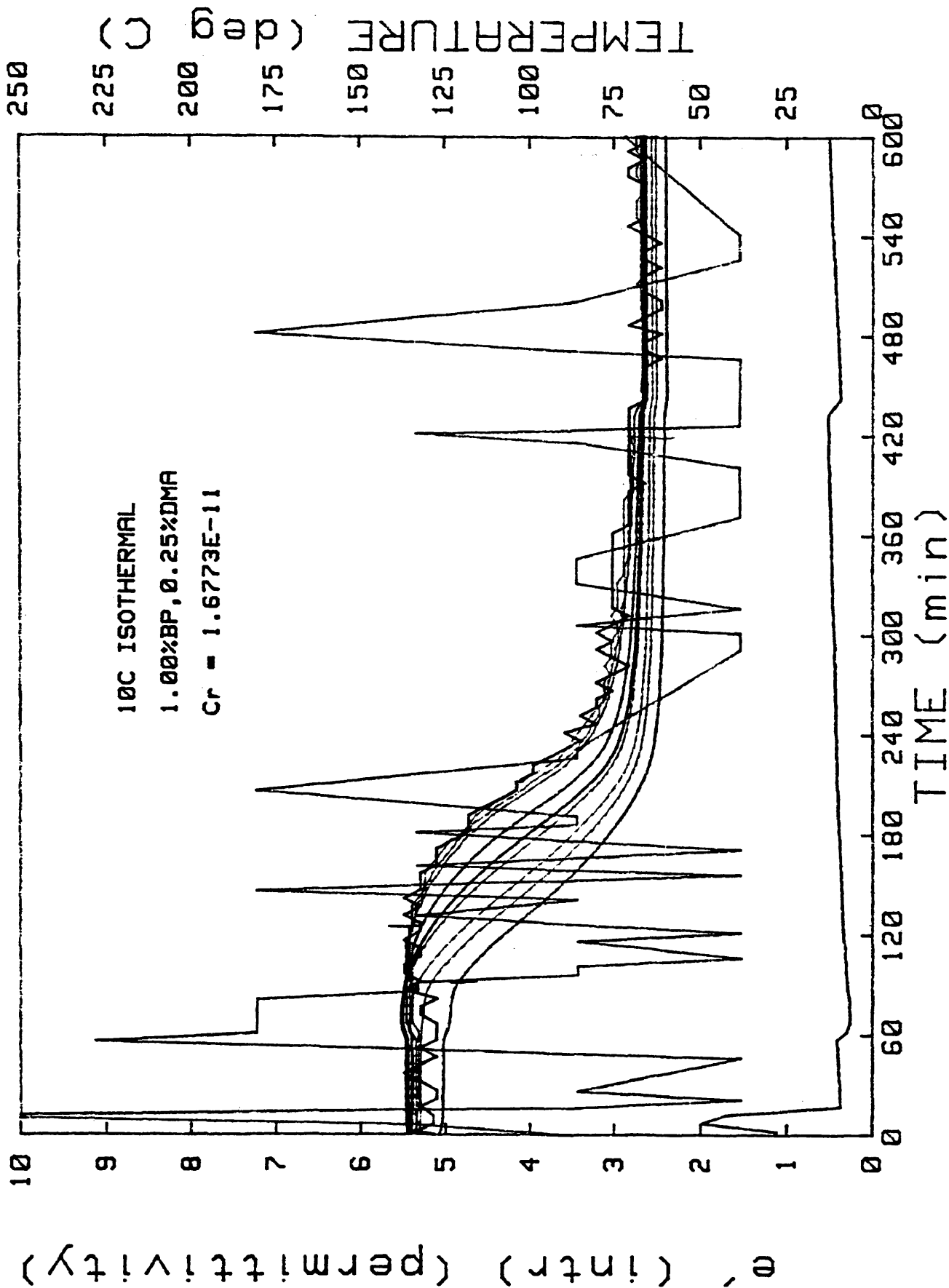


FIGURE 3.2

ARISTECH 24C

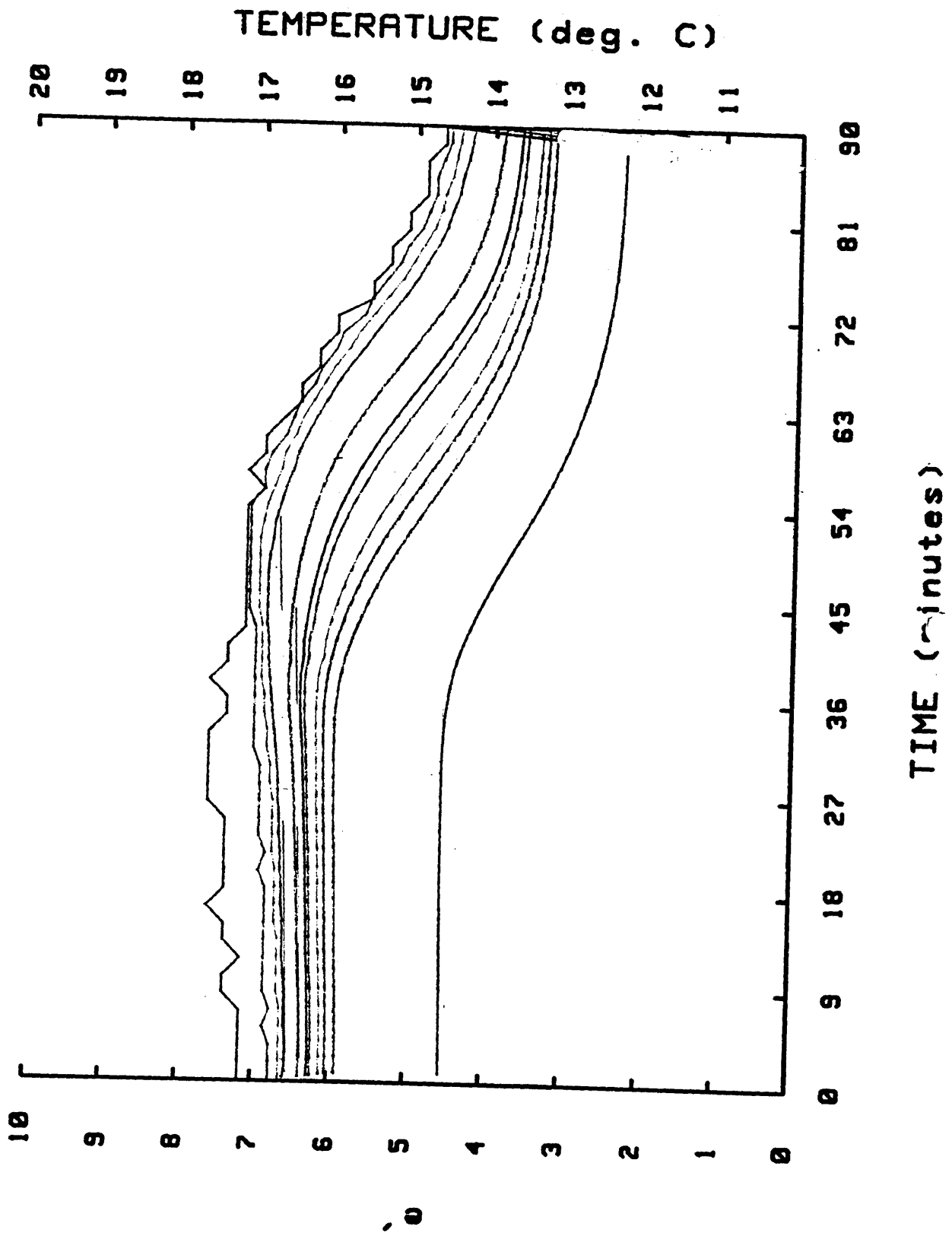


FIGURE 3.3

ARISTECH 30C ISOTHERMAL

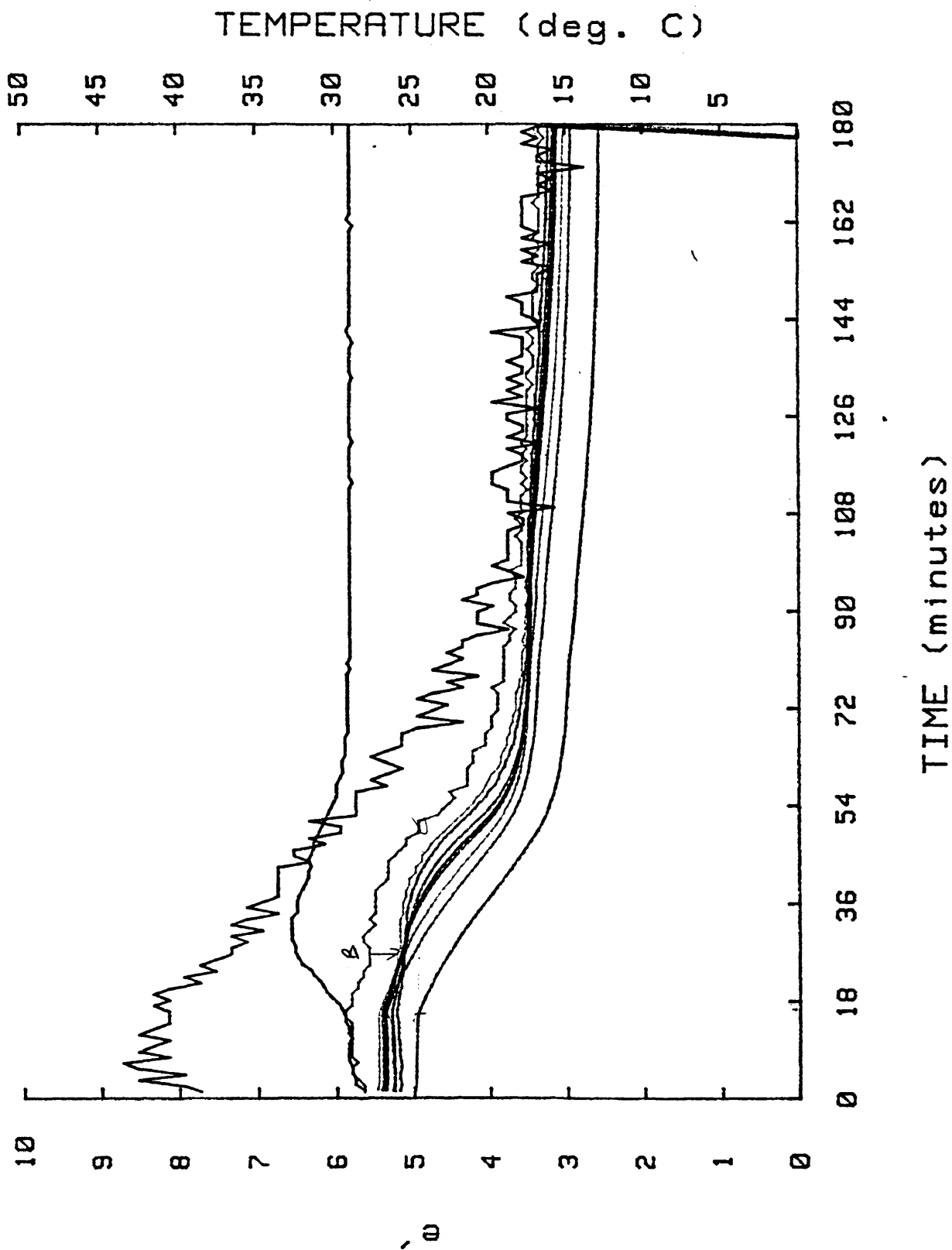


FIGURE 3.4

ARISTECH POLYESTER 35C

PT070788 Probe # 1

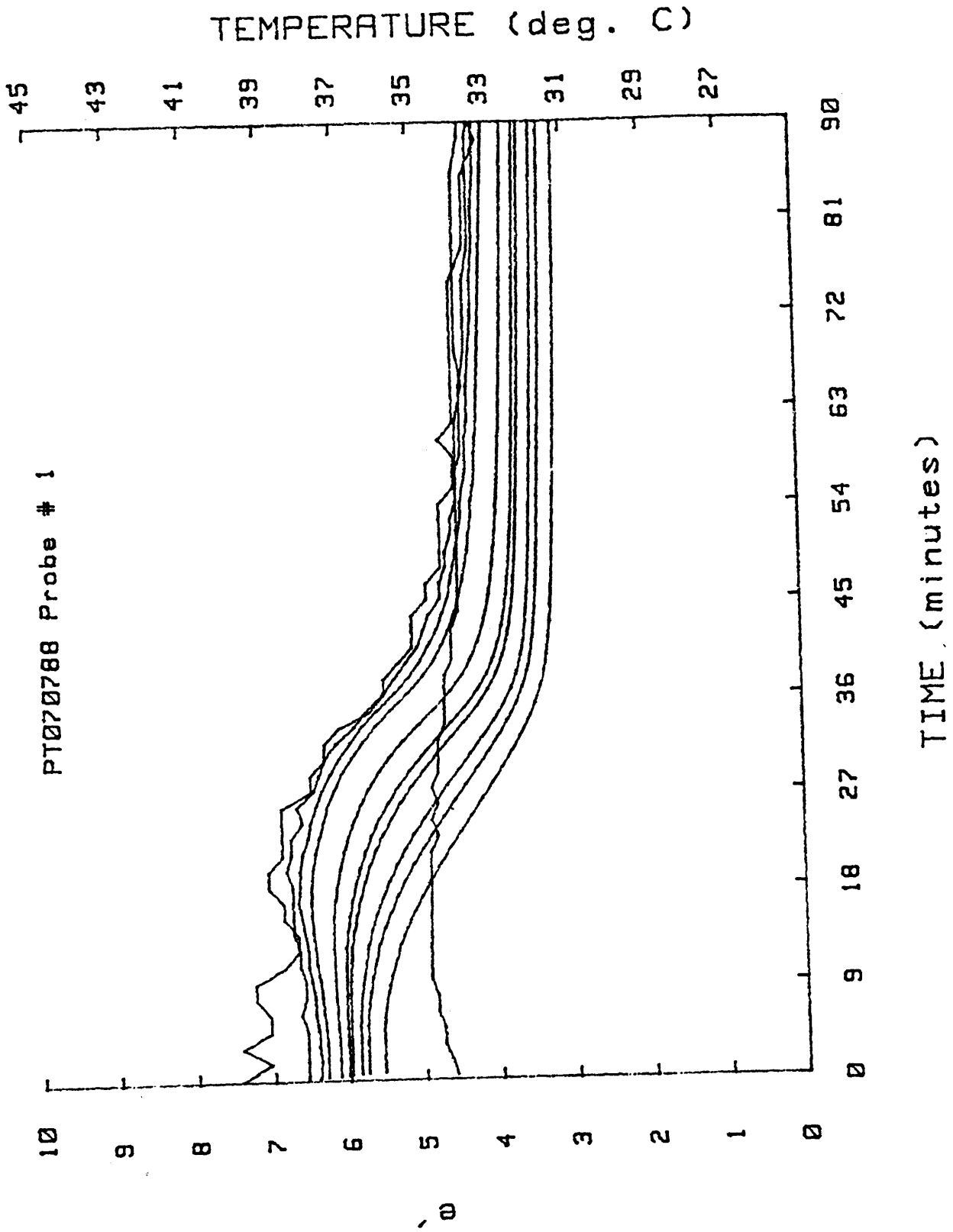


FIGURE 3.5

ARISTECH POLYESTER, 40C

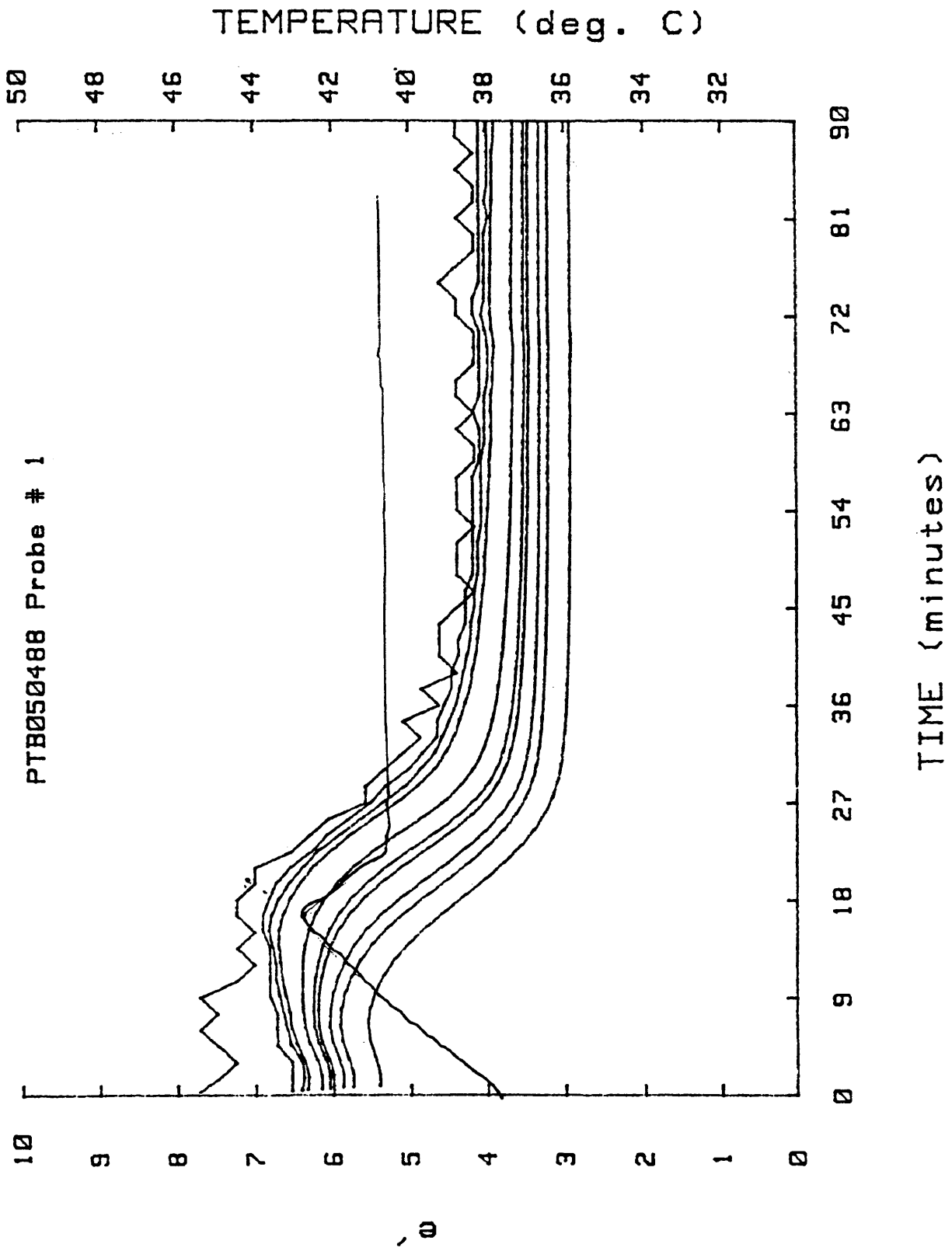


FIGURE 3.6

ARISTECH POLYESTER 45C

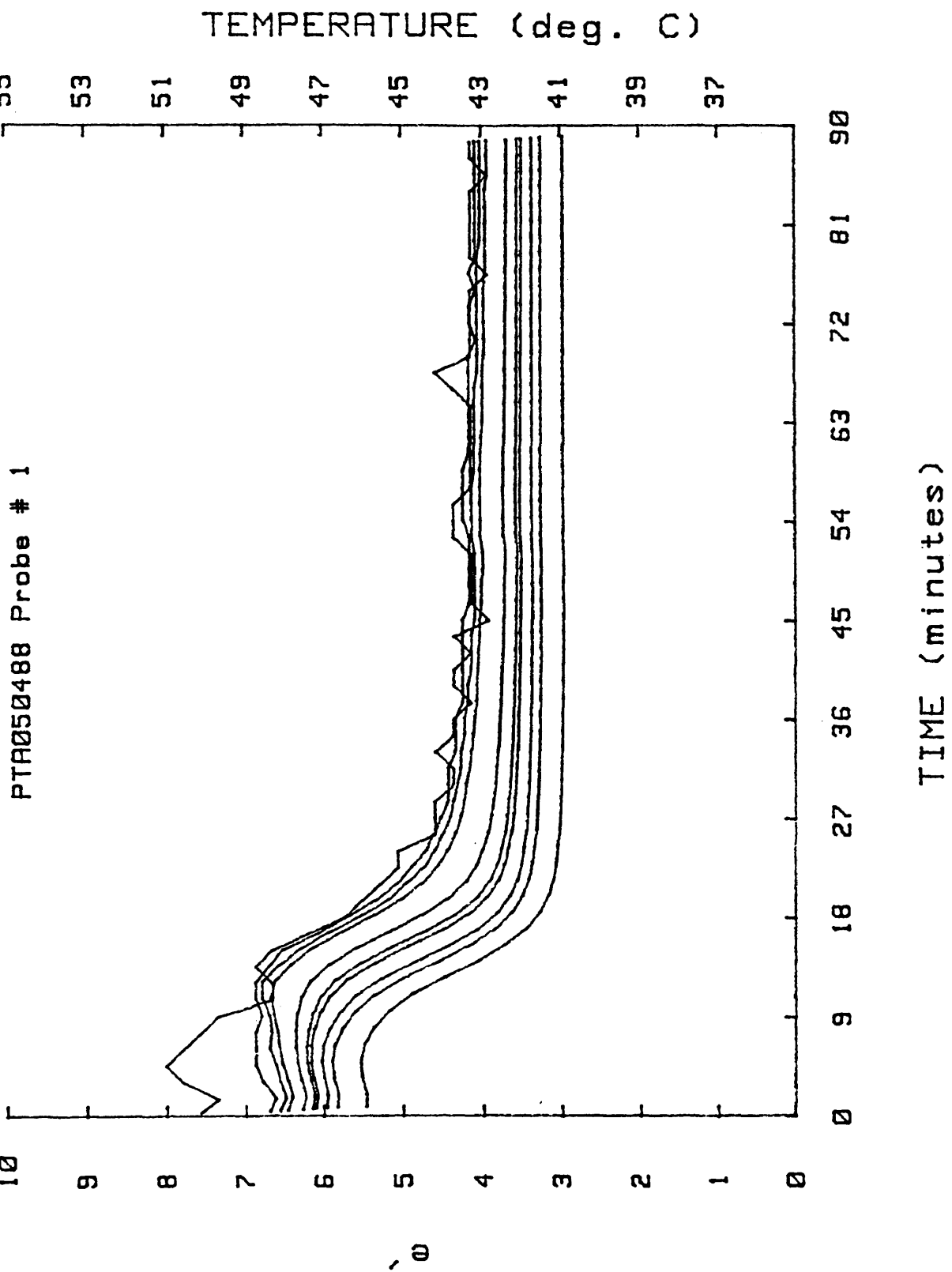


FIGURE 3.7



ARISTECH POLYESTER 60C

PHT050388 Probe # 1

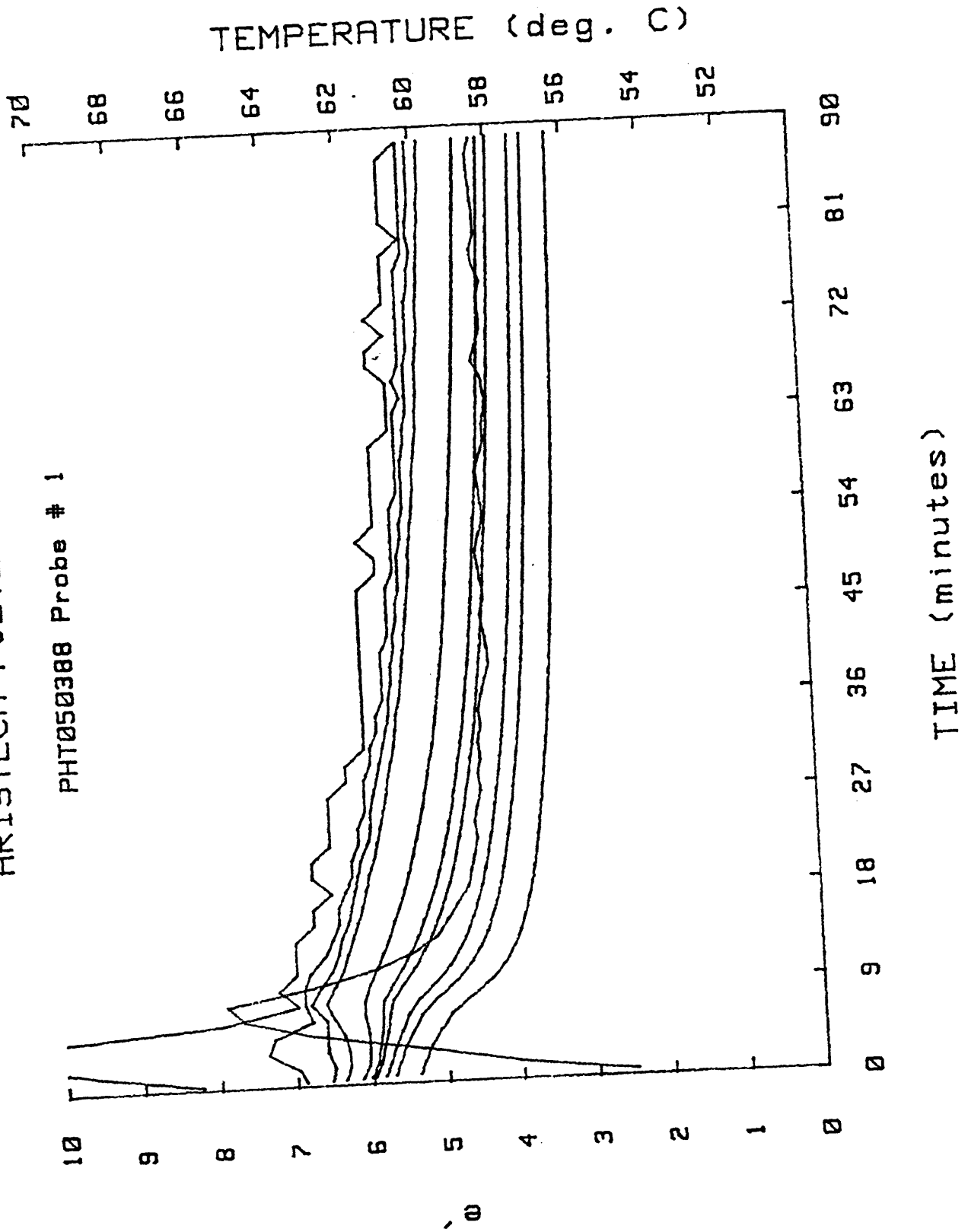


FIGURE 3.9

PH071687A:MEMORY, 0 Probe 1 ARISTECH

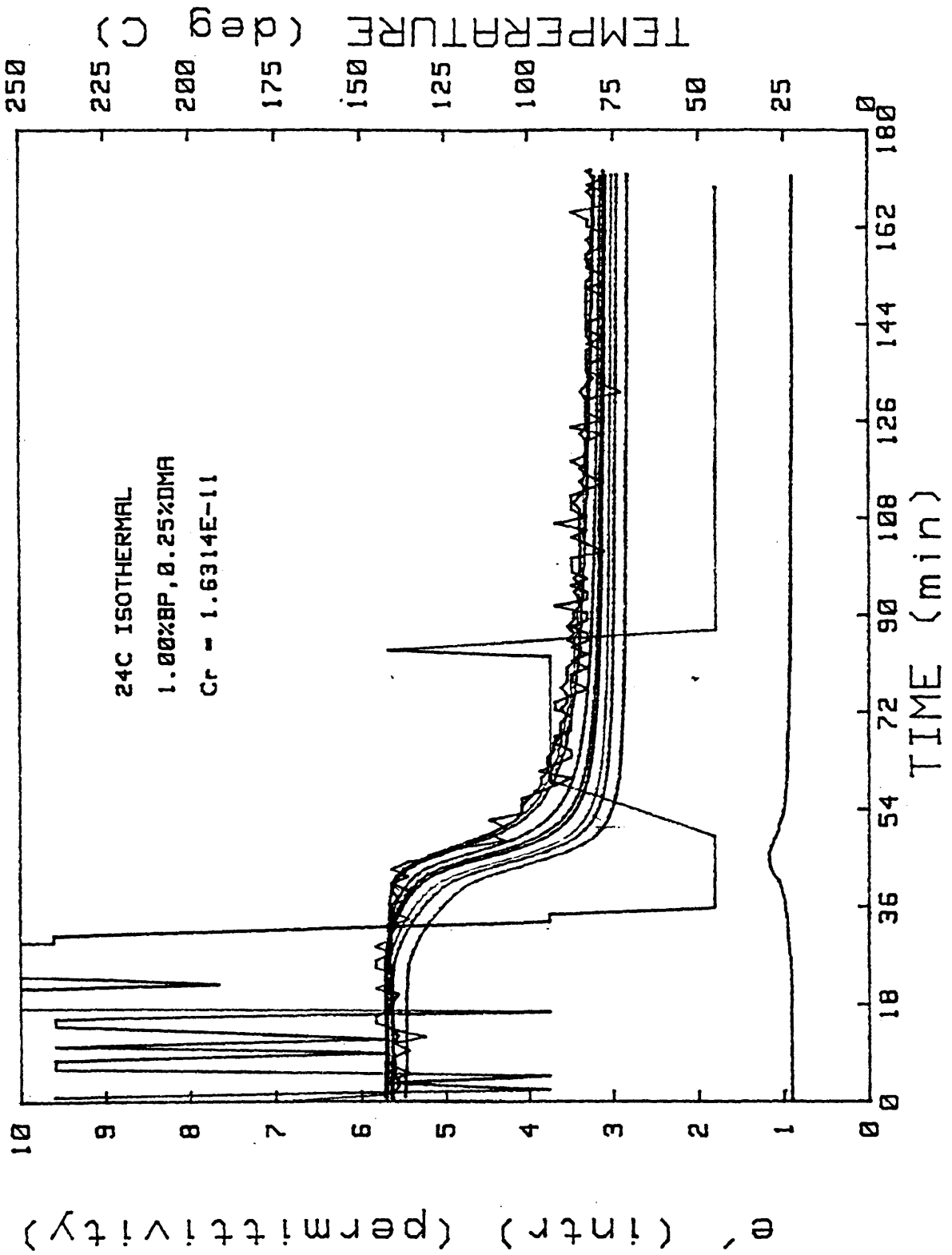


FIGURE 3.10

ARISTECH POLYESTER RESIN

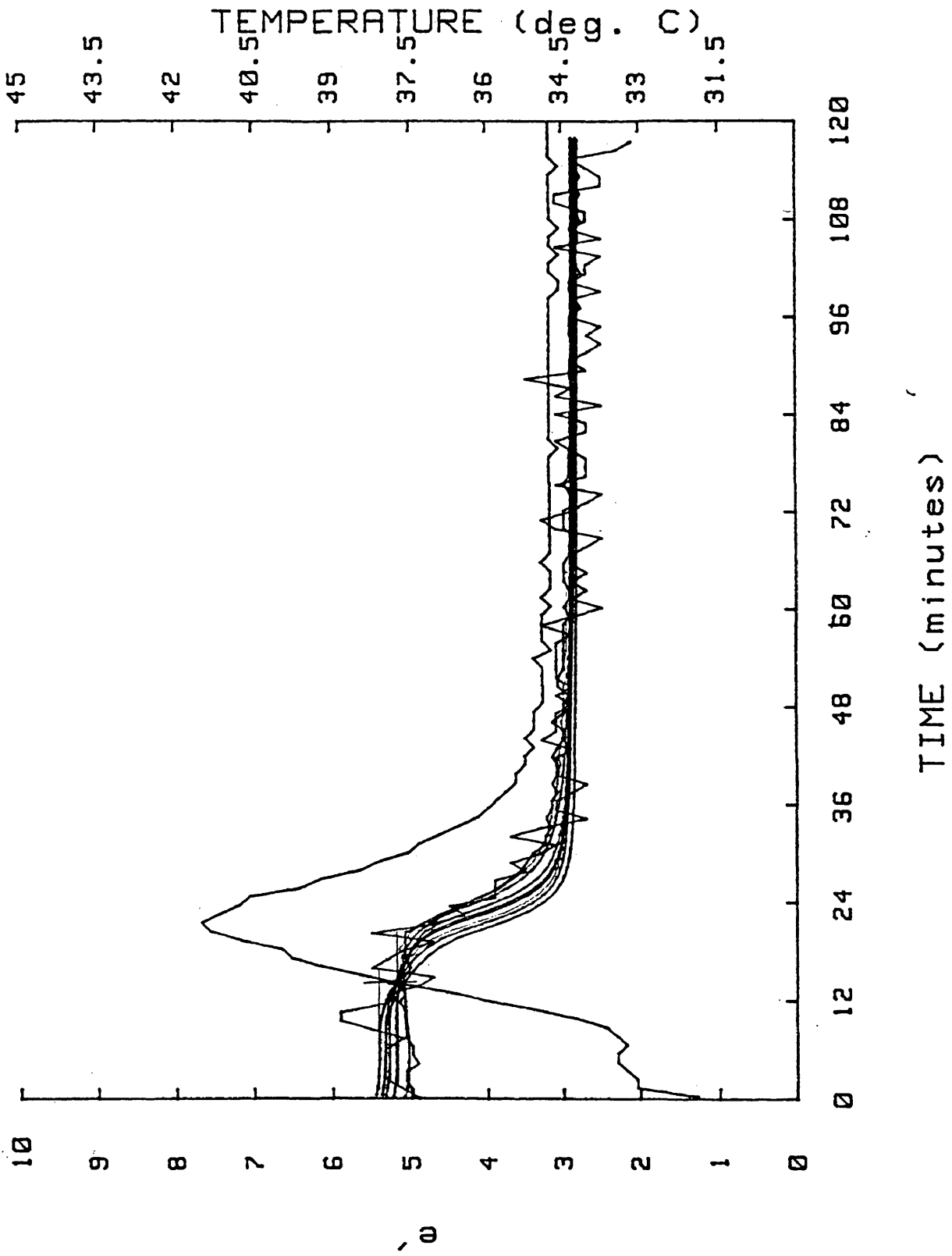


FIGURE 3.11

ARISTECH 0C ISOTHERMAL

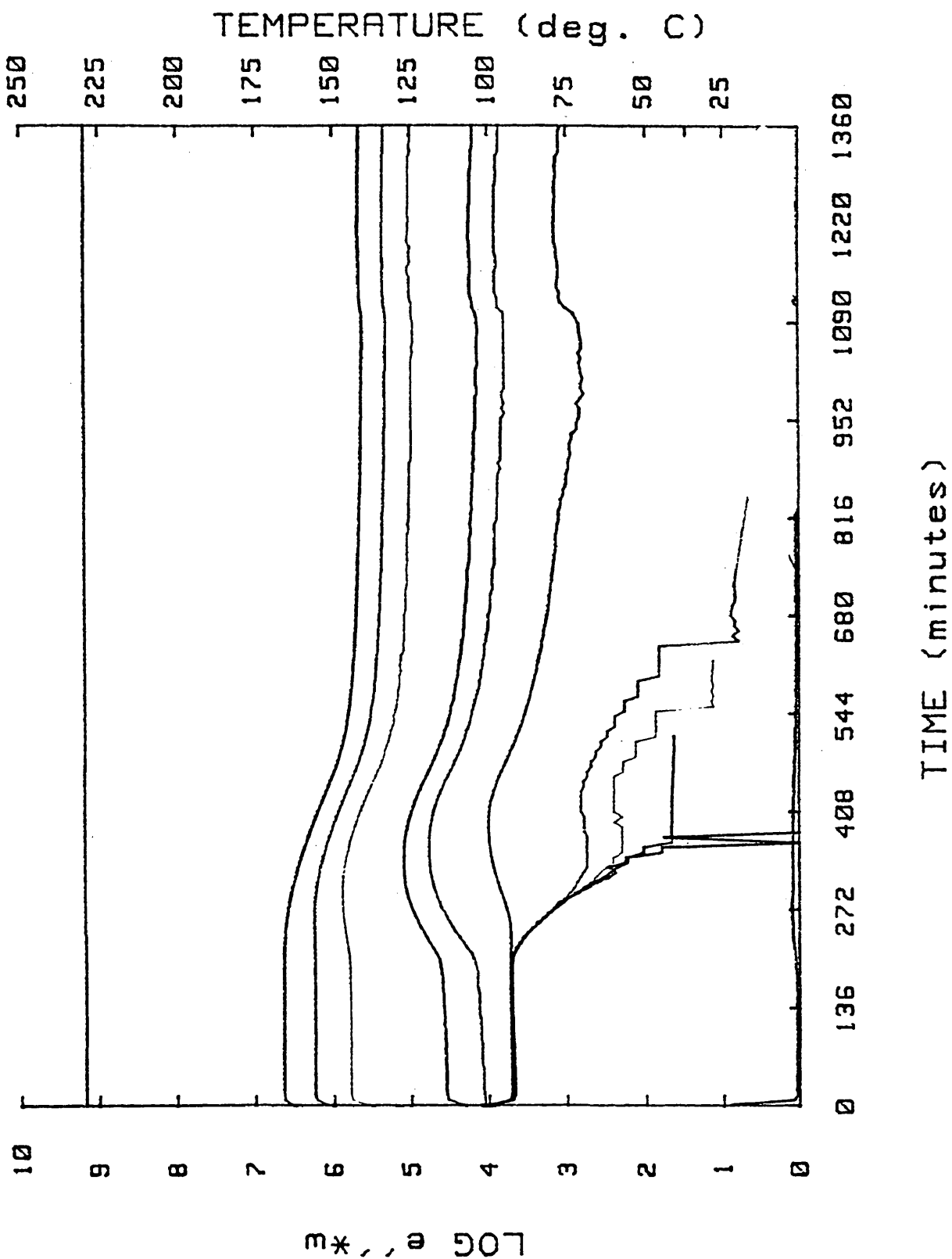


FIGURE 3.12

ARISTECH 15C

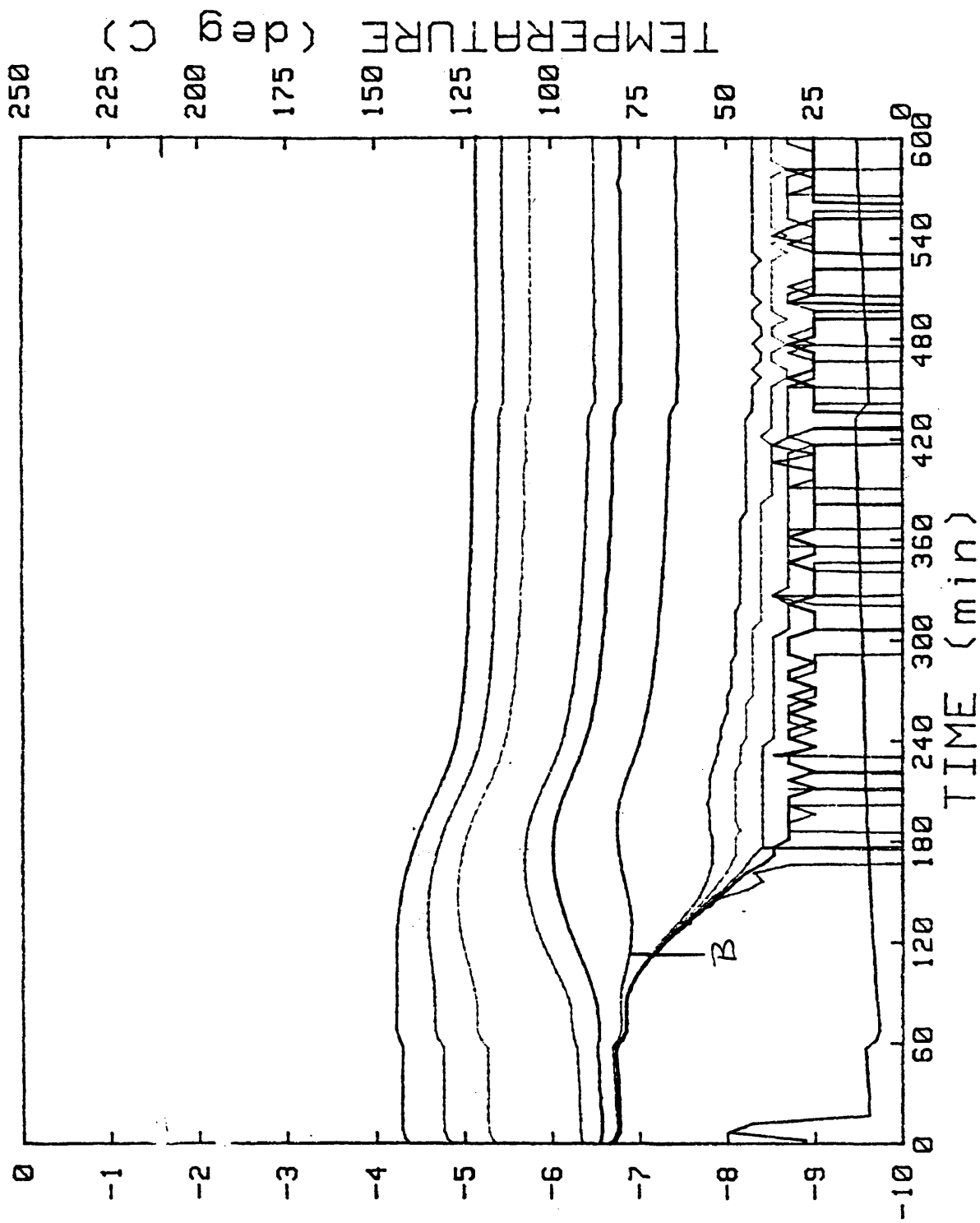


FIGURE 3.13

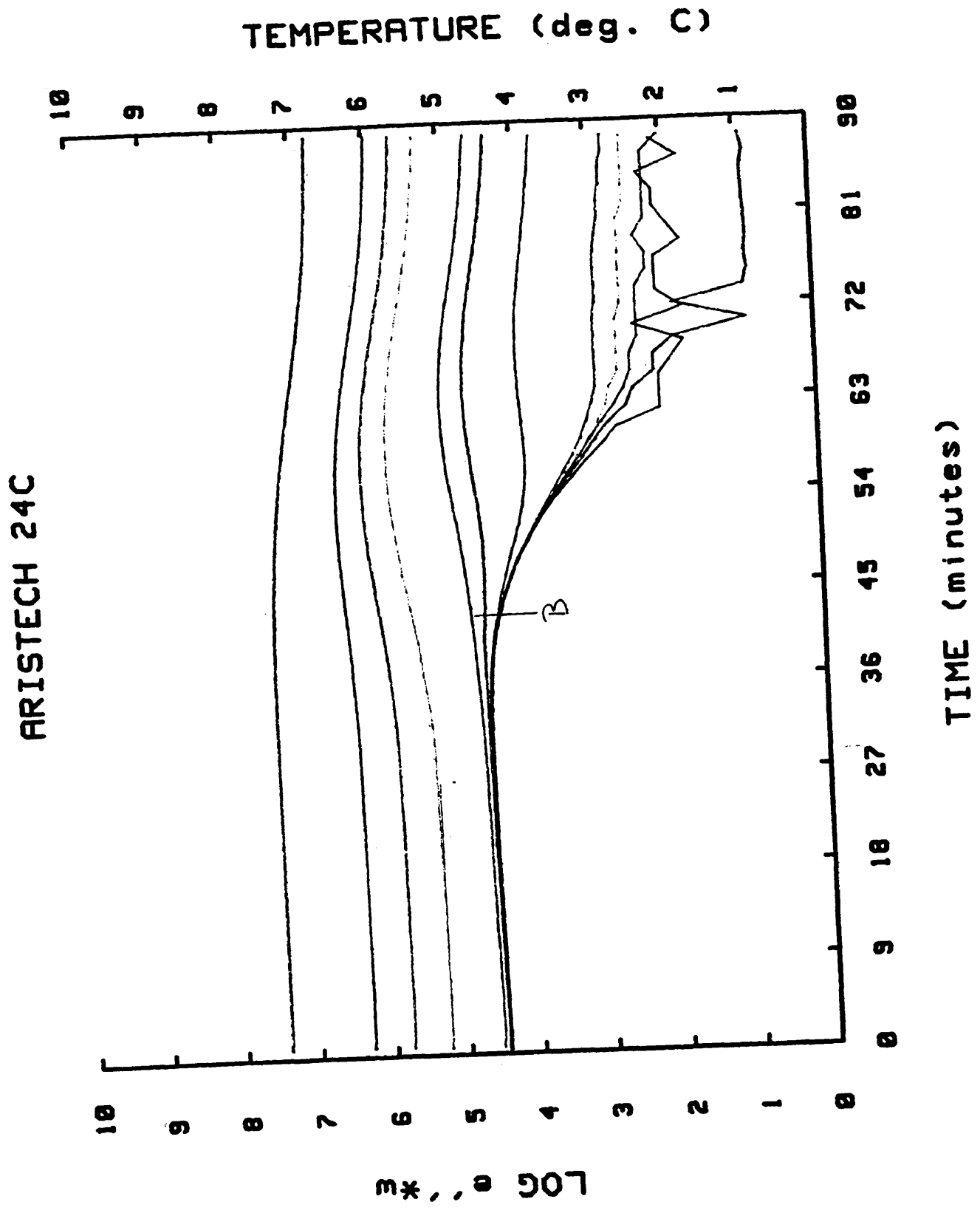


FIGURE 3.14

ARISTECH 30C ISOTHERMAL

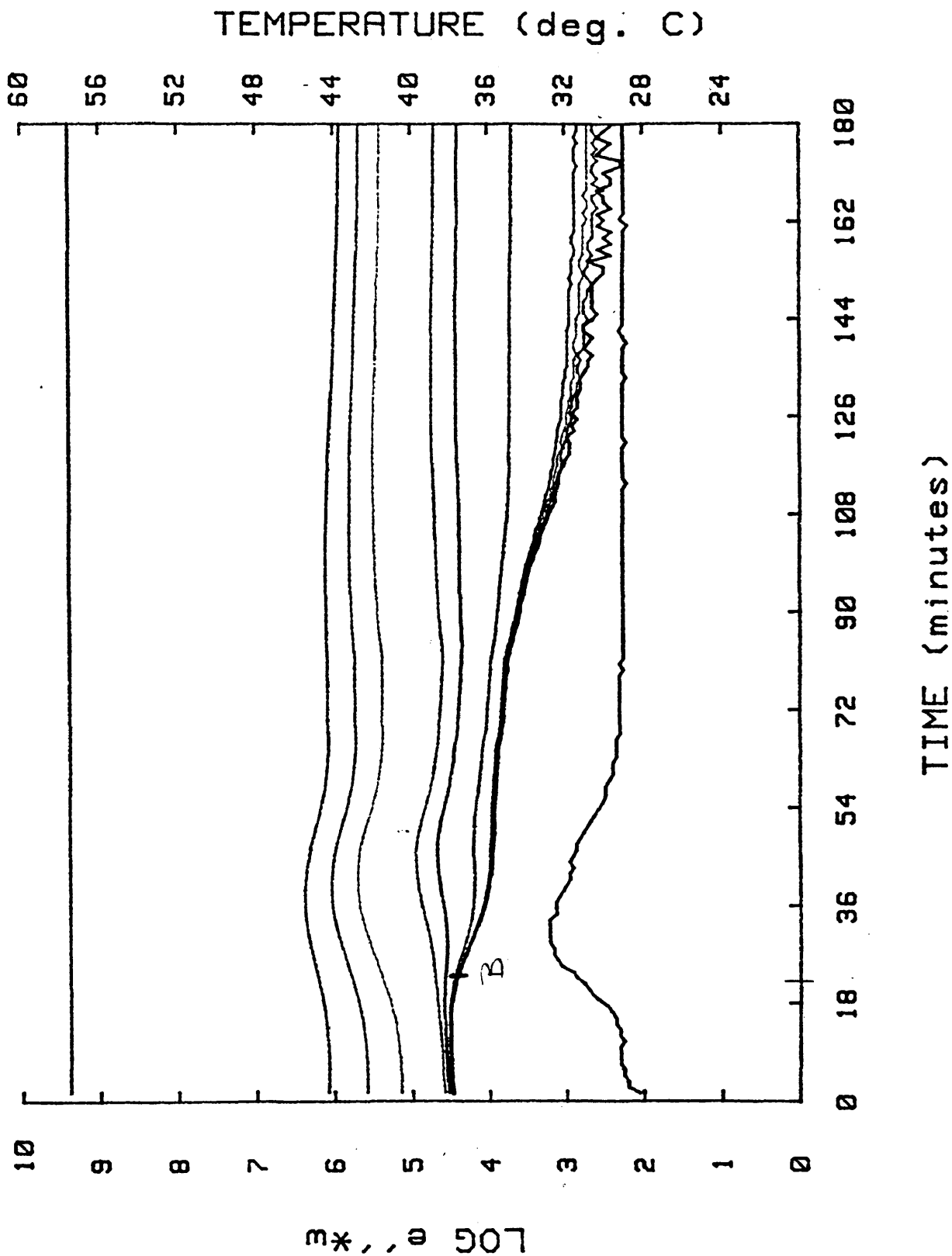
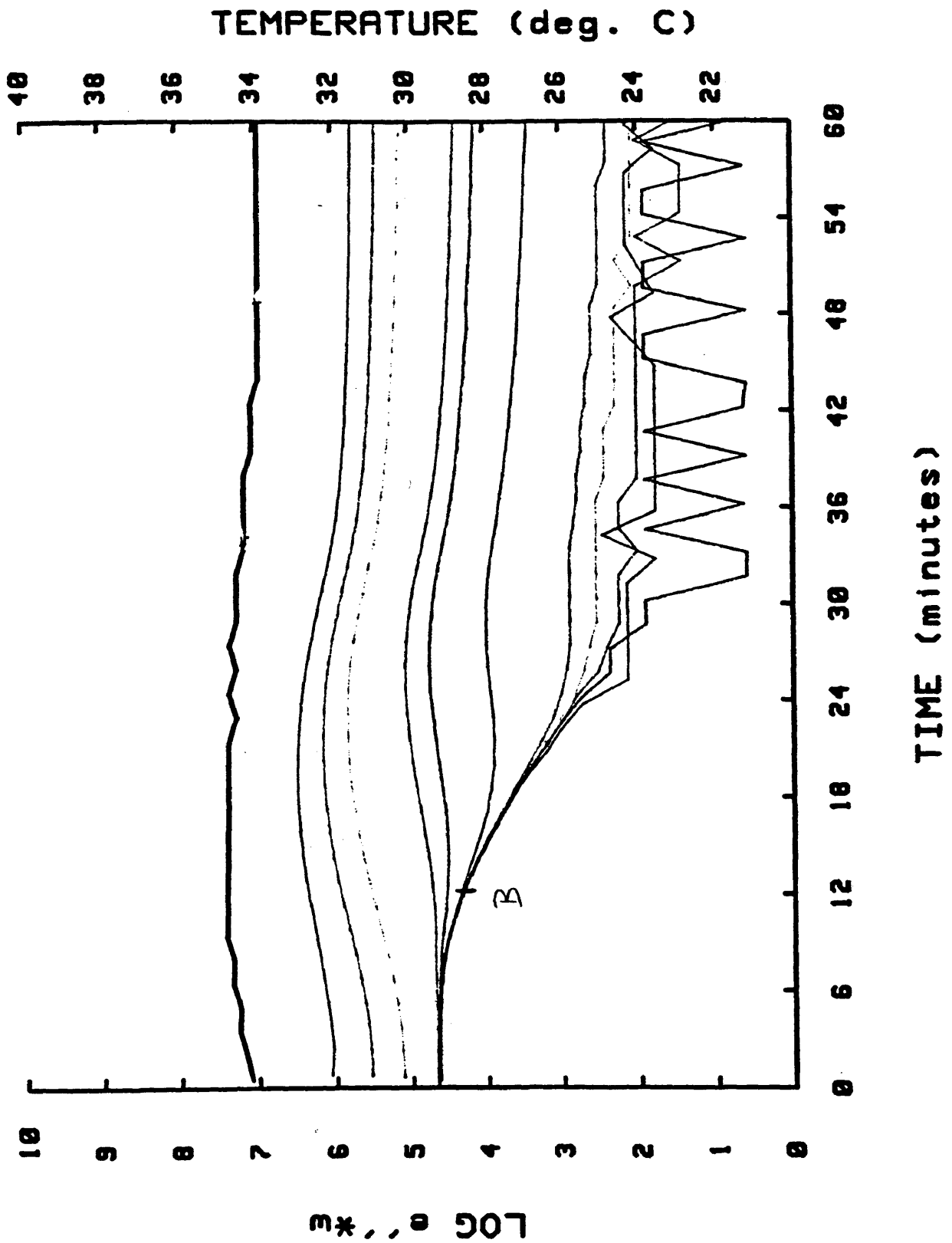


FIGURE 3.15

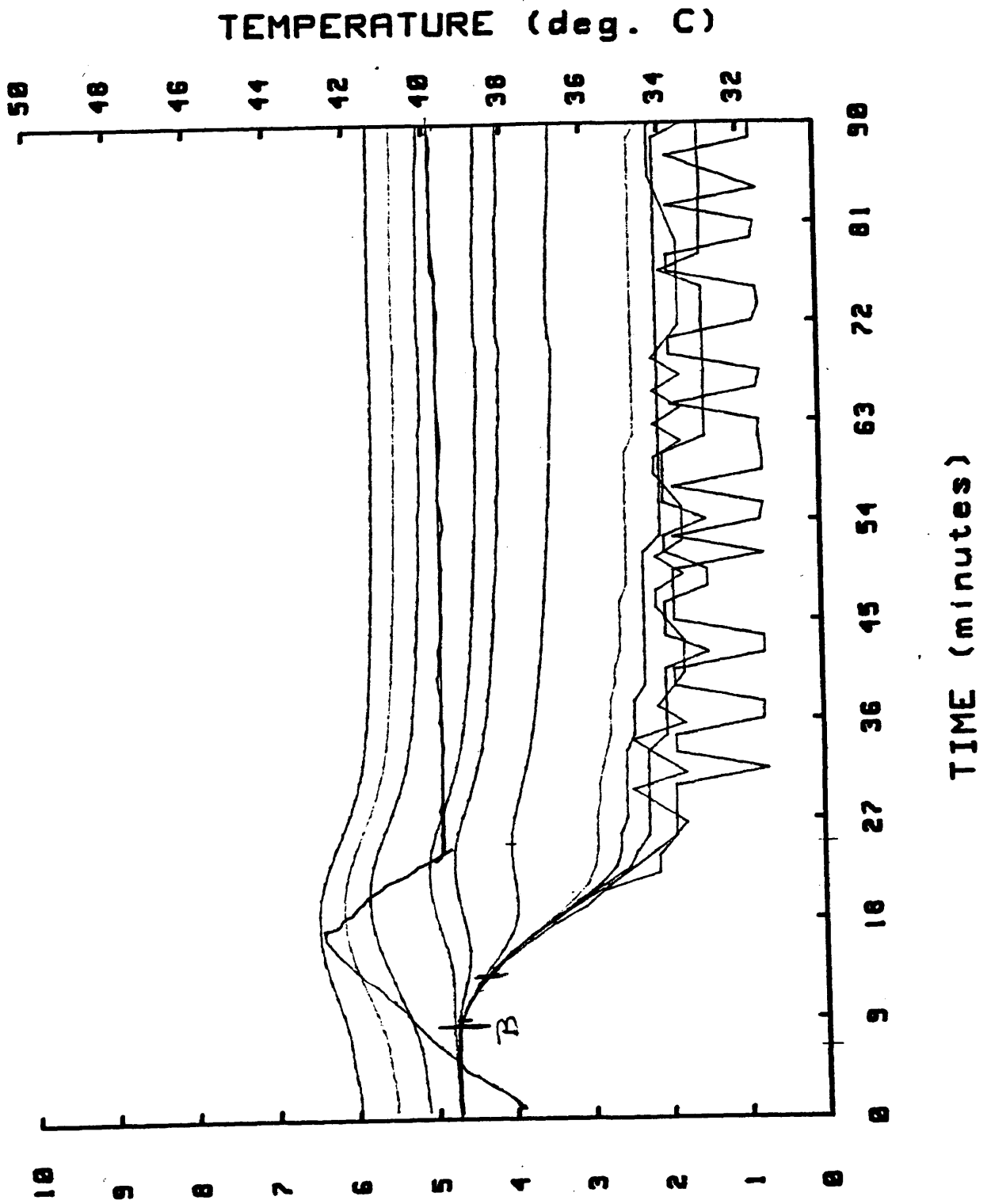
ARISTECH POLYESTER 35C



Log a

FIGURE 3.16

ARISTECH POLYESTER, 40C



LOC 507

FIGURE 3.17

ARISTECH POLYESTER 45C

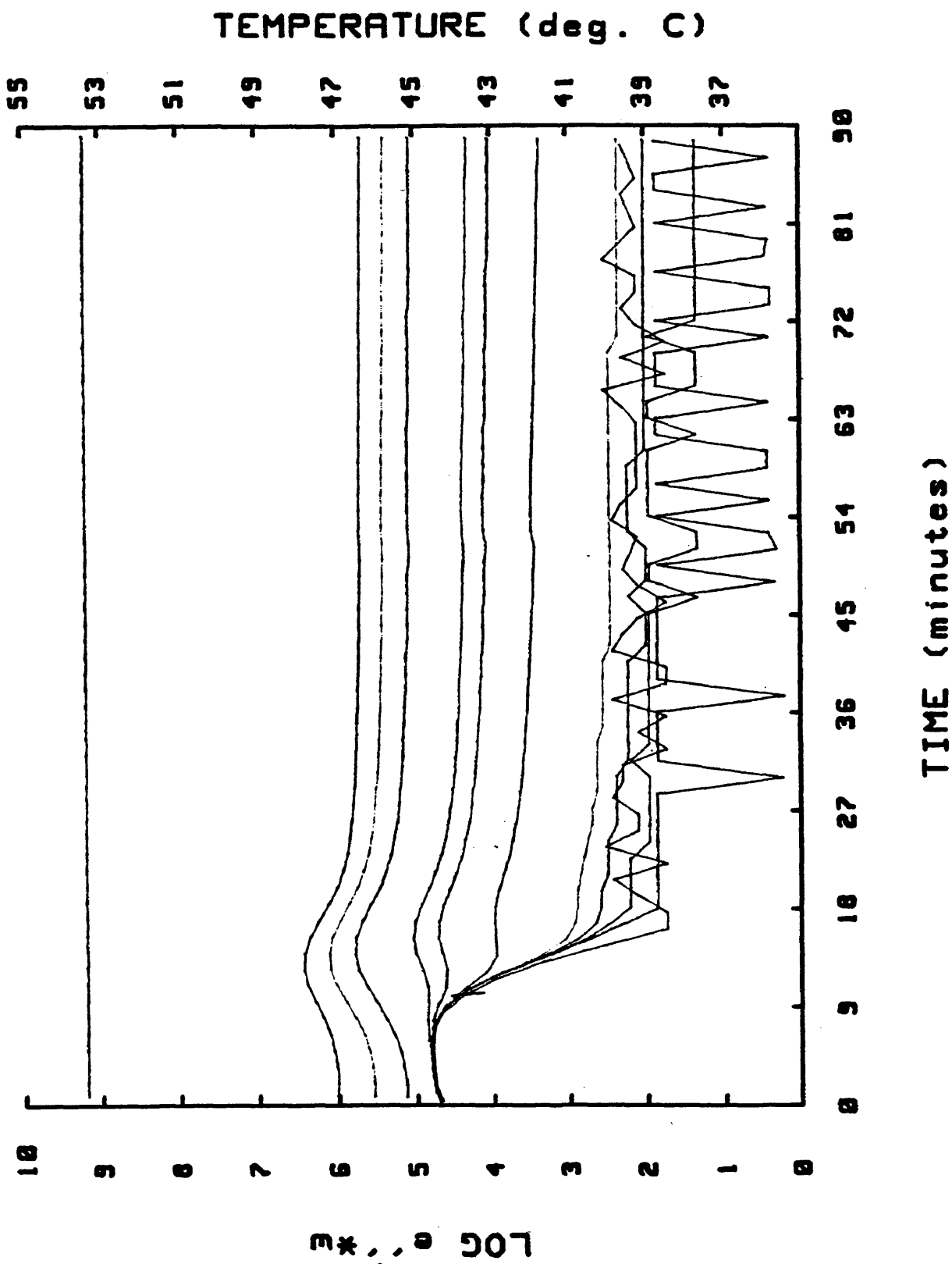


FIGURE 3.18

ARISTECH POLYESTER 50C

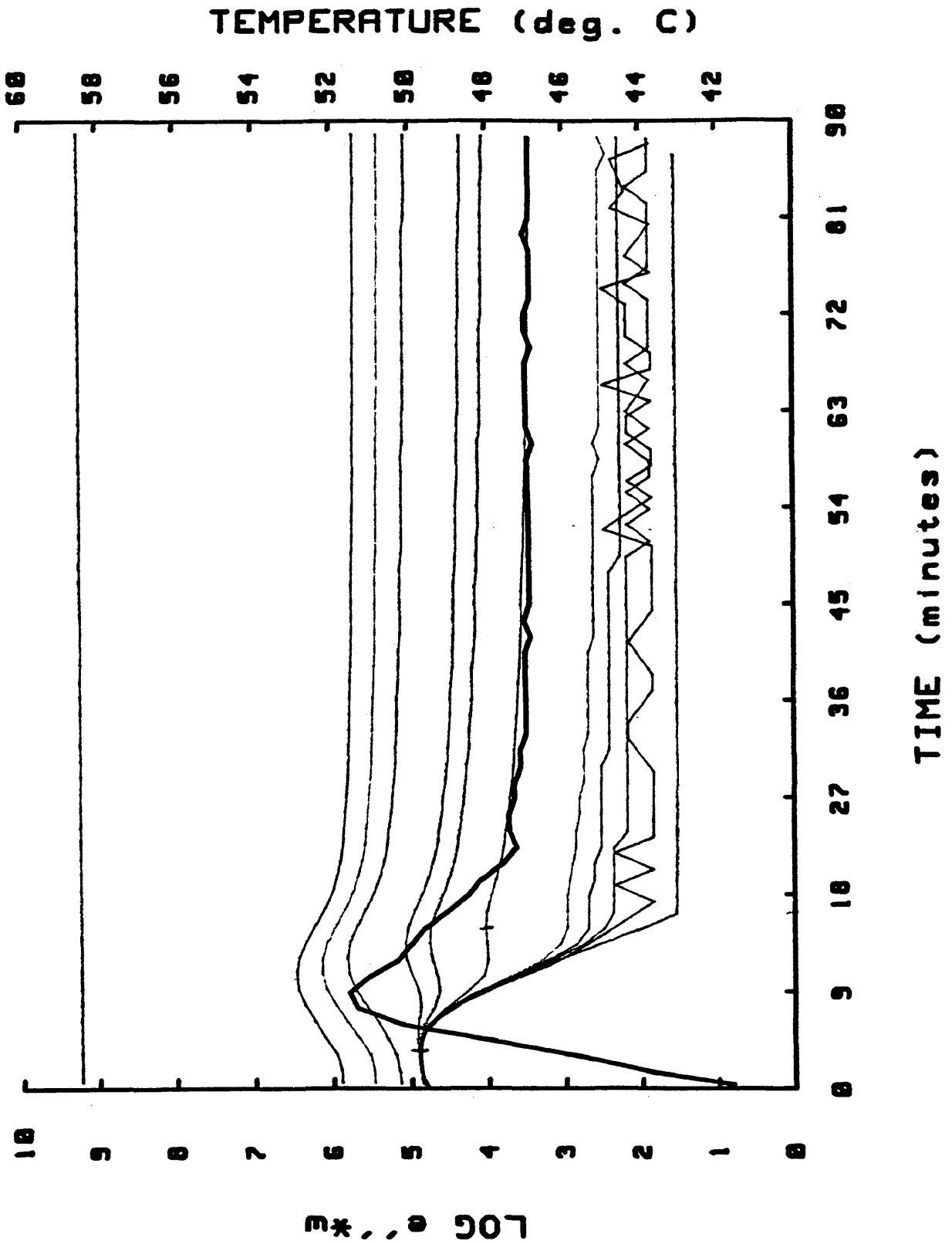


FIGURE 3.19

ARISTECH POLYESTER 60C

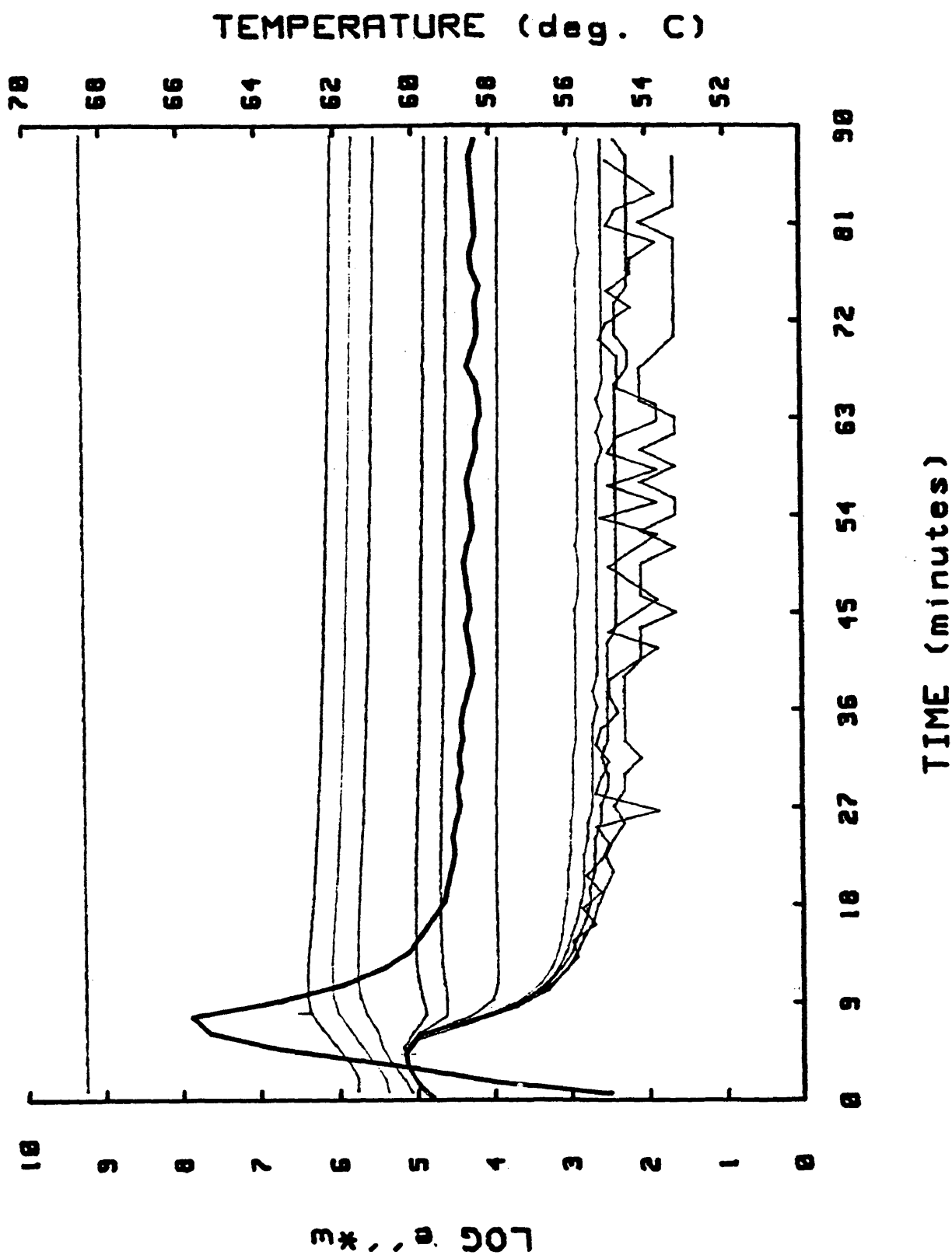
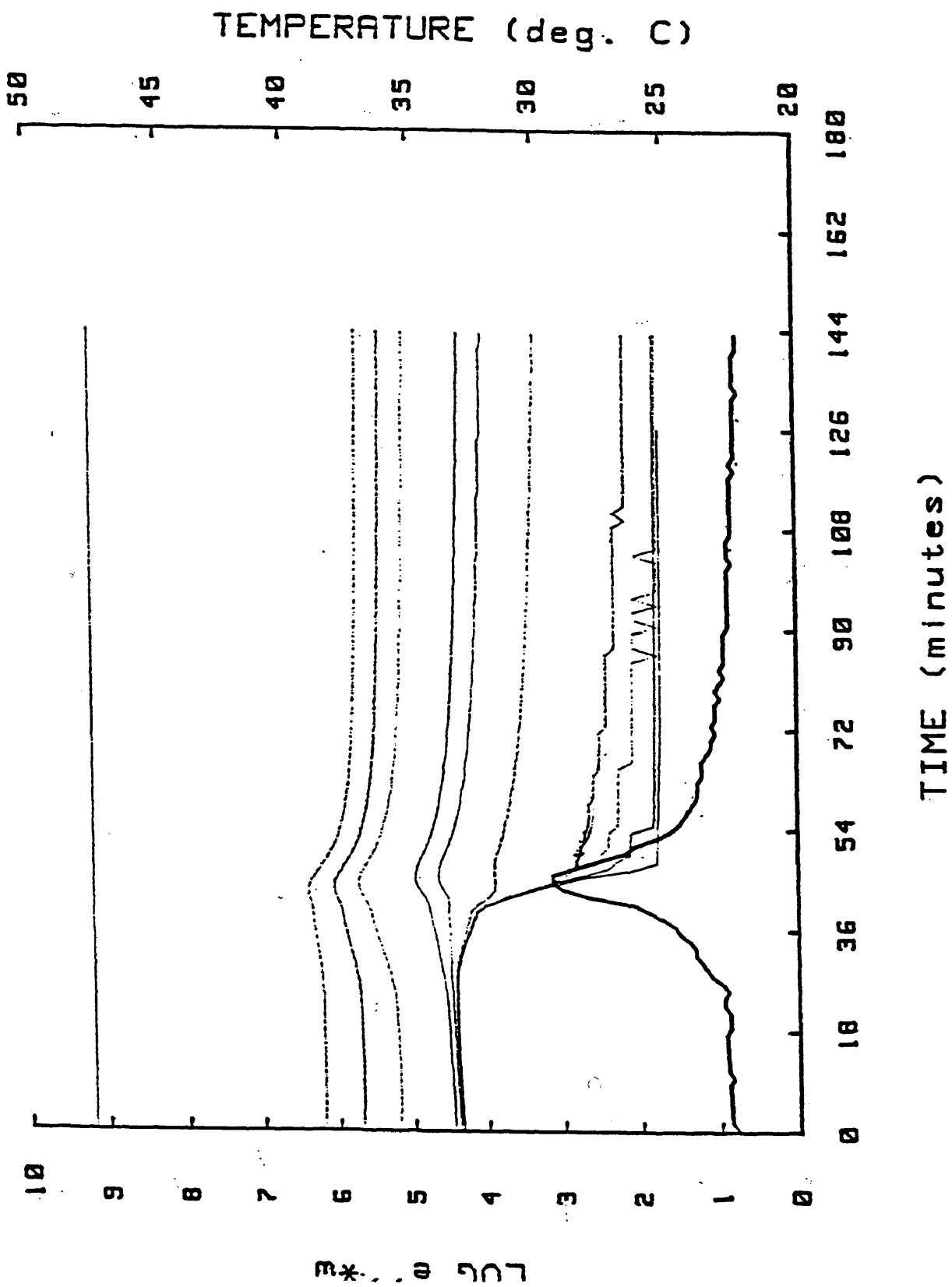


FIGURE 3.20

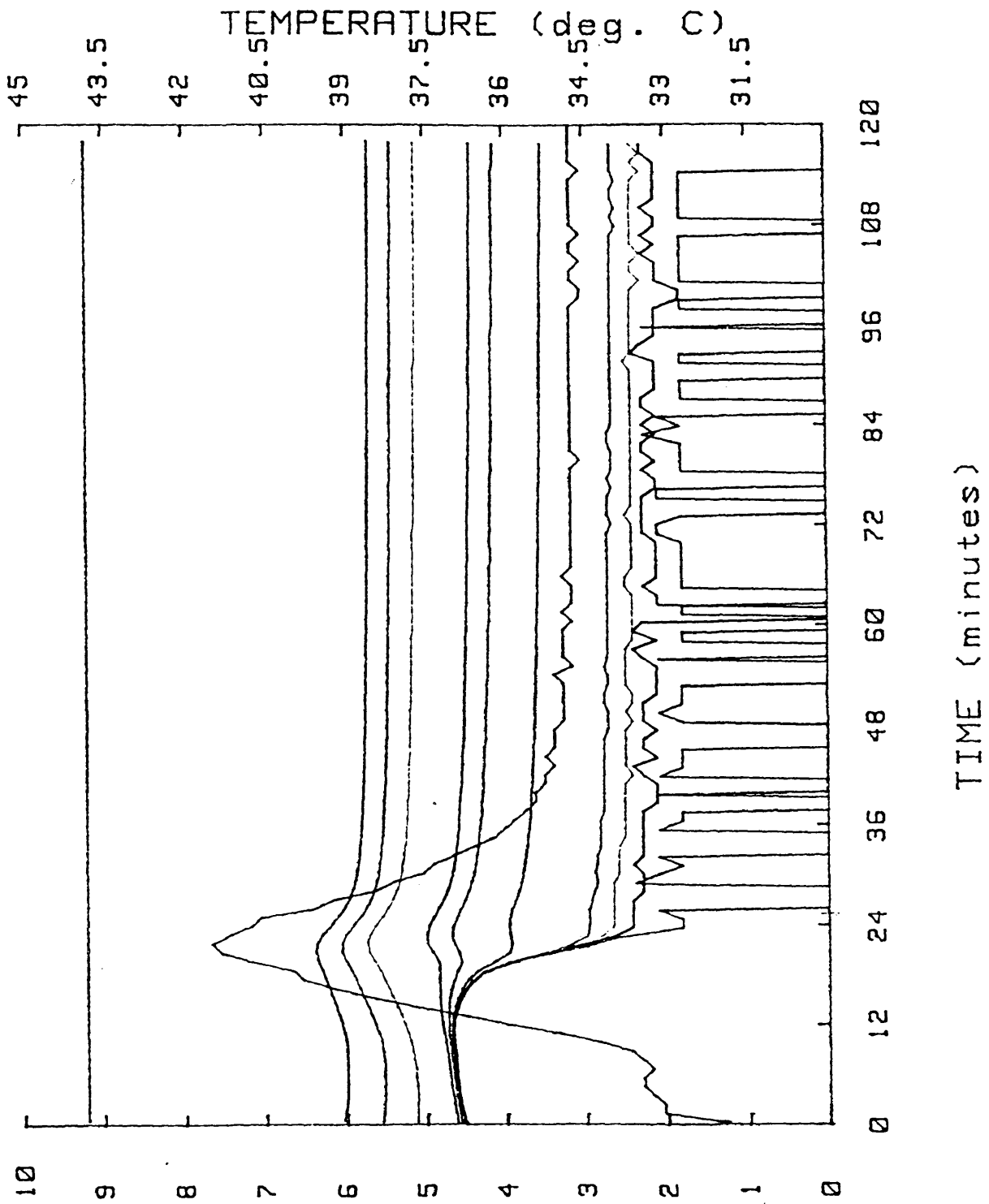
ARISTECH 24C ISOTHERMAL W/ EXOTHERM



ARISTECH 24C

FIGURE 3.21

ARISTECH 35C ISOTHERMAL W/ EXOTHERM



507, 0, \*

FIGURE 3.22

ARISTECH POLYESTER · 0C

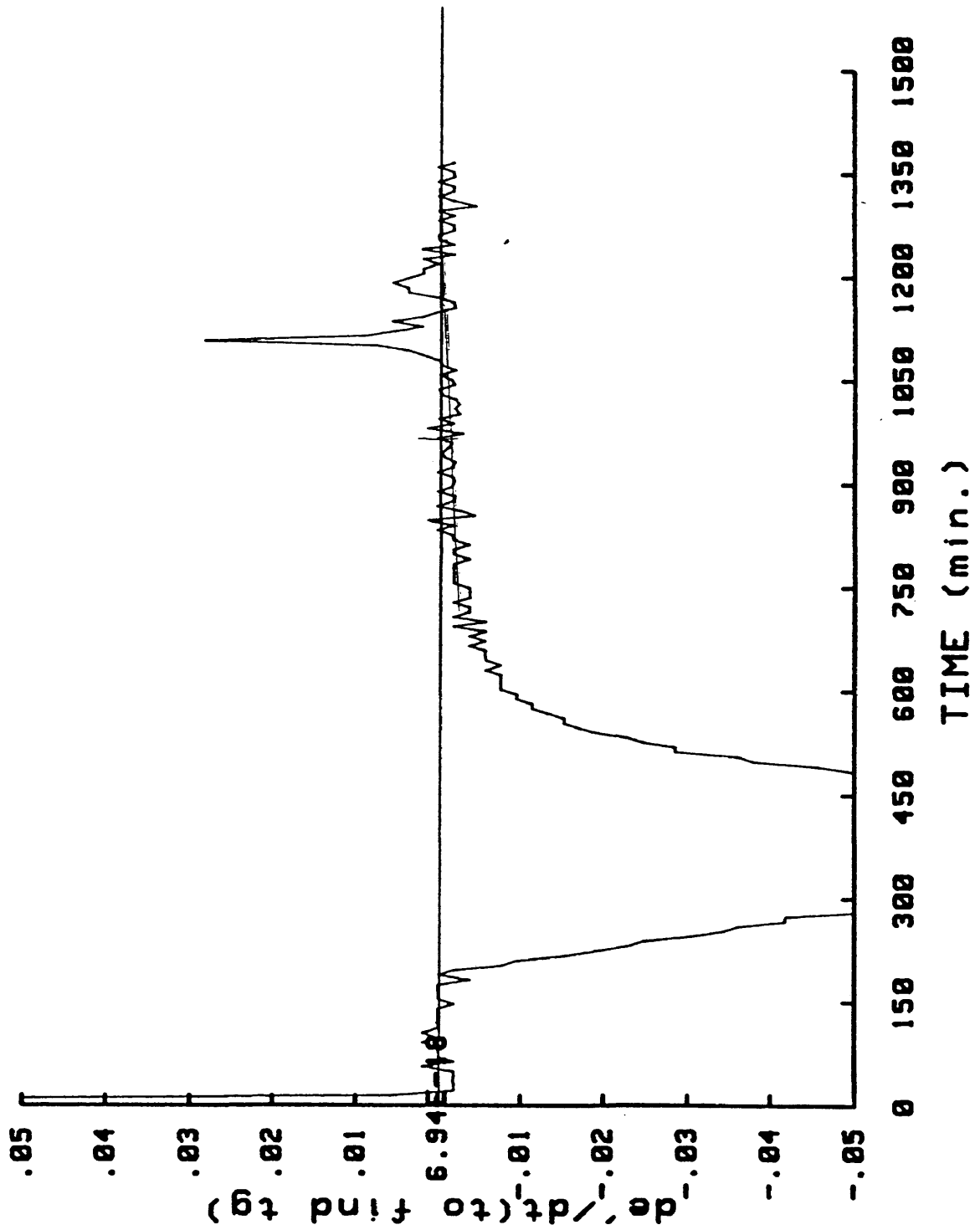


FIGURE 3.23

ARISTECH POLYESTER /ØC

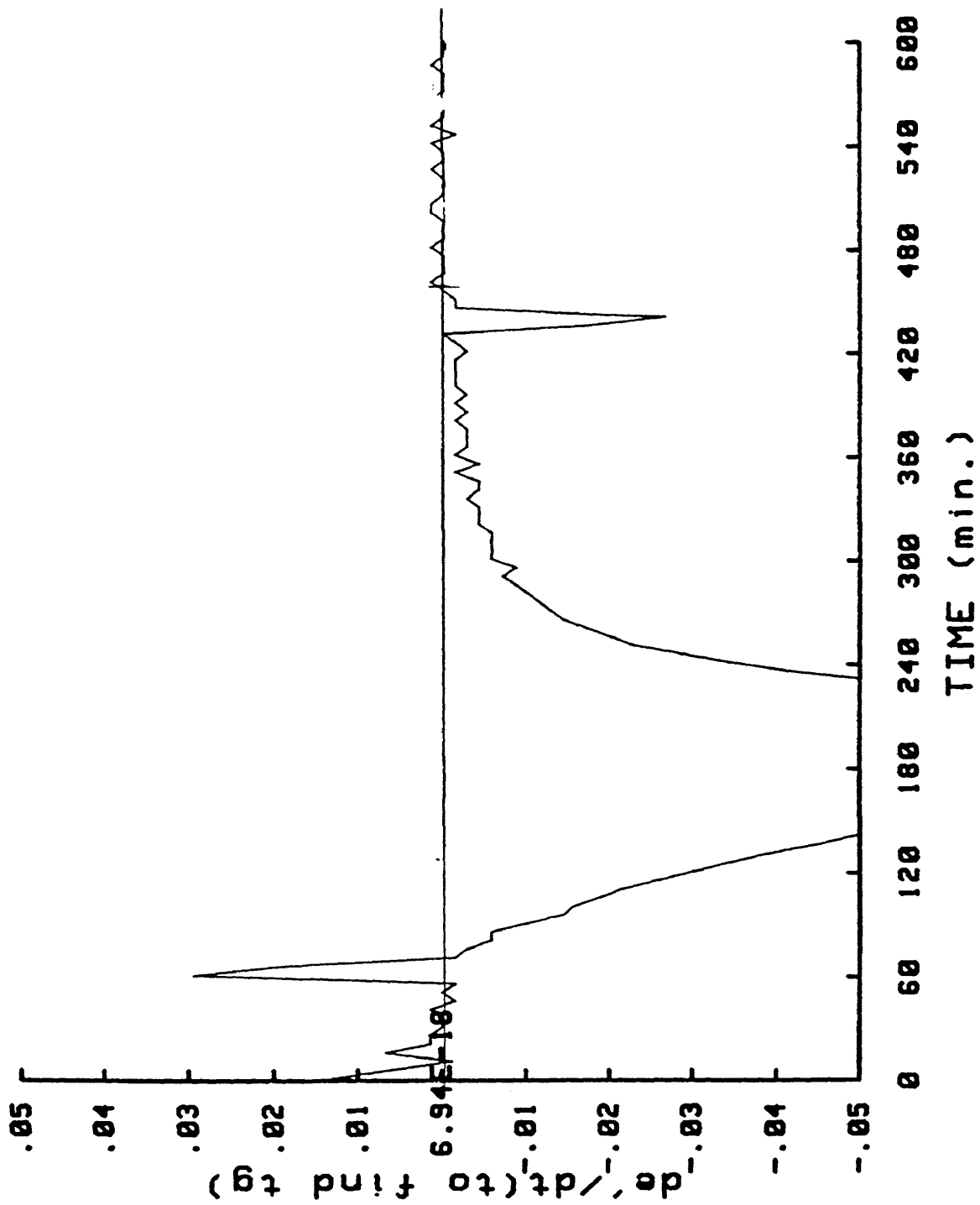


FIGURE 3.24

ARISTECH 24C ISOTHERMAL

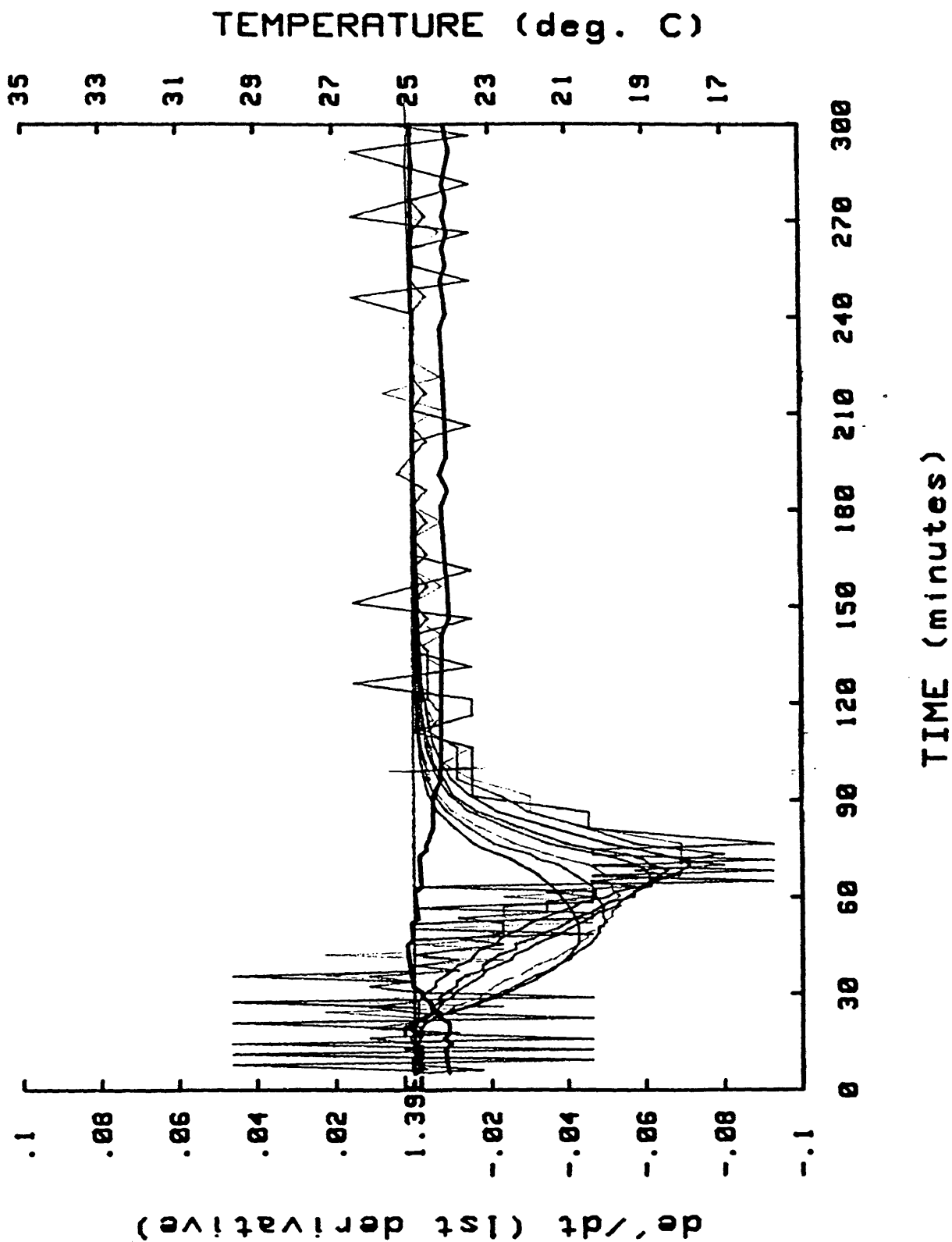
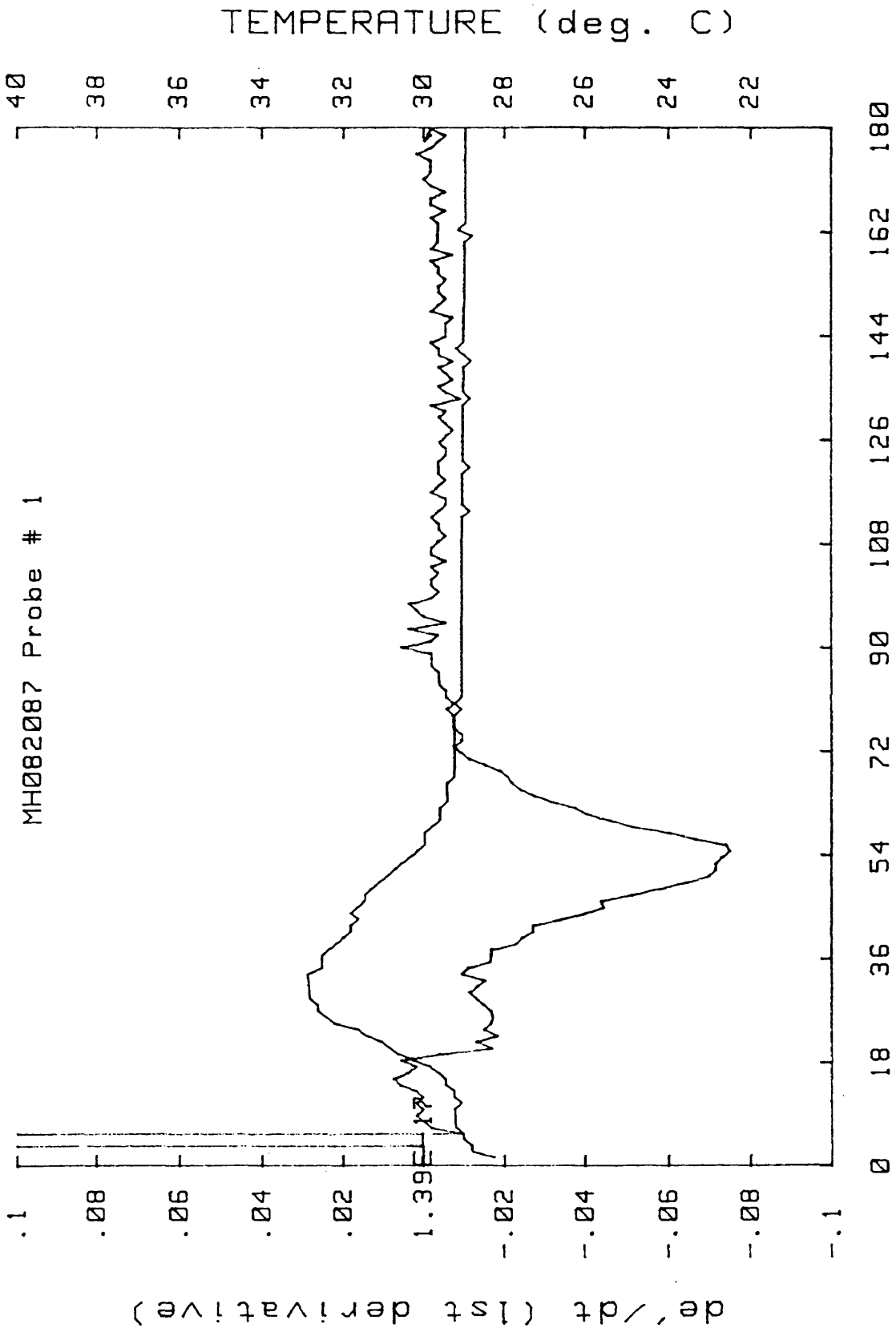


FIGURE 3.25

ARISTECH 30C ISOTHERMAL

MH082087 Probe # 1



TIME (minutes)

ARISTECH POLYESTER 35C

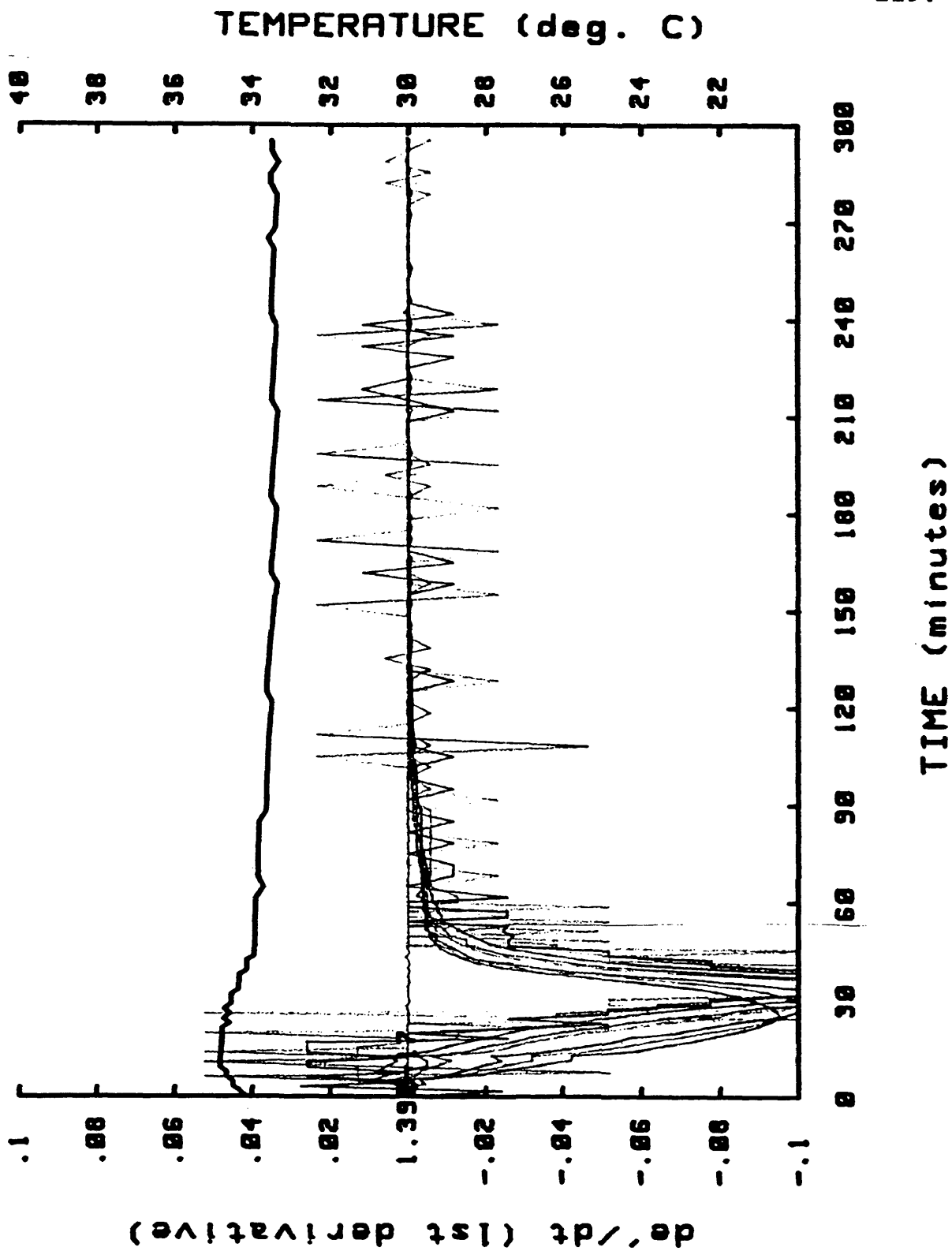


FIGURE 3.27

## ARISTECH POLYESTER, 40C

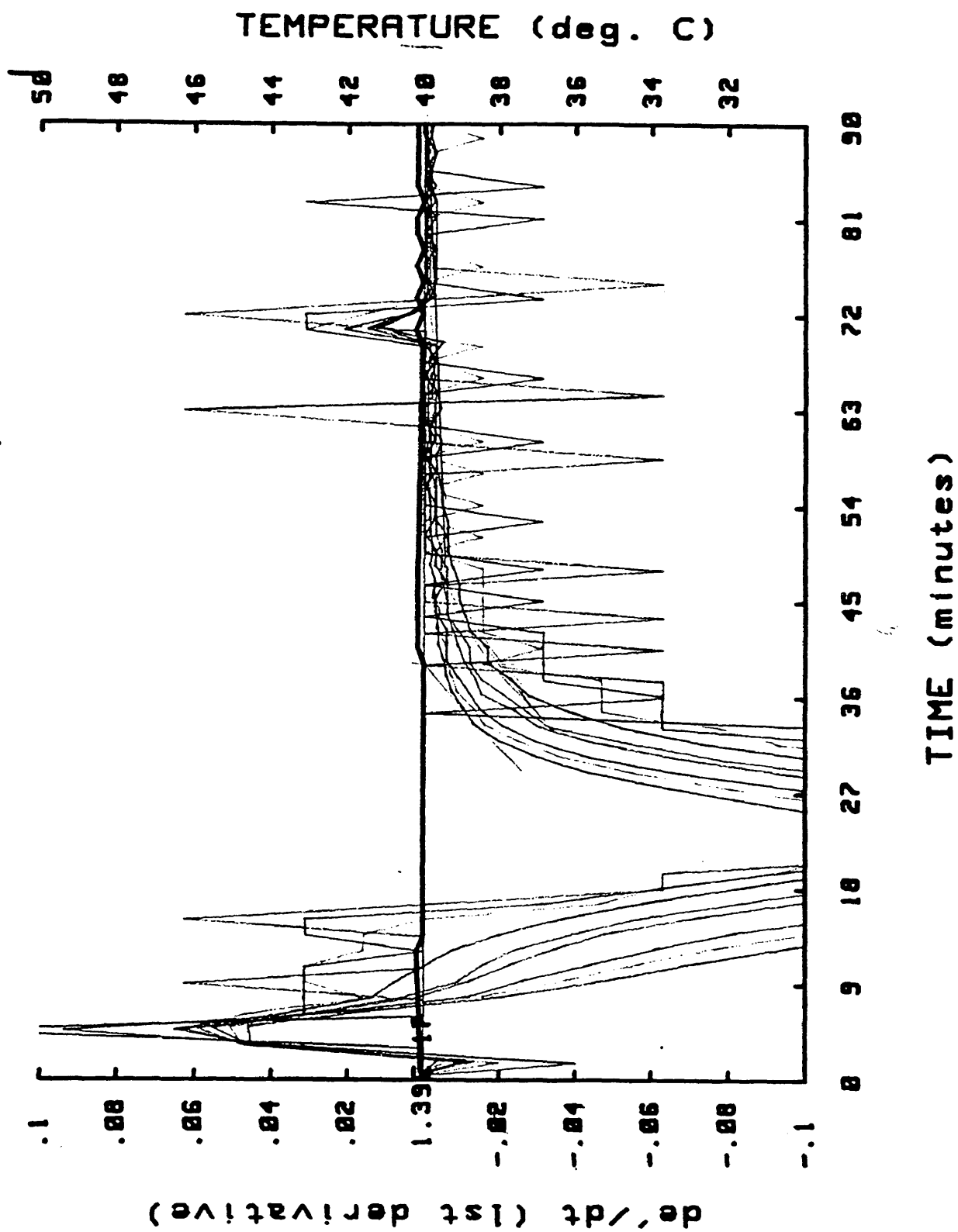


FIGURE 3.28

ARISTECH POLYESTER 45C

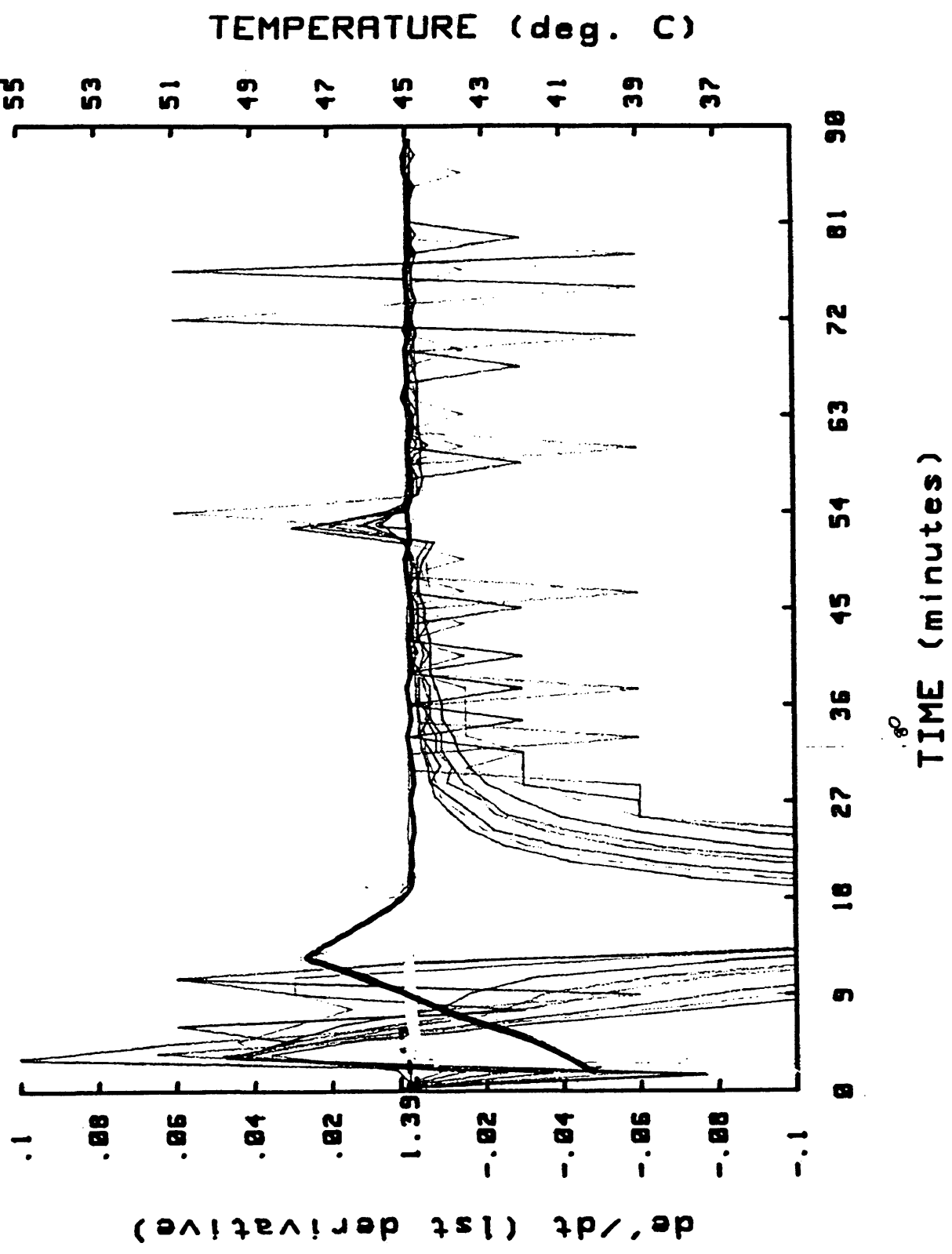


FIGURE 3.29

## ARISTECH POLYESTER 50C

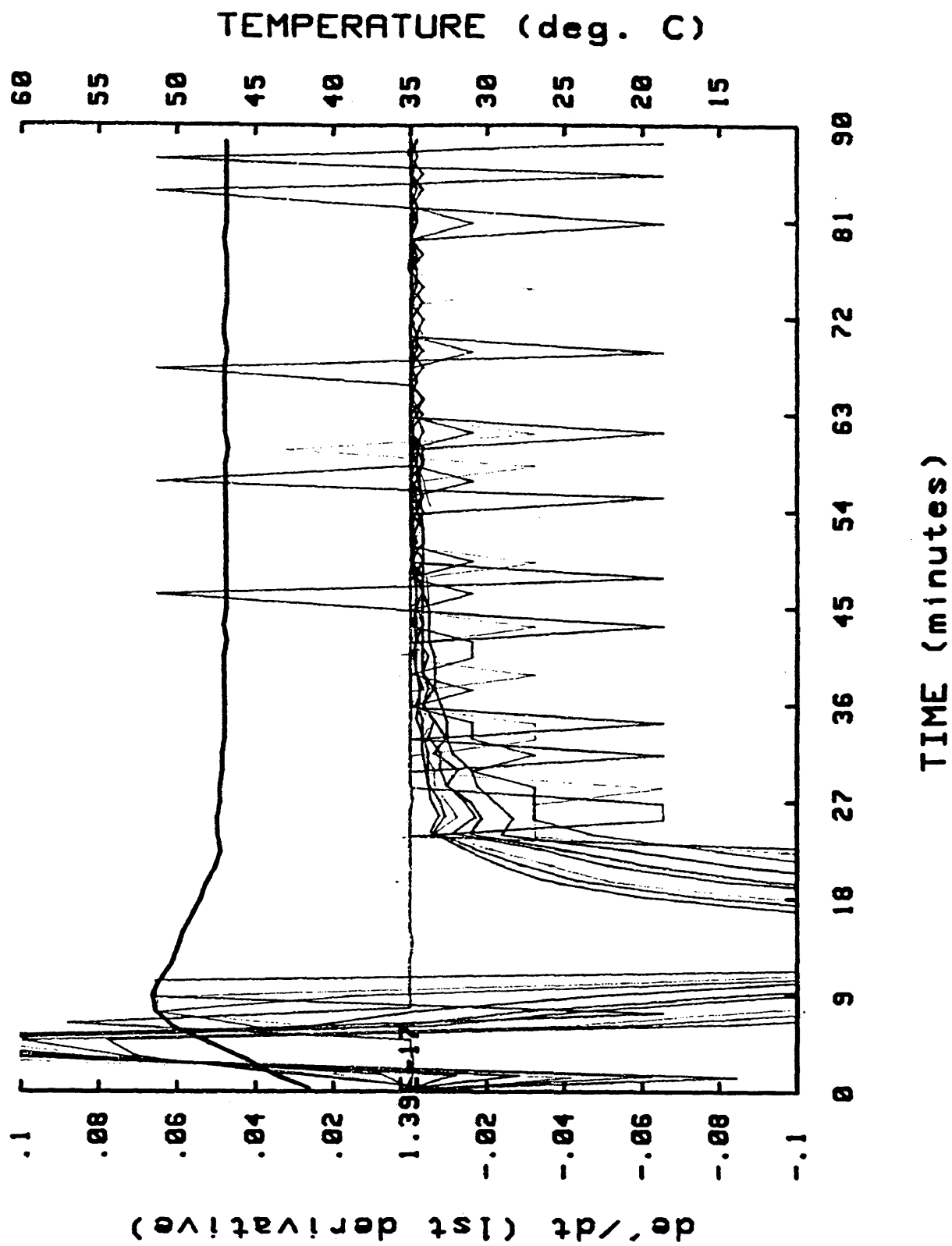


FIGURE 3.30

ARISTECH POLYESTER 60C

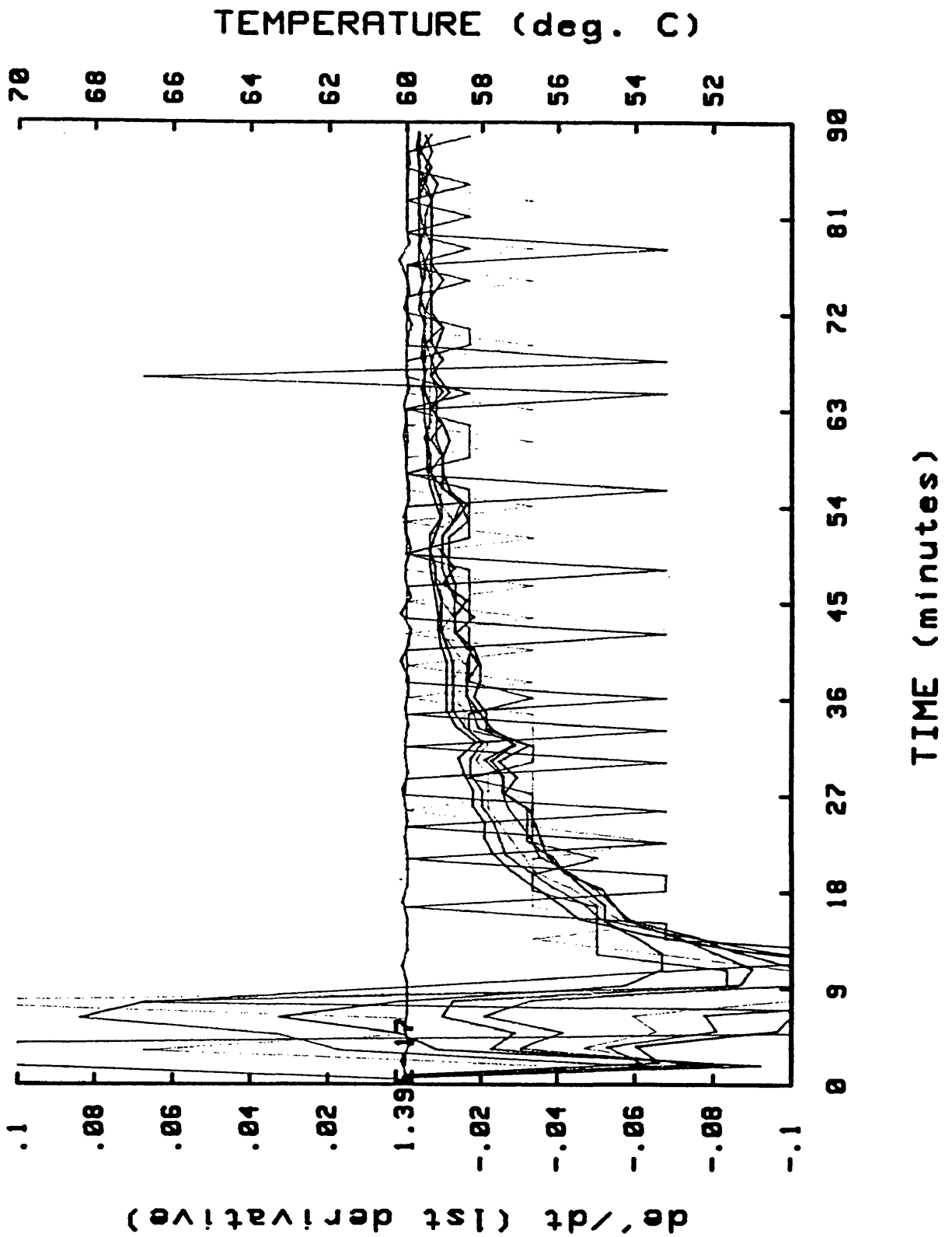


FIGURE 3.31

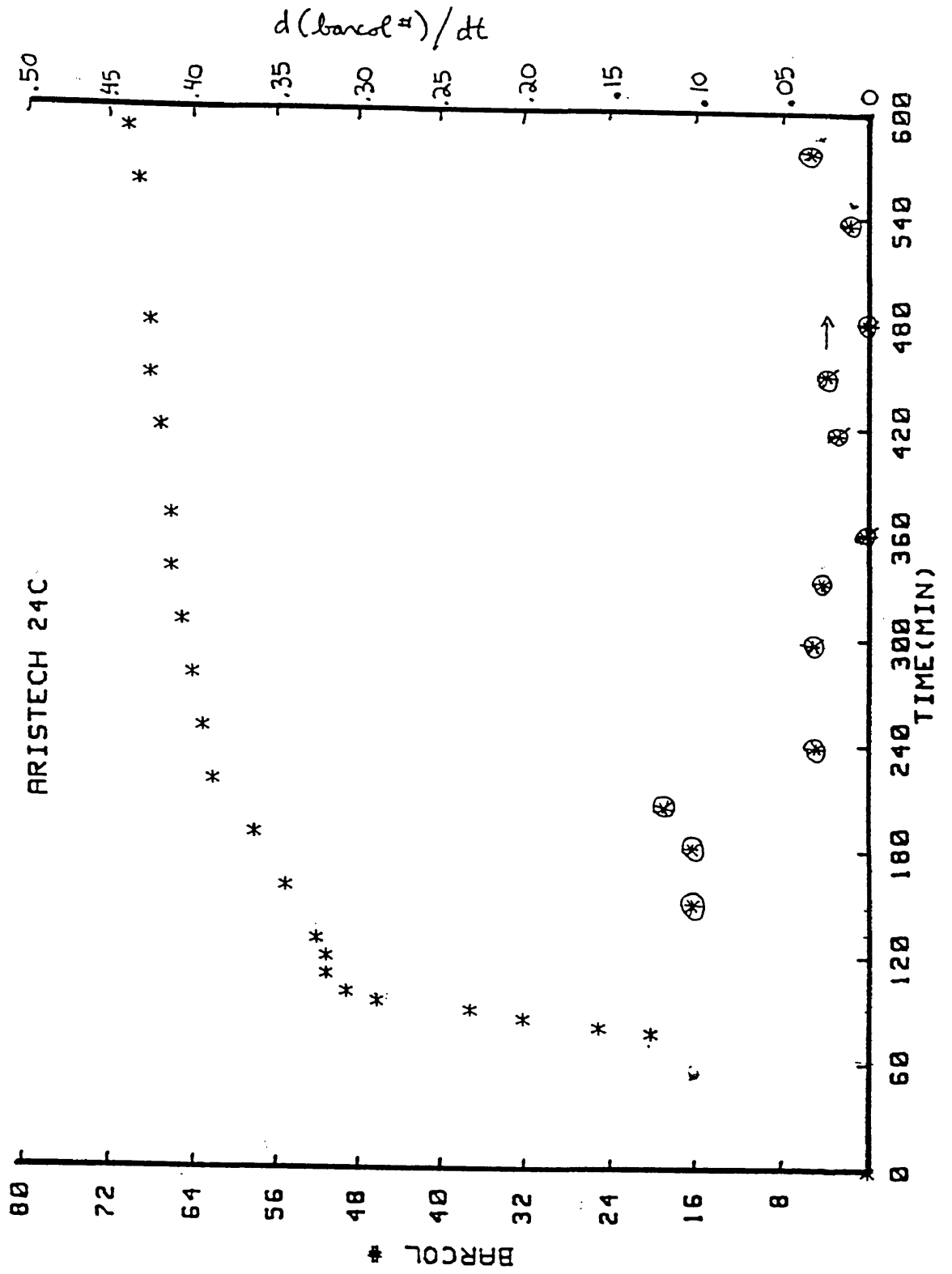


FIGURE 3.32

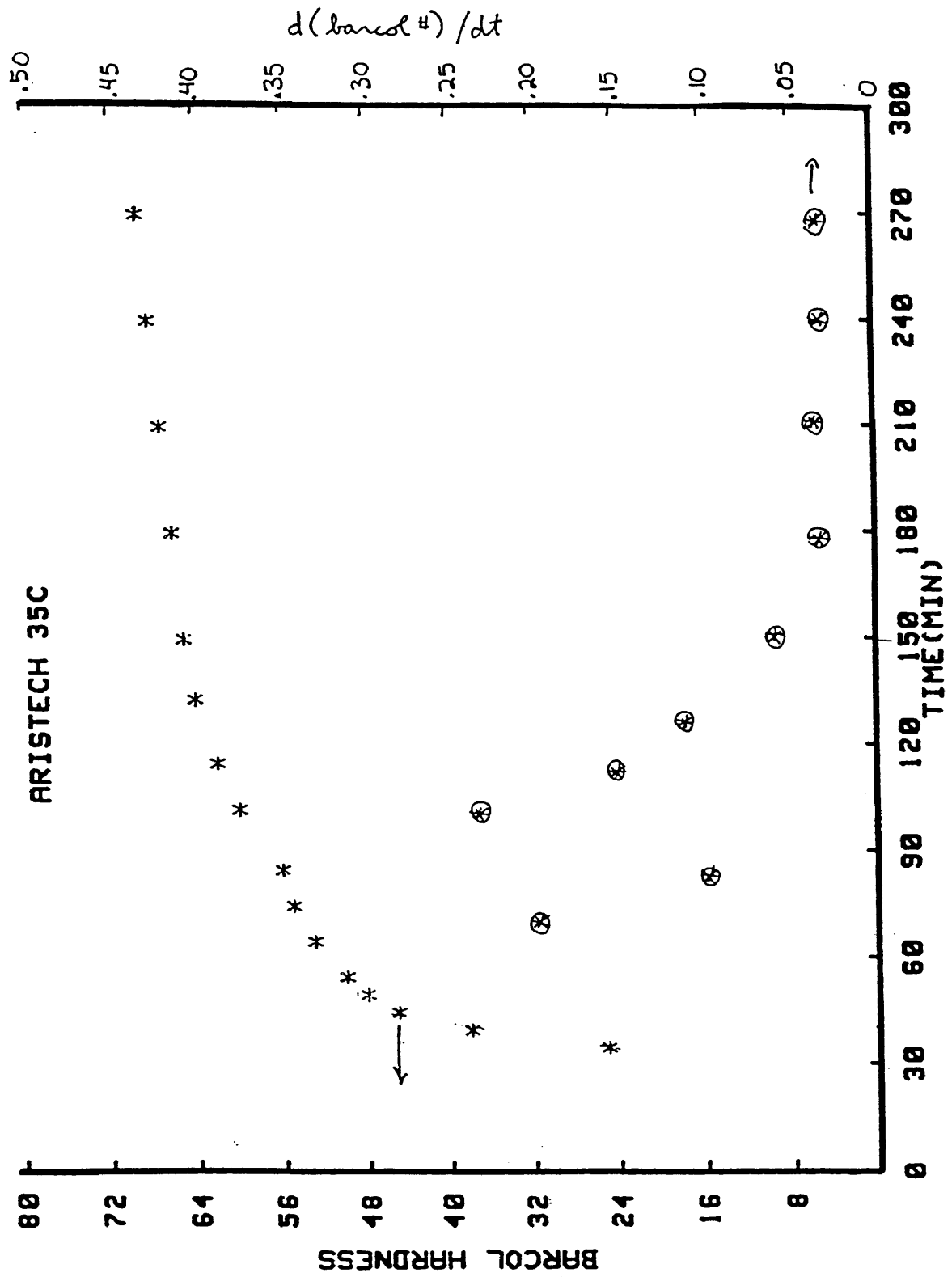


FIGURE 3.33

## 2. IONIC MOBILITY

The ionic mobility,  $\sigma$ , in the resin matrix is a function of the time and cure temperature as seen in figures 3.39 and 3.40. The graph displays constant values of log sigma taken after  $\sigma$  has maximized due to increased flow coupled with viscosity. The times to  $\sigma_{\max}$  are provided in the table below.

TABLE 3.6

TEMP	LOG $\sigma_{\max}$	TIME TO LOG $\sigma_{\max}$	ALPHA
25	-8.40	35	.11
30	-8.35	26	.13
35	-8.30	18	.10
40	-8.25	8	.02
45	-8.20	7	.13
50	-8.10	5	.11

The time to log  $\sigma_{\max}$  decreases with increasing temperature until 60°C;  $\sigma_{\max}$  increases with increasing temperature indicating that higher isothermal temperatures increase the ionic flow in the resin matrix. Examining figures E1-4, (pages 152-155) indicates that the corresponding intrinsic viscosity for the given times is approximately  $1 \times 10^3$ . These times exceed the  $t_{\text{gel}}$  (presented in Table 3.3) Ions in the system result from the reaction of benzoyl peroxide and DMA. These ions are then converted to radicals therefore, in the very early stage of the reaction, the DMA promotes radical formation.

TIME TO ALPHA AS A FUNCTION OF TEMPERATURE

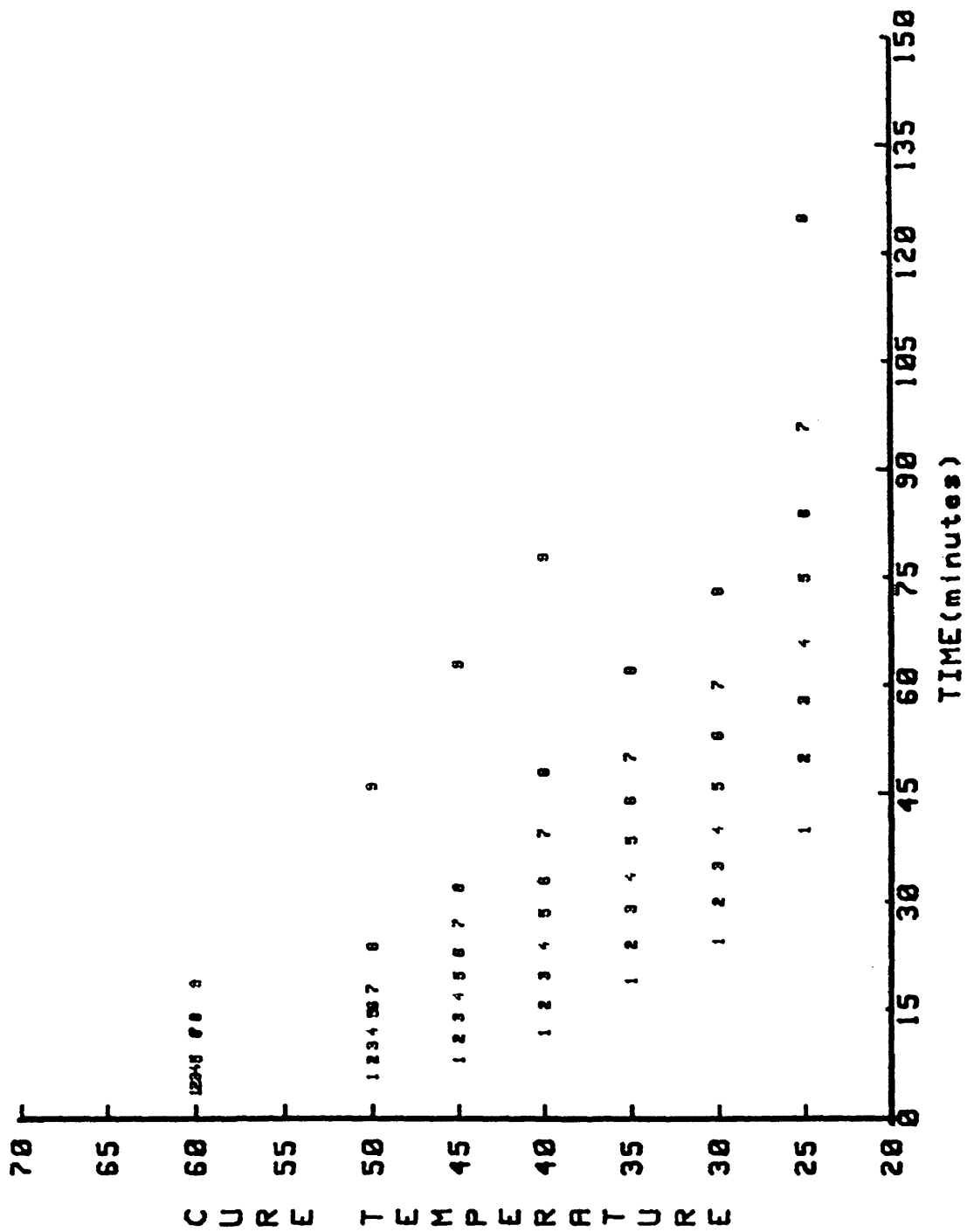


FIGURE 3.34



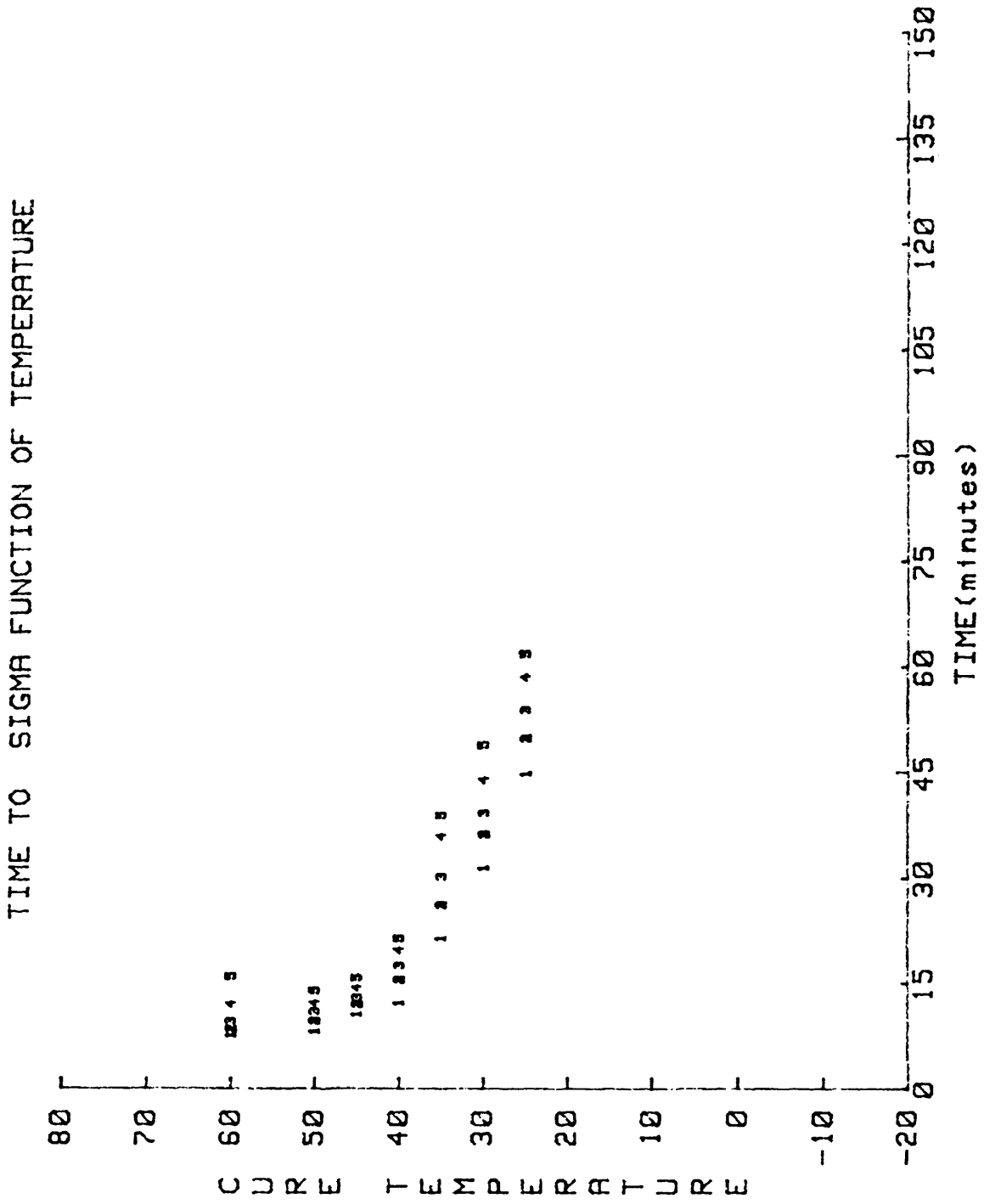


FIGURE 3.36

TIME TO ALPHA AS A FUNCTION OF TEMPERATURE

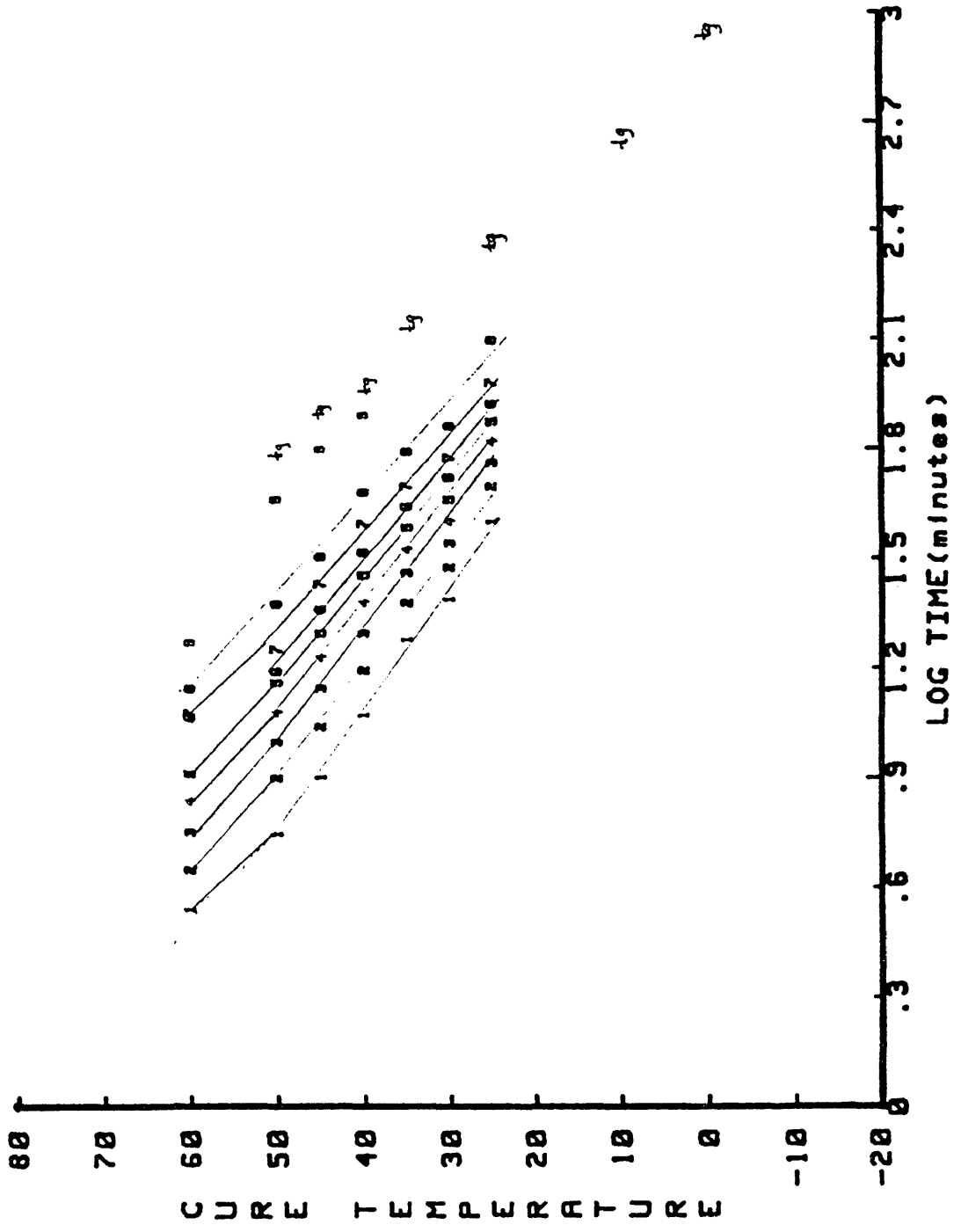


FIGURE 3.37

TIME TO TAU AS A FUNCTION OF TEMPERATURE

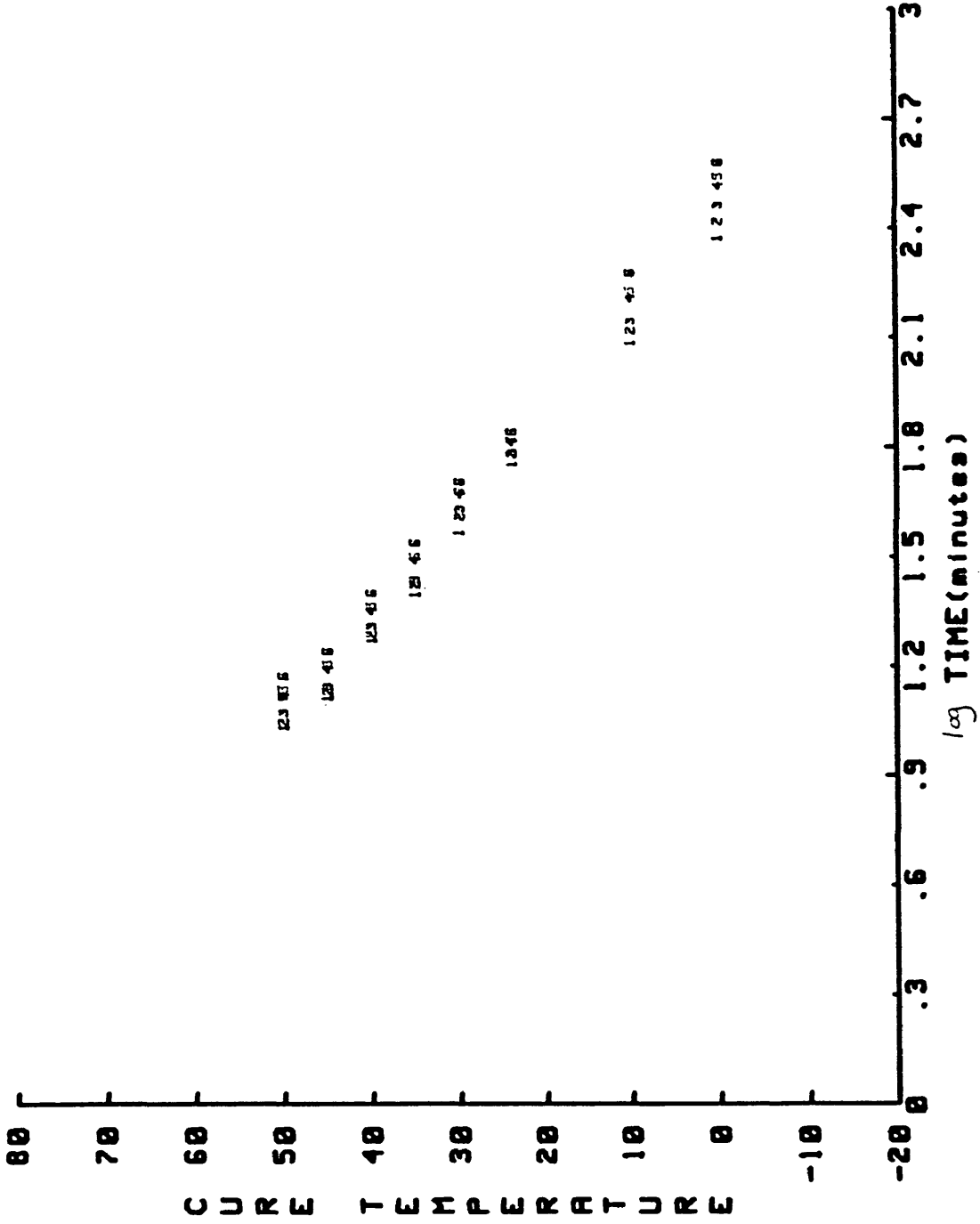


FIGURE 3.38

TIME TO SIGMA FUNCTION OF TEMPERATURE

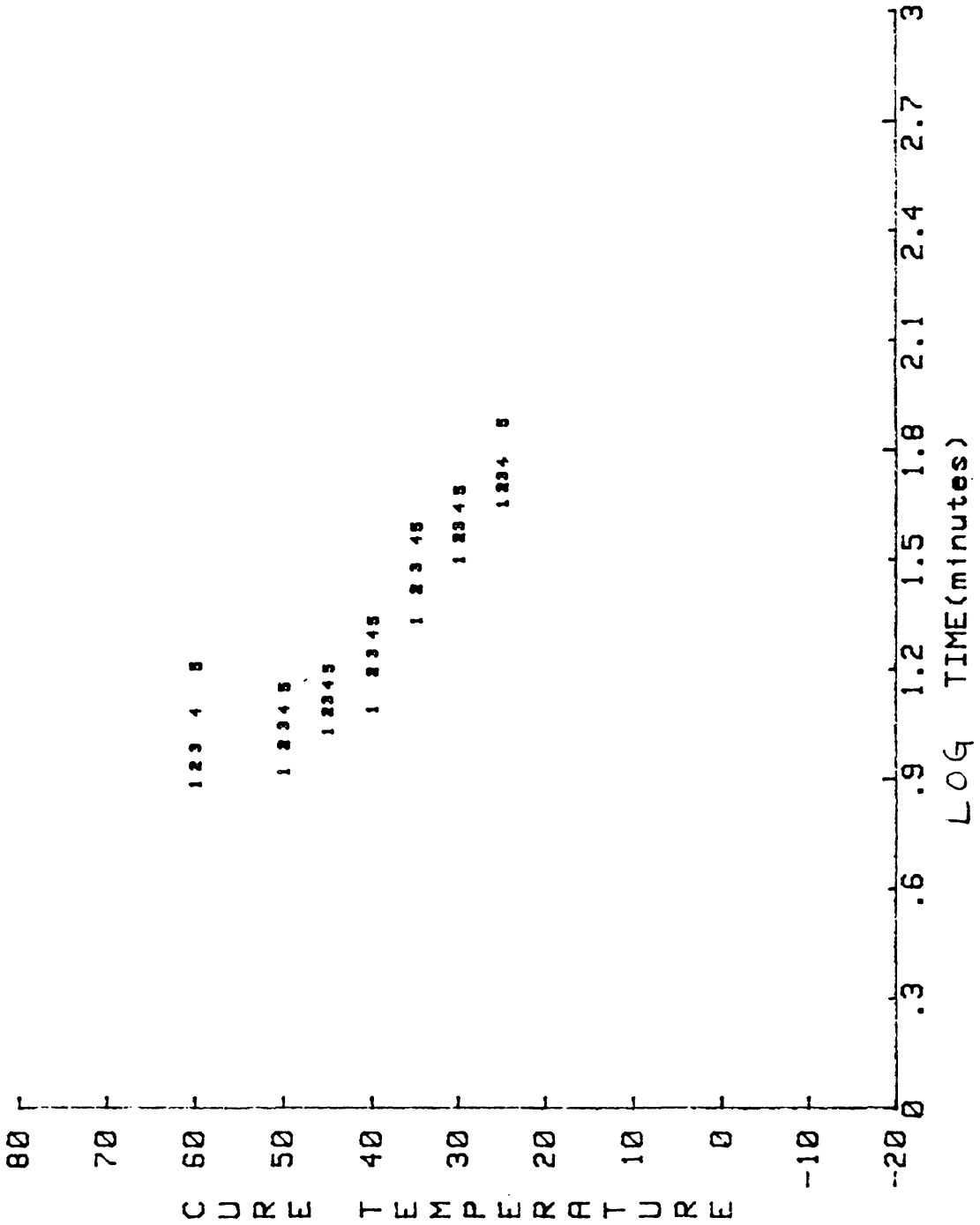


FIGURE 3.39

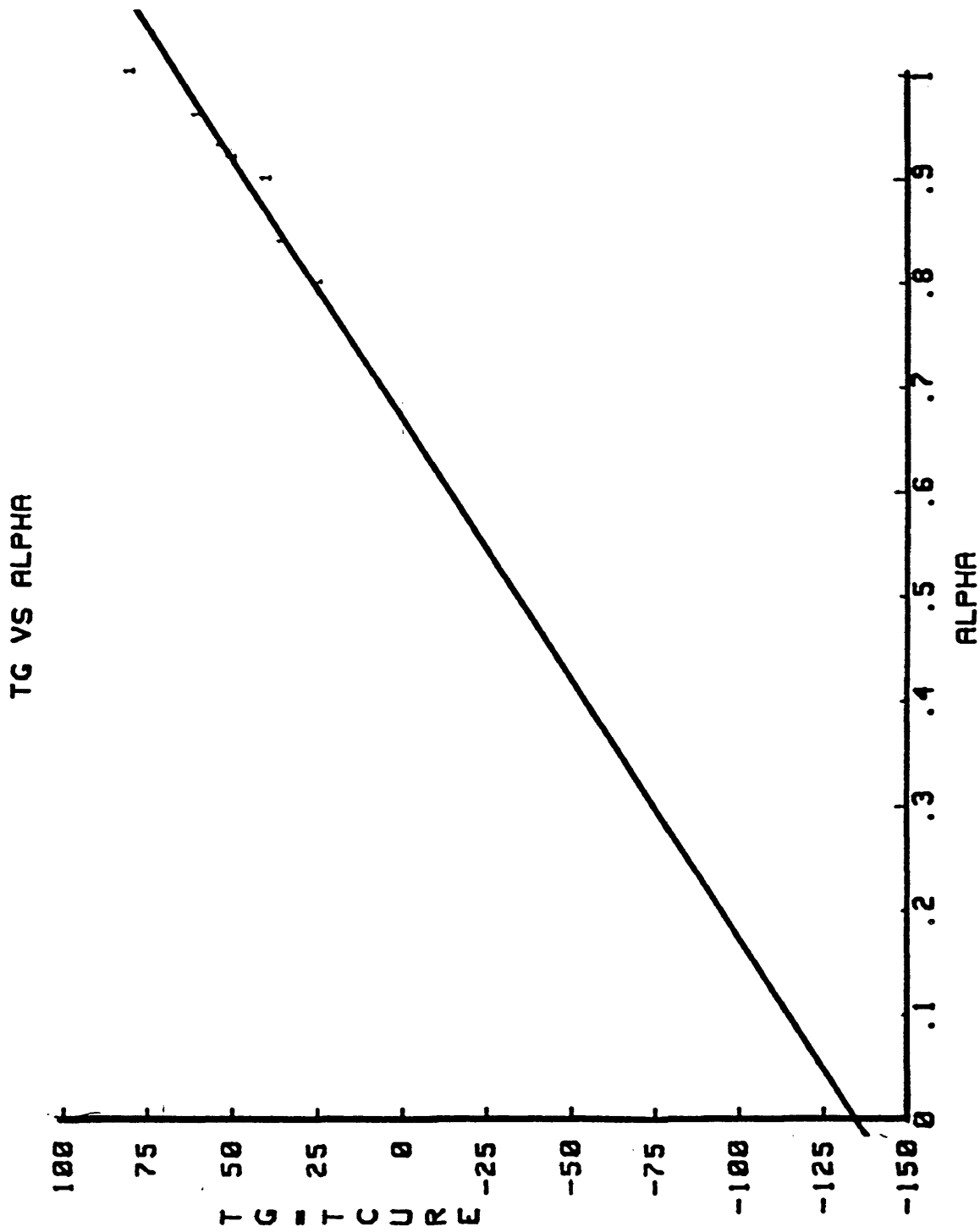


FIGURE 3.40

### Time-Temperature-Transition Plots

It is evident from figure 3.37 that  $t_g$  occurs at advanced degree of cure for the temperatures studied. Comparing the slope of the line represented by  $t_g$  with those represented by degree of cure shows the lower temperatures the degree of cure at  $t_g$  decreases- as expected. At some sufficiently low temperature the two lines will intersect. The tau data exhibits the same phenomenon; as temperature decreases dipolar relaxation and  $t_g$  become more closely associated. Ignoring the data at  $60^{\circ}\text{C}$ , ionic mobility evinces the same trend.

## CHAPTER IV: CONCLUSIONS

Of the fitting methods used, the Ryan Dutta most precisely predicts  $(d\alpha/dt)_{\max}$  and the time to  $(d\alpha/dt)_{\max}$ . The least square fit method is time consuming and restricted by the range. The approach used by Lam fails as the cure begins to shut down due to approach of glass transition. There is also intrinsic error in the equation in that  $d\alpha/dt=k_1(\alpha)^m(1-\alpha)^n$  does not account for the shoulder which is observed after  $(d\alpha/dt)_{\max}$  at all temperatures.

Ignoring the results of method #4 on the following page, the least square analysis gives no consistent trends in the predicted values of m and n. The sum m+n does, however, oscillate about  $2 \pm 0.5$ . Both the Lam and Ryan Dutta fits provide nearly constant values of m and n. The average value for m were .56 and .73 for the Ryan Dutta fit and the Lam fit respectively. It is interesting to note that the m=.56 is very close to the value of the theoretical exponent of initiator concentration of 0.50.

In determining the flow properties of the curing resin, DDA provided the times to onset of cure, onset of sol-gel transition, approach of glass transition as defined by tau relaxation and the times to  $T_g$ . While the DSC showed the

time to onset , it was ineffective in providing data on the glass transition region as the minute change in cure properities exceeded the instrument's sensitivity.

TABLE 4.1

method # 1= Lam

method # 2= LSF (with  $k_0$ )

method # 3= LSF (range  $m < 5$ ,  $n < 7$ )

method # 4= LSF (range  $m < 3$ ,  $n < 3$ )

method # 5= Ryan Dutta

Temp. ( $^{\circ}$ C)	Method	$k_1$	m	n	m+n
25	1	.049	.59	1.41	2.00
	2	.037	.50	1.56	2.06
	3	.099	.80	2.40	3.20
	4	.039	.39	1.47	1.86
	5	.038	.577	1.47	2.00
30	1	.076	.76	1.24	2.00
	2	.188	.903	1.81	1.08
	4	.060	.600	1.20	1.80
	5	.060	.527	1.47	2.00
35	1	.081	.760	1.24	2.00
	2	.120	.900	1.80	2.70
	3	.196	1.105	2.19	3.29
	4	.100	.750	1.72	2.47
	5	.060	.551	1.45	2.00

(TABLE 4.1 continued)

Temp. ( $^{\circ}\text{C}$ )	Method	$k_1$	m	n	m+n
40	1	.095	.660	1.34	2.00
	2	.099	1.010	1.40	2.0
	3	.096	.628	1.40	2.00
	4	.090	.600	1.40	2.00
	5	.060	.593	1.40	2.00
50	1	.187	.79	1.21	2.00
	2	.200	.900	1.50	2.40
	3	.200	.800	1.50	2.30
	4	.200	.800	1.50	2.30
	5	.152	.577	1.42	2.00
60	1	.328	.86	1.14	2.00
	2	.223	.510	1.18	1.69
	3	.204	.400	1.10	1.50
	4	.320	.402	1.40	1.80
	5	.195	.727	1.27	2.00

APPENDIX A

1

DSC Data File: 1210a  
 Sample Weight: 12.030 mg  
 Wed Dec 09 23:41:20 1987  
 PERKIN-ELMER  
 7 Series Thermal Analysis System  
 orietach polyester resin

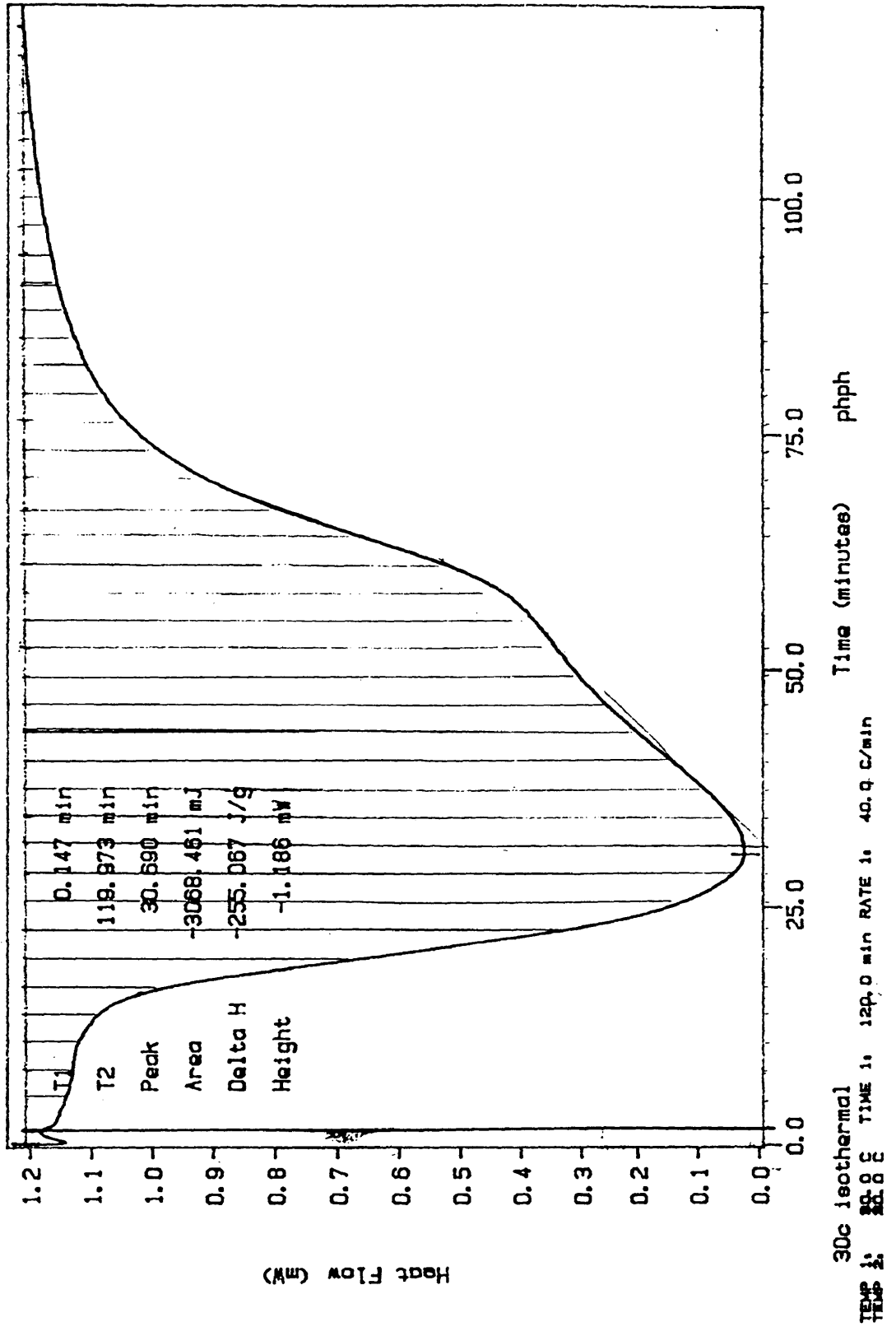


FIGURE A-1: 30°C ISOTHERMAL

DSC Data File: 01130  
 Sample Weight: 22.980 mg  
 Tue Jan 12 23:15:20 1988  
 Perkin-Elmer  
 7 Series Thermal Analysis System  
 Arlotech polyester resin

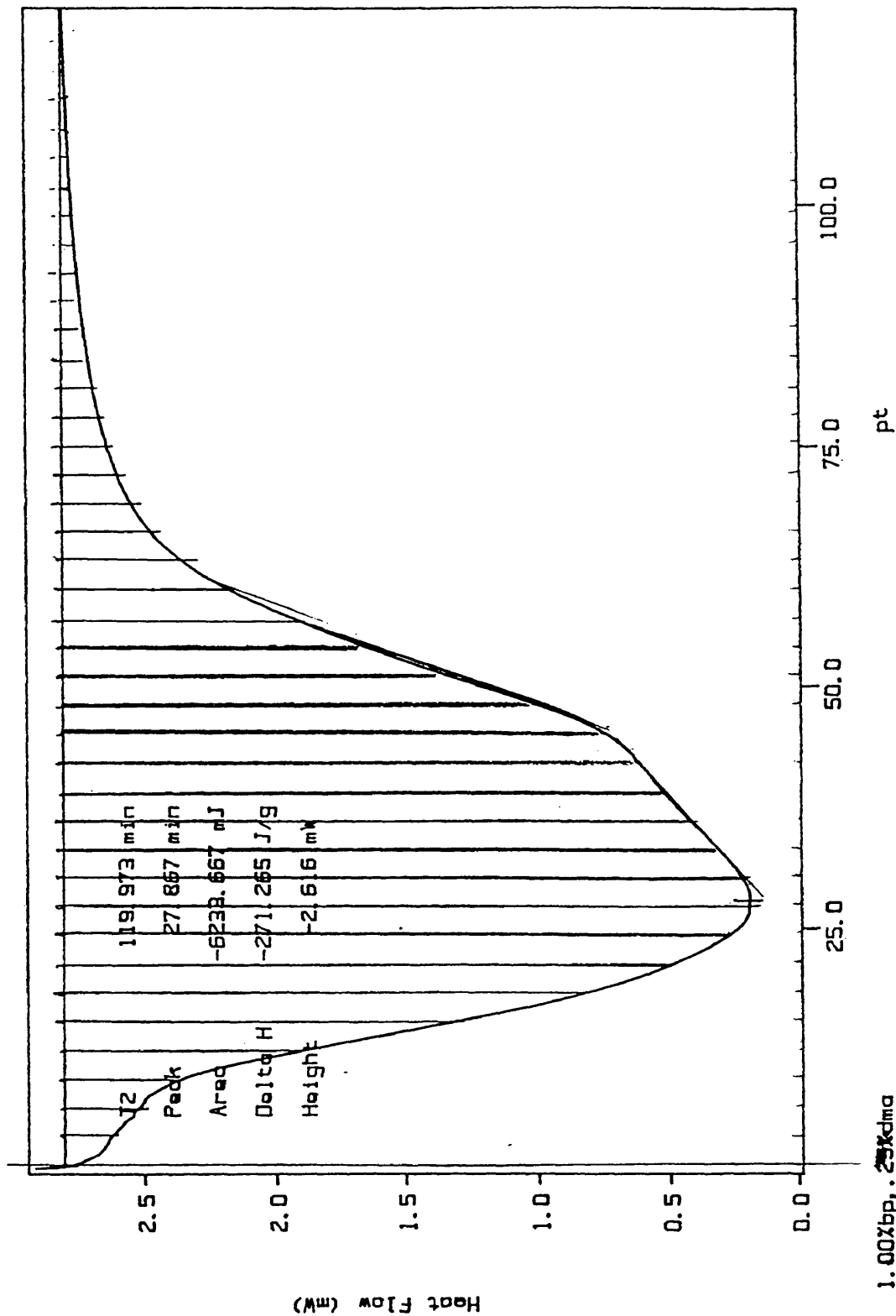
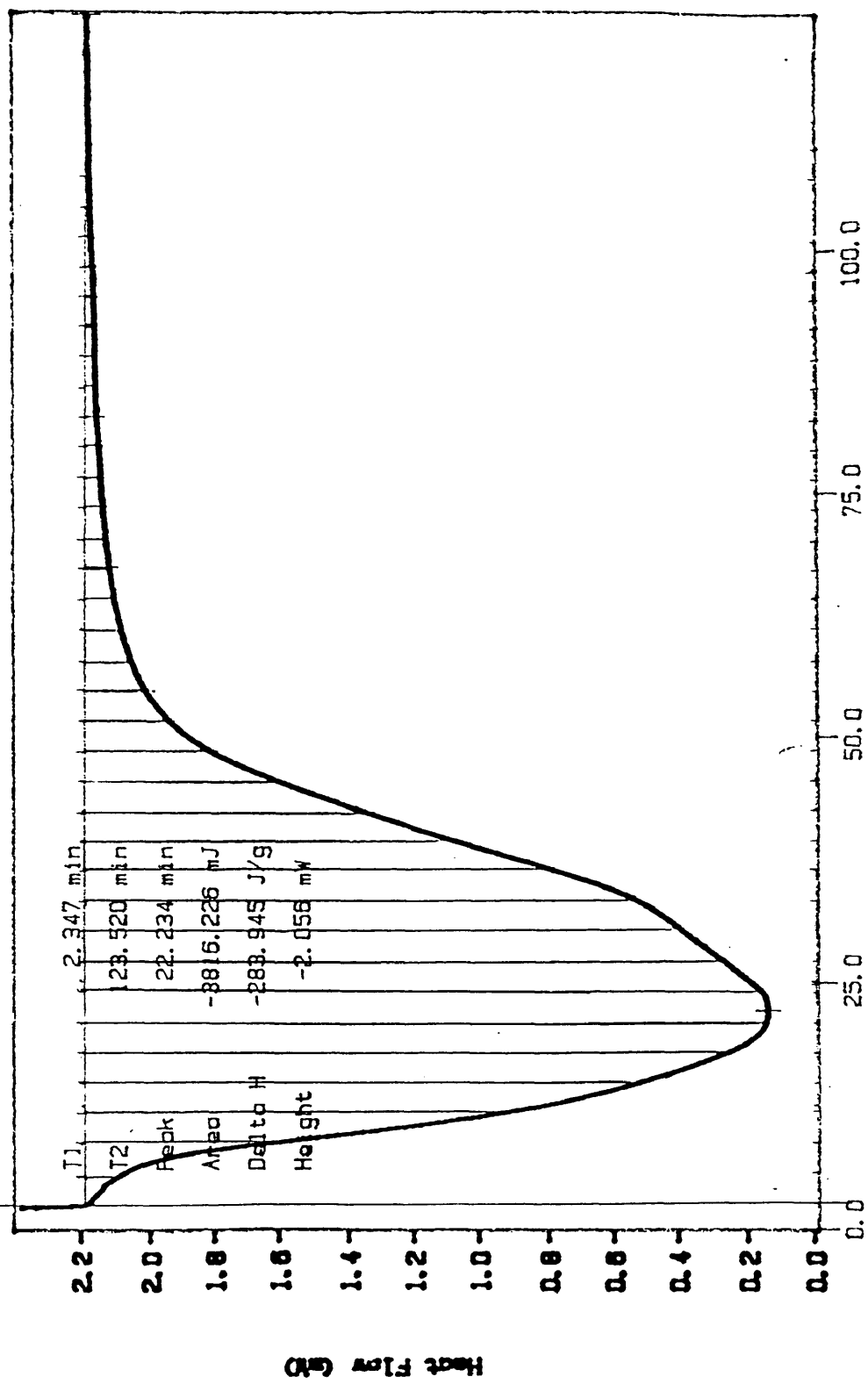


FIGURE A-2: 35°C ISOTHERMAL

TSC Data Files 0700bb  
 Sample Weight: 13.440 mg  
 Yed Jul 08 02:15:28 1987  
 Perkin-Elmer  
 7 Series Thermal Analysis System  
 crictechs 40p Isothermal



1.0000g, 0.251chm  
 TSC 40 23.52  
 TIME: 100.0 min RATE: 10.0 C/min  
 Time (minutes) ph

FIGURE A-3: 40°C ISOTHERMAL

DSC Data File: 0504a  
Sample Weight: 20.640 mg  
Tue May 03 22:45:25 1988  
Perkin-Elmer 7 Series Thermal Analysis System  
Cristech polyester resin, 45c

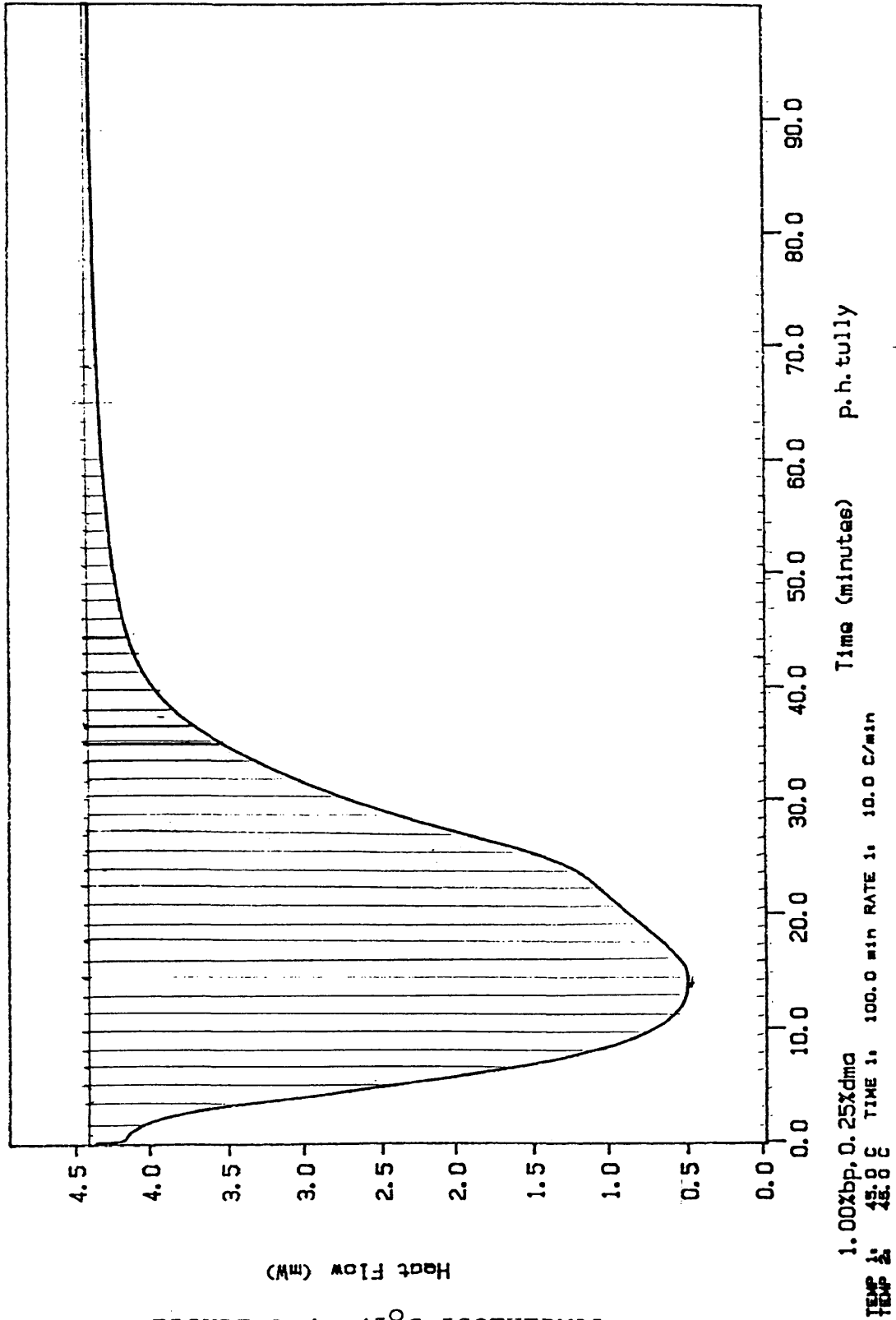


FIGURE A-4: 45°C ISOTHERMAL

DSC Data File: 0721a  
 Sample Weight: 12.750 mg  
 Tue Jul 21 02:09:40 1987  
 Perkin-Elmer  
 7 Series Thermal Analysis System  
 arstech; 50c isothermal

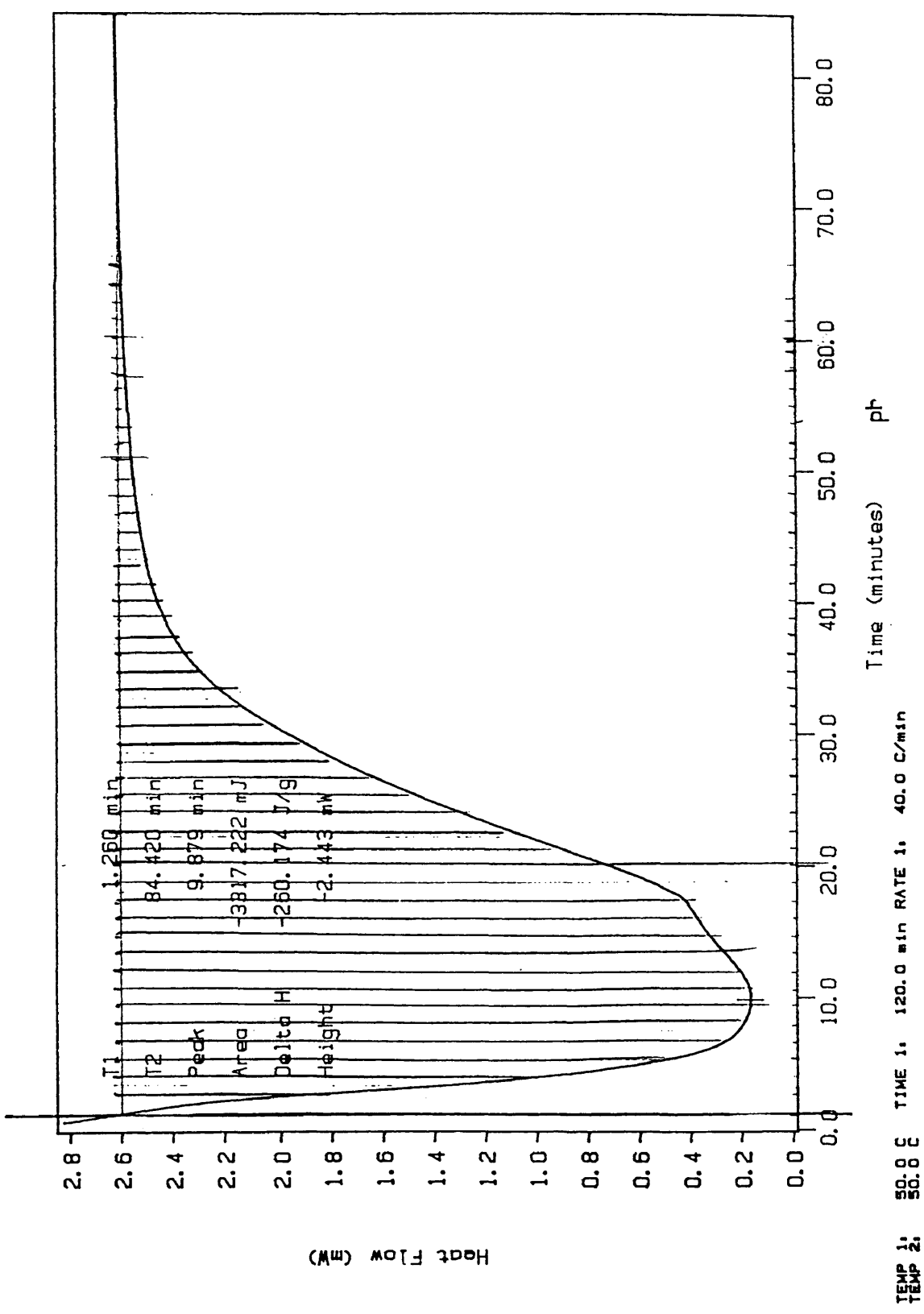


FIGURE A-5: 50°C ISOTHERMAL

DSC Data File: 0728a  
 Sample Weight: 18.580 mg  
 Tue Jul 28 02:24:00 1987  
 arlstech; 60b isothermal

PERKIN-ELMER

7 Series Thermal Analysis System

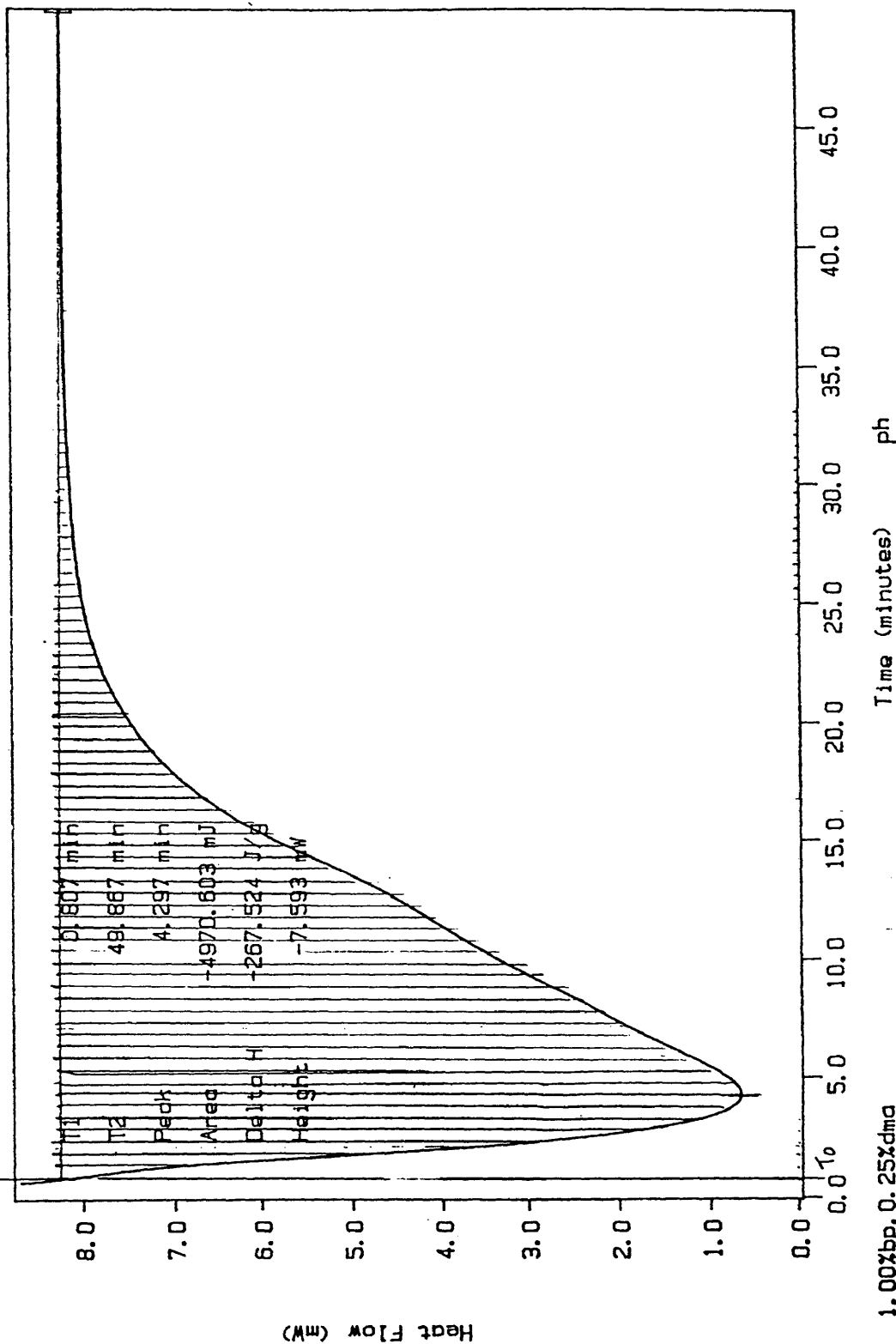


FIGURE A-6: 60°C ISOTHERMAL

APPENDIX B: LEAST SQUARE FIT PROGRAM

```

1 DATA TEMP;
2 infile bigg;
3 input x y;
4 ;

NOTE: INFILE BIGG IS:
DSNAME=WCHAMSH.ARIS.SIXTYIN.HALF.DATA,
UNIT=DISK,VOL=SER=PUBLO3,DISP=SHR,
DCB=(BLKSIZE=3120,LRECL=80,RECFM=FB)

NOTE: 19 LINES WERE READ FROM INFILE BIGG.
NOTE: DATA SET WORK.TEMP HAS 19 OBSERVATIONS AND 2 VARIABLES. 2346 OBS/TRK.
NOTE: THE DATA STATEMENT USED 0.19 SECONDS AND 384K.

5 PROC PRINT;
NOTE: THE PROCEDURE PRINT USED 0.22 SECONDS AND 516K AND PRINTED PAGE 1.

6 PROC NLIN METHOD=MARQUADT ITERATIONS=100 BEST=5;
7 PARAMETERS b0=0.00 TO 0.01 BY .001
8 R1=0.00 TO 1.0 BY .10
9 b2=0.50 TO 1.60 BY 0.10
10 b3=1.00 TO 3.00 BY 0.10;
11 d=x**b2;
12 e=(1-x)**b3;
13 model y=(b0+b1*x**b2)*(1-x)**b3;
14 der.b0=e;
15 der.b1=d*x;
16 der.b2=e*x*b2*(b2-1);
17 der.b3=(b0+b1*x*d)*b3*(1-x)**(b3-1);
18 output out=k Predicted=p Residual=r;
19 /*
20 end;

NOTE: THE DATA SET WORK.K HAS 19 OBSERVATIONS AND 4 VARIABLES. 1304 OBS/TRK.
NOTE: THE PROCEDURE NLIN USED 1250.78 SECONDS AND 840K AND PRINTED PAGES 2 TO
NOTE: SAS USED 840K MEMORY.

NOTE: SAS INSTITUTE INC.
SAS-CIRCLE
PO BOX 8000
CARY, N.C. 27511-8000

```

APPENDIX C: RYAN DUTTA DERIVATION FOR  $k_1$

1.  $d(\alpha)/dt = k(1-\alpha)^n + k_1\alpha^m(1-\alpha)^n$

2.  $d(\alpha)/dt = 0 =$

$$(-1)nk_0(1-\alpha)^{n-1} + [(k_1\alpha^m)(1-\alpha)^{n-1}(-n)] \\ + [mk_1(1-\alpha)^n](\alpha^{m-1})$$

3. Multiply through by  $(1-\alpha)^{-n+1}$ :

$$(-n)k_0 + (-n)k_1\alpha^m + mk_1\alpha + mk_1(1-\alpha)(\alpha^{m-1}) = 0$$

4. Multiply by  $\alpha^{1-m}$ :

$$(-n)k_0(\alpha^{1-m}) + (-n)k_1\alpha + mk_1\alpha - mk_1 = 0$$

5. Multiply by #4 by -1 and rearrange:

$$nk_0(\alpha^{1-m}) + k_1\alpha(m+n) - mk_1 = 0$$

6. Apply condition  $m+n=2$ :

$$(2-m)k_0\alpha^{1-m} + 2k_1\alpha - mk_1 = 0$$

7. Solve for  $k_1$  which is unknown:

$$k = \frac{(2-m)k_0(\alpha^{1-m})}{m - 2\alpha}$$

PPENDIX D: DERIVATION OF COMPLEX PERMITIVITY

In applying a steady field  $E_0$  with time, one can express the displacement as a function of time also:

$$1. D(t) = [\epsilon_s \epsilon_\infty + \epsilon_s - \epsilon_\infty \psi(t)] E_0$$

$\epsilon_s \epsilon_\infty E_0$  is the instantaneous response to the field]  
 $\psi(t) \epsilon_0 (\epsilon_s - \epsilon_\infty)$  represents slower response to the field due to polarization; this factor  $\psi(t)$  describes the time lag process.

$\psi(0) = 0, \psi(\infty) = 1$  allows for full spectrum of relaxation from  $\epsilon_s$  to  $\epsilon_\infty$ .

Recalling that the equilibrium value of dipolar polarization,  $P(\infty) = \epsilon_0 (\epsilon_s - \epsilon_\infty) E_0$

we assume that the rate at which dipolar polarization approaches this equilibrium value is proportional to its degree of departure from equilibrium.

$$1) \quad \dot{P}(t) = - \frac{P(\infty) - P(t)}{\tau}$$

2)  $P(t)$  = polarization with time

$P(\infty)$  = equilibrium polarization

$\tau$  = dielectric relaxation time, characteristic time constant

$P(t) - P(\infty)$  = departure from equilibrium polarization

Integrating equation #2:

$$3. \quad P(t) = P(\infty) (1 - e^{-t/\tau})$$

The time dependence on polarization is defined by:

$$4. \quad \psi(t) = (1 - e^{-t/\tau})$$

If polarization is a linear function of the applied field, then if a stronger field than  $E_0$  is applied at  $t_0$ :

$$5. \quad \bar{D}(t) = \epsilon_0 (\epsilon_\infty + (\epsilon_s - \epsilon_\infty) \psi(t)) (E_0 + E_1)$$

Applying the Boltzmann superposition principle and assuming that an extra field is applied at  $t_1$ , at a time greater than  $t_1$  the displacement will be

$$6. \quad \bar{D}(t) = \epsilon_0 (\epsilon_\infty + (\epsilon_s - \epsilon_\infty) \psi(t)) E_0 + \epsilon_0 (\epsilon_\infty + (\epsilon_s - \epsilon_\infty) \psi(t - t_1)) E_1$$

For a series of such increments in applied field:

$$7. \quad \bar{D}(t) = \sum_{t_i = -\infty}^{t_i = t} \epsilon_0 (\epsilon_\infty + (\epsilon_s - \epsilon_\infty) \psi(t - t_i)) E_i$$

For a continuously varying field:

$$8. \quad \bar{D}(t) = \epsilon_0 \epsilon_\infty \bar{E}(t) + \int_{-\infty}^t \epsilon_0 (\epsilon_s - \epsilon_\infty) \psi(t-s) \frac{d\bar{E}}{ds} ds$$

Equation #8 expresses the value of the dielectric

in terms of the entire past history of the material in the presence of the field. this equation may be integrated to give the following:

$$9. D(t) = \epsilon_0 \epsilon_\infty E(t) + \epsilon_0 (\epsilon_s - \epsilon_\infty) \int_{-\infty}^t \dot{\chi}(t-s) dS$$

From equation #4:

$$10. \dot{\chi}(t) = \frac{1}{\tau} (e^{-t/\tau})$$

Differentiating equation #9 with respect to time:

$$11. \frac{d(D(t))}{dt} = \epsilon_0 \epsilon_\infty \frac{dE(t)}{dt} + \epsilon_0 (\epsilon_s - \epsilon_\infty) \frac{d}{dt} \int \dot{\chi}(t-s) E(s) ds$$

And from equation #10, it follows:

$$12. \frac{d}{dt} \int_{-\infty}^t \dot{\chi}(t-s) E(s) ds = \dot{\chi}(0) E(0) - \frac{1}{\tau} \int_{-\infty}^t \dot{\chi}(t-s) E(s) ds$$

Combining equations 9, 11, and 12:

$$\tau \frac{d(D(t))}{dt} + D(t) = \tau \epsilon_0 \epsilon_\infty \frac{dE(t)}{dt} + \epsilon_0 \epsilon_s E(t)$$

## APPENDIX E: SUPPORTING EXPERIMENTATION

### RHEOLOGY.

The term viscoelasticity was coined to describe the mechanical behaviour of materials that exhibit properties of both solids and liquids. Under an applied stress (force), these materials deform as do liquids and solids. The difference lies in the response (strain) with time.

A body which is truly solid will maintain constant strain under constant stress. A viscoelastic material, however, continues to deform- creeps - under this same constant stress. A body which is truly liquid flows under constant stress. A viscoelastic material will recover part of the deformation when the stress is

removed. This elastic recoil is possible because the material does not dissipate all of the energy in the form of heat, as does a liquid; but rather it stores part of the energy for later recovery of conformation.

Given the dimensions of an ordinary macromolecule, the freedom of movement of the chains due to thermal energy, and their liquidlike and solidlike characteristics, the flow of these materials may be quite complex. A spectrum of response is observed when

studying the molecule. On one end of the spectrum, the entire chain responds to the field-slowly. On the other end, a small fragment of the chain, two or three units in length, responds rapidly in its continuously changing environment.

The study of the flow is rheology. Specifically, the viscosity of resin may be determined by applying a stress and measuring the rate of the deformation. Viscosity is the ratio of the stress to rate of strain, ideally, independent of the total strain itself.

As with the dielectric constant, it is useful to apply a sinusoidally oscillating stress to define and identify the storage and loss components of the stress/strain relationship of these unique materials. The dynamic viscosity is defined as the complex storage modulus,  $G^*$ , divided by the angular frequency,  $\omega$  time the complex quantity  $i$ .

$$\eta^* = G^* / i\omega = (\text{stress/strain}) / i\omega$$

$$\eta^* = (G'^2 + G''^2)^{.5} / \omega$$

where  $G'$  is the storage modulus and  $G''$  is the loss modulus. The rheometer measures  $G'$  and  $G''$  from which the viscosity is computed.

MD121787 : Polyester Resin 25°C Isothermal Cure.

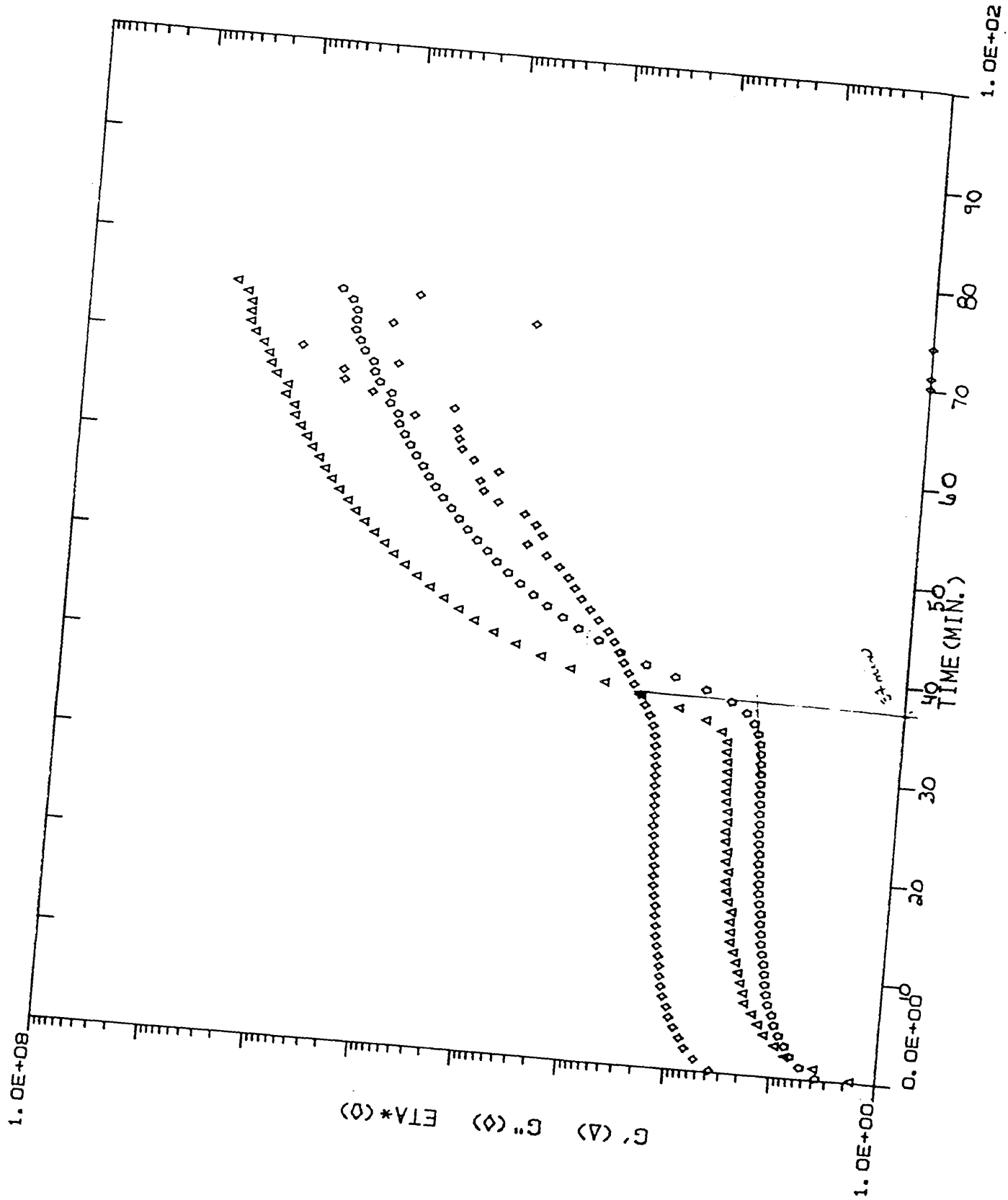


FIGURE E-1

MCI21787: Polyester Resin 30°C Isothermal 12-17-87 10  $\frac{wt}{sec}$

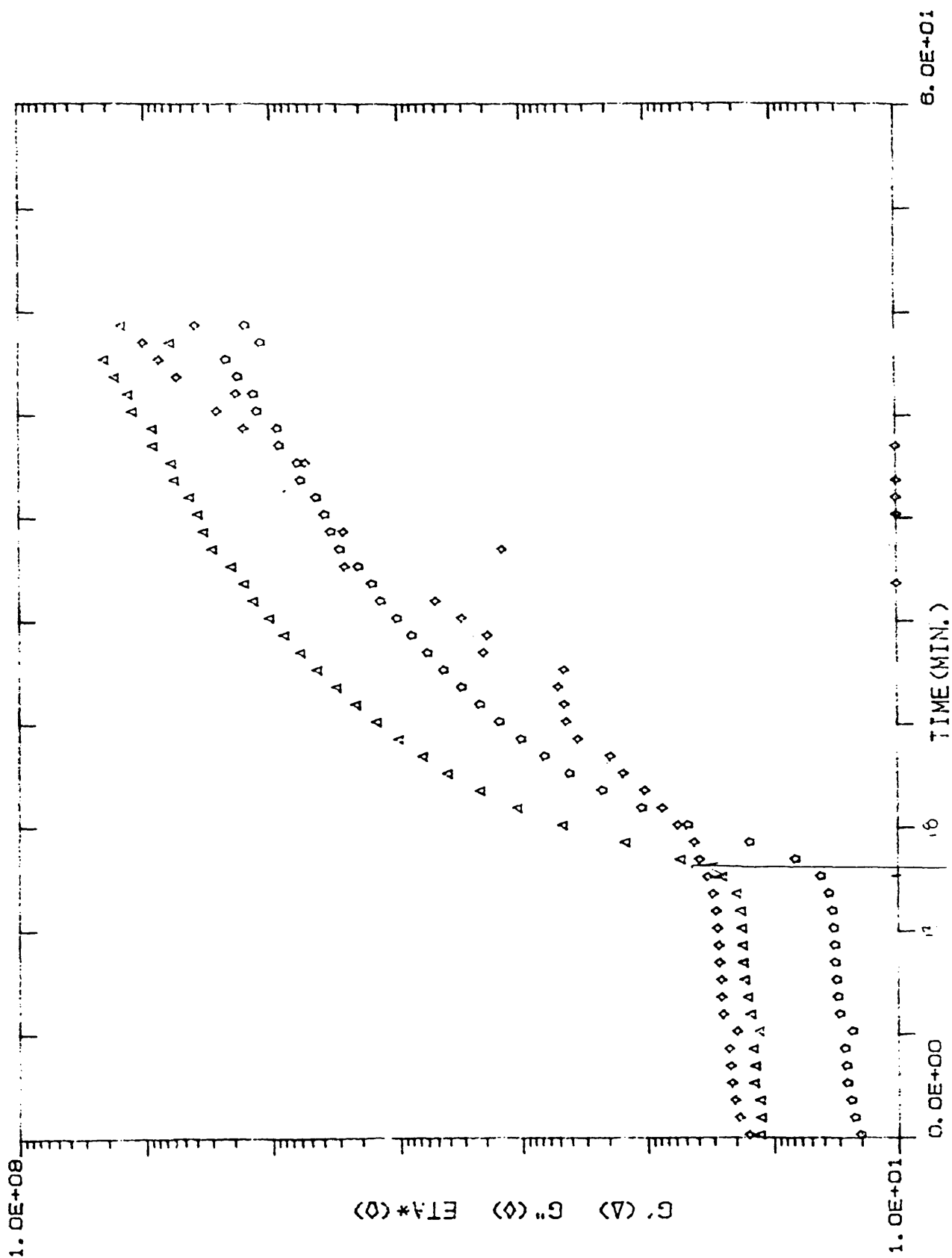


FIGURE E-2

MB121787: Polyester Resin 35°C Isothermal 12-17-87 10  $\frac{rad}{sec}$

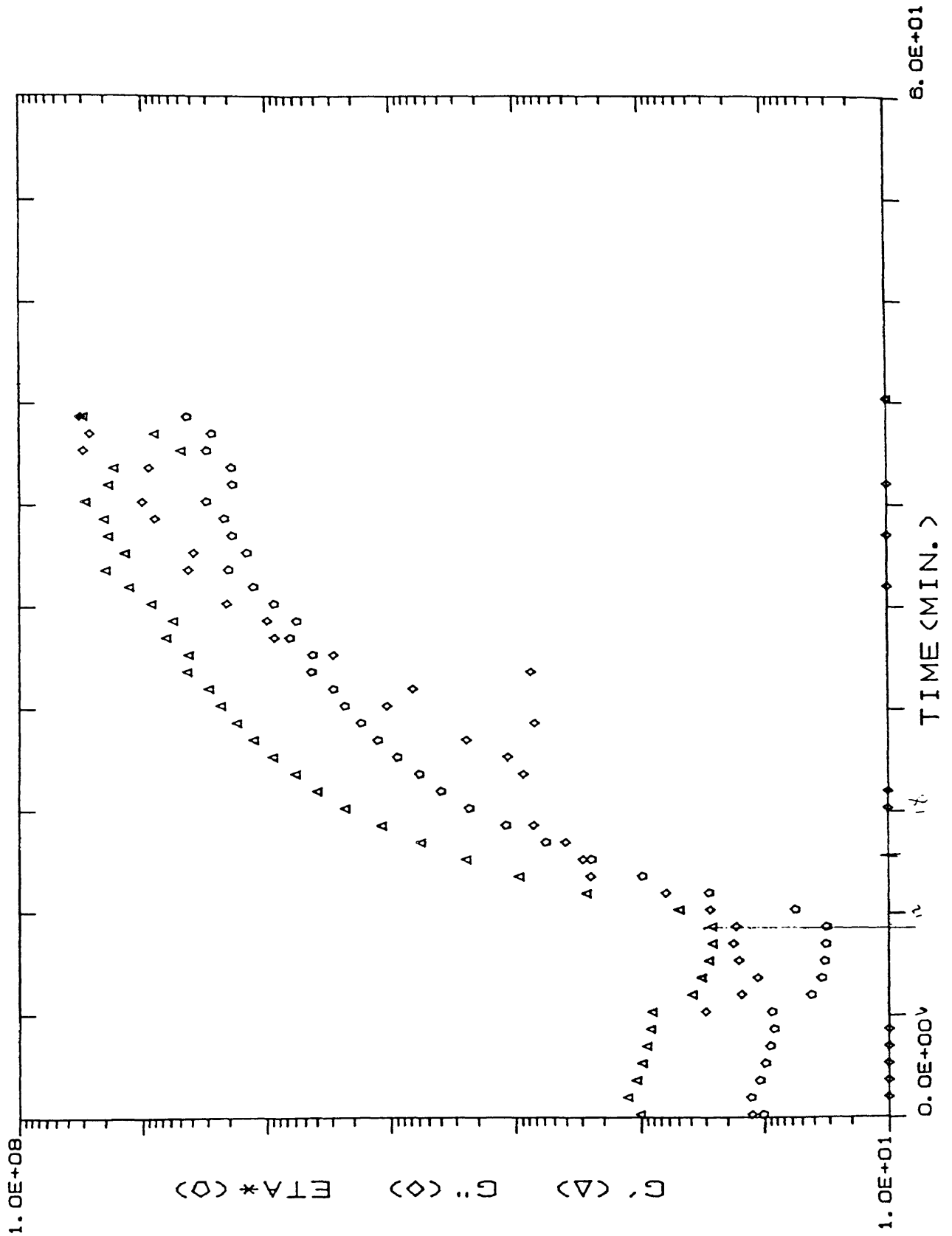


FIGURE E-3

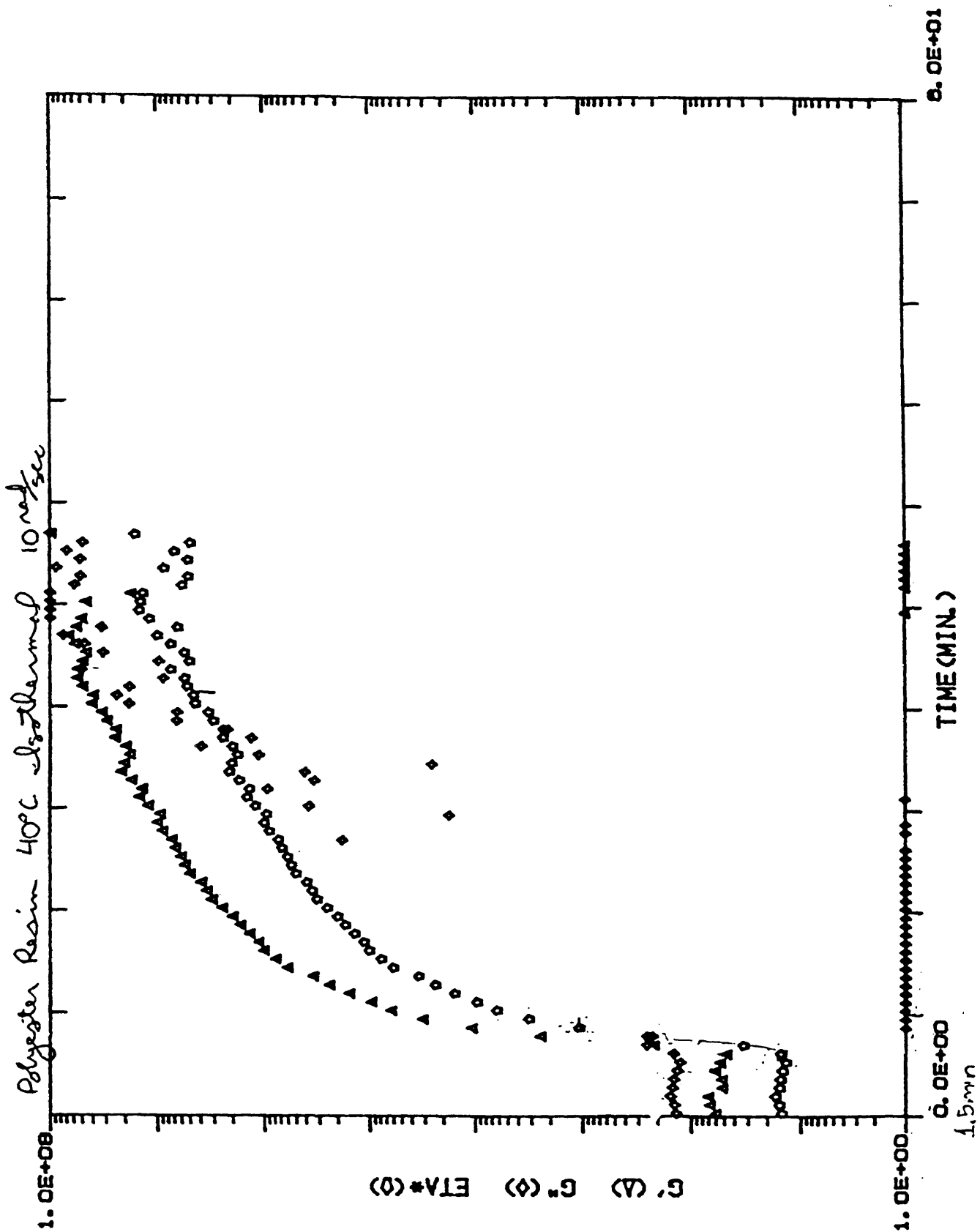


FIGURE E-4

## BARCOL HARDNESS

In an early study of polyester cure, Learmonth, Tomlinson, and Czerski used Barcol Hardness as a semi-empirical method for monitoring the degree of cure(1). Operating under the knowledge that the glass transition point is intimately connected with the ultimate degree of cure. They measured the build-up of the Barcol Hardness to completion of cure. The cure shuts down as the reacting groups are "frozen" into their configuration at the glass transition point, thereby determining the time to  $T_g$  at cure temperature.

A diagram of the general construction of a Barcol Hardness tester is shown in figure . The instrument is quite easy to operate in theory, but gives misleading results if the surface of the material tested is not completely flat. Resting the support leg on the surface, the body of the instrument is gripped and the plunger tip is pressed firmly and steadily into the curing resin. The spring-loaded needle penetrates the surface to a depth dependent on the hardness of the material. The more resistant to penetration, the higher the Barcol number. To allow for creep, the Plastics Technology Handbook suggests waiting ten seconds before recording a reading.

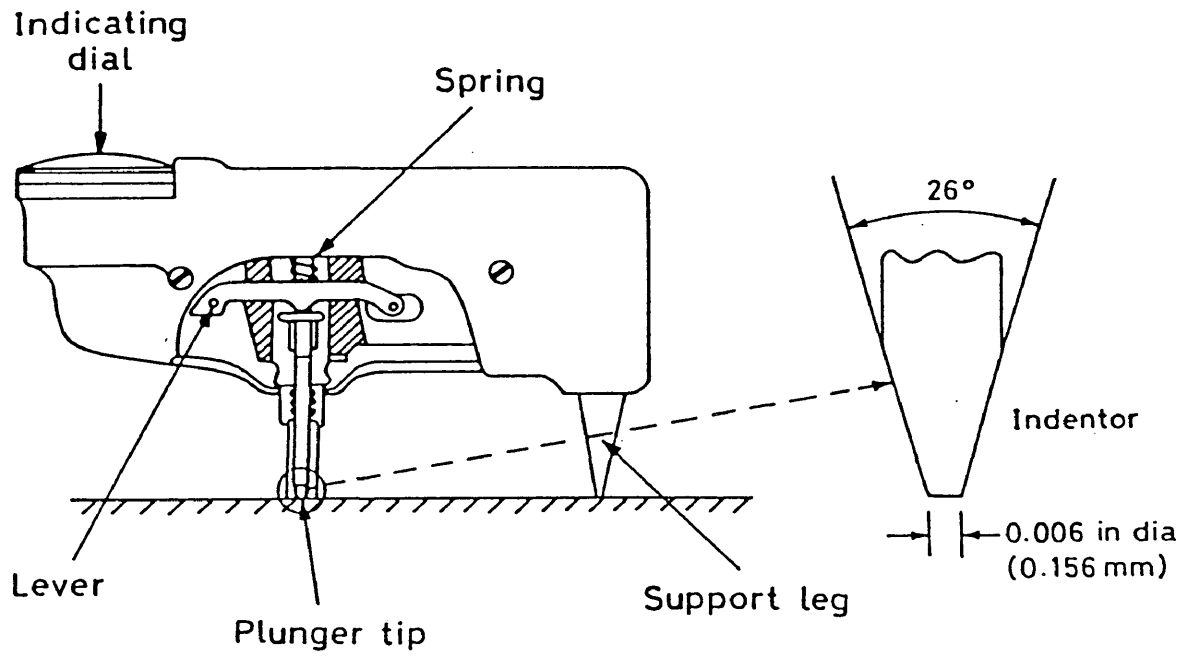


FIG. E.5 General construction of Barcol hardness tester.

## BIBLIOGRPHY

1. Allcock, Harry R. and Frederick W. Lampe, Contemporary Polymer Chemistry (New Jersey: Prentice-Hall, Inc., 1981), pp.436-442.
2. "Antioxidants," Encyclopedia of Polymer Science and Engineering, 1986 ed.
3. Batch, Gibson L. and Chrisotpher W. Macosko, "Kinetics of Crosslinking Free Radical Polymerization with Diffusion Limited Propagation," Antec, (1987), 974.
4. Batch,G. and C. Macosko, Antec (1988), 1039.
5. Blythe, A. R., Electrical Properties fo Polymers, (Cambridge: Cambridge University Press, 1977).
6. Manes, Chanda and Salel K. Roy, Plastics Technology Handbook(New York: Marcel Dekker Inc., 1987).
7. Enns, John B. and John K. Gillham, "Time-Temperature-Transformation (TTT) Cure Diagram: Modeling the Cure Behavoir of Thermosets," Journal of Applied Polymer Science, 28, (1983) 2567-2591.
8. Gibson,W. M., Basic Electricity (Harmondsworth: Penguin Books Ltd., 1969)
9. Han, Chang Dae and Dai Soo Lee, "Curing Bdhavoir of "Unsaturated Polyester Polyester Resin With Mixed Initiators," Journal of Applied Polymer Science, 34 (1987), 793.
10. S. W. Hockey, Fundamental Electrostatics, (London:

Methuen Educational Ltd., 1972).

11. Hoffman, R. D., D. E. Kranbuehl, P. Haverty and M. Hoff  
"Monitoring the Cure Processing Properties of  
Unsaturated Polyesters In-situ During Fabrication"
12. Kamal, Musa R., "Thermoset Characterization for  
Moldability Analysis," Polymer Engineering Science, 14,  
No. 3 (1974) 231.
13. Kamal, M. R. and S. Sourour, "Kinetics and Thermal  
Characterization of Thermoset Cure," Polymer Engineering  
and Science, 13, no. 1 (1973), 59.
14. Kranbuehl, David E., Cure Monitoring
15. Kranbuehl, D. E., S. E. Delos and P. K. Jue, Polymer,  
27 (1986), 11.
16. Lam, Patrick W., "The Characterization of Thermoset  
Cure Behaviour by Differential Scanning Calorimetry:  
Part 1 Isothermal and Dynamic Study," Polymer  
Composites, 18, No. 6 (1987), 427.
17. Learmonth, G. S., F. M. Tomlinson, and I. Czerski,  
"Cure of Polyester Resins I," Journal of Applied  
Polymer Science, 12 (1968), 403.
18. McNaughton, J. L. and C. T. Mortimer, Differential  
Scanning Calorimetry (rpt. London: Bttersworth, 1975).
19. Morton-Jones, David H. and John W. Willis, Polymer  
Products: Design, Materials and Processing (London:  
Chapman and Hall, 1986) 159-169.
19. "Polyesters, Unsaturated," Encyclopedia of Chemical  
Technology, 1982 ed.
20. "Polyesters, Unsaturated," Encyclopedia of Polymer  
Science and Engineering, 1986 ed.
21. Prime, R. Bruce, ed. Edith A. Turi, "Thermosets",

Thermal Characterizations of Polymeric Materials, (New York: Academic Press, Inc., 1981).

22. Pusatcioglu, S. Y., A. L. Fricke, and J. C. Hassler, "Heats of Reaction and Kinetics of a Thermoset Polyester," Journal of Applied Polymer Science, 24 (1979), 937.
23. Ryan, R. and A. Dutta "Kinetics of Epoxy Cure: A Rapid Technique for Kinetic Parameter Estimation," Polymer, 20 (1979), 203.
24. Salla, J. M. and J. L. Martin, "Dynamic Isothermal and Residual Heats of Curing of an Unsaturated Polyester Resin," Thermochemica Acta, 126 (1988) 339-354.
25. Sourour, S. and M. R. Kamal, "Differential Scanning Calorimetry for Characterization of Thermoset Cure," SPE Technical Papers, 18 (1972), 93.
26. Sourour, S. and M.R. Kamal, "Differential Scanning Calorimetry of Epoxy Cure: Isothermal Cure Kinetics," Thermochemica Acta, 14 (1976), 41.
27. Stevenson, James F., "Free Radical Models for Simulating Reactive Processing", Polymer Engineering and Science, 26, No. 11 (1986), 746.
28. Storey, Robson F., Dantiki Sudhakar and Melissa Hogue, "Tertiary Aromatic Amines as Cure Reaction Promoters for Unsaturated Polyester Resins: II Low Temperature Studies," Journal of Applied Polymer Science, 32 (1986), 4919.
29. Tipler, Paul A., Physics, 2nd ed. (New York: Worth Publishers Inc., 1982).

## VITA

### PATRICIA HAVERTY TULLY

Born in Suffolk, Virginia, March 18, 1965. Graduated from John F. Kennedy High School in that city June 1983. B.S. in Chemistry College of William and Mary in Williamsburg, Virginia May 1987.

In January 1989, the author entered the college of William and Mary as laboratory instructor of Organic Chemistry. Summer of 1986, the author participated in summer research at the afore mentioned institution. Summer of 1985, the author was employed as lab technician for Allied Colloids, Ltd. of Suffolk, Virginia.